2006

Two-Dimensional and High-Throughput Electrophoretic Separation of Proteins Using Polymeric Microchips

Hamed Shadpour
Louisiana State University and Agricultural and Mechanical College

TWO-DIMENSIONAL AND HIGH-THROUGHPUT ELECTROPHORETIC SEPARATION OF PROTEINS USING POLYMERIC MICROCHIPS

A Dissertation

Submitted to the Graduate Faculty of the
Louisiana State University and
Agricultural and Mechanical College
in partial fulfillment of the
requirements for the degree of
Doctor of Philosophy

in

The Department of Chemistry

by
Hamed Shadpour
B.S., University of Guilan, 1997
M.S., Amirkabir University of Technology (Tehran Polytechnic), 2000
December, 2006

DEDICATION

I would like to dedicate this dissertation to my loving parents for supporting me to go extra miles to achieve the very best.

ACKNOWLEDGEMENTS

I would like to express gratitude to my family members: Mom, Dad, and my Brother. Love is a reward that is appreciated by those that share it. I do cherish all those moments that we have shared as a family. I am sorry I missed so much, but I am sure you all realize. Definitely your compassion and love just never cease to amaze me. Thank you for the unfailing love, trust and support that you have given to me through my education. I love you all, and can never thank you enough for all that you have done for me. Mom and Dad, thank you for having faith in me since I was born and helping me my full potential in life. I share my degree with you two angels.

I would like to thank my advisor, Professor Steven A. Soper for his support, advice and constant encouragement during my graduate studies at Louisiana State University. You are an inspiration to many and a mentor whom I can always count on. Also, I want to thank my committee members, Professors Isiah M. Warner, Robert L. Cook**,** M. Graca H. Vicente, and Cathleen C. Williams for your direction and input that has kept me going. Professors Robin L. McCarley and Kermit K. Murray are greatly acknowledged for the use of their lab facilities with all their technical advises and supports.

To all my friends, you have been such a blessing to me. Thank you for your collective support, encouragement and for keeping me straight in more ways than one. I would like to thank the entire Super Soper Research Group, for the moments we shared as colleagues and friends. I share all my accomplishments, if there are any, with all my group members.

I greatly acknowledge the Center for Bio-Modular Multi-Scale Systems (CBM^2) and Center for Advance Microstructures and Devices (CAMD) for technical support of this dissertation. I also would like to thank the Department of Chemistry of Louisiana State University for all supports provided during my doctoral study.

TABLE OF CONTENTS

LIST OF TABLES

LIST OF FIGURES

SYMBOLS AND ABBREVATIONS

%T	Percent monomer composition
μ-CAE	Microchip capillary array electrophoresis
μ-CE	Microchip CE
μ-CEC	Micro-capillary electrochromatography
μ-CZE	Micro-capillary zone electrophoresis
μ_{eof}	Electroosmotic mobility
μ_{ep}	Electrophoretic mobility
μ–TAS	Micro-total analysis system
1-D	One-dimensional
2-D	Two-dimensional
3-D	Three-dimensional
4σ	Peak width
A	Area
A and *B*	Asymmetry peak parameters
ABS	Poly(acrylonitrile-butadiene-styrene)
AC	Actin
A_s	Asymmetry factor
ASE	Advanced silicon etching
BAL	Bronchoalveolar lavage
BSA	Bovine serum albumin
C	Concentration
CAE	Capillary array electrophoresis
CE	Capillary electrophoresis
CEC	Capillary electrochromatography
CF-PCR	Continuous-flow polymerase chain reaction
CF-TC	Continuous flow thermal cycler
CGE	Capillary gel electrophoresis
CNC	Computer numerical control
cmc	Critical micelle concentration
CO	Concanavalin
COMOSS	Collocated monolith support structures
C-PMMA	Clear acrylic
CSE	Capillary sieving electrophoresis
CTAB	Cetyltrimethylammonium bromide
CZE	Capillary zone electrophoresis
D	Diffusion coefficient
Da	Dalton
d_{chan}	Channel depth
DEEMO	Deep etching, electroplating, and molding
DIFE	Differential gel electrophoresis
DNA	Deoxyribonucleic acid
DSC	Differential scanning calorimetry
E	Electric field
EDC	1-ethyl-3-[3-dimethylaminopropyl] carbodiimide hydrochloride
EDM	Electrodischarge machining
EOF	Electroosmotic flow

ESI	Electrospray ionization
FAB	Fast atom bombardment
G	Conductivity
GC	Gas chromatography
GPI	Glycosylphosphatidylinositol
G-PMMA	Gray acrylic
H	Plate height
H_D	Height equivalent of a theoretical plate for longitudinal diffusion
HDPE	High-density polyethylene
H_{Joule}	Plate height contribution from Joule heating
h_{master}	Master height
HPA	*Helix pomatia* lectin
HPLC	High performance liquid chromatography
H_{TOT}	Total plate height
ICAT	Isotope-coded affinity tagging
IEF	Isoelectric focusing
IMAC	Immobilized metal affinity chromatography
IMS	Imaging mass spectrometry
ITP	Isotachophoresis
J	Joule heating
K (or K_c)	Cell constant
k_b	Thermal conductivity
L	Length (distance)
LC	Liquid chromatography
LCST	Lower critical solution temperature
LDPE	Low-density polyethylene
L_{eff}	Effective separation length
LIF	Laser-induced fluorescence
LiGA	Lithography, electroplating, and molding (a German word)
L_{inj}	Injection length
LOD	Limit of detection
L_{tot}	Total separation length
LX-PC	Lexan
MALDI TOF	Matrix-assisted laser desorption/ionization time-of-flight
MEEKC	Microemulsion Electrokinetic Chromatography
MEKC	Micellar electrokinetic chromatography
MG-PMMA	Medical-grade poly(methyl methacrylate)
MHEC	Methyl hydroxyl ethyl cellulose
mRNA	Messenger RNA
MS	Mass spectrometry
MS/MS	Tandem mass spectrometry
MT	Migration time
MW	Molecular weight
N	Separation efficiency
n	Number of channels
NDA	Naphthalene-2,3-dicarboxaldehyde
N_p	Practical peak capacity

NY	Nylon
O	Orthogonality
OV	Ovalbumin
P	Peak capacity
PA	Protein A
PBS	Phosphate buffered saline
PC	Polycarbonate
PCB	Printed circuit boards
PCR	Polymerase chain reaction
PDF	Pressure-driven flow
PDMS	Poly(dimethylsiloxane)
PET	Polyethylen terephtalate
PETG	Polyethylene terephthalate glycolate
pI	Isoelectric point
PMMA	Poly(methyl methacrylate)
PNA	Lectin peanut agglutinin
pNIPAAm	Poly(N-isopropylacrylamide)
PP	Polypropylene
PS	Polystyrene
PSU	Polysulfone
PTFE	Poly(tetrafluoroethylene)
PTM	Post-translational modification
PU	Polyurethane
q	Solute charge
R	Resistance
r	Correlation coefficient
R/W	Radius of curvature to channel width ratio
R_a/λ_a	Surface roughnesses
RE	Replication error
RIE	Reactive ion etching
RMS	Root mean square
RNA	Ribonucleic acid
RP-LC	Reverse-phase liquid chromatography
R_s	Resolution
SDS	Sodium dodecyl sulfate
SDS μ-CGE	Sodium dodecyl sulfate micro-capillary gel electrophoresis
SDS PAGE	Sodium dodecyl sulfate polyacrylamide gel electrophoresis
SELDI	Surface-enhanced laser desorption/ionization
SNR	Signal-to-noise ratios
SPE	Solid phase extraction
SPRI	Solid phase reversible immobilization
ST	Streptavidin
t	Time
T	Absolute temperature
TC	Thermal cycler
TCA	Trichloroacetic acid
TEAA	Triethylammonium acetate
T_g	Glass transition temperature

t_{mig}	Migration time
TR	Transferrin
tRNA	Transfer RNA
v_{eof}	Electroosmotic flow velocity
v_{ep}	Electrophoretic velocity
v_{tot}	Total velocity
$w_{0.1}$	Band width measured at one-tenth of the maximum height
WG	Wheat germ agglutinin
ε	Dielectric constant
ζ	Zeta potential
η	Viscosity
λ_+ and λ_-	Limiting ionic conductances
σ_{det}^2	Detection variance
σ_{inj}^2	Injection variance
σ_{tot}^2	Total variance

ABSTRACT

A major task in proteomics is to identify proteins from a biological sample using two-dimensional (2-D) separation prior to mass spectrometry of peptides generated via proteolytic digestion of the proteins. For 2-D separations, microfluidic devices are superior to bench top and capillary-based systems since they potentially provide higher separation efficiencies due to the minimal dead volumes produced during peak transfer between the two separation dimensions. In addition, fast separations can be envisioned because the column lengths are typically shorter in microfluidic platforms without scarifying peak capacity. High-throughput capabilities are extremely desirable for many types of bio-analytical analyses, such as understanding molecular interactions and the role they play in cellular functioning and drug discovery. Polymeric microchips possess a variety of physiochemical properties to match the intended application and their ease of fabrication increases the accessibility of technology to a large research base.

In this dissertation, a comprehensive 2-D separation platform for proteins using a polymeric microchip with the ability to perform high performance separations within a few minutes was established. The system combined sodium dodecyl sulfate micro-capillary gel electrophoresis (SDS μ-CGE) with micellar electrokinetic chromatography (MEKC) in a poly(methyl methacrylate), PMMA, microchip and was reported with a programmed pulse injection/separation protocol with laser-induced fluorescence for detection. A novel sixteen-channel polycarbonate (PC) microfluidic device for high-throughput separations of proteins was also presented using a process to pattern gold features as microelectrode array for sixteen parallel channels on microchips. The system was able to simultaneously analyze sixteen different samples in parallel consisting of native proteins, amino acids, peptides, and oligonucleotides with conductivity. Finally, due to the diverse nature of polymer properties and the large number of potential applications for microfluidic chips, the physiochemical properties of various polymers were investigated to guide researchers in selecting the best material for a given application including protein analysis.

CHAPTER 1

PROTEINS STRUCTURE AND ELECTROPHORESIS

1.1. Introduction to Proteins

1.1.1. Amino Acids

An amino acid is a molecule that contains both amine and carboxylic acid functional groups. Alpha amino acids represent those amino acids in which the amine and carboxylic acid groups are attached to the same carbon (i.e., α-carbon). The general structure of α-amino acids is shown in Figure 1.1, where R represents a side chain specific to each amino acid.

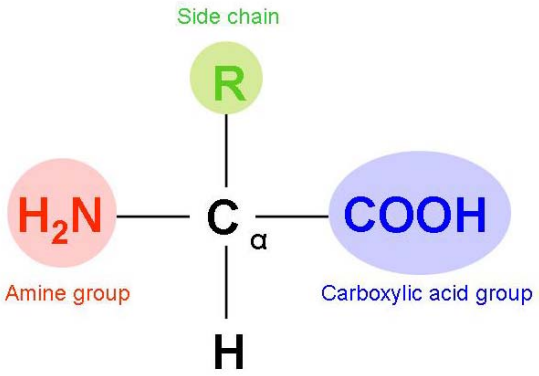

Figure 1.1. General structure of α-amino acids.

According to the properties of this side chain, amino acids can be classified into four groups. The side chain can make them acidic, basic, hydrophilic, if they are polar, and hydrophobic if they are non-polar. There are twenty standard amino acids used by cells in protein biosynthesis that are specified by the general genetic code.[1, 2] A list of standard amino acids, their chemical structures and side chain type is shown in Figure 1.2. Amino acids are the basic structural units of proteins. They form short polymer chains called peptides (see Section 1.1.2) or polypeptides, which in turn form structures called proteins (see Section 1.1.3).

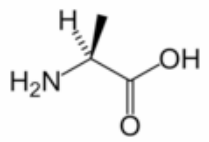

Alanine (Ala, A)

Hydrophobic

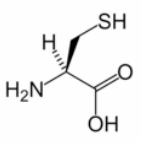

Cysteine (Cys, C)

Hydrophobic

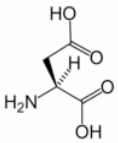

Aspartic acid (Asp, D)

Acidic

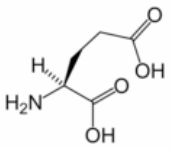

Glutamic acid (Glu, E)

Acidic

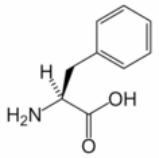

Phenylalanine (Phe, F)

Hydrophobic

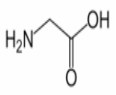

Glycine (Gly, G)

Hydrophobic

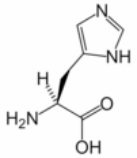

Histidine (His, H)

Basic

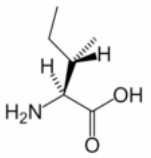

Isoleucine (Ile, I)

Hydrophobic

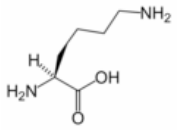

Lysine (Lys, K)

Basic

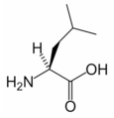

Leucine (Leu, L)

Hydrophobic

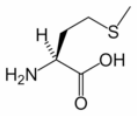

Methionine (Met, M)

Hydrophobic

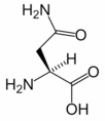

Asparagine (Asn, N)

Hydrophilic

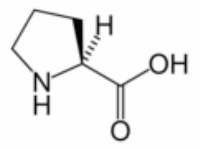

Proline (Pro, P)

Hydrophobic

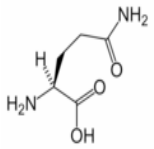

Glutamine (Gln, Q)

Hydrophilic

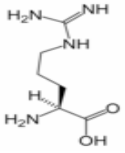

Arginine (Arg, R)

Basic

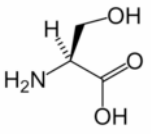

Serine (Ser, S)

Hydrophilic

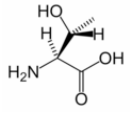

Threonine (Thr, T)

Hydrophilic

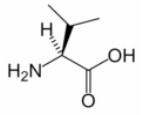

Valine (Val, V)

Hydrophobic

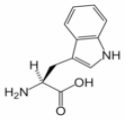

Tryptophan (Trp, W)

Hydrophobic

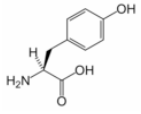

Tyrosine (Tyr, Y)

Hydrophobic

Figure 1.2. Standard amino acids and their side chain type.

1.1.2. Peptides

Peptide, a Greek term meaning “digestible”, is a family of short molecules formed from the linking of various α-amino acids. The link between one amino acid residue and the next one is through an amide bond, which is sometimes referred to as a peptide bond. As shown in Figure 1.3, a peptide bond is a chemical bond formed between two amino acid molecules when the carboxyl group of one molecule reacts with the amino group of the other molecule, releasing a molecule of water. This is called a dehydration synthesis reaction (also known as a condensation reaction).[3, 4]

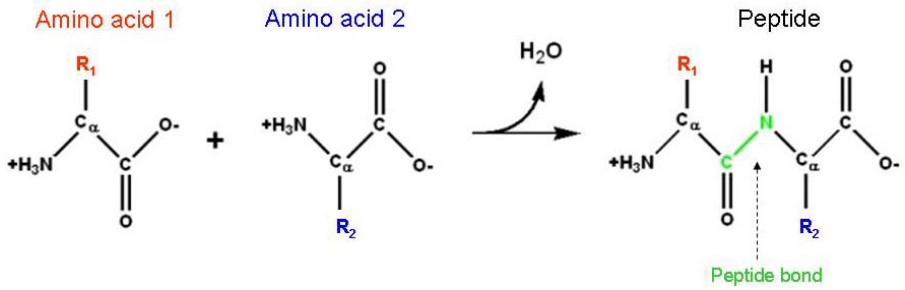

Figure 1.3. Formation of a peptide bond during a dehydration synthesis reaction between carboxyl (left) and amino (right) groups of two amino acid molecules.

1.1.3. Proteins

1.1.3.1. General Concepts

Proteins are bio-polymers made from amino acids arranged in a linear chain. The amino acids are linked together by peptide bonds as discussed previously. Once linked in the protein chain, an individual amino acid is often called a residue and the linked series of carbon, nitrogen, and oxygen atoms are known as the main chain or protein backbone. The name protein comes from the Greek term meaning "of primary importance" and was first described by Berzelius in 1838. Proteins are bio-polymers, whose amino acid sequence is specified by a gene encoded in the genetic code (see Section 1.1.3.2). Although this genetic code specifies twenty standard

amino acids (see Figure 1.2), the residues in a newly-synthesized protein are sometimes chemically altered in a process known as post-translational modification, (see Section 1.1.3.4), before the protein assumes its functional role in a cell. Similar to other biological molecules such as polysaccharides, lipids and nucleic acids, proteins are essential components of all living organisms. They are involved in every process within a living cell. Protein functions in biology will be reviewed in Section 1.1.3.5.

As discussed above, proteins are polypeptide molecules that consist of multiple polypeptide subunits. There are several different conventions to differentiate between peptides and proteins. One convention states that chains that are short enough to be made synthetically from the constituent amino acids should be called peptides rather than proteins. However, with the advent of better synthetic techniques, peptides as long as hundreds of amino acid residues can be made, including full proteins like ubiquitin. Chemical ligation has given access to the synthetic preparation of even longer proteins from peptide constituents, and so this convention is becoming out-dated.

Another convention places an informal dividing line at approximately 50 amino acid residues. However, this definition is somewhat arbitrary since some peptides, such as Alzheimer's beta peptide, can be considered a protein and some proteins, such as insulin, are close to the upper limit for peptides.[2-4]

1.1.3.2. Protein Synthesis

Deoxyribonucleic acid (DNA) and ribonucleic acid (RNA) are nucleic acid polymers consisting of nucleotide monomers. They consist of a pair of molecules, organized as strands running start-to-end and joined by hydrogen bonds along their lengths. Each strand is a chain of chemical building blocks, called nucleotides. There are four types of nucleotides in DNA

molecules including adenine (A), cytosine (C), guanine (G) and thymine (T). RNA contains uracil (U) and ribose rings unlike DNA, which contains deoxyribose and thymine.

Scientists for some time had suspected a link between DNA and proteins. Cells of developing embryos contain high levels of RNA. For example, rapidly growing *E. coli* has half its mass as ribosomes. Ribosomes are made of 2/3 RNA (a type of RNA known as ribosomal RNA or rRNA) and 1/3 protein. RNA is synthesized from viral DNA in an infected cell before protein synthesis begins. Information for protein synthesis in cell flows from DNA to RNA via the process of transcription, and thence to protein via translation as shown in Figure 1.4.

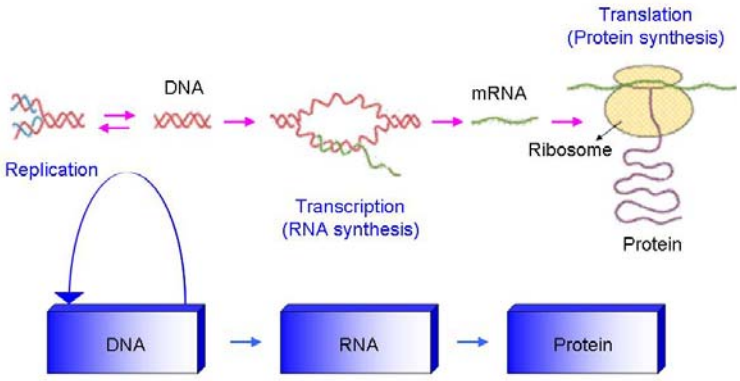

Figure 1.4. Simple scheme illustrating roles of DNA and RNA in protein synthesis. Transcription is the making of an RNA molecule off a DNA template. Translation is the construction of an amino acid sequence (polypeptide) from a messenger RNA (mRNA) molecule.

A brief explanation of protein synthesis in ribosomes during the translation step is shown in Figure 1.5. As shown in this figure, translation is the process of converting the mRNA codon (a sequence of three nucleotides in mRNA) sequences into an amino acid sequence. The initiator codon (i.e., AUG, the start command for protein synthesis) codes for the amino acid Met (see Figure 1.2). In other words, no transcription occurs without the AUG codon, and Met is always the first amino acid in a polypeptide chain, although frequently it is removed after translation.

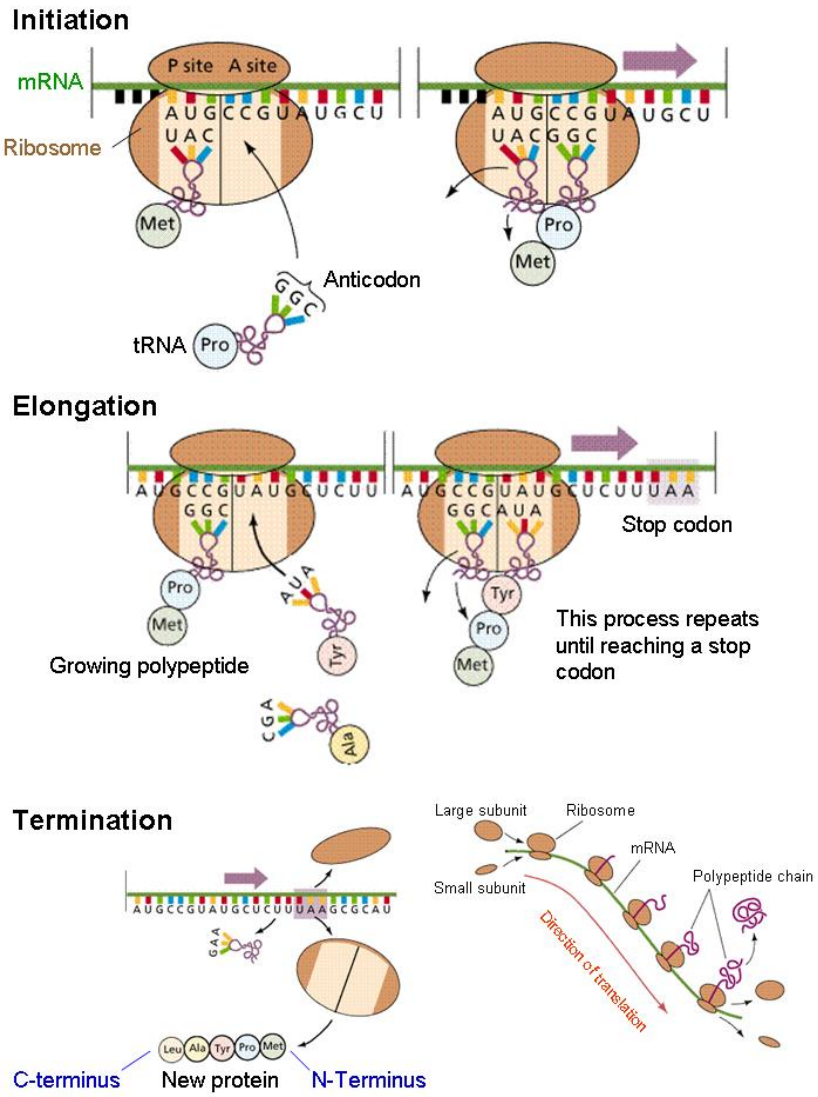

Figure 1.5. Phases involved in protein synthesis during translation process in a ribosome.

As shown in Figure 1.5, after the initiation phase the message gets longer during the elongation phase, which results in the growth of the polypeptide chain through the addition of amino acids. Next, the new tRNAs bring their amino acids to the open binding site on the ribosome/mRNA complex, forming a peptide bond between the amino acids. The complex then shifts along the mRNA to the next triplet, opening the A site. The new tRNA enters at the A site. When the codon in the A site is a termination codon, a releasing factor binds to the site, stopping

translation and releasing the ribosomal complex and mRNA. Therefore, translation in synthesis of proteins in ribosomes includes three phases including initiation, elongation and termination.[2-4]

The size of a synthesized protein is measured by the number of amino acids it contains and by its total molecular mass, which is normally reported in units of Dalton (Da). As an example, yeast proteins are on average 466 amino acids long and 53 kDa.[5] The largest known proteins are the titins, a component of the muscle sarcomere, with a molecular mass of almost 3,000 kDa and a total length of almost 27,000 amino acids.[6]

1.1.3.3. Protein Structure

Primary structure. The primary structure of proteins refers to the linear number and order of the amino acids present. The convention for the designation of the order of amino acids is that the N-terminal end (i.e., the end bearing the residue with the free α-amino group) is to the left (and the number one amino acid) and the C-terminal end (i.e., the end with the residue containing a free α-carboxyl group) is to the right.[2-4]

Secondary structure. The ordered array of amino acids in a protein confers regular conformational forms upon that protein. These conformations constitute the secondary structures of a protein. It is the partial double-bond character of the peptide bond that defines the conformations that a polypeptide chain may assume. Within a single protein, different regions of the polypeptide chain may assume different conformations determined by the primary sequence of the amino acids.

The α-helix is a common secondary structure encountered in proteins of the globular class.[2-4] The formation of the α-helix is spontaneous and is stabilized by hydrogen bonding between amide nitrogens and carbonyl carbons of peptide bonds spaced four residues apart. This orientation of hydrogen bonding produces a helical coiling of the peptide backbone such that the R groups lie on the exterior of the helix and perpendicular to its axis. Not all amino acids favor

the formation of the α-helix due to steric constraints of their R groups. Amino acids such as A, D, E, I, L and M (see Figure 1.2) favor the formation of α-helices, whereas, G and P favor disruption of the helix. This is particularly true for P, since it is a pyrrolidine-based imino acid (H–N=) whose structure significantly restricts movement about the peptide bond in which it is present, thereby, interfering with extension of the helix. The disruption of the helix is important as it introduces additional folding of the polypeptide backbone to allow the formation of globular proteins.

Whereas an α-helix is composed of a single linear array of helically disposed amino acids, β-sheets are composed of two or more different regions of stretches of at least 5 – 10 amino acids. The folding and alignment of stretches of the polypeptide backbone aside one another to form β-sheets is stabilized by hydrogen bonding between amide nitrogens and carbonyl carbons. However, the hydrogen bonding residues are present in adjacently opposed stretches of the polypeptide backbone as opposed to a linearly contiguous region of the backbone in the α-helix. β-Sheets are said to be pleated. This is due to positioning of the α-carbons of the peptide bond, which alternates above and below the plane of the sheet. β-Sheets are either parallel or anti-parallel. In parallel sheets, adjacent peptide chains proceed in the same direction (i.e., the direction of N-terminal to C-terminal ends is the same), whereas, in anti-parallel sheets, adjacent chains are aligned in opposite directions.[2-4]

Tertiary structure. Tertiary structure refers to the complete three-dimensional (3-D) structure of the polypeptide units of a given protein. Included in this description is the spatial relationship of different secondary structures to one another within a polypeptide chain and how these secondary structures fold themselves into the 3-D form of the protein. Secondary structures of proteins often constitute distinct domains. Therefore, tertiary structure also describes the relationship of different domains to one another within a protein. The interactions of different

domains are governed by several forces, such as hydrogen bonding, hydrophobic interactions, electrostatic interactions and van der Waals forces. Tertiary structure is largely maintained by disulfide bonds. Disulfide bonds are formed between the side chains of Cys (see Figure 1.2) by oxidation of two thiol (SH) groups to form a disulfide bond as shown in Figure 1.6.[2-4]

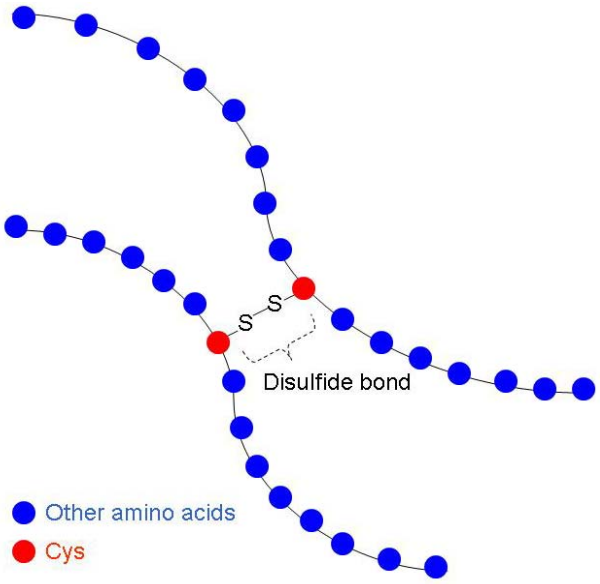

Figure 1.6. Formation of a disulfide bond (bridge) in a protein structure.

Quaternary structure. Many proteins contain two or more different polypeptide chains that are held in association by the same non-covalent forces that stabilize the tertiary structures of proteins. Proteins with multiple polypeptide chains are termed oligomeric proteins. The structure formed by monomer-monomer interaction in an oligomeric protein is known as its quaternary structure. Oligomeric proteins can be composed of multiple identical polypeptide chains or multiple distinct polypeptide chains. Proteins with identical subunits are termed homooligomers. Proteins containing several distinct polypeptide chains are termed heterooligomers.[7, 8] A simple illustration of protein structure is shown in Figure 1.7.

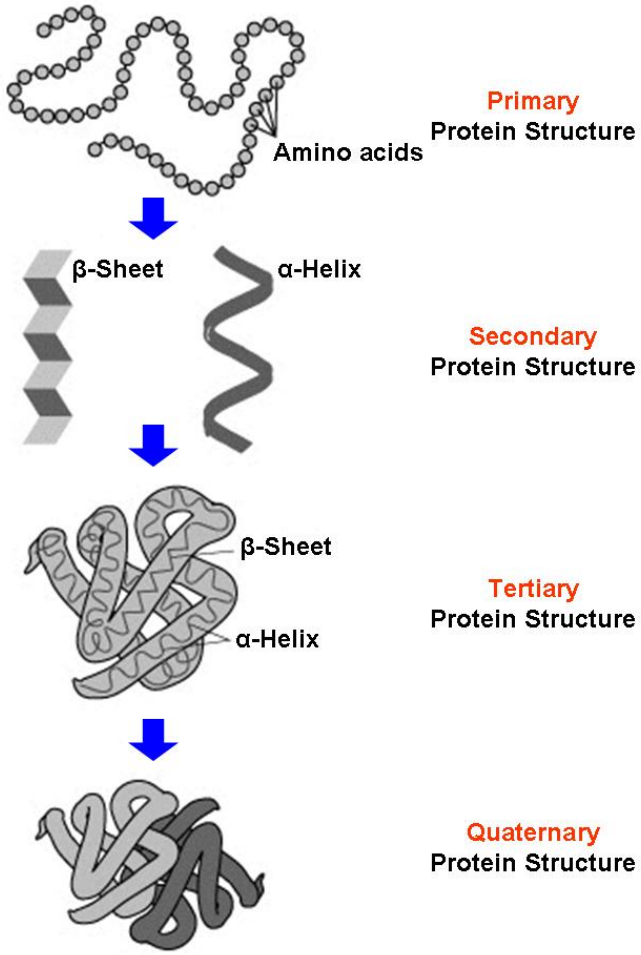

Figure 1.7. Illustrating different levels of protein structure.

1.1.3.4. Post-Translational Modification (PTM)

PTMs are the chemical modifications of a protein after it has been translated. PTM extends the range of functions of a protein by attaching to it other biochemical functional groups such as acetate, phosphate, various lipids and carbohydrates, by changing the chemical nature of an amino acid or by making structural changes. Furthermore, enzymes may remove amino acids from the amino end of a protein or cut the peptide chain in the middle. For instance, the peptide hormone insulin is cut twice after disulfide bonds are formed and a pro-peptide is removed from the middle of the chain. The resulting protein consists of two polypeptide chains connected by disulfide bonds. This phenomenon and other protein modifications are part of common

mechanisms for controlling the behavior of a protein or for activating or deactivating an enzyme.[9-11]

PTM is one of the lateral steps in protein biosynthesis for many proteins, which can determine its activity state, localization, turnover, and interactions with other proteins. In signaling, for example, kinase cascades are turned on and off by the reversible addition and removal of phosphate groups,[12] and in the cell cycle ubiquitination marks cyclins for destruction at defined time points.[13] Table 1.1 summarizes the features of important PTMs.[14]

Despite the great importance of PTMs for biological function, their study on a large scale has been hampered by a lack of suitable methods, and many key modifications have only been discovered late in the elucidation of various biological processes. As a result, we probably still do not realize the full extent and functional importance of protein modifications in the workings of the cell. Many PTMs have been discovered serendipitously during studies of individual proteins with the help of standard molecular techniques, such as deletion of the amino acids bearing the modification. Direct analysis of modifications requires isolation of the correctly processed protein in a sufficiently large amount for biochemical study.[11, 14]

As shown in Table 1.1, one of the most common PTMs in proteins is phosphorylation which will be explained in detail below. Addition of a phosphate group to a protein or a small molecule is called phosphorylation. In eukaryotes, protein phosphorylation is probably the most important regulatory event. Many enzymes and receptors are switched "on" or "off" by phosphorylation or de-phosphorylation. Phosphorylation is catalyzed by various specific protein kinases. Adding a phosphoryl group to a polar R group of an amino acid (see Figure 1.1) can actually turn a non-polar hydrophobic protein into an extremely hydrophilic molecule. Upon the deactivating signal, the protein becomes de-phosphorylated again and stops working.

Table 1.1. Most common and important types of PTMs of proteins.[14]

PTM Type	Stability*	Function and Notes
Phosphorylation		Reversible, activation / deactivation of enzyme activity, modulation of molecular interactions, signaling (see text for details)
pTyr	+ + +	
pSer, pThr	+ / + +	
Acetylation	+ + +	Protein stability, protection of N-terminus. Regulation of protein-DNA interactions
Methylation	+ + +	Regulation of gene expression
Acylation, fatty acid modification		Cellular localization and targeting signals, membrane tethering, mediator of protein-protein interactions
Farnesyl	+ + +	
Myristoyl	+ + +	
Palmitoyl	+ / + +	
Glycosylation		Excreted proteins, cell-cell recognition/signaling, reversible, regulatory functions
N-linked	+ / + +	
O-linked	+ / + +	
Glycosylphosphatidylinositol (GPI) anchor	+ +	GPI anchor, membrane tethering of enzymes and receptors, mainly to outer leaflet of plasma membrane
Hydroxyproline	+ + +	Protein stability and protein-ligand interactions
Sulfation (sTyr)	+	Modulator of protein-protein and receptor-ligand interactions
Disulfide bond formation	+ +	Intra- and inter-molecular crosslink, protein stability
Deamidation	+ + +	Possible regulator of protein-ligand and protein-protein interactions, also a common chemical artifact
Pyroglutamic acid	+ + +	Protein stability, blocked N-terminus
Ubiquitination	+ / + +	Destruction signal. After tryptic digestion, ubiquitination site is modified with the Gly-Gly dipeptide
Nitration of tyrosine	+ / + +	Oxidative damage during inflammation

* Stability: + Labile in mass spectrometry (MS), + + moderately stable in MS, + + + stable in MS.

It is estimated that 10% to 50% of proteins are phosphorylated (in some cellular stage). Since phosphorylation of any site on a given protein can change the function or localization

within a cellular compartment for that protein, understanding the state of a cell requires knowing the phosphorylation state of its proteins. Antibodies can be used as powerful tools to detect whether a protein is phosphorylated at any particular site. Such antibodies are called phospho-specific antibodies.[2-4, 11]

1.1.3.5. Protein Function

Proteins are the chief actors within the cell carrying out the duties specified by the information encoded in genes.[5] Proteins make up half the dry weight of an *E. coli* cell, while other macromolecules such as DNA and RNA make up only 3% and 20%, respectively.[15] One of the chief characteristic of proteins that enables them to carry out their diverse cellular functions is their ability to bind other molecules specifically. The region of the protein responsible for binding another molecule is known as its binding site. This binding ability is mediated primarily by the protein's tertiary structure (see Section 1.1.3.3), which defines the binding site pocket, and by the chemical properties of the side chains of the surrounding amino acids. Protein binding can be extraordinarily tight and specific, for example, the ribonuclease inhibitor protein binds to human angiogenin with a sub-femtomolar dissociation constant ($<10^{-15}$ M) but does not bind at all to its amphibian homolog onconase (dissociation constant >1 M). Extremely minor chemical changes, such as the addition of a single methyl group to a binding partner, can sometimes suffice to nearly eliminate binding. For example, the aminoacyl tRNA synthetase specific to the amino acid valine discriminates against the very similar side chain of the amino acid isoleucine. Proteins can bind to other proteins as well as to small-molecule substrates. When proteins bind specifically to other copies of the same molecule, they can oligomerize to form fibrils. This process occurs often in structural proteins that consist of globular monomers that self-associate to form rigid fibers. Protein-protein interactions also regulate enzymatic activity, control progression through the cell cycle, and allow the assembly of

large protein complexes that carry out many reactions with a common biological function. Proteins can also bind to, or be integrated into, cell membranes.

The best-known role of proteins in the cell is their duty as enzymes, which catalyze chemical reactions. Enzymes are usually highly specific catalysts that accelerate only one or a few chemical reactions. Enzymes affect most of the reactions involved in metabolism and catabolism as well as DNA replication, DNA repair, and RNA synthesis. Some enzymes act on other proteins to add or remove chemical groups in a process known as PTM as discussed previously. About 4,000 reactions are known to be catalyzed by enzymes. The molecules that bind and are acted upon by enzymes are known as substrates. Although enzymes can consist of hundreds of amino acids, it is usually only a small fraction of the residues that come in contact with the substrate and an even smaller fraction (typically 3-4 residues) that are directly involved in catalysis. The region of the enzyme that binds the substrate and contains the catalytic residues is known as the active site.[2-4]

Many proteins are involved in the process of cell signaling and signal transduction. Some proteins, such as insulin, are extra-cellular proteins that transmit a signal from the cell in which they were synthesized to other cells in distant tissues. Others are membrane proteins that act as receptors, whose main function is to bind a signaling molecule and induce a biochemical response in the cell. Many receptors are membrane proteins that have a binding site exposed on the cell surface and an effective domain within the cell. Antibodies are protein components of the adaptive immune system whose main function is to bind antigens or foreign substances in the body and target them for destruction. While enzymes are limited in their binding affinity for their substrates by the necessity of conducting their reaction, antibodies have no such constraints. An antibody's binding affinity to its target is extraordinarily high.

Many ligand-transport proteins bind small bio-molecules and transport them to other locations in the body of a multi-cellular organism. These proteins must have a high binding affinity when their ligand is present in high concentrations but must also release the ligand when it is present at low concentrations in the target tissues. The canonical example of a ligand-binding protein is hemoglobin, which transports oxygen from the lungs to other organs and tissues in all vertebrates and has close homologs in every biological kingdom. Transmembrane proteins can also serve as ligand-transport proteins that alter the permeability of the cell's membrane to small molecules and ions. The membrane alone has a hydrophobic core through which polar or charged molecules cannot diffuse. Membrane proteins contain internal channels that allow certain molecules to enter and exit the cell. Many ion channel proteins are specialized to select for only a particular ion, for example, potassium and sodium channels often discriminate for only one of the two ions.

Structural proteins confer stiffness and rigidity to other fluid biological components. Most structural proteins are fibrous proteins. For example, actin and tubulin are globular and soluble as monomers but polymerize to form long, stiff fibers that comprise the cytoskeleton, which allows the cell to maintain its shape and size. Collagen and elastin are critical components of connective tissue such as cartilage, and keratin is found in hard or filamentous structures such as hair, nails, feathers, hooves, and some animal shells. Other proteins that serve structural functions are motor proteins such as myosin, kinesin, and dynein, which are capable of generating mechanical forces. These proteins are crucial for cellular motility of single-celled organisms and the sperm of many sexually reproducing multi-cellular organisms.[2-4]

1.2. Proteomics

1.2.1. Background

Recent advances in human genome sequencing have brought many exciting opportunities to biological researchers. One of the great opportunities is proteomics, a contraction of PROTEin and genOMICS. Proteomes are the entire set of proteins expressed by cells of a certain organism at a certain point of time and, unlike genomes, are highly divergent between different cell types or tissues within the same organism. Proteomics is the study of the identity, structure and function of these proteins and how they interact with each other in cells, tissues or an organism at a given time or under certain environmental conditions.[16]

Now, it has become evident that the complexity of organisms is only to a small part the result of direct gene expression from the genome,[17-19] and it is also clear that the simple concept of one gene-one protein is incorrect. One important reason for this is that the product of one gene can be transformed to a whole family of gene products,[20, 21] i.e., one gene can produce multiple mature mRNAs via alternative splicing and other mechanisms.[22] Furthermore, the correlation between mRNA and protein concentrations has been demonstrated to be insufficient to predict protein expression levels from quantitative mRNA data, since protein levels are regulated by degradation as well.[23, 24] Although the correlation between mRNA levels and protein abundance is very good for a limited number of highly abundant proteins, it is poor for proteins with lower expression levels.[24] In this group, 30-fold differences in protein abundance are found for proteins with the same mRNA levels. Furthermore, PTMs produce further variations by increasing the number of components from the standard twenty amino acids to more than 140 possible amino acid forms.[11] These modifications undergo rapid changes and usually are not mutually exclusive.[14] Therefore, the study of the genome or even mRNA levels will reveal only a small spectrum of the response to a particular stimulus. In fact, even from the

diseases known to be based on specific genetic defects, only a very small number are likely to be monogenic, since cellular systems include complex interactions with a high level of redundancy.[25] Conversely, the function of a large number of the protein products that are encoded by these genes is still unclear.[26]

As a result, not only is it important for researchers to determine the identification and quantification of the proteome, but also to characterize its PTMs that can not be interrogated at the DNA or RNA level, understand the spatial distribution (compartmentalization) of its various constituents, measure half-lives, identify binding partners, determine various proteins 3-D structures, and finally define function of each protein (see Figure 1.8). Such information is necessary to secure for all proteins present in the proteome. As such, this ensemble of questions, and developments to address them, truly defines a new paradigm and a scientific field of proteomics.[27]

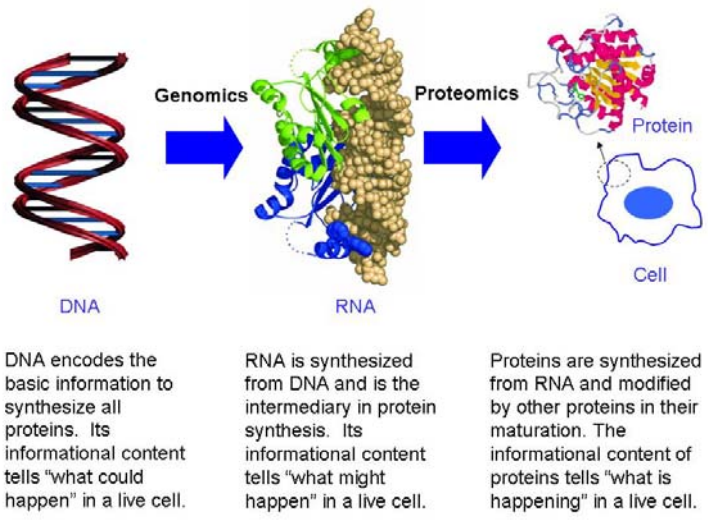

Figure 1.8. Correlation between genomics (DNA/RNA) and proteomics.

1.2.2. Challenges in Proteomics

From an analytical point of view, proteomics is a particularly challenging field. First, no amplification process, such as the polymerase chain reaction (PCR), exists in proteomic studies.

Thus, sensitivity and dynamic range are critical parameters, especially for low-abundant proteins and the large dynamic range of various proteins found in the cell. Usually, a cell can contain between one and more than 100,000 copies of a single protein.[28] It is now established that the dynamic range needed to analyze any proteome at the cellular level is $10^6 – 10^9$. For example, the concentrations of proteins in plasma vary from millimolar for albumin to around femtomolar for low-abundance components.[29-31] Therefore, if researchers try to identify proteins released in plasma, a dynamic range of 10^{12} may be required.[32] Furthermore, the proteome of organisms is dynamic and changes with environment and with time.[20]

Secondly, the proteome is very diverse. Proteins' size can range from a few tens of amino acids to several MDa, their isoelectric point, pI, (see Section 1.2.5.2, isoelectric focusing) can be as low as 3 or as high as 11, and for some proteins, their hydrophobicity can make them hardly recoverable in aqueous solutions or in gels.[33] From a quantitative point of view, there are at least 250 different types of human cells, each of which contains at least 2,000 – 6,000 different primary proteins,[34, 35] and PTMs are able to multiply this number.[14, 36-38] It has been estimated that the different types of human cells may differ from each other in ~400 unique proteins.[28] In fact, the complexity of proteomes is tremendous. For instance, if the number of human genes is about 30,000 – 50,000, and each gene gives 5 to 10 different proteins through differential splicing and PTMs, the analytical bio-chemist has to handle 150,000 – 500,000 different proteins in a single proteome, which is far beyond current analytical techniques. In order to study these proteins, considerable efforts and new technologies are required as we will discuss in the chapters of this dissertation.[27] Additionally, the amount of analyte that can be obtained is often limited especially in diagnostic applications.[27]

Typical samples in bio-medical fields are body fluids, such as plasma, urine, pleural fluid, pulmonary edema fluid, and cell lysates. These types of samples are complex mixtures of

proteins with a broad dynamic range of protein concentrations.[17, 21, 29] The expression and modification changes in low-abundant proteins (low copy number proteins, 10 – 1,000 copies per cell[26]) may be the most interesting ones. Their visualization is frequently obscured by highly expressed proteins (housekeeping proteins, ~10,000 copies per cell[26]). For example, plasma and pulmonary edema fluid contain large amounts of albumin (30 – 50 mg/mL in plasma and 20 – 25 mg/mL in pulmonary edema fluid) but comparatively small quantities of cytokines such as TNF-α or IL-1β (ng/mL to pg/mL range). Therefore, protein separation and purification techniques are key elements of proteome research that represent one of the major challenges.[34, 39, 40] Although the size of the proteome is unknown, the number of expressed proteins can be estimated from the open reading frames in a sequenced genome. It has been reported that 20% (1,484 proteins) from *Saccharomyces cerevisiae*[41] and ~61% of the predicted proteome of *Deinococcus radiodurans*[42] could be identified by a current multi-dimensional chromatography/MS approach. These results indicate that identification of a significant part of the proteome of a cell is feasible.

Other common problems in proteomics are more dependent on the individual sample and the specific techniques. The validity of the results of a proteomic experiment is dependent on the initial sample, the purity of cell and protein isolation, and the subsequent sample fractionation steps. Salts, mucus, and other contaminants may require purification procedures that lead to loss of proteins of interest. The presence of proteases in samples can cause additional cleavages of the investigated proteins, complicating protein identification and quantitation. Ongoing cellular protein synthesis and post-translational processing, by phospatases and kinases, for example, can influence the results as well.[21]

1.2.3. Approaches in Proteomics

Answering the multiplicity of questions and challenges raised by proteomics requires the development of new analytical tools and procedures, which in turn delineates some sub-fields such as profiling proteomics, functional proteomics and structural proteomics as shown below.

1.2.3.1. Profiling Proteomics

Profiling proteomics consists of identifying the protein present in a biological sample or the proteins that are differentially expressed between different samples. This approach is often used to make a list of proteins present in a sample and to discover proteins that are differentially expressed between different samples. Profiling proteomics can be performed to investigate the quality (i.e., expression proteomics) or quantity (i.e., quantitative proteomics) of protein samples.[43]

Protein profiling techniques take a global view at complex protein samples, such as plasma. Given the complexity of these samples, these techniques need to be streamlined to achieve high-throughput (see Chapter 5). The resulting protein patterns have diagnostic value as biomarkers on their own and indicate directions for more specific investigations. The application of protein profiling to tissue samples provides a combination of spatial information and protein profiles. The current results clearly indicate that these techniques are a valuable complement to histology. The continuing improvement in protein identification will provide further insights into pathological processes and will most likely be especially valuable in cancer research. The application of MS technology to the evaluation of protein modifications further extends the scope of proteomic analysis in depth. The physiological responses of an organism are only to a small part represented by changes in protein concentrations, especially, rapid responses to stimuli are transmitted by the modification of existing proteins. In spite of this complexity, this emerging field has, therefore, a large potential for clinically relevant research. Also, the

development of quantitative proteomics has widened the applicability of these techniques beyond a purely descriptive study design. Novel techniques in this field, namely differential gel electrophoresis (DIGE) and isotope-coded affinity tagging (ICAT), allow the direct comparison of samples, for example, of different disease states.[21] Because the profiling proteomics (especially expression proteomics) will be used in Chapter 4 of this dissertation, this technique will also be discussed in detail in Section 1.2.4.

1.2.3.2. Functional Proteomics

Functional proteomics studies the correlation of changes in the proteome with different states of the organism.[21] This approach attempts to discover protein functions based on the presence of specific functional groups or based on their involvement in protein-ligand interactions, such as protein complexes. Proteins need to interact with other molecules to perform their roles (see Section 1.1.3.5). Therefore, knowledge of interactions of a protein can help to discover its role in a cell. Similarly, pathways can be defined as a cascade of specific protein interactions required to activate cellular functions. PTMs such as phosphorylation, as discussed before, define the activity, localization and degradation of proteins and are key in understanding the functions of proteins in cells.[43]

1.2.3.3. Structural Proteomics

Finally, structural proteomics represents determining the tertiary structure (see Section 1.1.3.3) of proteins as well as the structure of protein complexes and small molecule-protein compounds. The x-ray crystallography and prediction of protein structures by computational biology are main methods used in this field of proteomics.[43]

1.2.4. Top-Down versus Bottom-Up Profiling Proteomics

Profiling proteomics traditionally have been divided into top-down and bottom-up approaches although there is some ambiguity about the usage of these two terms.[44] Both

approaches rely heavily on recent advances in MS.[45] The top-down techniques try to separate as many intact proteins as possible by techniques such as 2-D electrophoresis (see Chapter 4). Increased numbers of components are detected through increasingly complex fractionation of specimens before the final analysis and by increasing the number of dimensions (fractionation steps).[46] Bottom-up approaches start by breaking proteins with reagents, such as trypsin, into small peptides. The resulting peptides then are fractionated by chromatographic techniques and then analyzed by tandem MS instruments.[29, 47]

Top-down and bottom-up approaches each has advantages and disadvantages. Top-down approaches provide information about the variation, relative quantities and structures of the proteins that is lacking in the analysis of individual peptides in the bottom-up approach. As an example, analysis of plasma proteins by 2-D electrophoresis will yield multiple spots for most proteins, representing different PTMs, and spot intensities and positions provide information about abundance, molecular size, and pI. Bottom-up approaches exploit the higher chromatographic and MS resolution achieved for small peptides than for large proteins, and the sequence of small peptides can be determined in a very high-throughput fashion during analysis of peptides by this approach. Usually, this enables the sequence identification of a larger number of proteins than by the top-down approach, but the bottom-up approach does not identify what molecular form of the parent protein served as the source of the peptide. Sequence analysis by the top-down approaches tends to involve more laborious analysis of one protein at a time. Some of the top-down approaches, such as profiling by surface-enhanced laser desorption/ionization (SELDI) or matrix-assisted laser desorption/ionization time-of-flight (MALDI TOF) MS do not provide the sequence identification of peaks in an analysis.[29, 47] As a result, knowledge of variation, relative quantities and structures of proteins under proteomics

investigation is very important for clinical applications and this information can be obtained using a top-down approach.

1.2.5. Current Technologies in Top-Down Proteomics

The most traditional way to achieve top-down proteomics consists of protein extraction/preparation, protein separation, protein visualization and analysis, picking the protein spots to be analyzed, digestion of proteins and pooling of the released peptides, analysis of the peptide mass fingerprint for every digested protein using MS and matching peptide masses with protein databases to identify the proteins. Sometimes, further identification is necessary by acquisition of MS/MS spectra of selected peptides to confirm their sequences.[48, 49] An overview of the top-down proteomic strategy is shown in Figure 1.9.[48, 49] Each step will be discussed in detail below.

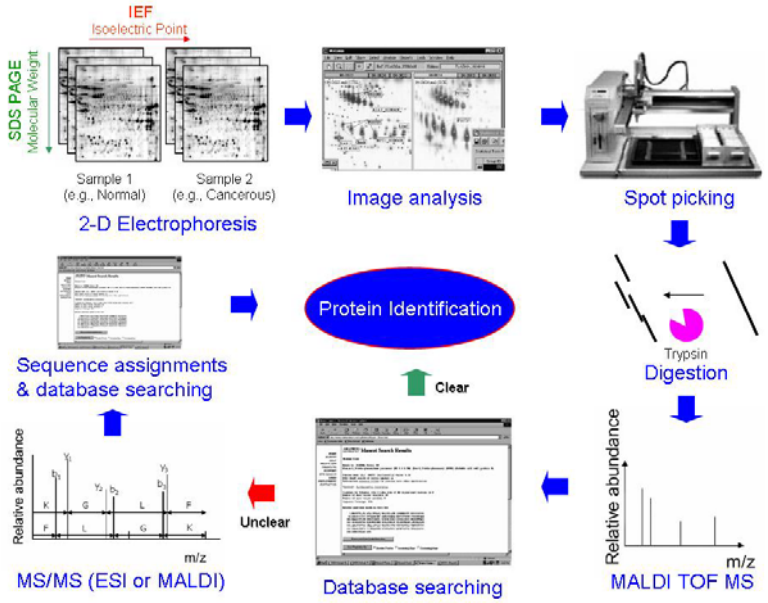

Figure 1.9. An overview of major steps in top-down proteomics strategy used to separate, analyze, identify and discover disease-associated proteins. Technology includes a separation step in which proteins of interest are separated by 2-D electrophoresis (see Section 1.2.5.2), protein visualization and image analysis, excising the protein spots to be analyzed, digestion of proteins and pooling of the released peptides, analysis of the peptide mass fingerprint for every digested protein using MALDI TOF MS, matching peptide masses against protein databases to identify proteins, and performing further identification (if necessary) by acquisition of MS/MS spectra of selected peptides to confirm their sequences.

1.2.5.1. Protein Extraction and Preparation

Protein extraction. Proteins can be obtained by lysis of cells. Cell disruption should be performed at cold temperatures. Cell disruption is often carried out in an appropriate solubilization solution for the proteins of interest.[50] The lysis methods include two categories, gentle lysis or vigorous lysis as discussed below.

The gentle lysis methods are generally employed when the sample of interest consists of easily lysed cells (such as tissue culture cells, blood cells and some micro-organisms). Gentle lysis methods can also be employed when only one particular sub-cellular fraction is to be analyzed. Most important gentle lysis methods include osmotic lysis,[51] freeze-thaw lysis,[50, 52, 53] detergent lysis[54, 55] and enzymatic lysis.[56, 57] Sometimes these techniques are combined (e.g., osmotic lysis following enzymatic treatment or freeze-thaw in the presence of detergent).

Vigorous lysis methods are employed when cells are less easily disrupted, for example, cells in solid tissues or cells with tough cell walls. These methods include sonication,[58-60] French pressure,[56, 57, 61] grinding,[59, 62-64] mechanical homogenization[51, 52, 65] and glass bead homogenization.[56, 57] Vigorous lysis methods usually result in complete disruption of the cells and care must be taken to avoid heating or foaming during these procedures.

Protection against proteolysis. When cells are lysed, proteases (enzymes that break peptide bonds in proteins) are often activated. Degradation of proteins through protease action greatly complicates the analysis of 2-D electrophoresis results, so actions should be taken to avoid this problem. If possible, inhibit proteases by disrupting the sample directly into strong denaturants such as 8 M urea, 10% trichloroacetic acid (TCA), or 2% sodium dodecyl sulfate (SDS).[66-68] Proteases are less active at lower temperatures, so sample preparation at low temperature is recommended. In addition, proteolysis can often be inhibited by preparing the sample in the presence of TRIS base, sodium carbonate or basic carrier ampholyte mixtures.[69, 70]

Precipitation procedure. Protein precipitation is an optional step in sample preparation for 2-D electrophoresis. Precipitation, followed by re-suspension in sample solution, is generally employed to selectively separate proteins in the sample from contaminating species such as salts, detergents, nucleic acids and lipids that would interfere with the 2-D result. Precipitation followed by re-suspension can also be employed to prepare a concentrated protein sample from a dilute source (e.g., plant tissues). No precipitation technique is completely efficient, and some proteins may not readily re-suspend following precipitation. Thus, employing a precipitation step during sample preparation can alter the protein profile of a sample. Precipitation and re-suspension should be avoided if the aim of a 2-D experiment is complete and accurate representation of all the proteins in a sample. If sample preparation requires precipitation, typically only one precipitation technique is employed. Most common protein precipitation techniques include ammonium sulfate precipitation,[71] TCA precipitation,[67, 72] acetone precipitation,[73] precipitation with TCA in acetone[59, 63, 66] and precipitation with ammonium acetate in methanol following phenol extraction .[74, 75] A review of precipitation techniques can be found elsewhere.[50, 71]

Protein purification. Because many components of biological samples interfere with 2-D analysis, it is necessary to remove them before study. Insoluble substances can be removed by centrifugation. For a 2-D electrophoresis followed by MS, it is necessary to remove salts before analysis. This can be achieved by dialysis, size exclusion filtering, protein precipitation or reverse-phase chromatography.[76, 77] Frequently, abundant proteins such as albumin or immunoglobulins need to be removed first.[29] Complex samples need to be fractionated before analysis to obtain simpler sub-fractions and to decrease the dynamic range of components, if possible.[29] Affinity purification is a powerful approach to reduce the complexity of a sample by specifically isolating individual proteins or protein complexes.[40] These preparation steps are

often more time consuming than the subsequent analysis steps and influence the sensitivity and discriminative power of MS-based protein identification.[77, 78]

1.2.5.2. Protein Separation

Electrophoresis. Electrophoresis is a class of separation techniques in which analytes are separated based on their ability to move through a conductive medium in response to an applied electric field. In the absence of other effects, cations migrate toward the electric field's negatively charged cathode, and anions migrate toward the positively charged anode. More highly charged ions and ions of smaller size, which means they have a higher charge-to-size ratio, migrate at a faster rate than larger ions, or ions of lower charge. Neutral species do not experience the electric field and remain stationary. As we will discuss later, under normal conditions even neutral species and anions migrate toward the cathode. In either case, differences in their rate of migration allow for the separation of complex mixtures of analytes.

In capillary electrophoresis (CE) the conducting buffer is retained within a capillary tube whose inner diameter is typically 25 – 200 μm. Samples are injected into one end of the capillary tube. As the sample migrates through the capillary, its components separate and elute from the column at different times. The resulting electropherogram looks similar to the chromatograms obtained in chromatography and provides both qualitative and quantitative information.[79, 80] A schematic of a CE instrument is shown in Figure 1.10.

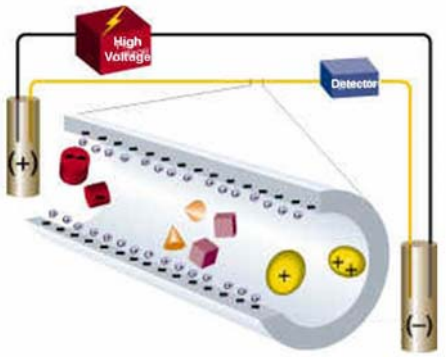

Figure 1.10. Diagram of a CE system.

When an electric field is applied to the capillary tube, the sample components migrate as the result of two types of mobility, electrophoretic mobility and electroosmotic mobility. Electrophoretic mobility is the solute's response to the applied electric field. As described earlier, cations move toward the negatively charged cathode and anions move toward the positively charged anode, and neutral species, which do not respond to the electric field, remain stationary. The other contribution to a solute's migration is the electroosmotic flow (EOF), which occurs when the buffer solution moves through the capillary in response to the applied electric field. Under normal conditions the buffer solution moves toward the cathode, sweeping most solutes, even anions, toward the negatively charged cathode. The velocity of a solute that moves in response to the applied electric field is called its electrophoretic velocity, v_{ep} which can be defined as:

$$v_{ep} = \mu_{ep} E \tag{1.1}$$

where μ_{ep} is the solute electrophoretic mobility, and E is the magnitude of the applied electric field. The electrophoretic mobility of a solute is defined as:

$$\mu_{ep} = q / (6\pi\eta r) \tag{1.2}$$

where q is the solute charge, η is the buffer viscosity, and r is the average solute radius. Since q is positive for cations and negative for anions, these species migrate in opposite directions. Neutral species, for which q is 0, have a $\mu_{ep} = 0$.

When an electric field is applied to a capillary filled with an aqueous buffer, we expect the buffer ions to migrate in response to their electrophoretic mobility. Because the solvent, H_2O, is neutral, we might reasonably expect it to remain stationary. What is observed under normal conditions, however, is that the buffer solution moves toward the cathode. This phenomenon is called the EOF. Electroosmosis occurs because the walls of the capillary tubing (glass or silica capillaries) are electrically charged. The surface of a silica capillary contains

large numbers of silanol groups (Si–OH). At pH levels greater than ~2, the silanol groups ionize to form negatively charged silanate ions ($Si–O^-$). Cations from the buffer are attracted to the silanate ions. Some of these cations bind tightly to the silanate ions, forming an inner or fixed layer. Other cations are more loosely bound, forming an outer or mobile layer. These two layers are called together the double layer. Cations in the outer layer migrate toward the cathode. Because these cations are solvated, the solution is also pulled along, producing the EOF.

Electroosmotic flow velocity (v_{eof}) is a function of the magnitude of E and the buffer solution's electroosmotic mobility, μ_{eof},

$$v_{eof} = \mu_{eof} E \tag{1.3}$$

Electroosmotic mobility is defined as:

$$\mu_{eof} = \varepsilon\zeta / (4\pi\eta) \tag{1.4}$$

where ε is the solution's dielectric constant and ζ is the zeta potential. Examining equations 1.3 and 1.4 shows that the zeta potential plays an important role in determining v_{eof}. Two factors determine the zeta potential and, therefore, v_{eof}. First, the zeta potential is directly proportional to the charge on the capillary walls, with a greater density of ions corresponding to a larger zeta potential. Second, the zeta potential is proportional to the thickness of the double layer. Increasing the buffer solution ionic strength provides a higher concentration of cations, decreasing the thickness of the double layer. The EOF profile is very different from that for a phase moving under forced pressure. It has a uniform and flat profile (see Section 2.3) that helps to minimize band broadening in CE, thus improving separation efficiency.

A solute's net or total velocity, v_{tot}, is the sum of its electrophoretic velocity and the electroosmotic flow velocity:

$$v_{tot} = v_{ep} + v_{eof} \tag{1.5}$$

and

$$\mu_{tot} = \mu_{ep} + \mu_{eof} \quad (1.6)$$

Under normal conditions the following relationships hold:

$v_{tot,\ cations} > v_{eof}$

$v_{tot,\ anions} < v_{eof}$

$v_{tot,\ neutrals} = v_{eof}$

Thus, cations elute first in an order corresponding to their electrophoretic mobilities, with small and highly charged cations eluting before larger cations of lower charge. Neutral species elute as a single band, with an elution rate corresponding to the electroosmotic flow velocity. Finally, anions are the last components to elute, with smaller and more highly charged anions having the longest elution time.[79, 80]

Joule heating. Power dissipation in the capillary has been known to cause heating of the electrolyte, a phenomenon often referred to as Joule heating.[81] The amount of heat generated in an electrical system can be simply calculated using the following equation:

$$J(t) = iVt = i^2Rt = (V^2t / R) = (V^2\sigma At /L) \quad (1.7)$$

where J is the heat generated (Joules) as a function of time (s), t, when a potential drop is applied across a capillary of resistance, R, area of cross-section, A, and length, L. This heat is dissipated across the capillary wall via natural or forced cooling.[81] It results from equation 1.7 that the problem of Joule heating gets worse with increasing capillary diameter, potential drop and time.

In the following sections, for the purpose of this dissertation, some methods of electrophoresis that will be used in this research are briefly discussed. Detail discussion of each method was out of focus of this dissertation and can be found in cited reviews at the end of each section.

Capillary zone electrophoresis (CZE). The separation mechanism in CZE is based on differences in the charge-to-mass ratio. Fundamentals to CZE are homogeneity of the buffer solution and constant E throughout the length of the capillary. Following the injection and application of voltage, the components of a sample mixture are separated into discrete zones as shown in Figure 1.11. More technical discussions can be found elsewhere.[82-84] The principle of migration and dispersion in CZE has been reviewed recently.[85]

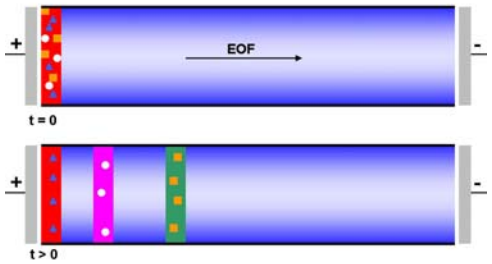

Figure 1.11. Schematic explanation of CZE separation. EOF is considered as driving force for current separation (normal-mode CZE).

In terms of protein separation, CZE has been a useful tool and a number of reviews have been published.[86-91] Understanding the electrophoretic properties of proteins in CZE is a challenge for theoretical protein chemistry. The current models rely on the primary amino acid composition of the protein and are good in estimating the effect of the molecular size on electrophoretic mobility. However, they are not able to determine the pK_a of the proteins.[92] Another technique currently used for a better understanding of protein ionization is based on behavior of protein charge ladders.[93, 94] In summary, proteins behave differently in CZE, in terms of separation efficiency than small molecules. The contribution of the length of the sampling zone of proteins to the final resolution has been studied.[95, 96]

Capillary electrochromatography (CEC). CEC is a hybrid separation method that couples the high separation efficiency of CZE with high performance liquid chromatography (HPLC), and

uses an electric field rather than hydraulic pressure to push the mobile phase through a packed or even an open tube (see Chapter 5). Since there is no back pressure, it is possible to use small diameter packing and thereby achieve very high efficiencies. An additional benefit of CEC compared to HPLC is the fact that the flow profile in a pressure driven system is parabolic, whereas in an electrically driven system it is linear (see Section 2.3) and therefore more efficient. Pretorius[97] first demonstrated the ability to use EOF in order to drive a mobile phase through a chromatography column. The advantages of using electrokinetic forces to push liquids through a packed bed are the same as in open capillaries, i.e., increased plate numbers as a result of the flat flow profile and the ability to use smaller particles leading to higher peak efficiency than is possible in pressure driven systems (i.e., HPLC).[98, 99]

The most promising developments in CEC rely on the use of monolithic stationary phases. For solid phase extraction (SPE), monomer solution is flowed into the capillary and polymerized in situ under UV light, which allows the precise localization of the solid phase within the flow stream. Critical parameters are (i) the pore size of the resulting monolith, so that fluid can be flowed easily through the bed, (ii) the surface charge of the monolith so that EOF can be generated, (iii) surface hydrophobicity, which can usually be easily achieved by using C8 or C18 functionalized co-monomers, and (iv) sticking of the monolith on the capillary walls, so that the stationary phase is not removed while the capillary is washed or reconditioned.[27]

Despite intensive work in the development of monolith or sol-gel solid phases for separations, very few studies have focused on peptide or protein separations. Most of the studies have focused on separation of drugs or neutral molecules using these materials. However, this approach is promising due to its ease of implementation in capillaries and the separation performances that are satisfactory.[27] This separation technique is recently reviewed in the literature either in general[99-108] or for proteins.[109-111]

Micellar electrokinetic chromatography (MEKC). Perhaps the most exciting mode of CE is MEKC (also called MECC). The use of micelle-forming surfactant solutions gives rise to separations that resemble reverse-phase liquid chromatography (RP-LC) with the benefits of CE. Micelles are amphiphilic aggregates of molecules known as surfactants. They are long chain molecules (10 – 50 carbon units) and are characterized as possessing a long hydrophobic tail and a hydrophilic head group. Normal micelles are formed in aqueous solution with the hydrophobic tails pointing inside micelles and the hydrophilic heads pointing outside into the aqueous solution. Micelles form as a consequence of the hydrophobic effect, that is, they form to reduce the free energy of the system. The hydrophobic tail of the surfactant cannot be solvated in an aqueous solution. Above a surfactant concentration known as the critical micelle concentration (cmc), the aggregate is completely formed. Physical changes such as surface tension, viscosity and the ability to scatter light come with micelle formation.

There are four major classes of surfactants: anionic, cationic, zwitterionic and nonionic. Examples of each group are shown in Table 1.2. Both synthetic and natural surfactants have been employed for MEKC separations. Synthetic components include anionic SDS and cationic cetyltrimethylammonium bromide (CTAB). Natural compounds such as bile salts (e.g., sodium taurocholate) are also useful.

SDS is the most widely used surfactant in MEKC (see Chapters 3 and 4). It is available in highly purified form and is inexpensive. Micelles have the ability to organize analytes at the molecular level based on hydrophobic and electrostatic interactions. Even neutral molecules can

Table 1.2. Major classes of surfactants.

Surfactant*	Type	cmc (M)	Aggregation Number
SDS	Anionic	8.3×10^{-3}	62
CTAB	Cationic	9.2×10^{-4}	170
Brij-35	Nonionic	1.0×10^{-4}	40
Sulfobetaine	Zwitterionic	3.3×10^{-3}	55

* Brij-35: polyoxyethylene-23-lauryl ether,
Sulfobetaine: N-dodecyl-N,N-dimethylammonium-3-propane-1-sulfonic acid.

bind to micelles since the hydrophobic core has very strong solubilizing power. Surfactant solutions have been employed in spectroscopy and chromatography to take advantage of these unique micellar properties. For example, room temperature phosphorescence is readily observable in micellar media since the micellar environment prevents many of the normal quenching mechanisms from operating. More significantly with regard to MEKC, these surfactant solutions can serve as chromatographic mobile phase modifiers. Micellar chromatography can mimic RP-LC. The analyte can partition between the micelle and the bulk phase, the micelle and the stationary phase, or the bulk and stationary phase. Therefore, "pseudo-phase" or micellar LC has more complex equilibria than conventional LC. This three-phase equilibrium can be likened to ion-pair chromatography in many cases. The complicating factor in MEKC is that analyte electrophoretic mobility often contributes to the overall separation. At neutral to alkaline pH, a strong EOF moves in the direction of the cathode. If SDS is employed as the surfactant, the electrophoretic migration of the anionic micelle is in the direction of the anode. As a result, the overall micellar migration velocity is slowed compared to the bulk flow of solvent. Suppressing EOF is one way to perform fast MEKC separations that will be discussed in Chapters 3 and 4. When an analyte is associated with a micelle, its overall migration velocity is reduced. When an uncharged analyte resides in the bulk phase, its migration velocity is that of the EOF. Therefore, analytes that have greater affinity for the micelle have slower migration velocities compared to analytes that spend most of their time in the bulk phase. When using a cationic surfactant, the EOF is reversed, therefore, the electrode polarity must also be reversed to detect the analyte. A schematic of MEKC is shown in Figure 1.12. Detail review of MEKC separation techniques can be found in literature.[112-126] There is also one review for MEKC of proteins.[127]

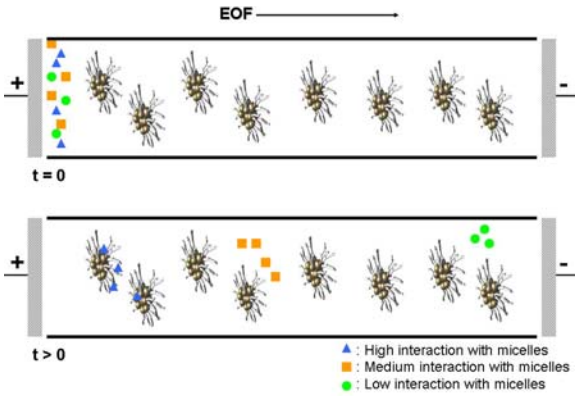

Figure 1.12. Schematic of MEKC separation. EOF is considered as driving force for this MEKC.

Isoelectric focusing (IEF). IEF is an electrophoresis method that is usually used for protein separation. It separates proteins according to their pI. Proteins are amphoteric molecules. They carry either positive, negative or zero net charge, depending on the pH of their surroundings. The net charge of a protein is the sum of all the negative and positive charges of its amino acid and carboxylic acid side chains (see Figure 1.1). The isoelectric point is the specific pH at which the net charge of the protein is zero. Proteins are positively charged at pH values below their pI and negatively charged at pH values above their pI. The presence of a pH gradient is critical to the IEF technique. In a pH gradient, under the influence of an electric field, a protein will move to the position in the gradient where its net charge is zero. A protein with a positive net charge will migrate toward the cathode, becoming progressively less positively charged as it moves through the pH gradient until it reaches its pI and vice versa for proteins with negative net charges. If a protein should diffuse away from its pI, it immediately gains charge and migrates back. This is the focusing effect of IEF, which concentrates proteins at their pIs and allows proteins to be separated on the basis of very small charge differences. IEF is performed at high voltages (typically in excess of 1,000 V). IEF performed under denaturing conditions gives the highest resolution. Commercial carrier ampholyte mixtures are comprised of hundreds of

individual polymeric species with pIs spanning a specific pH range. When a voltage is applied across a carrier ampholyte mixture, the carrier ampholytes with the highest pI (and the most negative charge) move toward the anode and the carrier ampholytes with the lowest pI (and the most positive charge) move toward the cathode. The other carrier ampholytes align themselves between the extremes, according to their pIs, and buffer their environment to the corresponding pHs. The result is a continuous pH gradient. A schematic of IEF is shown in Figure 1.13. Detail of IEF separation is out of the focus of this dissertation and can be found in the literature.[128-130] The application of IEF for separation of proteins is also reviewed by several people.[131-136]

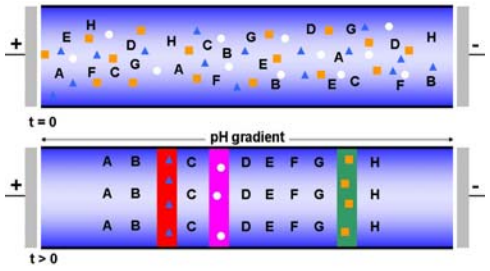

Figure 1.13. Schematic of IEF separation. Letters A to H refer to buffer with different pH gradients.

Gel-based electrophoreses. Traditional gel electrophoresis is carried out in an anti-convective medium such as polyacrylamide or agarose. The composition of the media also serves as a molecular sieve to perform size separations. Furthermore, the gel suppresses the EOF and minimizes the Joule heating. There are two fundamental classes of gels that can be employed in a gel-based electrophoretic separation. The "physical gel" obtains its porous structure by entanglement of polymers and is quite rugged to changes in the environment. Hydroxy-propylmethylcellulose and similar polymers can be used to form physical gels. On the other hand, "chemical gels" use covalent attachment to form their porous structure. These gels are less rugged, and it is difficult to change the running buffers once the gels are formed. In gel-based

CE, the capillary is usually filled with a physical gel by pressure. In each category, different types of gels can be used, which are reviewed in literature.[137]

Capillary gel electrophoresis (CGE) is typically performed in 50 – 200 μm capillaries in lengths of about 30 cm to 1 m. Better resolution is found for the longer capillaries, but the run times are long. The capillary gel composition is manipulated to optimize the resolution. For example, increasing the gel concentration improves resolution but decreases the molecular weight range accessible within the run. The voltage is somewhat limiting since field strengths above 500 V/cm may cause capillary heating and, finally, voids (see Chapter 4).

SDS polyacrylamide gel electrophoresis (SDS PAGE) is the most famous gel-based electrophoresis method for separating proteins according to their molecular weights (MW). This separation technique is performed in polyacrylamide gels containing SDS. The intrinsic electrical charge of the sample proteins is not a factor in the separation due to the presence of SDS in the sample and the gel. SDS and proteins form complexes with a necklace-like structure composed of protein-decorated micelles connected by short flexible polypeptide segments.[138] The result of the necklace structure is that large amounts of SDS are incorporated in the SDS-protein complex in a ratio of approximately 1.4 g SDS / g protein. SDS masks the charge of the proteins themselves and the formed anionic complexes have a roughly constant net negative charge per unit mass. Besides SDS, a reducing agent (e.g., 2-mercaptoethanol, see Chapter 4) is also added to break any disulfide bonds (see Section 1.1.3.3) present in the proteins. When proteins are treated with both SDS and a reducing agent, the degree of electrophoretic separation within a polyacrylamide gel depends largely on the MW of the proteins. In fact, there is an approximately linear relationship between the logarithm of the molecular weight and the relative distance of migration of the SDS-polypeptide complex (see Chapter 4). This linear relationship is only valid for a certain molecular weight range, which is

determined by the polyacrylamide percentage. The logarithm of the mobility versus the percent monomer composition (%T) of the gel is also linear. TRIS-containing buffers are the most commonly used buffer systems for SDS PAGE.[139, 140] This buffer system separates proteins at high pH, which confers the advantage of minimal protein aggregation and clean separation even at relatively heavy protein loads. A typical system for SDS PAGE separation is shown in Figure 1.14.

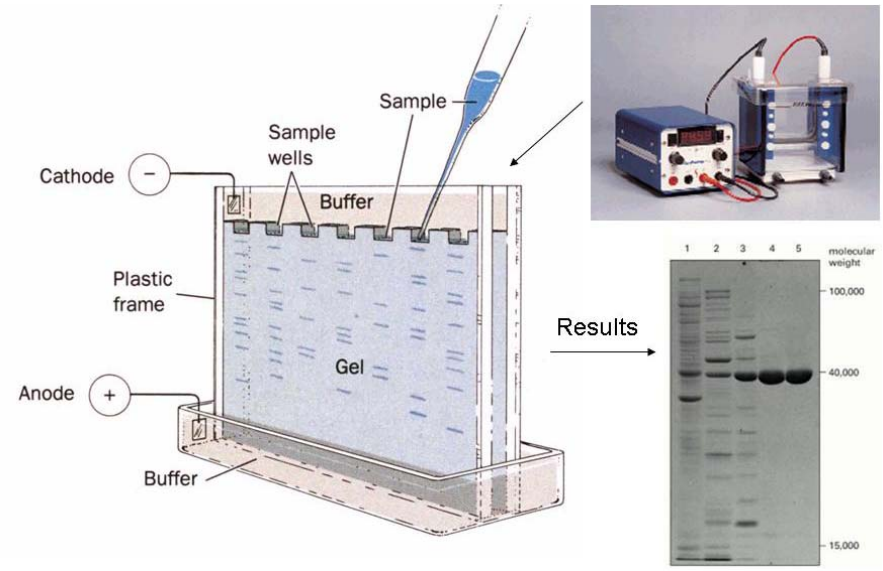

Figure 1.14. A typical SDS PAGE system used in laboratories.

Two-dimensional (2-D) versus one-dimensional (1-D) electrophoresis. The obtained peak capacities (the maximum number of compounds that can be resolved in a separation, see Chapter 4) of a 1-D separation technique are in the range of 150,[141] which is far from the required peak capacity in proteomics. Whereas a 1-D separation technique may be sufficient to map a single protein peptide digest (a few tens of peptides), it is likely that a five protein digest is already beyond the resolving power of most 1-D separation techniques. As first mentioned by Giddings,[142] the peak capacity of orthogonal separations (i.e., uncorrelated in their separation mechanism, see Chapter 4) is the product of individual peak capacities, so that the coupling of two 1-D separations can easily reach a peak capacity in the thousand range, which is best suited

to proteomic samples.[27] A comprehensive explanation of 2-D separation of proteins will be discussed in Chapter 4.

Historical perspective of 2-D separation techniques. Although the initial implementation of high-resolution 2-D is attributed to O'Farrell in 1975,[143] the original concept of 2-D protein separation by electrophoresis was proposed by Smithies and Poulik in 1956.[144] They recognized that "a combination of the two electrophoretic processes on a gel at right angles should therefore give a much greater degree of resolution than is possible with either separately." The two modes of resolution were (i) molecular size and (ii) free solution mobility on a starch gel. Five years later, Raymond[145] who named his 2-D experiments "orthogonal gel electrophoresis or orthacryl" realized that the combination of electrophoretic and molecular filtration produces new resolutions that could not be obtained by other electrophoretic procedures. Laurell, in 1965[146] devised a 2-D procedure for the separation of serum proteins whereby electrophoresis on an agarose gel was used in the first dimension, and affinity electrophoresis in the second dimension. 2-D IEF/SDS PAGE became the method of choice for biologists after its introduction by O'Farrell[143] for the separation of cellular proteins under denaturing conditions. The principle of 2-D IEF/SDS PAGE is resolution of proteins based on their pI in the first dimension and molecular mass in the second dimension (see previous sections for detail of each separation technique). Despite its limitations as will be discussed later, 2-D IEF/SDS PAGE is still the most widely used 2-D separation technique for the analysis of complex protein mixtures.

Common 2-D separation technique for top-down proteomics. IEF/SDS PAGE or simply called 2-D PAGE,[21, 28, 143, 147-160] has been the major method for the investigation of proteomes for a long time. As mentioned in the previous section, this method provides high resolution for the separation of complex protein mixtures.[142, 161] As shown in Figure 1.15, IEF/SDS PAGE combines two separation techniques, IEF and SDS PAGE that were discussed previously. As

shown in this figure, in this 2-D separation, proteins are separated in the first step (i.e., first dimension) based on their pI using an IEF separation in a gel media. This process is performed in an IEF unit (see Figure 1.15), which always has a flat geometry. This process usually takes between 2 h to 72 h depending on gel size, geometry and also separation parameters. Then, the IEF gel will be transferred to a second separation unit as shown in the figure to perform the SDS PAGE separation. This unit can be flat or vertical and usually takes between 1 h to 5 h. In this step, the unresolved protein spots in IEF will be separated based on their MW. The overall separation efficiency is therefore increased by coupling these separation techniques.

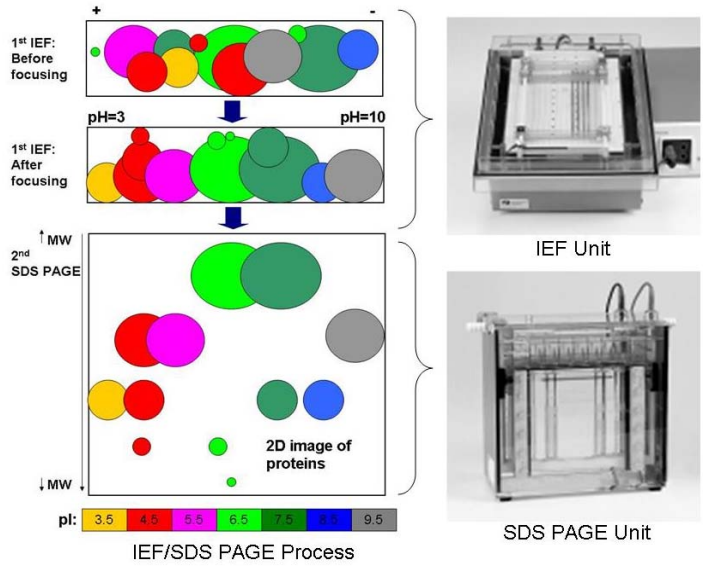

Figure 1.15. Conventional IEF/SDS PAGE technique for high efficiency separation of proteins.

Column-based 2-D separations. Recently, several efforts have been performed to couple two capillaries for performing a 2-D separation that will be discussed in Chapter 4. Basically, an increase in selectivity of a column-based 2-D system can only be obtained when the dimensions are based on different separation mechanisms. The second dimension of a 2-D separation system should not destroy the resolution achieved by the previous one.[142] Adequate interfacing is needed to transport the various fractions from the first to the second dimension. The interfacing

for column-based 2-D separation systems can be performed in various ways. The effluent of the first separation system can be transported to the next system manually (off-line) or automatically, e.g. with the aid of a robot (at-line), or via connecting tubing or a valve that directly transports a stream of liquid to the next system (on-line). In general, the on-line combination of separation systems enables a significantly faster analysis of a complex matrix in comparison with an off-line or at-line combination. In an on-line interface in a 2-D system, a loop or a column is generally used to trap a fraction of interest, where a switching valve is employed to inject this fraction into the next separation step.[162] If the separation of the complete sample in all dimensions is achieved, the system is considered to be completely 2-D or "comprehensive".[163] In this case the time required for performing a separation in the second dimension must be the same as for example filling a loop with effluent from the first dimension. Such a comprehensive on-line system can only be designed by making adjustments in the analytical dimensions (e.g., flow rates and column dimensions) of the system components, because the second dimension separations have to be performed much faster. An important reason for the development of comprehensive 2-D separation methods is the challenge to establish protein profiles of cells and other biological samples.[164]

If a coupled system separates only a fraction, retrieved from the first dimension, in the second dimension it is called a "heart-cut" 2-D system.[162] These systems are not comprehensive however such separations are important for the determination of closely related peptides and proteins in biological samples such as plasma and tissues, which require analytical methods with high selectivity and sensitivity. Heart-cut 2-D systems often offer sufficient selectivity and sensitivity for the assay of these compounds in a relatively short time.[165, 166,167-171]

1.2.5.3. Visualization and Evaluation of 2-D Results

For visualization, proteins in the gel are stained using a variety of different methods. A synopsis of the most widely employed staining methods is given in Table 1.3.[21] As examples, with the use of these staining methods, gel maps of body fluids such as human plasma[172-174] or bronchoalveolar lavage (BAL) fluid,[175, 176] have been reported. As discussed before, the large number of spots in a 2-D gel is partly due to PTMs of proteins, therefore, one protein may be present in several locations in the gel.[26] Although this phenomenon is potentially useful for further analysis of these modifications, the increased number of spots for analysis can lead to additional effort since >25% of the spots on one gel may be due to modified proteins[177] found elsewhere on the gel. The large number of protein spots in complex samples makes computer-assisted image analysis necessary. Digital image analysis is also needed for quantitative information. There are several image collection hardware and software suites for this purpose that are commercially available. In modern proteomics, IEF/SDS PAGE is most often used as a step before protein detection techniques especially MS. However, although it has been shown that MS can detect serially diluted and gel-embedded proteins down to the very low femtomole range,[178, 179] generally 5 – 50 ng (corresponding to 100 – 1,000 fmol for a 50 kDa protein, an amount visible by silver staining) are considered necessary for successful MS identification of proteins. Important reasons for this problem are the dynamic range of the current staining procedures (see Table 1.3) and poor recovery of the peptides from the gels. It has also been shown that in IEF/SDS PAGE, several classes of proteins are systematically underrepresented. This limitation is relevant for many of the potential proteins of interest in pulmonary research.[180-186] These weaknesses are constantly motivating efforts to improve 2-D techniques and to find alternative methods (e.g., microchip-based 2-D techniques) to supplement or replace it as will be discussed in the next chapters.[43]

Table 1.3. Different staining methods for 2-D electrophoresis.[21]

Stain	Sensitivity (g of protein)	Dynamic Range	Visualization	Price	Compatibility with MS	Advantages	Disadvantages
Silver staining	10^{-9}	10 fold	Visual	$$	Not good	- Sensitivity - Inexpensive - Ease of use	- Certain proteins stain Poorly - Complex and time consuming
Coomassie blue	10^{-8}	10 fold	Visual	$	Good	- Fast - Ease of use	- Sensitivity
Colloidal coomassie staining	10^{-8}	10 fold	Visual	$$	Not good	- Fast - Ease of use	- Sensitivity
Radioactive gel visualization	10^{-10}	4,000 fold	Photography	$$$$	Good	- Application of several samples to the same gel - Can be combined with other staining methods	- Radioactivity - Complex and time Consuming, - Visualization requires equipment
Fluorescence detection systems	10^{-9}	1,000 fold	Photography	$$$	Good	- Relatively fast - Good reproducibility and dynamic range	- Visualization requires equipment
Differential gel electrophoresis	10^{-5}-10^{-9}	10,000 fold	Ozone-free Xenon lamp	$$$	Not good	- Application to up to three samples on the same gel - Very small variability with different gels and operators - Better correlation between spot density and protein content than silver staining	- Can cause changes in protein migration in isoelectric focusing - Visualization requires equipment

1.2.5.4. Further Analysis of Protein Spots

Background. Traditionally, protein patterns in 2-D PAGE were identified by matching with a master 2-D PAGE pattern (e.g., SWISS-2D PAGE), with reference proteins[159, 175, 176, 187] or with Western immunoblots.[188] Important progress in the identification of gel spots was made by the

development of automated NH_2-terminal (Edman) sequencing used in a large number of studies.[187, 189-191] Later, MS has rapidly replaced Edman sequencing for protein identification due to faster analysis times and much higher sensitivity.[154, 192, 193]

MS provides highly accurate measurements of the molecular weight and charge of the proteins or peptides in a sample. In addition, with the use of enzymatic digestion and peptide mass fingerprinting (see below), proteins can be identified. By adding a second mass analyzer (tandem mass spectrometry or MS/MS), the amino acid sequence of peptides can also be determined directly due to the fact that peptides create fragments in a predictable fashion.[194] After acquisition, the data are interrogated against protein sequence databases in an automated fashion[181, 195] or interpreted manually.[154, 196, 197] An overview of mass spectrometers currently being used for protein identification is provided in Table 1.4.[21]

Protein identification. Mass measurements of the intact proteins provide a mass balance and rapid and valuable information on the protein profile of a sample. It is, however, not practical to attempt to identify a protein solely on the basis of its mass-to-charge ratio. This is mainly due to splice and sequence variation from database entries combined with a heterogeneous set of PTMs, which lead to variable differences in the molecular weight of a protein compared with the theoretical mass derived from the database. Therefore, additional strategies have been developed for protein identification, and these can be used separately or in combination.[21]

Peptide mass fingerprinting is based on mass measurements of peptide fragments derived from a single protein. Before mass spectrometry, spot of proteins of interest (or all spots) are picked using a spot picker that is shown in Figure 1.16. Next, the picked proteins are cleaved into peptides at specific and reproducible points in their amino acid sequence using chemical agents or proteases. A protein covalent modification will only be reflected in one or a few of the peptide mass values, whereas the rest will remain unchanged. Because of its highly reproducible

Table 1.4. Overview of different MS techniques used in proteomics.[21]

Technique	Description	Advantages	Limitations
Electrospray ionization (ESI)	- Proteins are solubilized and ionized at atmospheric pressure by pumping the solute through a capillary at high voltage - As the micromolar-sized droplets enter the mass spectrometer, solvent is removed by heat or energetic collisions with a gas and impart charge onto analyte molecules - Proteins and peptides acquire multiple charge state	- Can be interfaced online with chromatographic separations - More accurate than MALDI	- More susceptible to contamination - Capillary can become blocked - Requires more maintenance
MALDI (MALDI TOF)	- The sample is co-crystallized with the matrix on a metal slide (target) - The target is positioned in front of the ion source - A laser pulse irradiates each spot, causing a rapid excitation of the matrix - The ions are accelerated by an electric field that directs them toward a mass detection unit	- Sensitivity in combination with a TOF analyzer - A mass accuracy of a few parts per million can be obtained with internal calibration - MALDI is most often coupled with TOF analyzers, which are highly sensitive and have a wide mass range - Robustness to low levels of salts and buffers - Spectra are relatively easy to interpret	- Fragmentation of singly charged peptides can be less informative
SELDI	- Modification of MALDI, in which the target is a protein chip array composed of various chromatographic, immunologic or enzymatic surfaces - Several different probe surfaces are available - Using different chip arrays, SELDI can be modified for use with proteins of cationic, anionic, hydrophobic, hydrophilic and other properties	- For surface-enhanced affinity capture, a 100-fold dynamic range was reported - May be useful in the high-throughput discovery of new drug targets and biomarkers	- Difficult to identify the proteins that contribute to the mass profile - Peptide fingerprinting and MS/MS requires purification and enzymatic digestion steps that are difficult to integrate with this approach
Imaging mass spectrometry (IMS)	- IMS utilizes MALDI MS for the direct analysis of tissue samples - A slice of frozen tissue is coated with crystallization matrix or the tissue is blotted on a target coated with C18 beads	- Successfully used to identify disease markers - IMS generates ion images of samples and maps them to the original sample, combining spatial information of peptide/ protein distributions	- Difficult to identify proteins in the profile - Potential overlay of different cell layers in tissue specimens

cleavage on the COOH-terminal side of arginine and lysine residues (see Figure 1.2), trypsin is the proteolytic enzyme that is used most often. With the use of this specificity, the anticipated mass values of all peptides in virtual digests of all proteins in the database are calculated. The protein identity is determined by comparing the measured peptide mass values with those calculated.[186, 192, 198-201] The reliability of peptide mass fingerprinting is dependent on the mass accuracy of the peptide measurements,[192] the number of matched versus unmatched peaks in the spectrum, the number of peptides that could be matched to a single protein, and the number of proteins that are present in the digested sample. With the use of two sequential mass analyzers (i.e., MS/MS), primary structural analysis of the amino acid sequence can be obtained by fragmenting one or more of the peptides.[193, 194, 197, 202]

Figure 1.16. Photograph of a spot picker instrument which is used to select and pick the protein spots appeared in a 2-D PAGE (Reproduced from http://www1.amershambiosciences.com).

Protein profiling techniques. Protein profiling is the rapid screening of samples by MS with limited or no sample preparation. The resulting profile of mass-to-charge ratio peaks of different samples (that can be body fluids, cell lysates or even tissue samples) can then be compared, and differences in the relative abundance of proteins can be identified. The samples can then be further purified by chromatography and identified by techniques such as peptide fingerprinting or

MS/MS. These techniques provide a complementary method to 2-D PAGE for protein visualization.[21]

Quantitative proteomics. With the use of MS/MS technique, the sequence of one peptide can be sufficient to identify an entire protein. This simplification of protein identification has triggered the development of methods that aim at increasing throughput by performing protein separation and identification in one suite of experiments.[203] Because cutting out individual gel spots from a 2-D gel is a very time-consuming procedure, many recently introduced approaches use chromatography for sample separation. These techniques either couple LC directly to ESI MS/MS or robotically spot the chromatographically separated fractions to a MALDI target. However, 2-D PAGE provides quantitative information that has only been obtained to a very limited extent from mass spectrometry-based methods.[21]

Interpretation of MS data (bioinformatics). Given the complexity of the proteome, an adequate proteomics approach requires the identification of thousands rather than several or a few proteins at a time.[18] Therefore, bioinformatics plays a key role in proteomic studies.[204, 205] The data obtained from MS must be interpreted by interrogation against protein databases, the quality of which is crucial for protein identification. Both peptide masses and peptide sequence information can be used for protein identification. There are several protein databases readily available over the internet that differ in the frequency with which they are updated and the amount of redundancy.[21]

1.2.5.5. Limitation of Common 2-D Separation Technologies

As discussed above, using current 2-D electrophoresis techniques (e.g., IEF/SDS PAGE) only the most abundant proteins can be identified. The lack of sensitivity of conventional 2-D electrophoresis technologies is caused mainly by a lack of separating or resolving power because, as discussed before, high abundance proteins mask the identification of low abundance

proteins. Loading more protein on the gel does not improve the situation because the Gaussian tails of the high abundant spots contaminate the low abundant proteins. Additionally, during peptide extraction following in-gel digestion procedures, the sample is exposed to many surfaces and losses can be substantial, particularly for low abundance proteins.[206]

Other limitations of conventional 2-D electrophoresis include extensive sample handling, time consuming, difficult to automate, decreased resolving power for proteins with a molecular mass of <15 kDa as a result of their high mobility in the gel and finally the gel cannot be coupled on-line to MS. Moreover, quantitation in 2-D gel electrophoresis is also a problem. After staining, the spots can be detected, but a direct quantitative detection method is not available.[147-149] Though the 2-D gel electrophoresis presents some limitations,[180] it still remains the workhorse for protein separation and identification.[160]

As alternatives, by using column-based 2-D systems that were discussed previously, direct quantitative detection with UV absorbance, laser-induced fluorescence (LIF) or MS is possible. Off-line 2-D chromatographic or electrophoretic systems have been applied for profiling in proteomics research.[207-210] If the column-based 2-D system is on-line coupled, there are additional advantages such as limited loss of analyte due to adsorption to the walls of vials or pipettes, which often occurs in analysis of peptides or proteins in the pmol range.[211] Moreover, increased reproducibility of the method can be achieved due to the lack of manual sample treatment necessary for the transfer of the analytes from the first to the second dimension.[162] On-line coupling is also easy to automate[162] and operator participation is reduced.[211]

Disadvantages of on-line coupling are the increased complexity of the system which may result in a higher risk of peak broadening due to dead volumes (caused by interface between the two CE dimensions, see Chapter 4),[162] and the necessity for relatively long retention or migration times in the first dimension to enable the coupling.[142] Microchip-based 2-D electrophoretic

techniques are the most recent technologies that can mainly overcome these limitations and will be discussed in Chapter 4.

1.3. References

(1) Doolittle, R. F. *Predictions of Protein Structure and the Principles of Protein Conformation* Plenum Press: New York, 1989.

(2) Nelson, D. L.; Cox, M. M. *Lehninger Principles of Biochemistry*; Worth Publishers: New York, 2000.

(3) Hames, D.; Hooper, N. *Biochemistry, 3rd Edition. (BIOS Instant Notes.)*, 2005.

(4) Voet, D.; Pratt, C. W.; Voet, J. G. *Fundamentals of Biochemistry, 2nd Edition*, 2004.

(5) Lodish, H.; Berk, A.; Matsudaira, P.; Kaiser, C. A.; Krieger, M.; Scott, M. P.; Zipurksy, S. L.; Darnell, J. *Molecular Cell Biology* WH Freeman and Company: New York, 2004.

(6) Fulton, A. B.; Isaacs, W. B. *Bioessays* **1991**, *13*, 157-161.

(7) Branden, C.; Tooze, J. *Introduction to Protein Structure*; Garland Publishing: New York, 1999.

(8) Ramachandran, G. N.; Sasisekharan, V. *Advances in Protein Chemistry* **1968**, *23*, 283-438.

(9) Malakhova, O. A.; Yan, M.; Malakhov, M. P.; Yuan, Y. Z.; Ritchie, K. J.; Kim, K. I.; Peterson, L. F.; Shuai, K.; Zhang, D. E. *Genes & Development* **2003**, *17*, 455-460.

(10) Wilson, V. G. *Sumoylation: Molecular Biology and Biochemistry*; Horizon Bioscience: Norfolk, 2004.

(11) Krishna, R. G.; Wold, F. *Proteins* **1998**, 121-206.

(12) Cohen, P. *Trends in Biochemical Sciences* **2000**, *25*, 596-601.

(13) Tyers, M.; Jorgensen, P. *Current Opinion in Genetics & Development* **2000**, *10*, 54-64.

(14) Mann, M.; Jensen, O. N. *Nature Biotechnology* **2003**, *21*, 255-261.

(15) Voet, D.; Voet, J. G. *Biochemistry*; Wiley: Hoboken, 2004.

(16) Chang, H.-T.; Huang, Y.-F.; Chiou, S.-H.; Chiu, T.-C.; Hsieh, M.-M. *Current Proteomics* **2004**, *1*, 325-347.

(17) Aebersold, R.; Goodlett, D. R. *Chemical Reviews (Washington, D. C.)* **2001**, *101*, 269-295.

(18) Godovac-Zimmermann, J.; Brown, L. R. *Mass spectrometry reviews* **2001**, *20*, 1-57.

(19) Rappsilber, J.; Mann, M. *Trends in Biochemical Sciences* **2002**, *27*, 74-78.

(20) Ideker, T.; Thorsson, V.; Ranish, J. A.; Christmas, R.; Buhler, J.; Eng, J. K.; Bumgarner, R.; Goodlett, D. R.; Aebersold, R.; Hood, L. *Science (Washington, DC, United States)* **2001**, *292*, 929-934.

(21) Hirsch, J.; Hansen, K. C.; Burlingame, A. L.; Matthay, M. A. *American Journal of Physiology* **2004**, *287*, L1-L23.

(22) Poly, W. J. *Comparative biochemistry and physiology. Part A, Physiology* **1997**, *118*, 551-572.

(23) Chen, G.; Gharib, T. G.; Huang, C.-C.; Thomas, D. G.; Shedden, K. A.; Taylor, J. M. G.; Kardia, S. L. R.; Misek, D. E.; Giordano, T. J.; Iannettoni, M. D.; Orringer, M. B.; Hanash, S. M.; Beer, D. G. *Clinical Cancer Research* **2002**, *8*, 2298-2305.

(24) Gygi, S. P.; Rochon, Y.; Franza, B. R.; Aebersold, R. *Molecular and Cellular Biology* **1999**, *19*, 1720-1730.

(25) Strohman, R. *Bio/Technology* **1994**, *12*, 156-164.

(26) Blackstock, W. P.; Weir, M. P. *Trends in Biotechnology* **1999**, *17*, 121-127.

(27) Lion, N.; Rohner, T. C.; Dayon, L.; Arnaud, I. L.; Damoc, E.; Youhnovski, N.; Wu, Z.-y.; Roussel, C.; Josserand, J.; Jensen, H.; Rossier, J. S.; Przybylski, M.; Girault, H. H. *Electrophoresis* **2003**, *24*, 3533-3562.

(28) Celis, J. E.; Gromov, P. *Current Opinion in Biotechnology* **1999**, *10*, 16-21.

(29) Anderson, N. L.; Anderson, N. G. *Molecular and Cellular Proteomics* **2002**, *1*, 845-867.

(30) Lescuyer, P.; Hochstrasser, D. F.; Sanchez, J.-C. *Electrophoresis* **2004**, *25*, 1125-1135.

(31) Omenn, G. S.; States, D. J.; Adamski, M.; Blackwell, T. W.; Menon, R.; Hermjakob, H.; Apweiler, R.; Haab, B. B.; Simpson, R. J.; Eddes, J. S.; Kapp, E. A.; Moritz, R. L.; Chan, D. W.; Rai, A. J.; Admon, A.; Aebersold, R.; Eng, J.; Hancock, W. S.; Hefta, S. A.; Meyer, H.; Paik, Y.-K.; Yoo, J.-S.; Ping, P.; Pounds, J.; Adkins, J.; Qian, X.; Wang, R.; Wasinger, V.; Wu, C. Y.; Zhao, X.; Zeng, R.; Archakov, A.; Tsugita, A.; Beer, I.; Pandey, A.; Pisano, M.; Andrews, P.; Tammen, H.; Speicher, D. W.; Hanash, S. M. *Proteomics* **2005**, *5*, 3226-3245.

(32) Corthals, G. L.; Wasinger, V. C.; Hochstrasser, D. F.; Sanchez, J.-C. *Electrophoresis* **2000**, *21*, 1104-1115.

(33) Herbert, B. *Electrophoresis* **1999**, *20*, 660-663.

(34) Celis, J. E.; Ostergaard, M.; Jensen, N. A.; Gromova, I.; Rasmussen, H. H.; Gromov, P. *FEBS Letters* **1998**, *430*, 64-72.

(35) Duncan, R.; McConkey, E. H. *Clinical Chemistry (Washington, DC, United States)* **1982**, *28*, 749-755.

(36) Miklos, G. L. G.; Maleszka, R. *Proteomics* **2001**, *1*, 169-178.

(37) Wold, F. *Annual Review of Biochemistry* **1981**, *50*, 783-814.

(38) Wold, F.; Moldave, K. *Methods in enzymology* **1984**, *107*, 13-16.

(39) Ajuh, P.; Kuster, B.; Panov, K.; Zomerdijk, J. C. B. M.; Mann, M.; Lamond, A. I. *EMBO Journal* **2000**, *19*, 6569-6581.

(40) Bauer, A.; Kuster, B. *European Journal of Biochemistry* **2003**, *270*, 570-578.

(41) Washburn, M. P.; Wolters, D.; Yates, J. R. *Nature Biotechnology* **2001**, *19*, 242-247.

(42) Lipton, M. S.; Pasa-Tolic, L.; Anderson, G. A.; Anderson, D. J.; Auberry, D. L.; Battista, J. R.; Daly, M. J.; Fredrickson, J.; Hixson, K. K.; Kostandarithes, H.; Masselon, C.; Markillie, L. M.; Moore, R. J.; Romine, M. F.; Shen, Y.; Stritmatter, E.; Tolic, N.; Udseth, H. R.; Venkateswaran, A.; Wong, K.-K.; Zhao, R.; Smith, R. D. *Proceedings of the National Academy of Sciences of the United States of America* **2002**, *99*, 11049-11054.

(43) Figeys, D. *Analytical Chemistry* **2003**, *75*, 2891-2905.

(44) Wehr, T. *LCGC North America* **2006**, *24*, 1004, 1006-1010.

(45) Diamandis, E. P. *Molecular and Cellular Proteomics* **2004**, *3*, 367-378.

(46) Anderson, N. L.; Polanski, M.; Pieper, R.; Gatlin, T.; Tirumalai, R. S.; Conrads, T. P.; Veenstra, T. D.; Adkins, J. N.; Pounds, J. G.; Fagan, R.; Lobley, A. *Molecular and Cellular Proteomics* **2004**, *3*, 311-326.

(47) Hortin, G. L.; Jortani, S. A.; Ritchie, J. C., Jr.; Valdes, R., Jr.; Chan, D. W. *Clinical Chemistry (Washington, DC, United States)* **2006**, *52*, 1218-1222.

(48) Alaiya, A.; Al-Mohanna, M.; Linder, S. *Journal of proteome research* **2005**, *4*, 1213-1222.

(49) Monteoliva, L.; Albar, J. P. *Briefings in Functional Genomics & Proteomics* **2004**, *3*, 220-239.

(50) Bollag, D. M.; Edelstein, S. J.; Editors *Protein Methods*, 1991.

(51) Dignam, J. D. *Methods in Enzymology* **1990**, *182*, 194-203.

(52) Lenstra, J. A.; Bloemendal, H. *European Journal of Biochemistry* **1983**, *135*, 413-423.

(53) Toda, T.; Ishijima, Y.; Matsushita, H.; Yoshida, M.; Kimura, N. *Electrophoresis* **1994**, *15*, 984-987.

(54) Sanchez, J.-C.; Appel, R. D.; Golaz, O.; Pasquali, C.; Ravier, F.; Bairoch, A.; Hochstrasser, D. F. *Electrophoresis* **1995**, *16*, 1131-1151.

(55) Portig, I.; Pankuweit, S.; Lottspeich, F.; Maisch, B. *Electrophoresis* **1996**, *17*, 803-808.

(56) Cull, M.; McHenry, C. S. *Methods in Enzymology* **1990**, *182*, 147-153.

(57) Jazwinski, S. M. *Methods in enzymology* **1990**, *182*, 154-174.

(58) Kawaguchi, S.-i.; Kuramitsu, S. *Electrophoresis* **1995**, *16*, 1060-1066.

(59) Goerg, A.; Postel, W.; Guenther, S. *Electrophoresis* **1988**, *9*, 531-546.

(60) Teixeira-Gomes, A. P.; Cloeckaert, A.; Bezard, G.; Dubray, G.; Zygmunt, M. S. *Electrophoresis* **1997**, *18*, 156-162.

(61) Ames, G. F. L.; Nikaido, K. *Biochemistry* **1976**, *15*, 616-623.

(62) Goerg, A.; Boguth, G.; Obermaier, C.; Posch, A.; Weiss, W. *Electrophoresis* **1995**, *16*, 1079-1086.

(63) Goerg, A.; Postel, W.; Domscheit, A.; Guenther, S. *Electrophoresis* **1988**, *9*, 681-692.

(64) Posch, A.; van den Berg, B. M.; Berg, H. C. J.; Goerg, A. *Electrophoresis* **1995**, *16*, 1312-1316.

(65) Gegenheimer, P. *Methods in enzymology* **1990**, *182*, 174-193.

(66) Damerval, C.; De Vienne, D.; Zivy, M.; Thiellement, H. *Electrophoresis* **1986**, *7*, 52-54.

(67) Wu, F. S.; Wang, M. Y. *Analytical Biochemistry* **1984**, *139*, 100-103.

(68) Harrison, P. A.; Black, C. C. *Plant Physiology* **1982**, *70*, 1359-1366.

(69) Rabilloud, T. *Electrophoresis* **1996**, *17*, 813-829.

(70) Theillet, C.; Delpeyroux, F.; Fiszman, M.; Reigner, P.; Esnault, R. *Planta* **1982**, *155*, 478-485.

(71) Englard, S.; Seifter, S. *Methods in Enzymology* **1990**, *182*, 285-300.

(72) Meyer, Y.; Grosset, J.; Chartier, Y.; Cleyet-Marel, J. C. *Electrophoresis* **1988**, *9*, 704-712.

(73) Matsui, N. M.; Smith, D. M.; Clauser, K. R.; Fichmann, J.; Andrews, L. E.; Sullivan, C. M.; Burlingame, A. L.; Epstein, L. B. *Electrophoresis* **1997**, *18*, 409-417.

(74) Hurkman, W. J.; Tanaka, C. K. *Plant Physiology* **1986**, *81*, 802-806.

(75) Granier, F. *Electrophoresis* **1988**, *9*, 712-718.

(76) Badock, V.; Steinhusen, U.; Bommert, K.; Otto, A. *Electrophoresis* **2001**, *22*, 2856-2864.

(77) Issaq, H. J.; Conrads, T. P.; Janini, G. M.; Veenstra, T. D. *Electrophoresis* **2002**, *23*, 3048-3061.

(78) Peng, J.; Gygi, S. P. *Journal of Mass Spectrometry* **2001**, *36*, 1083-1091.

(79) Schiewe, J. *Drugs and the Pharmaceutical Sciences* **2003**, *128*, 1-21.

(80) Harvey, D. *Modern Analytica Chemistry, 1st Edition*; McGraw-Hill Higher Education, 2000.

(81) Rathore, A. S. *Journal of Chromatography, A* **2004**, *1037*, 431-443.

(82) Swadesh, J. K. *HPLC (2nd Edition)* **2001**, 427-441.

(83) Issaq, H. J. *Journal of Liquid Chromatography & Related Technologies* **2002**, *25*, 1153-1170.

(84) Whatley, H. *Clinical and Forensic Applications of Capillary Electrophoresis* **2001**, 21-58.

(85) Porras, S. P.; Riekkola, M.-L.; Kenndler, E. *Electrophoresis* **2003**, *24*, 1485-1498.

(86) Dolnik, V. *Electrophoresis* **1999**, *20*, 3106-3115.

(87) Jia, L.; Terabe, S. *Metabolome Analyses* **2005**, 83-101.

(88) Righetti, P. G. *Journal of Chromatography, A* **2005**, *1079*, 24-40.

(89) Veuthey, J.-L. *Analytical and Bioanalytical Chemistry* **2005**, *381*, 93-95.

(90) Righetti, P. G.; Hamdan, M.; Antonucci, F.; Verzola, B.; Bossi, A. *Journal of Chromatography Library* **2004**, *69B*, 633-668.

(91) Bossuyt, X. *Clinical Chemistry and Laboratory Medicine* **2003**, *41*, 762-772.

(92) Adamson, N. J.; Reynolds, E. C. *Journal of Chromatography, B: Biomedical Sciences and Applications* **1997**, *699*, 133-147.

(93) Carbeck, J. D.; Colton, I. J.; Gao, J.; Whitesides, G. M. *Accounts of Chemical Research* **1998**, *31*, 343-350.

(94) Colton, I. J.; Anderson, J. R.; Gao, J.; Chapman, R. G.; Isaacs, L.; Whitesides, G. M. *Journal of the American Chemical Society* **1997**, *119*, 12701-12709.

(95) Radko, S. P.; Chrambach, A.; Weiss, G. H. *Journal of Chromatography, A* **1998**, *817*, 253-262.

(96) Radko, S. P.; Weiss, G. H.; Chrambach, A. *Journal of Chromatography, A* **1997**, *781*, 277-286.

(97) Pretorius, V.; Hopkins, B. J.; Schieke, J. D. *Journal of Chromatography* **1974**, *99*, 23-30.

(98) Smith, N. *Capillary Electrochromatography*; beckman Coulter Inc.: London, 1999.

(99) Simal-Gandara, J. *Critical Reviews in Analytical Chemistry* **2004**, *34*, 85-94.

(100) Vegvari, A.; Guttman, A. *Electrophoresis* **2006**, *27*, 716-725.

(101) Eeltink, S.; Kok, W. T. *Electrophoresis* **2006**, *27*, 84-96.

(102) Xie, C.; Fu, H.; Hu, J.; Zou, H. *Electrophoresis* **2004**, *25*, 4095-4109.

(103) Liu, C.-Y.; Lin, C.-C. *Electrophoresis* **2004**, *25*, 3997-4007.

(104) Laemmerhofer, M.; Lindner, W. *Journal of Chromatography Library* **2003**, *67*, 489-559.

(105) Colon, L. A.; Maloney, T. D.; Anspach, J.; Colon, H. *Advances in Chromatography (New York, NY, United States)* **2003**, *42*, 43-106.

(106) Mistry, K.; Krull, I.; Grinberg, N. *Journal of Separation Science* **2002**, *25*, 935-958.

(107) Rathore, A. S. *Electrophoresis* **2002**, *23*, 3827-3846.

(108) Svec, F. *Advances in Biochemical Engineering/Biotechnology* **2002**, *76*, 1-47.

(109) Li, Y.; Xiang, R.; Wilkins, J. A.; Horvath, C. *Electrophoresis* **2004**, *25*, 2242-2256.

(110) Bandilla, D.; Skinner, C. D. *Journal of Chromatography, A* **2004**, *1044*, 113-129.

(111) Mistry, K.; Grinberg, N. *Journal of Liquid Chromatography & Related Technologies* **2004**, *27*, 1179-1202.

(112) Pappas, T. J.; Gayton-Ely, M.; Holland, L. A. *Electrophoresis* **2005**, *26*, 719-734.

(113) Simms, P. J. *Chemical Analysis (New York, NY, United States)* **2004**, *163*, 175-208.

(114) Terabe, S. *Analytical Chemistry* **2004**, *76*, 240A-246A.

(115) Welsch, T.; Michalke, D. *Journal of Chromatography, A* **2003**, *1000*, 935-951.

(116) Molina, M.; Silva, M. *Electrophoresis* **2002**, *23*, 3907-3921.

(117) Pyell, U. *Fresenius' Journal of Analytical Chemistry* **2001**, *371*, 691-703.

(118) Bandilla, D.; Banks, P. R. *Journal of Liquid Chromatography & Related Technologies* **2001**, *24*, 1929-1934.

(119) Otsuka, K.; Terabe, S. *Bulletin of the Chemical Society of Japan* **1998**, *71*, 2465-2481.

(120) Otsuka, K.; Terabe, S. *Molecular Biotechnology* **1998**, *9*, 253-271.

(121) Nielsen, K. R.; Foley, J. P. *Capillary Electrophoresis, 2nd Edition;* **1998**, 135-182.

(122) Khaledi, M. G. *Chemical Analysis (New York)* **1998**, *146*, 77-140.

(123) Mazzeo, J. R. *Handbook of Capillary Electrophoresis (2nd Edition)* **1997**, 49-73.

(124) Terabe, S. *Analytical chemistry* **2004**, *76*, 241A-246A.

(125) Terabe, S. *Chromatographic Science Series* **1993**, *64*, 65-87.

(126) Terabe, S.; Chen, N.; Otsuka, K. *Advances in Electrophoresis* **1994**, *7*, 87-153.

(127) Strege, M. A.; Lagu, A. L. *Journal of Chromatography, A* **1997**, *780*, 285-296.

(128) Wehr, T. *Separation Science and Technology (San Diego, CA, United States)* **2005**, *7*, 181-210.

(129) Schwartz, H. E.; Guttman, A.; Vinther, A. *Capillary Electrophoresis, 2nd Edition;* **1998**, 363-396.

(130) Fawcett, J. S. *Methodological Developments in Biochemistry* **1973**, *2*, 61-80.

(131) Righetti, P. G.; Bossi, A. *Analytica Chimica Acta* **1998**, *372*, 1-19.

(132) Righetti, P. G.; Gelfi, C.; Conti, M. *Journal of Chromatography, B: Biomedical Sciences and Applications* **1997**, *699*, 91-104.

(133) Bier, M.; Marquez, R. B. *Techniques in Protein Chemistry V, [Papers from the Symposium of the Protein Society], 7th, San Diego, July 24-28,* **1994**, 249-258.

(134) Delincee, H. *Izotoptechnika* **1986**, *29*, 1-26.

(135) Hjelmeland, L. M. *Journal of Chromatography Library* **1983**, *18B*, 117-119.

(136) Vesterberg, O. *Protides of the Biological Fluids* **1969**, *17*, 383-387.

(137) Righetti, P. G.; Gelfi, C. *Journal of chromatography. B, Biomedical sciences and applications* **1997**, *699*, 63-75.

(138) Ibel, K.; May, R. P.; Kirschner, K.; Szadkowski, H.; Mascher, E.; Lundahl, P. *European Journal of Biochemistry* **1990**, *190*, 311-318.

(139) Laemmli, U. K. *Nature (London, United Kingdom)* **1970**, *227*, 680-685.

(140) Schaegger, H.; Von Jagow, G. *Analytical Biochemistry* **1987**, *166*, 368-379.

(141) Culbertson, C. T.; Jacobson, S. C.; Ramsey, J. M. *Analytical Chemistry* **2000**, *72*, 5814-5819.

(142) Giddings, J. C. *Analytical Chemistry* **1984**, *56*, 1258A-1270A.

(143) O'Farrell, P. H. *Journal of Biological Chemistry* **1975**, *250*, 4007-4021.

(144) Smithies, O.; Poulik, M. D. *Nature (London, United Kingdom)* **1956**, *177*, 1033.

(145) Raymond, S. *Annals of the New York Academy of Sciences* **1964**, *121*, 350-365.

(146) Laurell, C. B. *Analytical Biochemistry* **1965**, *10*, 358-361.

(147) Sickmann, A.; Dormeyer, W.; Wortelkamp, S.; Woitalla, D.; Kuhn, W.; Meyer, H. E. *Electrophoresis* **2000**, *21*, 2721-2728.

(148) Nilsson, I.; Utt, M.; Nilsson, H.-O.; Ljungh, A.; Wadstrom, T. *Electrophoresis* **2000**, *21*, 2670-2677.

(149) Marcus, K.; Immler, D.; Sternberger, J.; Meyer, H. E. *Electrophoresis* **2000**, *21*, 2622-2636.

(150) Klose, J. *Humangenetik* **1975**, *26*, 231-243.

(151) Gharbi, S.; Gaffney, P.; Yang, A.; Zvelebil, M. J.; Cramer, R.; Waterfield, M. D.; Timms, J. F. *Molecular and Cellular Proteomics* **2002**, *1*, 91-98.

(152) Tyers, M.; Mann, M. *Nature (London, United Kingdom)* **2003**, *422*, 193-197.

(153) Unlu, M.; Morgan, M. E.; Minden, J. S. *Electrophoresis* **1997**, *18*, 2071-2077.

(154) Clauser, K. R.; Hall, S. C.; Smith, D. M.; Webb, J. W.; Andrews, L. E.; Tran, H. M.; Epstein, L. B.; Burlingame, A. L. *Proceedings of the National Academy of Sciences of the United States of America* **1995**, *92*, 5072-5076.

(155) Devlin, R. B.; Koren, H. S. *American Journal of Respiratory Cell and Molecular Biology* **1990**, *2*, 281-288.

(156) Gorg, A.; Obermaier, C.; Boguth, G.; Harder, A.; Scheibe, B.; Wildgruber, R.; Weiss, W. *Electrophoresis* **2000**, *21*, 1037-1053.

(157) Herbert, B. R.; Harry, J. L.; Packer, N. H.; Gooley, A. A.; Pedersen, S. K.; Williams, K. L. *Trends in Biotechnology* **2001**, *19*, S3-S9.

(158) Klose, J.; Nock, C.; Herrmann, M.; Stuhler, K.; Marcus, K.; Bluggel, M.; Krause, E.; Schalkwyk, L. C.; Rastan, S.; Brown, S. D. M.; Bussow, K.; Himmelbauer, H.; Lehrach, H. *Nature Genetics* **2002**, *30*, 385-393.

(159) Lindahl, M.; Staahlbom, B.; Svartz, J.; Tagesson, C. *Electrophoresis* **1998**, *19*, 3222-3229.

(160) Rabilloud, T. *Proteomics* **2002**, *2*, 3-10.

(161) Davis, J. M.; Giddings, J. C. *Analytical Chemistry* **1985**, *57*, 2178-2182.

(162) Powell, M. *Multidimensional Chromatography Edited by L. Mondello, A. C. Lewis, K. D. Bartle*, 2002.

(163) Bushey, M. M.; Jorgenson, J. W. *Analytical Chemistry* **1990**, *62*, 161-167.

(164) Stroink, T.; Ortiz, M. C.; Bult, A.; Lingeman, H.; de Jong, G. J.; Underberg, W. J. M. *Journal of Chromatography, B: Analytical Technologies in the Biomedical and Life Sciences* **2005**, *817*, 49-66.

(165) Stroink, T.; Schravendijk, P.; Wiese, G.; Teeuwsen, J.; Lingeman, H.; Waterval, J. C. M.; Bult, A.; de Jong, G. J.; Underberg, W. J. M. *Electrophoresis* **2003**, *24*, 1126-1134.

(166) Stroink, T.; Wiese, G.; Teeuwsen, J.; Lingeman, H.; Waterval, J. C. M.; Bult, A.; de Jong, G. J.; Underberg, W. J. M. *Electrophoresis* **2003**, *24*, 897-903.

(167) Clarke, N. J.; Crow, F. W.; Younkin, S.; Naylor, S. *Analytical Biochemistry* **2001**, *298*, 32-39.

(168) Stroink, T.; Wiese, G.; Lingeman, H.; Bult, A.; Underberg, W. J. M. *Analytica Chimica Acta* **2001**, *444*, 193-203.

(169) Stroink, T.; Wiese, G.; Teeuwsen, J.; Lingeman, H.; Waterval, J. C. M.; Bult, A.; de Jong, G. J.; Underberg, W. J. M. *Journal of Pharmaceutical and Biomedical Analysis* **2002**, *30*, 1393-1401.

(170) Visser, N.; Lingeman, H.; Irth, H. *Chromatographia* **2003**, *58*, 691-699.

(171) Ruiz-Calero, V.; Puignou, L.; Galceran, M. T.; Diez, M. *Journal of Chromatography, A* **1997**, *775*, 91-100.

(172) Anderson, L.; Anderson, N. G. *Proceedings of the National Academy of Sciences of the United States of America* **1977**, *74*, 5421-5425.

(173) Manabe, T.; Mizuma, H.; Watanabe, K. *Electrophoresis* **1999**, *20*, 830-835.

(174) Pieper, R.; Gatlin, C. L.; Makusky, A. J.; Russo, P. S.; Schatz, C. R.; Miller, S. S.; Su, Q.; McGrath, A. M.; Estock, M. A.; Parmar, P. P.; Zhao, M.; Huang, S.-T.; Zhou, J.; Wang, F.; Esquer-Blasco, R.; Anderson, N. L.; Taylor, J.; Steiner, S. *Proteomics* **2003**, *3*, 1345-1364.

(175) Noel-Georis, I.; Bernard, A.; Falmagne, P.; Wattiez, R. *Journal of Chromatography, B: Analytical Technologies in the Biomedical and Life Sciences* **2002**, *771*, 221-236.

(176) Wattiez, R.; Hermans, C.; Cruyt, C.; Bernard, A.; Falmagne, P. *Electrophoresis* **2000**, *21*, 2703-2712.

(177) Celis, J. E.; Rasmussen, H. H.; Gromov, P.; Olsen, E.; Madsen, P.; Leffers, H.; Honore, B.; Dejgaard, K.; Vorum, H.; et al. *Electrophoresis* **1995**, *16*, 2177-2240.

(178) Courchesne, P. L.; Luethy, R.; Patterson, S. D. *Electrophoresis* **1997**, *18*, 369-381.

(179) Figeys, D.; Ducret, A.; Yates, J. R., III; Aebersold, R. *Nature Biotechnology* **1996**, *14*, 1579-1583.

(180) Gygi, S. P.; Corthals, G. L.; Zhang, Y.; Rochon, Y.; Aebersold, R. *Proceedings of the National Academy of Sciences of the United States of America* **2000**, *97*, 9390-9395.

(181) Shevchenko, A.; Jensen, O. N.; Podtelejnikov, A. V.; Sagliocco, F.; Wilm, M.; Vorm, O.; Mortensen, P.; Shevchenko, A.; Boucherie, H.; Mann, M. *Proceedings of the National Academy of Sciences of the United States of America* **1996**, *93*, 14440-14445.

(182) Gygi, S. P.; Han, D. K. M.; Gingras, A.-C.; Sonenberg, N.; Aebersold, R. *Electrophoresis* **1999**, *20*, 310-319.

(183) Boucherie, H.; Sagliocco, F.; Joubert, R.; Maillet, I.; Labarre, J.; Perrot, M. *Electrophoresis* **1996**, *17*, 1683-1699.

(184) Garrels, J. I.; Futcher, B.; Kobayashi, R.; Latter, G. I.; Schwender, B.; Volpe, T.; Warner, J. R.; McLaughlin, C. S. *Electrophoresis* **1994**, *15*, 1466-1486.

(185) Ducret, A.; Van Oostveen, I.; Eng, J. K.; Yates, J. R., III; Aebersold, R. *Protein Science* **1998**, *7*, 706-719.

(186) Sabounchi-Schutt, F.; Astrom, J.; Eklund, A.; Grunewald, J.; Bjellqvist, B. *Electrophoresis* **2001**, *22*, 1851-1860.

(187) Lindahl, M.; Stahlbom, B.; Tagesson, C. *Electrophoresis* **1999**, *20*, 3670-3676.

(188) Griese, M.; Von Bredow, C.; Birrer, P. *Electrophoresis* **2001**, *22*, 165-171.

(189) Aebersold, R. H.; Leavitt, J.; Saavedra, R. A.; Hood, L. E.; Kent, S. B. H. *Proceedings of the National Academy of Sciences of the United States of America* **1987**, *84*, 6970-6974.

(190) Wattiez, R.; Hermans, C.; Bernard, A.; Lesur, O.; Falmagne, P. *Electrophoresis* **1999**, *20*, 1634-1645.

(191) Witzmann, F. A.; Bauer, M. D.; Fieno, A. M.; Grant, R. A.; Keough, T. W.; Kornguth, S. E.; Lacey, M. P.; Siegel, F. L.; Sun, Y.; Wright, L. S.; Young, R. S.; Witten, M. L. *Electrophoresis* **1999**, *20*, 3659-3669.

(192) Clauser, K. R.; Baker, P.; Burlingame, A. L. *Analytical Chemistry* **1999**, *71*, 2871-2882.

(193) Mann, M.; Hendrickson, R. C.; Pandey, A. *Annual Review of Biochemistry* **2001**, *70*, 437-473.

(194) Biemann, K.; Scoble, H. A. *Science (Washington, DC, United States)* **1987**, *237*, 992-998.

(195) Yates, J. R., III; Eng, J. K.; McCormack, A. L. *Analytical Chemistry* **1995**, *67*, 3202-3210.

(196) Biemann, K. *Biomedical & environmental mass spectrometry* **1988**, *16*, 99-111.

(197) Medzihradszky, K. F.; Burlingame, A. L. *Methods (San Diego)* **1994**, *6*, 284-303.

(198) Henzel, W. J.; Billeci, T. M.; Stults, J. T.; Wong, S. C.; Grimley, C.; Watanabe, C. *Proceedings of the National Academy of Sciences of the United States of America* **1993**, *90*, 5011-5015.

(199) James, P.; Quadroni, M.; Carafoli, E.; Gonnet, G. *Protein Science* **1994**, *3*, 1347-1350.

(200) Mann, M.; Hoejrup, P.; Roepstorff, P. *Biological Mass Spectrometry* **1993**, *22*, 338-345.

(201) Yates, J. R., III; Speicher, S.; Griffin, P. R.; Hunkapiller, T. *Analytical Biochemistry* **1993**, *214*, 397-408.

(202) Aebersold, R.; Mann, M. *Nature (London, United Kingdom)* **2003**, *422*, 198-207.

(203) Gygi, S. P.; Aebersold, R. *Current Opinion in Chemical Biology* **2000**, *4*, 489-494.

(204) Patterson, S. D. *Nature Biotechnology* **2003**, *21*, 221-222.

(205) Vihinen, M. *Biomolecular Engineering* **2001**, *18*, 241-248.

(206) Timperman, A. T.; Aebersold, R. *Analytical Chemistry* **2000**, *72*, 4115-4121.

(207) Kachman, M. T.; Wang, H.; Schwartz, D. R.; Cho, K. R.; Lubman, D. M. *Analytical Chemistry* **2002**, *74*, 1779-1791.

(208) Yan, F.; Subramanian, B.; Nakeff, A.; Barder, T. J.; Parus, S. J.; Lubman, D. M. *Analytical Chemistry* **2003**, *75*, 2299-2308.

(209) Wang, H.; Kachman, M. T.; Schwartz, D. R.; Cho, K. R.; Lubman, D. M. *Electrophoresis* **2002**, *23*, 3168-3181.

(210) Wall, D. B.; Parus, S. J.; Lubman, D. M. *Journal of Chromatography, B: Analytical Technologies in the Biomedical and Life Sciences* **2002**, *774*, 53-58.

(211) Opiteck, G. J.; Jorgenson, J. W.; Anderegg, R. J. *Analytical Chemistry* **1997**, *69*, 2283-2291.

CHAPTER 2

MICROCHIP PROTEOMICS

2.1. Principles of Microchip Proteomics

Besides the well-established technologies used the analysis of proteomes, new tools are evolving for analyzing proteins that are based on the use of microfluidics.[1, 2] The term "microfluidics" refers to analytical tools where fluids can be driven in microstructured channels and reservoirs. The first successful marriage between microchip technology and chemistry is certainly to be found in the field of genomics, where two types of devices are now included in the chemist/biologist toolbox, namely microarrays and CE microchips. The concept of a microarray, simultaneously introduced by several teams,[3-6] relies on the parallelization of hundreds to thousands of recognition reactions with immobilized probes. Microarrays found their most successful application in genomics, because a binding reaction directly gives sequence information. DNA surface chemistry allows either direct on-chip synthesis of short oligonucleotides or post-synthesis immobilization of PCR products. The other successful alliance of microchip technology was the development of CE microchips for DNA sizing.[7] In this case, the success does not rely solely on parallelization, but on separation efficiency due to microdimensions, integration of sample preparation, labeling, gel loading, and detection.[8, 9] From these examples, it should be noted that key success factors for microfluidics are the high degree of parallelization they offer for several similar functions on the same chip due to micrometer dimensions and integration of different functions.[10] While genomics has been the primary driver for micro-analytical tools developments, new efforts are now being forged to provide valuable microfluidic systems for the analysis of proteomes.

As discussed in Chapter 1, proteomic studies requires protein samples to be subjected to sequences of analytical processes, including protein extraction/preconcentration, protein separation, enzymatic protein digestion followed by separation of the resulting peptide fragments prior to being injected into a mass spectrometer. Several issues have been raised concerning the preparation process. For the analysis of complex protein samples comprised of thousands of individual components using non-miniaturized systems, the analysis time is typically several days, the sample volume lies in the μL range and the transfer of the sample from one step of the protocol to the next is a source of material loss and contamination. In this context it is advantageous to work with a miniaturized and integrated system, since this allows reduction of the material consumption and analysis time as well as eliminates most sample handling issues. These advantages have been highlighted and reviewed by a number of groups.[1, 11, 12] To summarize, a situation that involves a substantial number of different processing steps, one may say that the goal of these studies is to integrate the protein preparation steps and couple them as closely as possible to the ion source of the MS.

2.1.1. Integrated Microchips for Protein Analysis

Foote and co-workers[13] developed a microfabricated device with the ability to electrophoretically concentrate fluorescently labeled proteins prior to a separation unit (see Figure 2.1). They were able to concentrate proteins using a porous silica membrane between adjacent microchannels that allowed for the passage of buffer ions, but excluded larger migrating molecules. Concentrated proteins were then injected into a separation column for analysis. Pre-concentration factors of ~600 fold were achieved using this on-chip format, which was followed by SDS micro-capillary gel electrophoresis (SDS μ-CGE) separation of the proteins. Using this microfluidic, fluorescently labeled ovalbumin was detected at initial concentrations as

low as 100 fM by using a combination of field-amplified injection and preconcentration at a membrane prior to microchip CE (μ-CE).

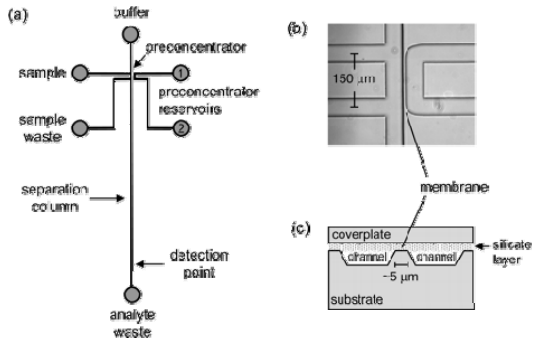

Figure 2.1. (A) Schematic of microchip layout used for preconcentration. (B) Microscopic image of preconcentrator-injector channels. (C) Schematic cross section through injector and preconcentrator channels (Reproduced from Analytical Chemistry 77, 2005, 57-63).

In a work performed by Yue et al.,[14] an integrated glass microfluidic device for proteomics, which directly coupled proteolysis with affinity selection, was described (see Figure 2.2). Initial results with standard phosphorpeptide fragments from β-casein in peptide mixtures showed selective capture of the phosphorylated fragments using immobilized metal affinity chromatography (IMAC) beads packed into a microchannel. Complete selectivity was seen with angiotensin, with capture of only the phosphorylated forms.

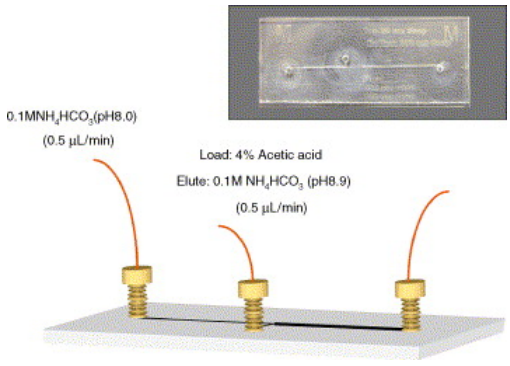

Figure 2.2. Diagram of the integrated trypsin digestion and affinity capture process along with a picture of the actual microdevice (Reproduced from Analytica Chimica Acta 564, 2006, 116-122).

Peterson et al.[15] reported a microfluidic device with a dual function containing both a solid phase extractor and an enzymatic microreactor (see Figure 2.3). This device was fabricated from a 25 mm long porous poly(butyl methacrylate-co-ethylene dimethacrylate) monolith prepared within a 50 μm i.d. capillary. This capillary with a pulled 9 – 12 μm needle tip was used as a nanoelectrospray emitter coupling the device to ESI MS. Photografting with irradiation through a mask was then used to selectively functionalize a 20 mm long portion of the monolith, introducing reactive poly(2-vinyl-4,4-dimethylazlactone) chains to enable the subsequent attachment of trypsin, thereby creating an enzymatic microreactor with high proteolytic activity. The other 5 mm of unmodified hydrophobic monolith served as a micro solid phase extractor. To test device functionality, different volumes of myoglobin solution ranging from 2 to 20 μL were loaded into the device, and a sequence coverage of ~80% was achieved for the highest loading.

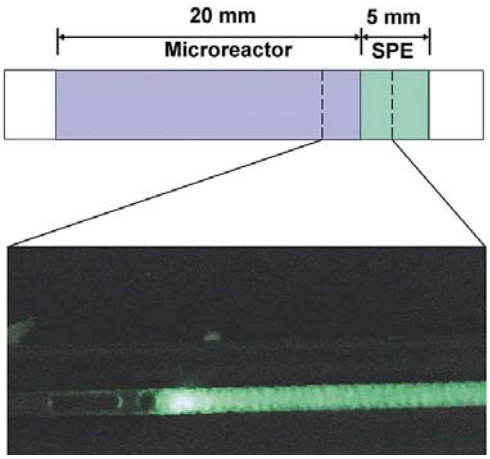

Figure 2.3. Schematic and fluorescence microscopic image of the monolithic dual-function device used in the digestion-SPE isolation for the analysis of labeled proteins and the capture of fluorescent peptides (Reproduced from Analytical Chemistry 75, 2003, 5328-5335).

An integrated poly(dimethylsiloxane), PDMS, microchip for SPE and CE followed by ESI/TOF MS has been developed and evaluated by Dahlin and co-workers.[16] The microchip

(see Figure 2.4) was fabricated in a novel one-step procedure where mixed PDMS was cast over steel wires in a mold. The removed wires defined 50 μm cylindrical channels. Fused-silica capillaries were then successfully inserted into the structure in a tight fit connection. The inner walls of the inserted fused-silica capillaries and the PDMS microchip channels were modified with a positively charged polymer, Poly E-323. In this approach, the chip was fabricated in a two-level cross design. The channel at the lower level was packed with 5 μm hyper-cross-linked polystyrene beads acting as a SPE medium used for desalting. The upper level channel acted as a CE channel and ended in an integrated emitter tip coated with conducting graphite powder to facilitate the electrical contact for ESI. To evaluate the microchip, six-peptide mixtures were dissolved in physiological salt solution, injected, desalted, separated, and sprayed into MS for analysis with a limit of detection in the femtomole regime.

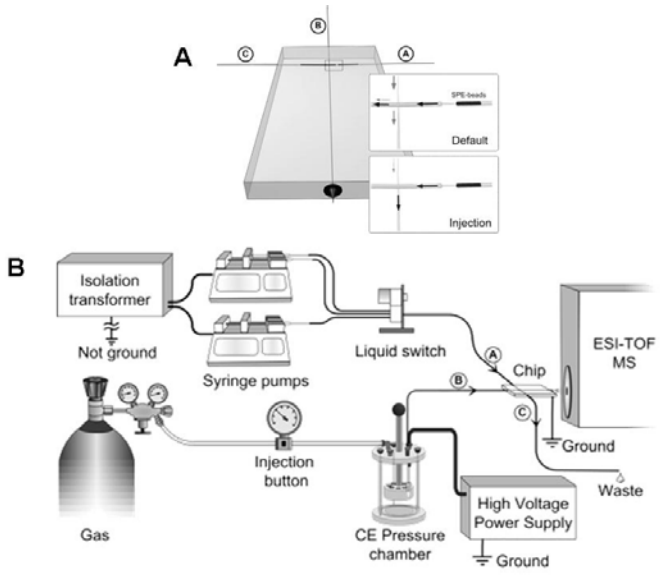

Figure 2.4. (A) Schematic of a PDMS microchip device. Channel A: sample inlet, channel B: CE, channel C: waste channel. (B) Schematic showing the instrumental setup and the connection of the microchip to the ESI/TOF MS (Reproduced from Analytical Chemistry, 77, 2005, 5356-5363).

In a similar effort to combine preconcentration with electrophoretic separations, Fortier et al.[17] investigated the analytical performances of a fabricated microfluidic device, which

included an enrichment column, a reversed phase separation channel, and a nanoelectrospray emitter embedded together in polyimide layers (see Figure 2.5). This configuration minimized transfer lines and connections and reduced post-column peak broadening and dead volumes. The compact microchip was interfaced to both ion trap and TOF MS, and its analytical potentials were evaluated in the context of proteomic applications. Sensitivity measurements were performed on a dilution series of protein digests spiked into rat plasma samples and provided a detection limit of 1 – 5 fmol.

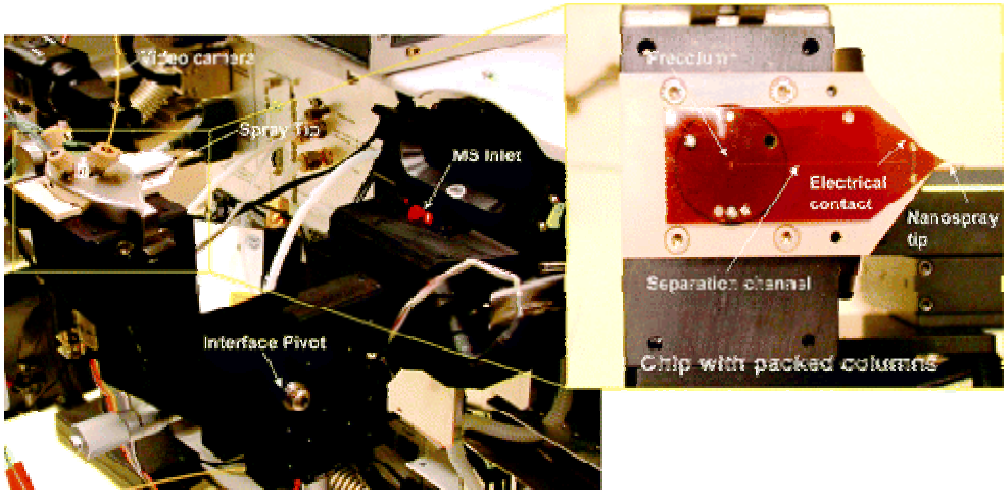

Figure 2.5. Microchip system interfaced to an ion trap MS. The chip was placed on an articulated manifold, which was comprised of a valve rotor with a clamping mechanism ensuring proper port alignment and sealing. A two-way translation stage provided easy positioning of the device in front of the sampling orifice when the manifold was inserted into the MS inlet. The inset shows a close up view of the chip device with the precolumn, separation channel, and nanospray tip (Reproduced from Analytical Chemistry, 77, 2005, 1631-1640).

In another study, Gao and co-workers[18] developed an integrated microchip for rapid and sensitive protein identification by on-line protein digestion and analysis of the digested proteins using ESI MS or transient capillary isotachophoresis/CZE with MS. A miniaturized membrane reactor was constructed by fabricating a PDMS microchip and coupling the microfluidic to a poly(vinylidene fluoride) porous membrane with adsorbed trypsin (see Figure 2.6), which

produced a large surface area-to-volume ratio by the porous membrane media with adsorbed trypsin to provide ultrahigh catalytic turnover. The residence time of protein analytes inside the trypsin-adsorbed membrane, the reaction temperature, and the protein concentration controlled the extent of protein digestion.

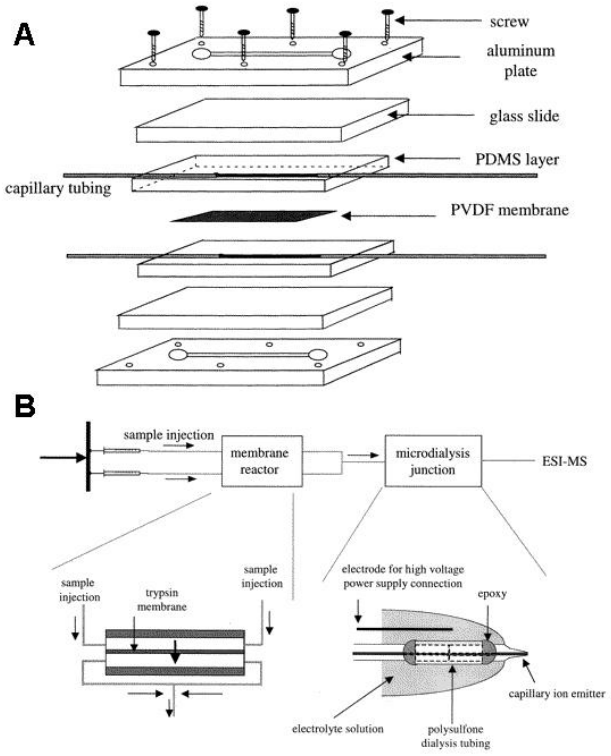

Figure 2.6. (A) Schematic of a membrane reactor assembly. (B) Schematic of the setup for performing ESI MS analysis of peptide mixtures from a trypsin membrane reactor (Reproduced form Analytical Chemistry, 73, 2001, 2648-2655).

A microfluidic device was also described by Wang and co-workers[19] in which an electrospray interface to MS was integrated with a CE channel, an injector and a protein digestion bed situated on a monolithic substrate (see Figure 2.7). To perform analysis, a 800 μm wide, 150 μm deep and 15 mm long channel served as a reactor bed for trypsin, which was immobilized on 40 – 60 μm diameter beads. Separation was performed in channels feeding into

a capillary, attached to the chip with a low dead volume coupler. Then, sample including melittin, cytochrome C and bovine serum albumin (BSA), was pumped through the reactor bed at flow rates between 0.5 and 60 μL/min and the application of the device for rapid digestion, separation and identification of proteins was demonstrated. A flow rate of 1 or 0.5 μL/min was found to be adequate for complete digestion of cytochrome C or BSA, corresponding to a digestion time of 3 – 6 min at room temperature.

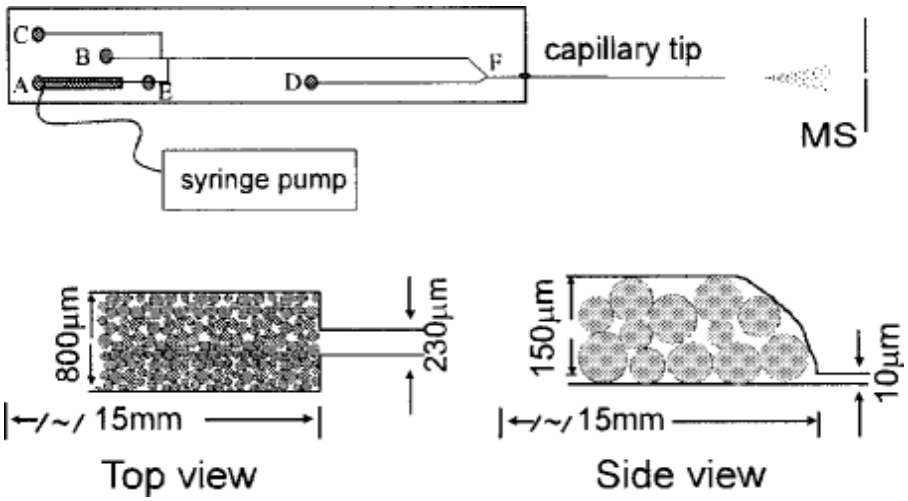

Figure 2.7. Schematic of an integrated enzyme reaction bed and CE microchip. Top and side views show a blow up of the packed trypsin bead (Reproduced from Rapid Communications in Mass Spectrometry, 14, 2000, 1377-1383).

According to Gottschlich et al.[20], a microfluidic device was developed that integrated enzymatic reactions, electrophoretic separation of the reactants from the products and post-separation labeling of proteins and peptides prior to fluorescence detection was accomplished (see Figure 2.8). A tryptic digestion of oxidized insulin β-chain was performed in 15 min under stopped flow conditions in a heated channel serving as the reactor and the separation was completed in 60 s. Localized thermal control of the reaction channel was achieved using a resistive heating element. The separated reaction products were then labeled with naphthalene-2,3-dicarboxaldehyde (NDA) and detected by fluorescence detection.

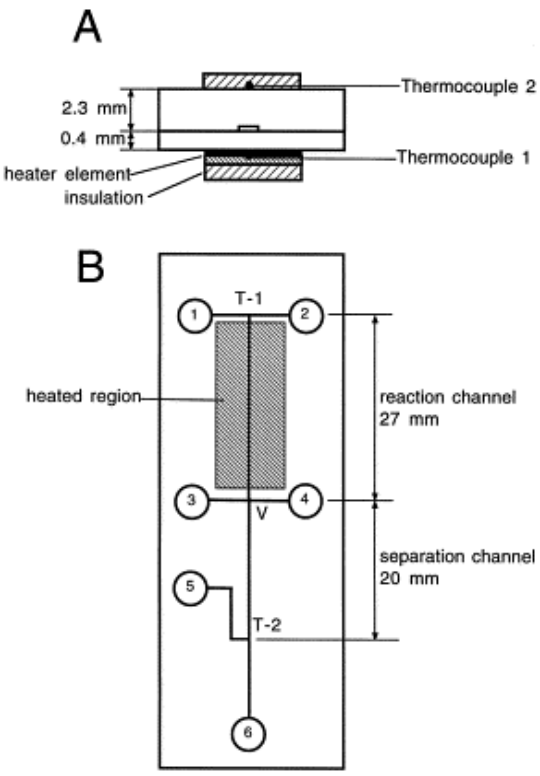

Figure 2.8. (A) Cross-sectional view of a microchip, heating element, and thermocouples. (B) Diagram of the microchip used for on-chip proteolytic reactions, separations and postcolumn labeling for generating fluorescent moieties. The fluid reservoirs are: (1) substrate, (2) enzyme, (3) buffer, (4) sample waste, (5) NDA, and (6) waste (Reproduced from Journal of Chromatography B, Biomedical Sciences and Applications, 745, 2000, 243-249).

Recently, a PDMS microfluidic device has been reported by Dodge and co-workers[21] that combined on-line protein electrophoretic separation, selection, and digestion of a protein of interest for identification by MS (see Figure 2.9). The microfluidic system included eight integrated valves and one micropump dedicated to control of flow operations. To evaluate the system performance, myoglobin was successfully isolated from BSA, then selected using integrated valves and digested in a rotary micromixer. Proteolytic peptides were recovered from the micromixer for protein identification. Total analysis from sample injection to protein identification was performed in under 30 min, with sample volumes in the range of tens of nanoliters.

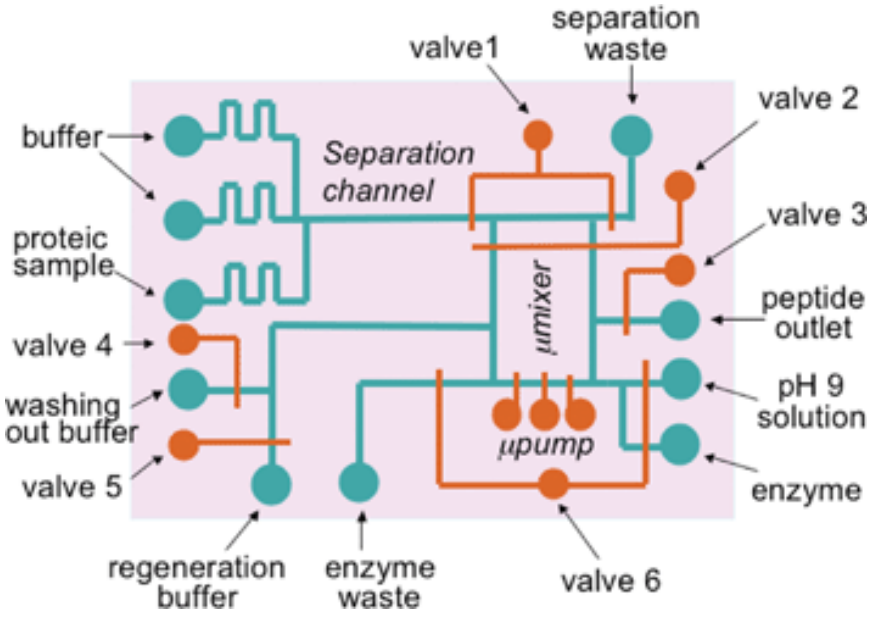

Figure 2.9. Drawing of an integrated PDMS microfluidic device. It was comprised of four modules: an injection/separation module in which pumping was entirely supported by electroosmotics; a protein trapping module; a circular micromixer where pumping was mechanically achieved; and an enzyme reaction module. Fluidic channels are in red, actuation channels are in blue-green. Valve actuation channels were filled with water in order to avoid air entering the fluidic channels through the PDMS membranes. Integrated valves are numbered from 1 to 6 (Reproduced from The Analyst, 131, 2006, 1122-1128).

2.1.2. Our Approach to Integrated Microchips for Protein Analysis

As shown above, none of the previous studies integrated the entire protein processing steps onto a single chip. They succeeded to integrate some parts of the proteomics processing on microchip including preconcentration with 1-D separation of proteins,[13] proteins SPE with enzymatic digestion of the concentrated proteins,[14, 15] SPE of peptides with separation of the concentrated peptides,[16, 17] protein separation with digestion or protein digestion with separation of the resulting peptide fragments.[18-21] As a result, the problem of transferring samples between units involved in proteomics remains unanswered. In other word, it will be essential to transfer samples from the reported microchip units to other missing parts in proteomics processing. This should be done either off-line or by using capillary inter-connects, which affect the overall efficiency and speed of analysis by introducing contaminants and void volumes.[1, 11, 12]

In addition, none of these reports used a 2-D platform for separation of proteins. As discussed in Chapter 1 (see Section 1.2.5.2), 1-D separation techniques are not able to provide suitable resolving power needed for protein analyses. As a result, incorporation of a microchip 2-D separation unit is absolutely essential in any integrated microchip for protein analysis.

Our approach to overcome the reported problems in proteomics includes an integrated microfluidic protein analysis system, which covers almost all proteomics steps and can be interfaced to a variety of different biological MS formats, such as MALDI or ESI. Figure 2.10 shows a schematic of the integrated microfluidic system proposed in this work, which consists of several processing units, including a cell lysis and protein extraction unit (I, optional), a 2-D microchip electrophoresis unit (II), a solid-phase proteolytic nano-reactor (III) and a micro-capillary electrophoresis unit (IV).[22, 23] The system input can be whole cells that are lysed and the protein components isolated using nanopillars decorated with thermally-responsive polymers, such as poly(N-isopropylacrylamide), pNIPAAm. pNIPAAm is a thermally responsive polymer that has been previously considered as an intelligent substrate to harvest intact cells.[24-27] It has a sharp lower critical solution temperature, LCST (~32 °C). pNIPPAm is a solid at temperatures greater than LCST, and undergoes a solid–liquid phase transition as it is cooled to lower temperatures and can dissolve in a surrounding aqueous medium.[25, 28] The isolated proteins are then separated using microchip 2-D electrophoresis and subsequently digested in a solid phase nano-reactor consisting of micro-pillars functionalized to allow covalent attachment of proteolytic enzymes for digesting the individual proteins for MS fingerprinting. Finally, the generated peptide fragments are sorted by electrophoretic techniques (e.g., CZE) and fed to a mass spectrometer for identification and protein fingerprinting.

Figure 2.11 represents further details on the configuration and operation of this integrated protein analysis system along with some primary data for each of the proposed units. To affect

isolation of the series of proteins from whole cell lysates, nanopillar arrays (see Figure 2.11A) can be dynamically coated with pNIPAAm, which shows super-hydrophobicity at a temperature above its LCST (contact angle ~90^{o}), and super-hydrophilicity below its LCST (contact angle 0^{o}), which served as a highly efficient solid-phase capture-bed for hydrophobic proteins (see Figure 2.11B).[29]

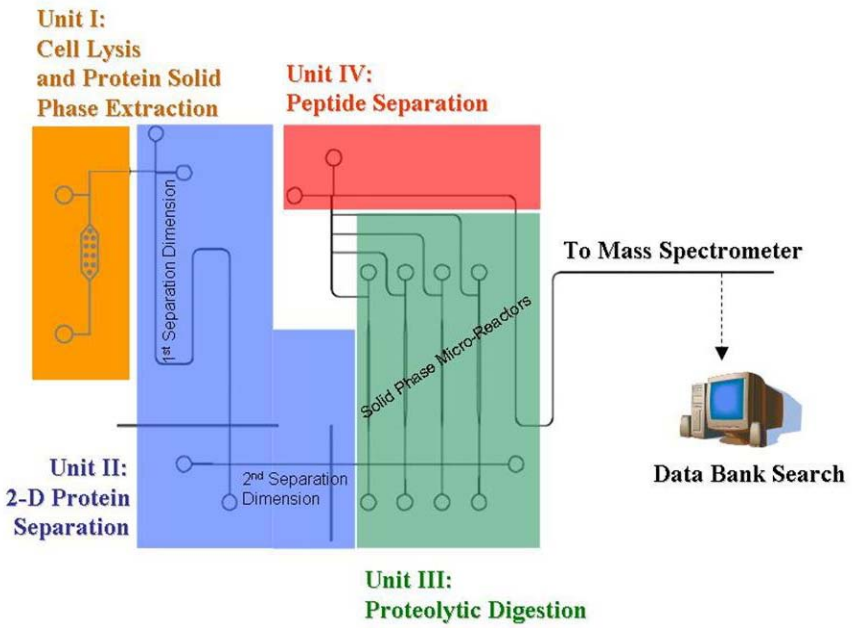

Figure 2.10. Schematic layout of the integrated microfluidic chip, which will preferably be fabricated in poly(methyl methacrylate), PMMA, due to its excellent operational properties for microchip electrophoresis and its ease for surface functionalizaiton. The system consists of a cell lysis/solid phase extraction unit, 2-D electrophoresis separation unit, solid-phase micro-reactors, separation of the peptides using electrophoretic techniques such as CZE or CEC, and on-line interfacing to MS, for example using a rotating ball or other interface (see text for detail).

Following protein isolation, the microfluidic network for the 2-D separation employs two electrophoresis techniques, for example, SDS μ-CGE in the first dimension and MEKC in the second dimension (see Figure 2.11C). In Chapter 4, we broadly discuss the function of this unit as the most important part of the protein analysis microchip. The sorted protein components are then digested using a micro-pillar solid-phase proteolytic reactor. Trypsin can be surface-

immobilized onto the micro-pillar structures following UV-254 nm exposure of the PMMA and incubation with 1-ethyl-3-[3-dimethylaminopropyl] carbodiimide hydrochloride (EDC). The proteolytic reactor has been tested with several proteins to evaluate its performance, which indicated improved protein identification efficiencies due to fast (<4 s digestion times) and efficient (>80% sequence coverage) protein digestions (see Figure 2.11D). Additional information about this unit can be found elsewhere.[30]

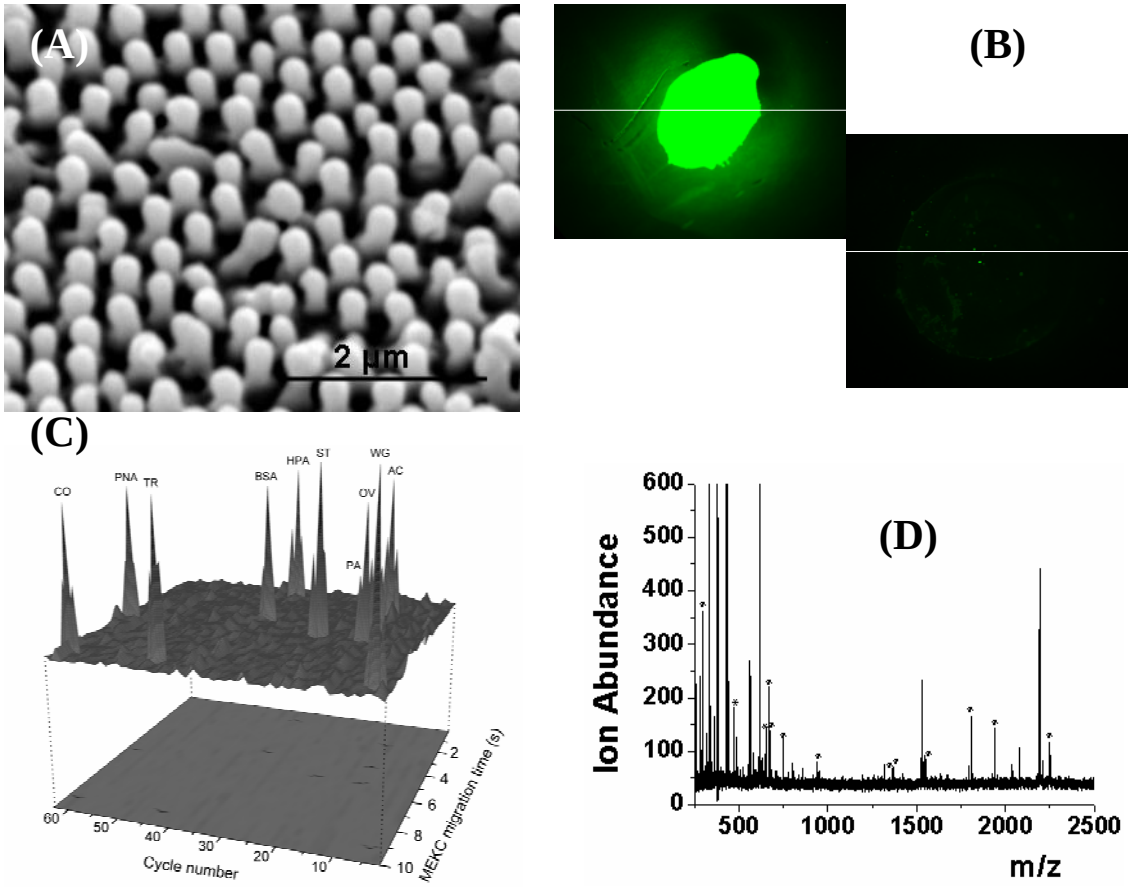

Figure 2.11. (A) Micrograph showing high aspect ratio nanopillars fabricated by nano-templating. (B) The nanopillars were dynamically coated with pNIPAAm and used to capture avidin that was labeled with a fluorescent dye. The first image shows the material above its LCST, in which the protein is captured and the second micrograph shows the release of avidin by dropping the temperature below the LCST. (C) 2-D SDS µ-CGE × MEKC electrophoretic separation of model proteins. The detection was accomplished using laser-induced fluorescence of proteins labeled with Alexa-Fluor 633. See Chapter 4 for details. (D) Mass spectrum showing the MALDI TOF MS analyses of peptides fragments generated from cytochrome C that were subjected to solid-phase protein digestion using trypsin immobilized onto micro-pillars.

In unit 4, since each protein can produce several peptides and before directing into the mass spectrometer, the resulting peptides will be separated using a simple 1-D separation technique, such as CZE. This separation can be performed either in a single channel format (shown in Figure 2.11) or by using a high-throughput platform using parallel channels that will be discussed in Chapter 5. In the case of the parallel format, the number of channels should be equal to the number of channels used for unit III, and this format will minimize both total protein analysis time and the throughput of the entire microchip for protein analysis.

In the following sections of this chapter, a brief overview of current microfabrication processes used to produce microfluidic structures, especially polymer-based microchips, will be presented. Then, a discussion on different detection techniques for proteins will be briefly presented with emphasis on techniques used with microfluidic applications.[10]

2.2. Microfabrication

2.2.1. Historical Aspects

In the 1970s in a remarkable effort, Terry et al.[31] miniaturized a gas chromatography (GC) system that was integrated onto a silicon wafer. Unfortunately, this work went unnoticed for more than a decade until the concept of micro-total analysis system (μ-TAS) was published in 1990.[32] This article triggered an avalanche of developments and discoveries, which led to a truly exponential growth of this field, first in the academic arena, and then from a commercial basis .[33] For the most part, microfluidic devices were fabricated using silicon wafers.[34] However, when electrophoretic techniques were transitioned to microfluidic devices, various types of glass[35-39] and quartz[40-42] were used as the substrate materials due to the well-established fabrication processes appropriate for these materials and the fact that the electrical conductivity of silicon proved problematic for the application of high voltages needed for EOF.[43] The fabrication methods, however, were the same; isotropic wet etching, using hydrofluoric acid or potassium

hydroxide as an etchant. However, for the commercialization of this technology, these fabrication processes represent certain disadvantages:[33]

I. Cost of substrate material. As many microfluidic devices have a relatively large footprint (typically several cm^2) to achieve either a long separation channel length or a high parallelization of their functions, the cost of the substrate material is an important factor for mass production. Polymers, such as PMMA, are of the order of 0.2 – 2.0 cents per cm^2, while boro-float glasses (e.g., Corning Pyrex) are of the order of 10 – 20 cents per cm^2. While the size of a microchip could become smaller, the area of a microfluidics often cannot be decreased in size due to scaling issues, which can produce a loss in performance.[33]

II. Many steps (i.e., cleaning, resist coating, photolithography, development, and wet etching) and harmful wet chemistry (e.g., hydrochloric acid) are involved for glass/quartz processing. Despite the fact that these steps are well known in the microelectronics industry and can be fully automated, each device goes through this fabrication process serially, which increases the fabrication time, and therefore the cost as well as the risk of fabrication errors. In addition, the costs are significant due to the reagents involved as well as their disposal.[33]

III. Limitations in geometrical design due to the isotropicity of the etching process, which allows only shallow, mainly semicircular channel cross sections in glass substrates, is another disadvantage. For many applications, however, channel cross sections (e.g., high-aspect ratio square channels, channels with a defined but arbitrary wall angle, or channels with different heights) are desirable. These cannot be achieved with standard microfabrication methods in glass or quartz substrates. In silicon, due to the

advanced silicon dry etch processes,[44] a larger variety of geometries can be produced, however, the cost per unit substrate area is significant.[33]

IV. The surface chemistry of silicon substrates poses a problem, as biomolecules tend to adsorb to silicon surfaces. This can be prevented with a surface coating (e.g., silanization), but carries with it the need of an additional process step.

Polymers as substrates for microfluidics, offer a solution to these fabrication challenges poised by glass and related materials, due to the fact that they lend themselves to inexpensive mass production of devices. Their wide range of material properties, relatively low cost and the development of suitable polymer microfabrication methods have attracted interest in the area of polymer microfluidics. Polymers provide the opportunity for high-volume production of disposable microfluidic devices, which could allow for the successful commercialization of the μ-TAS concept.[33]

2.2.2. Polymers

Polymers are macromolecules with a relative molecular mass between 10,000 Da and 100,000 Da and more than 1,000 monomeric units. The polymerization process is started by an initiator or a change in the physical parameters (e.g., light, pressure, or temperature). In most cases, polymers are amorphous or in some cases microcrystalline, where the length of the polymer chains is larger than the size of the crystallites. The chain length of the polymer chain varies in bulk material, therefore, a polymeric material does not necessarily have a narrow melting temperature range. Glass transition temperature (T_g) is the temperature at which a liquid changes to an amorphous or glassy solid. This is an important parameter in microchip fabrication protocols (see Chapter 3) because if the temperature is increased above T_g, the material becomes viscous and can be molded. It is important during the molding protocol to cool the material below its T_g before de-molding otherwise the geometric stability of the molded

component may suffer due to material relaxation during de-molding. Softeners can be used to reach lower T_g for the material. The elasticity, impact strength, and expansion of the polymer increase and the hardness decreases due to these softeners.

Polymers can be classified into the following three categories according to their molding behavior, which is determined by the interconnection of the monomer units in the polymer chain:

I. Thermoplastic polymers: These polymers consist of unlinked or weakly linked chains. At a temperature above the T_g, these materials become malleable and can be molded into specific shapes.

II. Elastomeric polymers: These are very weakly cross-linked polymer chains. If an external force is applied, the molecular chains will stretch and return to their original state (higher entropy) once the external force is removed. Elastomers do not melt before reaching their decomposition temperature.

III. Duroplastic polymers: In these materials, the polymer chains are cross-linked heavily, and therefore a molecular movement for a change in shape is not easily obtained. These materials must be cast into their final shape. They are harder and more brittle than thermoplastics and soften very little before they reach their decomposition temperature.

2.2.3. Replication Technologies

The key to commercial success of polymer microfabrication in microfluidics lies in the establishment of a low-cost micro-manufacturing process. Replication technologies are good for this application because the principles behind these processes are well known in the macro-world, and in the case of injection molding, represent a standard technology for macroscopic polymer component manufacturing. The underlying principle is the replication of a microfabricated mold tool, which represents the negative (inverse) structure of the desired final

part. The expensive microfabrication step is therefore only necessary for the fabrication of the master, which then can be replicated many times into the final product. In addition to the cost advantages, replication technologies also offer the benefit of freedom of design. The master can be fabricated with a large number of different microfabrication technologies, which allow various geometries to be realized. Nevertheless, some restrictions apply to these replication techniques:[33]

I. The surface quality of the mold tool. In general, the smoother the tool surface, the lower the frictional forces on the tool as well as the polymer microstructure in the de-molding step. Typically, surface roughness values of better than 100 nm root mean square (RMS) are necessary for reliable replication.

II. The interface chemistry between tool material and substrate polymer is also a critical factor. If the two materials form any kind of chemical or physical bond during the replication step, this adds to forces during the de-molding step. Release agents that are often used to aid mold release of complex structures are often not suitable for microfluidic devices as they might diffuse into the polymer and contaminate the analysis.

2.2.3.1. Master Fabrication

Micromachining methods. Modern micromachining technologies (i.e., sawing, cutting, milling, and turning) are capable of producing mold tools with lateral dimensions to a few μm. Their advantage is the wide range of materials, which can be machined. In addition, the development times for micromachined tools can be shorter as no mask fabrication and lithography steps are involved. Relatively simple channel structures with straight walls are well-suited geometries for these techniques. Channel crossings, high aspect ratio structures, very deep holes or very small structures, however, cannot be fabricated without drawbacks.

Special mention should be made of micro-electrodischarge machining (micro-EDM), which allows the fabrication of quasi 3-D structures in conducting materials. Here the material is removed due to the high energy electric discharge between an electrode and the work surface. This technique offers a high degree of flexibility in terms of materials and geometries, but produces a relatively rough surface. Very simple structures have reportedly been fabricated by replicating thin chromel wires.[45]

Electroplating methods. The most commonly used method for master fabrication employs an electroplating step, resulting in a replication master made out of nickel or a nickel alloy such as Ni-Co or Ni-Fe. The process starts with photolithography, in which a photoresist-coated substrate with a conducting electroplating layer is exposed to light and subsequently developed so that the areas to be electroplated are free of resist. This structure is then placed into a galvanic bath where, due to the migration of metal ions between the bath and the conducting starting layer, the metal starts to grow in the resist-free area. After the plated structure is overgrown with the metal, the resist and starting layer can be developed (removed) and the resulting metal structure is processed further.

Conventional photoresist technologies allow structural heights on the order of 10 – 40 μm. Other techniques to produce electroplating masters are the LiGA technique, which is a German acronym for Lithographie (lithography), Galvanoformung (electroplating), Abformung (molding), where thick PMMA layers are exposed to synchrotron radiation[46] or the laser-LiGA process,[47] where the synchrotron radiation is replaced by pulsed UV-light, which ablates the polymer material. With these techniques, the surface roughness is quite small (LiGA down to ~10 nm RMS) and the resulting nickel tool has a good surface quality (i.e., low surface roughness). Drawbacks are the comparatively slow growth rate of nickel in the electroplating process (a typical rate is typically between 10 μm/h and 100 μm/h), the high stress levels in thick

nickel layers, which tend to bend the master, and the radial dependency of the growth rate, which can result in a different height of the nickel structure in the middle and at the rim of a nickel wafer.[33]

Silicon micromachining. As silicon itself has suitable material properties for a mold tool (high level of stiffness, high heat conductivity) and a large variety of silicon surface micromachining techniques exist, attempts have been made to use silicon as a replication tool directly. Several micromachining technologies have been under investigation, the simplest one being wet etching of silicon. A wet etching step of 100-silicon results in a structure with a wall angle of ~55 degrees, which forms a trapezoidal channel. The slant in the wall allows good mold release and the surface roughness of the wet etching process of well-oriented monocrystalline silicon wafers is excellent.[45, 48, 49] Obviously, the channel cross section in this case is limited, although some isotropic etching techniques for silicon exist to allow the production of relatively tall and narrow structures (i.e., low machining aspect ratio, where the aspect ratio is defined as the structure height divided by its width).

Dry etching methods, such as reactive ion etching (RIE), advanced silicon etch (ASE) or the Bosch process,[44] allow deep structures with vertical walls to be fabricated although with a surface roughness that strongly depends on the etch rate. Fast etches produce a very rough surface, which for practical reasons limits the achievable depth of the structures. Typical depths range between 10 μm and 40 μm for a conventional dry etch and up to more than 200 μm in the case of an ASE process, with etch rates on the order of 1 – 5 μm/min. All silicon tools, however, have the common problem of potential sticking with many polymers due to their surface chemistry. A combination of silicon etching and electroplating exists, which is called DEEMO (deep etching, electroplating, and molding).[50] In this technique, the micromachined silicon is used as a base for an electroplating step.[33]

2.2.3.2. Hot Embossing

Currently the most widely used replication process to fabricate channel structures for microfluidic applications is hot embossing.[33] The microfabrication process of hot embossing itself is quite straightforward.[51] After fabrication of the master, it is mounted in the embossing system together with the planar polymer substrate. Both are heated separately in a vacuum chamber to a temperature just above the T_g of the polymer material. The vacuum is necessary to prevent the formation of air bubbles due to entrapment of air in small cavities. It also allows water vapor (that is driven out of the polymer substrate during the process,) to be removed. Additionally, it increases the lifetime of nickel tools as it prevents corrosion of the nickel at these elevated temperatures. The tool is brought into contact with the substrate and then embossed with a controlled pressure and temperature. While maintaining the embossing pressure, the tool-substrate sandwich is then cooled to just below the T_g. To minimize thermally induced stress in the material as well as replication errors (RE) due to the different thermal expansion coefficients of the tool and substrate, this thermal cycle should be as short as possible. After reaching the lower cycle temperature, the embossing tool is mechanically driven apart from the substrate, which now contains the desired features. This is usually the most critical step, as now the highest forces act on the polymer microstructure, particularly if a structure with vertical walls and a high aspect ratio is desired. Therefore, an automated mold release is crucial for a higher production yield. The microstructured polymer wafer can now be processed further. Figure 2.12 shows a diagram of a hot embossing machine.[33]

Figure 2.12. Diagram of hot embossing machine (left), and the embossing machine with its counterparts (right).

2.2.4. Bonding Techniques to Make a Complete Microfluidic Structure

In order to form closed micro-capillary structures, the microchannels, which are normally open after the fabrication step, have to be enclosed. This should be utilized without clogging the channels, changing their physical parameters or altering their dimensions. This often represents a big challenge for higher volume fabrication methods. Several methods have been reported in the literature and are outlined below.

2.2.4.1. Lamination

In the lamination process, a thin polyethylenterephtalate (PET) foil (typical thickness about 30 µm) coated with a melting adhesive layer (typical thickness 5 – 10 µm) is rolled onto the structure with a heated roller.[52] The adhesive layer melts in this process and combines the lid foil with the channel plate. This method is widespread in the macro-world for encapsulation of paper and polymers in a polymer film and works well for larger channels. With very small channels, however, the adhesive tends to block the channel. Due to the difference in the materials used, an inhomogeneous interface between the lid and channel plate is created, which leads to a sudden change of parameters, such as refractive index and EOF.[33]

2.2.4.2. Gluing

A simple technique to realize bonding at low temperature is the use of an intermediate gluing layer. For example, two component epoxy resins can be used for gluing together two microchip components. To perform this on glass microchips before bonding, a glass substrate with a 1-µm thick layer of glue is heated at 80°C until the glue starts to harden. At the moment, the glue is still soft enough to bond well and its viscosity is sufficiently high to prevent filling of the channel, the second glass substrate is brought into contact with the first one. A pressure of about 1 MPa is applied during hardening of the glue, permitting a uniform bonding. A clear advantage of this method is its simplicity and very low temperature; however, a potential drawback is the interference of the hardened epoxy material with the chemical analysis experiments.[53]

2.2.4.3. Application of Heat and Pressure (Thermal Annealing)

Several researchers use sealing of structures by heating the polymer and applying a force to enclose the channels (see Chapter 3).[54] Care has to be taken not to damage the structures; therefore this method is suitable mainly for designs with relatively small structured areas.[33] A schematic diagram of the thermal annealing process for polymeric microchips is shown in Figure 2.13. The annealing process is done in a temperature-controlled atmosphere.

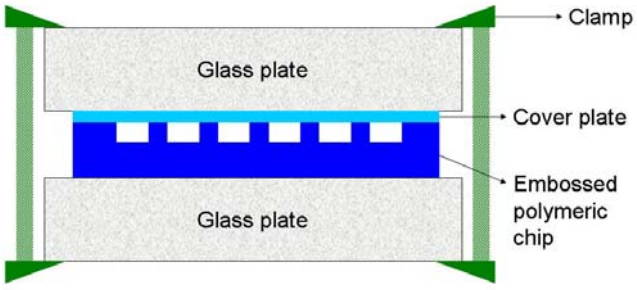

Figure 2.13. Schematic diagram of thermal annealing used for polymeric microchips.

2.2.4.4. Laser Welding

Polymers can be joined by local melting due to heat generated by a laser. This has been successfully demonstrated in the fabrication of micro-pumps,[55] but so far no reports have been published on microchannel applications. The main reason for this is the fact that all welding lines have to be drawn with the laser, which in the case of microchannels amounts to large distances and therefore long welding times.[33]

2.2.4.5. Ultrasonic Welding

A method well known in the macroworld is ultrasonic fusion of two polymer layers, where a local melting of the polymer is achieved by the energy density of an ultrasonic sound wave. This bonding technique as well as other bonding technologies reported above need very clean processing conditions, as particle contamination reduces the bond quality and yield dramatically. Clean-room processing is therefore highly advised.[33]

2.3. Fluid Mobilization in Microfluidics

There are basically two ways of mobilizing fluids in microfluidic systems: (i) Fluids can be pumped by external devices, such as syringe pumps or pneumatic pressure. The advantage of pressure-driven flow (PDF) is proper control of flow rates down to a few tens of nL/min as well as tight control of delivered volumes, irrespective of the microchannel wall surface charge, chemistry or capillary forces. But PDF results in parabolic flow profiles, which can in turn induce sample plug dispersion. An elegant approach has been undertaken by two companies, Gyros and Tecan, that use centrifugal forces to move fluids in microfluidic systems; microchannels are designed radially on a compact disk-like platform and rotation of the disk moves samples through the microchannel due to centrifugal forces. Such devices have been designed for MALDI sample preparation as well as screening assays.[56] (ii) Electrokinetic mobilization is induced by an applied electric field and provides a flat flow profile, which

produces high sample plug definition and is much easier to integrate into microfluidic systems,[57] but requires proper control of the microchannel wall surface charge and chemistry, as well as the sample ionic strength, which can be problematic when dealing with real-world samples. Moreover, the use of open channels, as is usually the case in electrokinetic mobilization, can pose technical problems; a slight difference in fluid levels in the reservoirs can induce a PDF. A comprehensive investigation of pressure effects in microfluidic systems has been reported in the literature.[58] Despite extensive work, fluid mobilization in open-channel microfluidic devices remains the major obstacle to reach satisfactory reproducibility.

2.4. Detection Methods for Microchip Electrophoresis

The diversity of μ-CE detection requirements makes it desirable to use a variety of detection principles. Several performance criteria must be considered when choosing the appropriate detector for any particular analysis. The criteria include sensitivity, selectivity, linear range and noise characteristics as well as footprint and hardware requirements for the device. Detector response should produce a known and reproducible relationship with amount/concentration of a solute and analytical signal, which should also have a large linear-response range. In other cases, it is preferable to use a detector that is "universal" and responds similarly to all solutes. Detectors for μ-CE as for other separation techniques should respond independent of the buffer, should not contribute to extra-column broadening, and should be reliable and convenient to use. Unfortunately, no single detector provides all these properties; therefore, an appropriate detector must be chosen based on the particular application.[59]

There are two main types of detectors: bulk-property and specific-property detectors. The bulk-property detector measures the difference in some physical property of the solute relative to that of the buffer alone. These include reflective index, conductivity and indirect methods. These detectors are generally more universal than specific property detectors.

However, these detectors usually have poorer limits of detection and smaller dynamic ranges compared to specific property detectors. This is because the detector signal depends not only on the properties of the solutes, but also on the differences in the properties of the solute and the buffer. Specific-property detectors measure the specific properties of the solutes and include such examples as UV absorbance, LIF, MS, and electrochemical. These methods limit detection to only those analytes that possess the required specific properties. Use of a selective detector is very advantageous when the sample matrix is complex and in situations where it is desirable to minimize "background" artifacts. These types of detectors normally provide impressive limits of detection compared to bulk-property detectors, possess wider linear ranges, provide more acceptable signal-to-noise ratios (SNR), and is used most often in μ-CE.[59]

Detection of the small analyte volumes in μ-CE can be accomplished either while they are migrating through the capillary (i.e., on-column detection such as UV absorbance, fluorescence, conductivity, and refractive index) or as they elute from the capillary (i.e., off-column detection such as electrochemical or MS). For on-column detection, the detection cell is part of the electrophoresis capillary; thus, zone broadening due to joints, fittings, and connectors is eliminated. In off-column detection, the detection region usually contributes to band broadening and needs to be evaluated by utilizing specific off-column detection techniques.[59]

2.4.1. UV Absorbance

The strong absorption of the peptide bond O=C–NH in the 185 – 220 nm wavelengths region can allow for the detection of proteins or peptides directly without any labeling with a chromophore. Detection sensitivity is increased at the lower end of this wavelength region, however, the user should be careful in selecting a buffer and microchip substrate material that will not absorb radiation at the selected detection wavelengths. In addition, proteins that contain

an aromatic amino acid residue in their structure can be detected by UV absorption from 275 – 280 nm.[60]

2.4.2. Fluorescence

Native proteins or peptides containing aromatic amino acid residues in their structure can also be detected by fluorescence in the 200 – 300 nm wavelength range. The detection of native proteins by fluorescence depends on the quantum yield of the three aromatic amino acids. Surveys of the literature reporting on the use of native fluorescence has indicated that: (i) The quantum yield is highest for tryptophan and lowest for phenylalanine; and (ii) the detection limits of these peptides using a Kr-F UV laser operating at 248 nm were at least two orders of magnitude lower when compared to UV absorption at 214 nm.[61] Other lasers have been used in the range of 200 – 300 nm for the detection of native proteins and/or peptides. The optimum excitation was found to be 275 nm. In most cases, proteins/peptides are detected by fluorescence following covalent or non-covalent labeling of these entities using fluorescent dyes. Additional information about fluorescence detection with and without labeling can be found elsewhere.[62]

Most commercial CE instruments are equipped with UV-absorption or fluorescence detectors. Although these optical detection methods have proven to be valuable techniques, they also have limitations as not all analytes absorb light or possess a fluorescent functionality. Some non-fluorescent analytes can be labeled with a fluorescent compound; however, these labeling reactions are not applicable to many simple ions, such as inorganic ions. Additionally, labeling reactions can be time-consuming, may introduce experimental errors, and can be difficult to perform at low analyte concentrations. For non-UV-absorbing solutes, UV-absorbing buffer additives can be used to facilitate indirect absorbance detection. By analogy, addition of fluorescent compounds to the buffer allows indirect fluorescence detection. However, indirect detection is not always desirable due to possible complications and/or restraints on buffer

compositions which are imposed to prevent the occurrence of system peaks, unstable baselines, or peak broadening due to incompatibility of the motilities of the analyte and background co-ions. Additionally, detection limits are generally higher as a result of somewhat compromised sensitivity when measuring a small signal on a relatively high and noisy background. The short detection path length in narrow-bore capillaries often results in unfavorable detection limits for absorbance-based detection methods, even when these are applied to UV absorbing analytes. Therefore, alternative, robust detection methods are required for CE, especially when downscaling to the microchip format.[63]

2.4.3. Mass Spectrometry

MS is being investigated as an alternative method of detection for microfluidic devices. However, when thinking of MS, an image of a large bulky piece of instrumentation comes to mind. Microchips should provide an excellent means of performing sample preparation for mass spectrometers. Sample preparation protocols such as SPE, digestion, preconcentration and separation methods (e.g., 2-D) can be conveniently performed on a microchip, making sample preparation for the mass spectrometer faster and more efficient. The mass spectrometer and the microchip are well-matched, due to the similarity in flow rates generated by the microchip with those required for most techniques in MS (e.g., ESI MS), despite the mismatch in physical dimensions.[64]

As discussed in Chapter 1, MS, especially when coupled to CE, is one of the most important tools in proteomics research for peptide mapping, for the confirmation of protein sequence and for the investigation of PTMs. It is also used for quantification of proteins by employing isotope-labeling techniques.[65] Mass spectrometry and finger printing MS are ideal detection techniques for proteins and peptides because of their universality, selectivity and most importantly, the wealth of structural information that they provide. The recent success of MS as

a detection technique for proteomic studies has evolved as a result of three analyte introduction techniques; continuous flow fast atom bombardment (FAB),[66] ESI[67] and MALDI TOF.[68] These three MS analyte introduction techniques solved the problem of introduction of polar, nonvolatile compounds, such as proteins into the MS. According to Thomas et al.,[69] ESI MS is useful for probing a wide range of biological problems as a detector for CE, in the study of non-covalent complexes, and for obtaining structural information. Advantages and limitations of different MS techniques used in proteomics are shown in Chapter 1 (see Table 1.4). Detail about the role of MS in proteomics is reviewed.[70]

2.4.4. Electrochemical Detections

Electrochemical detection techniques, including amperometry, potentiometry, and conductivity detection, have the advantages of relatively high sensitivity, high selectivity, and large dynamic range.[71] These detection techniques are concentration sensitive and miniaturization of the detection electrodes can result in improved sensitivity due to reduced noise (see Chapter 5).[72] In HPLC, ~5% of detection has been performed using amperometric detectors to measure the current associated with the oxidation or reduction of analytes as they are eluted from the column.[71] The suitability of amperometric detection depends on the redox characteristics of the analyte molecules in the environment of the mobile phase.

While amperometric is typically considered the most sensitive of the analytical electrochemical detection strategies, the success of readout depends upon the presence of an electrophore within the molecular structure of the analyte or the ability to append (either covalently or non-covalently) an electrophore to the analyte. In contrast, conductivity detection is considered a more "universal" electrochemical readout approach in that most any analyte can be detected as long as it has a conductance different from that of the carrier electrolyte or mobile phase used in the analytical separation. A further advantage of conductivity detection is that

direct contact of the detector with the solution under measurement is not essential, as conductivity detection can be performed in a contactless mode, exploiting capacitive coupling with the liquid inside the capillary or channel. This represents a viable method to eliminate interferences by the high separation voltage with the detection electronics.[63] In addition, since the electrodes are not in contact with the separation medium and analytes, electrode fouling due to non-specific adsorption is not present. The following section is a brief explanation of the principle of contact conductivity detection.

For conductivity detection, the analytical response (G, conductivity) is described through the following equation;

$$G = C(\lambda_+ + \lambda_-)/(1000K) \quad (2.1)$$

where λ_+ and λ_- (S cm^2 equiv^{-1}, S = siemens) are the limiting ionic conductances of cations and anions in solution, respectively, C is the concentration, and K is the cell constant (K = L/A, where L is the distance between the electrode pair and A is the area of the electrodes).[73] Clearly, increasing the area of the electrodes and/or reducing the spacing between the electrodes can improve the signal response of the conductivity measurement. In addition, one must reduce the contribution of Faradaic currents to the measured current to assist in reducing noise. One approach to accomplish this is to use a bipolar pulse waveform.[74-77] In this format, successive voltage pulses of equal amplitude and duration but opposite polarity are applied to the conductivity electrodes with the current passing between the electrodes measured at the end of the second pulse. If the pulse frequency is appropriately chosen with respect to the cell time constant (defined as the time to charge the double layer), the electrical double layer does not have sufficient time to form, which can minimize Faradaic reactions from occurring at the electrodes. In addition, since the bipolar pulses are of equal amplitude and time duration but opposite polarity, the measured current is effectively free from charging currents. Therefore, the

measured current primarily results from solution Ohmic resistance. The attractive feature of this format is that the electrodes can be configured directly on-column. Table 2.1 shows an overview of work performed on microchips integrated with contact conductivity detection.[63]

Table 2.1. Contact conductivity detection in microchips.[63]

Microchip Material	Channel Dimensions, μm (width × height)	Electrode	Number of Electrode, Electrode Configuration	Separation Technique
PMMA-PTFE[1] hybrid	1000 × 200	Pt	2, potential gradient detection	CZE
PDMS	350 × 50	White Au	1 and 2 in parallel leaving 200 um gap	ITP[3]
PDMS	324 × 56	25 μm ø Pt-iridium	1	ITP
PMMA	300 × 400	200 μm ø Pt	2, facing and flush with channel walls	ITP
PMMA	200 × 300	75 μm ø Pt	2, facing and flush with channel walls	ITP
PS[2]	200 × 200	160 μm wide, 200 μm high 40% carbon fiber-filled	2, facing and flush with channel walls	ITP
Zeonor	100 × 400	160 μm wide and 200 μm high 40% carbon fiber-filled nylon 6/6	2, facing and flush with channel walls	N/A
PMMA	200 × 200	Pt, 200 nm thick, 50 μm wide	2, facing leaving 80 μm gap	ITP, CZE
Fused corundum ceramics	50 × 20	Au	2, in parallel	CZE
Glass	80 × 21	Pt, 200 nm thick, 50 μm wide	2, in parallel leaving 25 μm gap	CZE
Silicon nitride, deposited on Si master	50 × 27	Pt, 200 nm thick, 50 μm wide	2, facing leaving 25 μm gap	CZE
PMMA	15 × 85	127 μm ø Pt	2, facing, flush with channel walls	CEC
PMMA	15 × 85	127 μm ø Pt	2, facing, leaving 20 μm gap	CZE, CEC, MEKC
PET	50 × 40	Carbon ink 100 μm wide and 20 μm high	2, facing flush with channel walls	CZE
PET	50 × 45	Carbon ink 100 μm wide and 55 μm high	2, parallel with 200 μm gap	CZE
Glass-PDMS hybrid	90 μm wide	Pt wire	Potential gradient detection	CZE

1. PTFE: Poly(tetrafluoroethylene); 2. PS: Polystyrene; 3. ITP: isotachophoresis.

2.5. References

(1) Laurell, T.; Marko-Varga, G. *Proteomics* **2002**, *2*, 345-351.

(2) Laurell, T.; Nilsson, J.; Marko-Varga, G. *TrAC, Trends in Analytical Chemistry* **2001**, *20*, 225-231.

(3) Ekins, R.; Chu, F.; Biggart, E. *Analytica Chimica Acta* **1989**, *227*, 73-96.

(4) Fodor, S. P. A.; Read, J. L.; Pirrung, M. C.; Stryer, L.; Lu, A. T.; Solas, D. *Science (Washington, DC, United States)* **1991**, *251*, 767-773.

(5) Khrapko, K. R.; Lysov, Y. P.; Khorlyn, A. A.; Shick, V. V.; Florent'ev, V. L.; Mirzabekov, A. D. *FEBS Letters* **1989**, *256*, 118-122.

(6) Southern, E. M.; Maskos, U.; Elder, J. K. *Genomics* **1992**, *13*, 1008-1017.

(7) Paegel, B. M.; Emrich, C. A.; Wedemayer, G. J.; Scherer, J. R.; Mathies, R. A. *Proceedings of the National Academy of Sciences of the United States of America* **2002**, *99*, 574-579.

(8) Mueller, O.; Hahnenberger, K.; Dittmann, M.; Yee, H.; Dubrow, R.; Nagle, R.; Ilsley, D. *Electrophoresis* **2000**, *21*, 128-134.

(9) Bousse, L.; Mouradian, S.; Minalla, A.; Yee, H.; Williams, K.; Dubrow, R. *Analytical Chemistry* **2001**, *73*, 1207-1212.

(10) Lion, N.; Rohner, T. C.; Dayon, L.; Arnaud, I. L.; Damoc, E.; Youhnovski, N.; Wu, Z.-y.; Roussel, C.; Josserand, J.; Jensen, H.; Rossier, J. S.; Przybylski, M.; Girault, H. H. *Electrophoresis* **2003**, *24*, 3533-3562.

(11) O'Connor, C. D.; Pickard, K. *Microarrays & Microplates* **2003**, 61-88.

(12) Chang, H.-T.; Huang, Y.-F.; Chiou, S.-H.; Chiu, T.-C.; Hsieh, M.-M. *Current Proteomics* **2004**, *1*, 325-347.

(13) Foote, R. S.; Khandurina, J.; Jacobson, S. C.; Ramsey, J. M. *Analytical Chemistry* **2005**, *77*, 57-63.

(14) Yue, G. E.; Roper, M. G.; Balchunas, C.; Pulsipher, A.; Coon, J. J.; Shabanowitz, J.; Hunt, D. F.; Landers, J. P.; Ferrance, J. P. *Analytica Chimica Acta* **2006**, *564*, 116-122.

(15) Peterson, D. S.; Rohr, T.; Svec, F.; Frechet, J. M. J. *Analytical Chemistry* **2003**, *75*, 5328-5335.

(16) Dahlin, A. P.; Bergstroem, S. K.; Andren, P. E.; Markides, K. E.; Bergquist, J. *Analytical Chemistry* **2005**, *77*, 5356-5363.

(17) Fortier, M.-H.; Bonneil, E.; Goodley, P.; Thibault, P. *Analytical Chemistry* **2005**, *77*, 1631-1640.

(18) Gao, J.; Xu, J.; Locascio, L. E.; Lee, C. S. *Analytical Chemistry* **2001**, *73*, 2648-2655.

(19) Wang, C.; Oleschuk, R.; Ouchen, F.; Li, J.; Thibault, P.; Harrison, D. J. *Rapid Communications in Mass Spectrometry* **2000**, *14*, 1377-1383.

(20) Gottschlich, N.; Culbertson, C. T.; McKnight, T. E.; Jacobson, S. C.; Ramsey, J. M. *Journal of Chromatography, B: Biomedical Sciences and Applications* **2000**, *745*, 243-249.

(21) Dodge, A.; Brunet, E.; Chen, S.; Goulpeau, J.; Labas, V.; Vinh, J.; Tabeling, P. *Analyst (Cambridge, United Kingdom)* **2006**, *131*, 1122-1128.

(22) Soper, S. A.; McCarley, R. L.; Chen, G.; Shadpour, H.; Musyimi, H. K.: Patent disclosure filed for U.S. Patent Office (Louisiana State University, Reference No. 0622), **2006**.

(23) Musyimi, H. K.; Shadpour, H.; Chen, G.; McCarley, R. L.; Murray, K. K.; Soper, S. A. *Micro Total Analysis Systems 2006, Proceedings of the μ-TAS 2006 Symposium,* **2006**, in press.

(24) Yamato, M.; Konno, C.; Utsumi, M.; Kikuchi, A.; Okano, T. *Biomaterials* **2001**, *23*, 561-567.

(25) Okano, T.; Yamada, N.; Sakai, H.; Sakurai, Y. *Journal of Biomedical Materials Research* **1993**, *27*, 1243-1251.

(26) Yamato, M.; Utsumi, M.; Kushida, A.; Konno, C.; Kikuchi, A.; Okano, T. *Tissue Engineering* **2001**, *7*, 473-480.

(27) Chen, G.; Ito, Y.; Imanishi, Y. *Biotechnology and Bioengineering* **1997**, *53*, 339-344.

(28) Shimizu, T.; Yamato, M.; Kikuchi, A.; Okano, T. *Tissue engineering* **2001**, *7*, 141-151.

(29) Chen, G.; Bolivar, J. G.; Soper, S. A.; McCarley, R. L. *Micro Total Analysis Systems 2005, Proceedings of the mTAS 2005 Symposium* **2005**, 1261-1263.

(30) Musyimi, H. K.; Shadpour, H.; Murray, K. K.; Soper, S. A., **2006**, in submission.

(31) Terry, S. C.; Jerman, J. H.; Angell, J. B. *IEEE Transactions on Electron Devices* **1979**, *ED-26*, 1880-1886.

(32) Manz, A.; Graber, N.; Widmer, H. M. *Sensors and Actuators, B: Chemical* **1990**, *B1*, 244-248.

(33) Becker, H.; Gartner, C. *Electrophoresis* **2000**, *21*, 12-26.

(34) Manz, A.; Fettinger, J. C.; Verpoorte, E.; Luedi, H.; Widmer, H. M.; Harrison, D. J. *TrAC, Trends in Analytical Chemistry* **1991**, *10*, 144-149.

(35) Harrison, D. J.; Fluri, K.; Seiler, K.; Fan, Z.; Effenhauser, C. S.; Manz, A. *Science (Washington, DC, United States)* **1993**, *261*, 895-897.

(36) Fan, Z. H.; Harrison, D. J. *Analytical Chemistry* **1994**, *66*, 177-184.

(37) Effenhauser, C. S.; Manz, A.; Widmer, H. M. *Analytical Chemistry* **1993**, *65*, 2637-2642.

(38) Jacobson, S. C.; Hergenroeder, R.; Koutny, L. B.; Ramsey, J. M. *Analytical Chemistry* **1994**, *66*, 2369-2373.

(39) Jacobson, S. C.; Hergenroder, R.; Moore, A. W., Jr.; Ramsey, J. M. *Analytical Chemistry* **1994**, *66*, 4127-4132.

(40) Jacobson, S. C.; Moore, A. W.; Ramsey, J. M. *Analytical Chemistry* **1995**, *67*, 2059-2063.

(41) Jacobson, S. C.; Ramsey, J. M. *Electrophoresis* **1995**, *16*, 481-486.

(42) Becker, H.; Lowack, K.; Manz, A. *Journal of Micromechanics and Microengineering* **1998**, *8*, 24-28.

(43) Kopp, M. U.; Crabtree, H. J.; Manz, A. *Current Opinion in Chemical Biology* **1997**, *1*, 410-419.

(44) Jansen, H.; Gardeniers, H.; de Boer, M.; Elwenspoek, M.; Fluitman, J. *Journal of Micromechanics and Microengineering* **1996**, *6*, 14-28.

(45) Martynova, L.; Locascio, L. E.; Gaitan, M.; Kramer, G. W.; Christensen, R. G.; MacCrehan, W. A. *Analytical Chemistry* **1997**, *69*, 4783-4789.

(46) Ehrfeld, W.; Muenchmeyer, D.; Schmidt, D.; (Kernforschungszentrum Karlsruhe Gmbh, 7500 Karlsruhe, De, Germany). Germany, 1991.

(47) Arnold, J.; Dasbach, U.; Ehrfeld, W.; Hesch, K.; Loewe, H. *Applied Surface Science* **1995**, *86*, 251-258.

(48) McCormick, R. M.; Nelson, R. J.; Alonso-Amigo, M. G.; Benvegnu, D. J.; Hooper, H. H. *Analytical Chemistry* **1997**, *69*, 2626-2630.

(49) Becker, H.; Heim, U. *IEEE International Conference on Micro Electro Mechanical Systems, Technical Digest, 12th, Orlando, FL., Jan. 17-21,* **1999**, 228-231.

(50) Elders, J.; Jansen, H. V.; Elwenspoek, M.; Ehrfeld, W. *Proceedings - IEEE Micro Electro Mechanical Systems, 8th, Amsterdam, Jan. 29-Feb. 2,* **1995**, 238-243.

(51) Heckele, M.; Bacher, W. *Nachrichten - Forschungszentrum Karlsruhe* **1998**, *30*, 231-236.

(52) Roberts, M. A.; Rossier, J. S.; Bercier, P.; Girault, H. *Analytical Chemistry* **1997**, *69*, 2035-2042.

(53) Sayah, A.; Solignac, D.; Cueni, T.; Gijs, M. A. M. *Sensors and Actuators, A: Physical* **2000**, *A84*, 103-108.

(54) Paulus, A.; Williams, S. J.; Sassi, A. P.; Kao, P.; Hongdong, T.; Hooper, H. H. *Proceedings of SPIE-The International Society for Optical Engineering* **1998**, *3515*, 94-103.

(55) Kamper, K. P.; Dopper, J.; Ehrfeld, W.; Oberbeck, S. *Proceedings - IEEE Annual International Workshop on Micro Electro Mechanical Systems: An Investigation of Micro*

Structures, Sensors, Actuators, Machines and Systems, 11th, Heidelberg, Jan. 25-29, **1998**, 432-437.

(56) Felton, M. J. *Analytical Chemistry* **2003**, *75*, 302A-306A.

(57) Bousse, L.; Cohen, C.; Nikiforov, T.; Chow, A.; Kopf-Sill, A. R.; Dubrow, R.; Parce, J. W. *Annual Review of Biophysics and Biomolecular Structure* **2000**, *29*, 155-181.

(58) Crabtree, H. J.; Cheong, E. C. S.; Tilroe, D. A.; Backhouse, C. J. *Analytical Chemistry* **2001**, *73*, 4079-4086.

(59) Grossman, P. D.; Colburn, J. C.; Editors *Capillary Electrophoresis: Theory & Practice*, 1992.

(60) Issaq, H. J. *Electrophoresis* **2001**, *22*, 3629-3638.

(61) Chan, K. C.; Janini, G. M.; Muschik, G. M.; Issaq, H. J. *Journal of Liquid Chromatography* **1993**, *16*, 1877-1890.

(62) Issaq, H. J.; Chan, K. C. *Electrophoresis* **1995**, *16*, 467-480.

(63) Guijt Rosanne, M.; Evenhuis Christopher, J.; Macka, M.; Haddad Paul, R. *Electrophoresis* **2004**, *25*, 4032-4057.

(64) Oleschuk, R. D.; Harrison, D. J. *TrAC, Trends in Analytical Chemistry* **2000**, *19*, 379-388.

(65) Gygi, S. P.; Rist, B.; Gerber, S. A.; Turecek, F.; Gelb, M. H.; Aebersold, R. *Nature Biotechnology* **1999**, *17*, 994-999.

(66) Suter, M. J. F.; Caprioli, R. M. *Journal of the American Society for Mass Spectrometry* **1992**, *3*, 198-206.

(67) Loo, J. A.; Udseth, H. R.; Smith, R. D. *Analytical Biochemistry* **1989**, *179*, 404-412.

(68) Walker, K. L.; Chiu, R. W.; Monnig, C. A.; Wilkins, C. L. *Analytical Chemistry* **1995**, *67*, 4197-4204.

(69) Thomas, J. J.; Bakhtiar, R.; Siuzdak, G. *Accounts of Chemical Research* **2000**, *33*, 179-187.

(70) Gygi, S. P.; Aebersold, R. *Current Opinion in Chemical Biology* **2000**, *4*, 489-494.

(71) LaCourse, W. R. *Encyclopedia of separation science*: New York, 2000.

(72) Zemann, A. J. *TrAC, Trends in Analytical Chemistry* **2001**, *20*, 346-354.

(73) Galloway, M.; Stryjewski, W.; Henry, A.; Ford, S. M.; Llopis, S.; McCarley, R. L.; Soper, S. A. *Analytical Chemistry* **2002**, *74*, 2407-2415.

(74) Johnson, D. E.; Enke, C. G. *Analytical Chemistry* **1970**, *42*, 329-335.

(75) Caserta, K. J.; Holler, F. J.; Crouch, S. R.; Enke, C. G. *Analytical Chemistry* **1978**, *50*, 1534-1541.

(76) Dasgupta, P. K.; Bao, L. *Analytical Chemistry* **1993**, *65*, 1003-1011.

(77) Kar, S.; Dasgupta, P. K.; Liu, H.; Hwang, H. *Analytical Chemistry* **1994**, *66*, 2537-2543.

CHAPTER 3

PHYSIOCHEMICAL PROPERTIES OF VARIOUS POLYMERIC MICROCHIPS AND THEIR EFFECTS ON MICROCHIP ELECTROPHORESIS PERFORMANCE*

3.1. Introduction

Microchip capillary electrophoresis of biological samples is a growing area of interest in a variety of applications due to the inherent advantages associated with this separation platform including: short development times; multi-channel capabilities to increase sample processing throughput; high separation efficiencies; the ability to integrate sample preparation steps into the device; small reagent and sample consumption; and the implementation of standard fabrication technologies to efficiently produce a large number of devices. In addition, μ-CE has the capability to separate a variety of analytes, such as large macromolecules like proteins, nucleic acids (RNAs, DNAs), and small molecules, for example amino acids, peptides, and pharmaceutics.[1] μ-CE is not restricted to separating only molecular targets, but can also be used to sort large assemblies, such as cells and particles.[2]

μ-CE separations have been performed in a variety of materials with the most common being glass or silicon.[3-5] The motivation for using these materials stems from their similarity to fused silica, the foundation of conventional capillary electrophoresis. The well-entrenched literature base for CE has provided well-characterized modification chemistries, EOF profiles and non-specific adsorption properties from which to guide transitioning established CE separations to a microchip format. In addition, established silicon-based fabrication technologies provide standard methods for chip production. Also, the favorable optical properties of glass and quartz substrates permit the detection of analytes using a variety of optical readout modalities such as LIF,[2, 3] electrochemiluminescence,[2, 6] absorbance,[2, 7] or refractive index.[8]

* Reprinted from *Journal of Chromatography A*, Vol. 1111, Hamed Shadpour, Harrison K. Musyimi, Jifeng Chen, and Steven A. Soper, Physiochemical properties of various polymers and their effects on microchip electrophoresis performance, pp. 238-251. Copyright 2006, with permission from Elsevier.

The production of microfluidic devices using polymer substrates has generated recent attention due primarily to the unique fabrication methods that are available to produce polymer-based μ-CE systems.[3, 5, 9, 10] For example, the use of replication-based microtechnologies has fostered the ability to manufacture inexpensive devices in large numbers without the need of extensive infrastructure (for example, clean rooms), thus providing access to this separation platform to researchers who have limited microfabrication expertise and resources. There are several characteristics that should be associated with any material to allow it to serve as a viable substrate for μ-CE applications and these are listed below:

I. Support a stable EOF: In most cases, the EOF represents a large contribution to the apparent mobility. Therefore, if the EOF is not stable, changes in apparent mobilities provide irreproducible results and makes peak identification by migration time matching difficult. Also, surface heterogeneity can create "hot spots" in which the surface charge density is not uniform, causing localized changes in the EOF, which can affect separation efficiency.[11, 12]

II. Good optical clarity: In most cases, detection is based on optical schemes and as such, the substrate must be optically clean at the monitoring wavelengths. For example, if UV absorption detection is used, the substrate material must possess small extinction coefficients at those wavelengths. In the case of fluorescence, the excitation wavelength must not produce large backgrounds due to either scattering (Raman or Rayleigh) or autofluorescence. Of course, non-optical-based detection techniques are not fraught with this limitation, for example, electrochemical detection or mass spectrometry.

III. Easily micromachined: The device requires the microfabrication of channels with micrometer dimensions. Therefore, the material should provide accessibility to a

variety of microfabrication technologies to make the prerequisite structures with high reproducibility and the required lateral dimensions and aspect ratios. In addition, the fabrication of structures with the intended dimensions should produce fairly smooth side walls.

IV. Established modification/surface chemistries: The substrate material many times requires chemical modification of its surface to modify or suppress the EOF, add an immobile phase (i.e., CEC) or covalent attachment of capture elements, for example antibodies. Therefore, stable and diverse modification chemistries must be supported by the intended substrate material.

V. Compatibility with the running buffer: The μ-CE separation may require the use of an aqueous buffer, an organic carrier electrolyte or a binary carrier electrolyte (mixed organic/aqueous phases). Therefore, the substrate must show good wettability with a range of electrolytes and also, must not swell or show appreciable solubility in the electrolyte, which would cause microstructure collapse or deformation.

VI. Good thermal/electrical properties: To minimize Joule heating or dielectric breakdown effects when operated at modest to high electric field strengths, the μ-CE substrate should possess good thermal conductivity with favorable electrical insulating properties.

While glass or quartz substrates meet or exceed many of the aforementioned material criteria for μ-CE, the limited choices in simple microfabrication techniques to manufacture the necessary structures limit their use. Polymers, on the other hand, provide a diverse range of fabrication technologies that can make exquisite structures using rather simple equipment and processing steps that are often not accessible to glass-based devices. Indeed, using replication technologies, polymer-based μ-CE chips can be produced at high production rates and at moderate costs.[13]

However, there are several physicochemical properties associated with polymers in general that diminish their capacity to provide performance characteristics for μ-CE similar to glass, such as potentially inferior optical clarity, poorly defined and unstable EOF, a lack of different modification protocols and thermal/electrical properties that vary tremendously with the type of polymer.

In this chapter, we will evaluate some physiochemical properties of a number of different polymers that can potentially be used as substrates for μ-CE applications. The intent is to provide a list of polymer properties that can be used to direct the choice of substrate material appropriate for a particular μ-CE application. As a demonstration to show the importance of how the polymer's physiochemical properties affect μ-CE performance, a set of model proteins will be analyzed using several different polymers with divergent physiochemical properties.

Sixteen different polymers were evaluated in this study. For selecting the optimal conditions for embossing and assembling devices using a thermal bonding technique to attach a cover plate to enclose the fluidic channels, the T_g of the polymers was measured. We also measured the optical clarity (i.e., UV/Vis absorbance, autofluorescence levels) of these materials since for our model investigations, LIF was used for readout during the separations. Several polymers were then used for an electrophoretic separation of proteins that were labeled with a fluorescent dye. The substrate-dependent electrophoresis performance was evaluated in terms of migration times, efficiencies, resolutions, and run-to-run/chip-to-chip reproducibilities.

While protein separations have been reported in a variety of polymers, for example PMMA,[14-21] polycarbonate (PC),[22-25] PET,[23] polyester[16, 26] and PDMS,[24, 27-31] little attention has been offered to explain how the material properties affect performance and reproducibility in the μ-CE separation. Different methods of detection such as LIF,[15, 18, 21, 27] UV/Vis,[23, 26] MS,[22] conductivity[14, 17, 19] and digital imaging[16, 20, 23-25, 28-31] have also been demonstrated in polymer

chips for protein separations. In addition, dynamic wall coatings were evaluated for several polymers to minimize solute-wall interactions or to suppress the EOF. The coating consisted of flushing the channels with a protein solution, such as BSA, prior to performing the electrophoresis.[23-25, 32, 33]

3.2. Experimental Details

3.2.1. Microchip Fabrication

Table 3.1 provides a list of polymers used in this study. These polymers were selected from a pool of substrates commonly used in fabricating microdevices. The monomer unit structures of these polymers are shown in Figure 3.1. PMMA, PET and nylon (NY) were purchased from Goodfellow (Devon, PA). Medical-grade PMMA (MG-PMMA) was purchased from Vista Optics Limited (Cheshire, UK). All other polymers in Table 3.1 were obtained from MSC (Melville, NY). The glass chip used in these studies was obtained from Micralyne (Edmonton, Canada).

The fluidic devices were embossed using Ni electroforms fabricated via LiGA following techniques detailed in our previous work.[14] Briefly, the embossing system consisted of a PHI Precision Press model TS-21-HC-4A-5 (City of Industry, CA). A vacuum chamber was installed into this press (pressure <0.1 bar) to allow complete filling of the die. The wafers inserted into the press were 133 mm in diameter, which permitted a maximum area of 7,850 mm^2 to be patterned over the wafer. Before molding, all residual water present in the polymer was removed by baking them in an oven at 50°C overnight. The die was coated with a release agent, MoldWiz (Axel, Woodside, NY), to improve demolding. During embossing, the molding die was heated and pressed into the polymer wafer with a pressure of 900 – 1,100 psi for a few minutes (see Table 3.1). During this process, the molding die was heated to a temperature greater than the T_g of the polymer. The press was then opened and the polymer piece removed and cooled to

room temperature. The entire fluidic channels were covered with a thin polymer cover plate by clamping the plastic pieces between two glass plates and thermal annealing in a GC oven (see Table 3.1 for conditions). The assembled microfluidic devices were configured in a "T" type geometry and included the following features: 5 mm length sample injection and waste channels; 40 mm separation channel (effective separation channel length = 30 mm); all channels were 50 μm in width and 85 μm in depth.

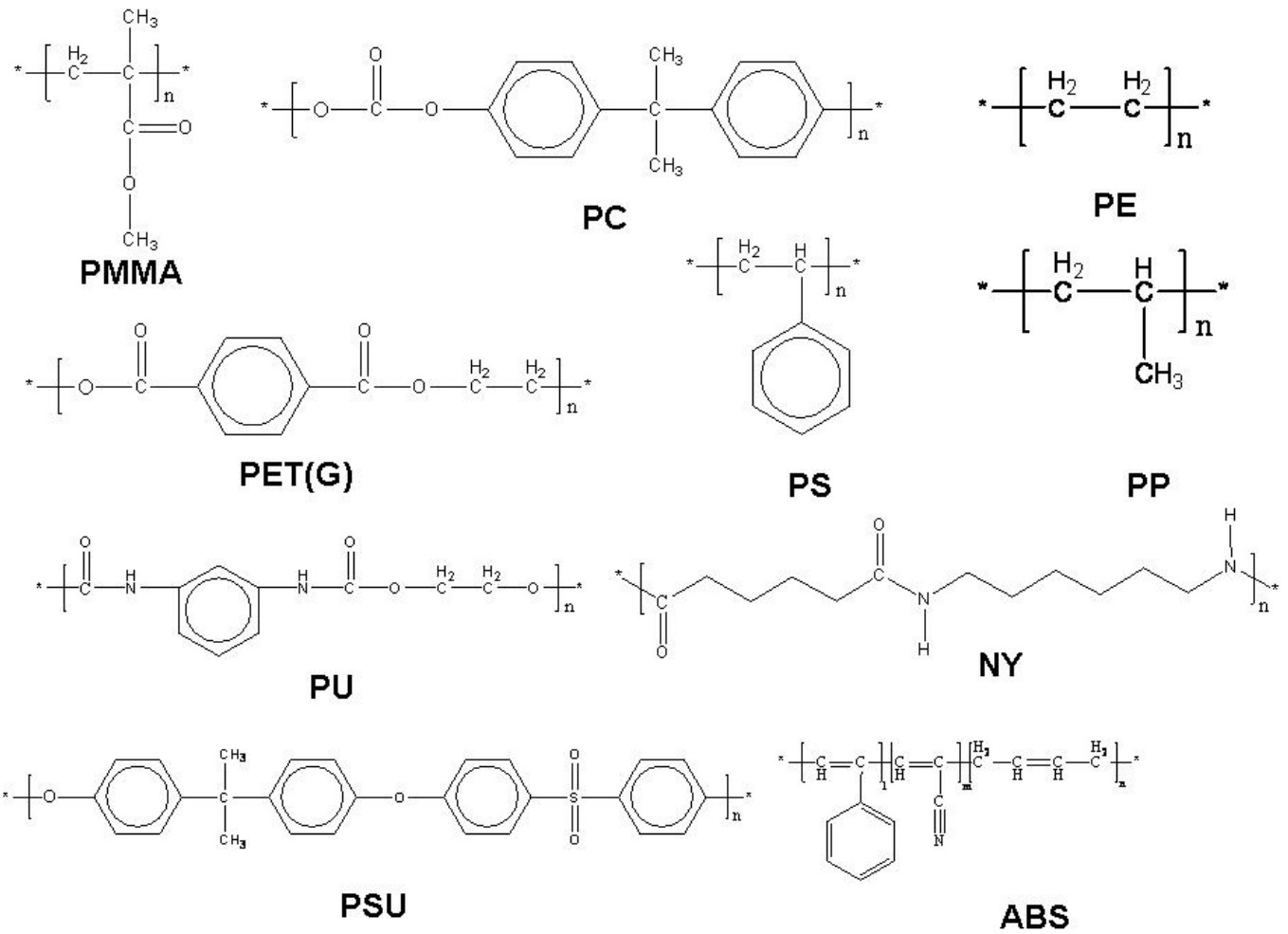

Figure 3.1. Monomer units of the selected polymers evaluated in this study as potential microchip electrophoresis substrates. The microstructures were fabricated using hot embossing.

Table 3.1. A list of polymers evaluated in this study along with their T_g, and optimal embossing and assembly conditions.

Polymer	Symbol	Tg[1] (°C)	Embossing					Annealing[2]	
			Temperature (°C)	Pressure (psi)	Time (s)	Channel Depth (μm)	Replication Error (%RE)	Temperature (°C)	Time (min)
Poly (methyl methacrylate)	PMMA	106 ± 2	155	950	150	81.2 ± 1.1	4.5	107	20
Clear acrylic	C-PMMA	117 ± 3	160	1100	410	80.3 ± 1.4	5.5	120	20
Gray acrylic	G-PMMA	115 ± 4	144	1100	190	81.4 ± 1.0	4.2	120	20
Medical grade PMMA	MG-PMMA	125 ± 1	165	950	180	83.4 ± 2.0	1.8	130	20
Polycarbonate	PC	148 ± 2	185	900	270	84.7 ± 1.1	0.4	150	20
Lexan	LX-PC	159 ± 5	170	1100	220	84.2 ± 3.3	0.9	165	15
High-density polyethylene	HDPE	-	140	1100	330	84.6 ± 0.9	0.5	130	20
Low-density polyethylene	LDPE	-	115	1100	480	73.4 ± 5.1	13.6	110	20
Polyethylene terephthalate	PET	75 ± 4	225	1100	600	76.8 ± 2.8	9.6	N/A	N/A
Polyethylene terephthalate glycolate	PETG	81 ± 2	100	900	180	82.4 ± 0.6	3.0	85	20
Polystyrene	PS	105 ± 5	140	1000	160	80.8 ± 3.4	4.9	110	15
Polypropylene	PP	-	155	1100	300	74.5 ± 4.8	12.3	150	20
Polyurethane	PU	-	190	1100	330	77.0 ± 4.1	9.4	N/A	N/A
Nylon	NY	57 ± 4	200	1100	540	83.3 ± 3.7	2.0	N/A	N/A
Polysulfone	PSU	182 ± 4	190	750	330	83.8 ± 1.1	1.4	185	30
Poly(acrylonitrile-butadiene-styrene)	ABS	110 ± 1	140	1000	180	79.7 ± 1.3	6.2	115	20

1. The T_g was determined using DSC. 2. N/A: Unable to thermally anneal a cover plate to the embossed fluidic network.

3.2.2. Contact Angle Measurements

Sessile water contact angle measurements were performed using 18 MΩ cm water on a VCA 2000 contact angle system equipped with a CCD camera (VCA, Billerica, MA). Approximately 5 μL of 18 MΩ cm water was placed on the polymer surface using a syringe. The left and right contact angles of the water drops were measured immediately after placement on the polymer surface. Contact angles were calculated using the software provided by the manufacturer. Each value reported was the average of a minimum of five measurements secured at separate positions on any given substrate.

3.2.3. EOF Measurements

The current-monitoring method was used to measure EOF in the microfabricated channel.[34] A straight channel between two reservoirs was used for the measurements. Initially, the entire chip was filled with 5.0 mM TRIS/HCl, pH 9.2 (Bio-Rad Laboratories, Hercules, CA) and run with an electric field of 300 V/cm while the current passing through the channel was monitored. After ~20 min, one reservoir was emptied and filled with 4.5 mM TRIS/HCl, pH 9.2 (Bio-Rad Laboratories). The electric filed was then applied to the reservoirs containing the low and high ionic strength buffer and the current was monitored continuously. After the current plateaued, the time to reach this plateau was secured from the plot from which the linear velocity could be calculated. Dividing this linear velocity by the electric field strength (300 V/cm) produced the EOF ($cm^2/V\ s$).

3.2.4. UV/Vis, Autofluorescence, Surface Profile, and T_g Measurements

An Ultrospec 4000 UV/Vis spectrophotometer (Pharmacia Biotech, Cambridge, UK) was used for measuring the absorbance of the polymer sheets. The absorbance values for each polymer were measured at six different wavelengths. The average absorbance for each polymer was divided by the absorption obtained for glass at that same wavelength in order to normalize

the data with respect to glass. The LIF background was measured for each polymer using an in-house constructed LIF detection system (see Section 3.2.7 for brief discussion of this system), which was operated at 488 nm, 632.8 nm and 780 nm excitation wavelengths. The fluorescence intensities were normalized with respect to glass, which was used as a reference material.

A surface profiler (P-11 Tencor, Santa Clara, CA) was used to measure channel dimensions and surface roughness of the embossed polymer microchips. The embossed polymer was scanned at 20 μm/s. Five replicate measurements were made for each polymer to ascertain RE following embossing. The surface roughness of the channel floors was obtained by measuring R_a, the average deviation in height, and λ_a, the average distance between roughness features. The ratio of R_a/λ_a, was used to evaluate the surface roughness inside the embossed channels.[35]

To obtain the T_g for different polymers, differential scanning calorimetry (DSC) measurements were performed using a Seiko heat-flux DSC-6200 EXSTAR system (Thermo Haake, Madison, WI) with a heating rate of 2°C/min (1°C/min for cooling) coupled to a Seiko II data acquisition and analysis system. Fifty microliter aluminum pans (Seiko P/N SSC000E031, Thermo Haake), sealed to withstand a pressure of 30 atm, were used as the sample holders. An empty pan served as the reference. The DSC pans were filled with the polymer powder (~2 mg) and weighed. The sample was heated from an initial temperature of 20°C at a rate of 2°C/min to a final temperature of 200°C under nitrogen gas. T_g values were measured at the onset of a change in heat capacity of the polymer sample using the available Seiko II software. Additional details of these measurements are reported elsewhere.[36]

3.2.5. Reagents and Preparation of Electrophoresis Chips

With the exception of the protein labeling kit (Molecular Probes, Eugene, OR) and TRIS/HCl (Bio-Rad Laboratories), all reagents were purchased from Sigma (St. Louis, MO) and

used as received. A suitable amount of SDS powder was added to TRIS/HCl to prepare the MEKC buffer. The buffer pH then was adjusted by adding HCl. Carbonic anhydrase, phosphorylase B, β-galactosidase, and myosin were also obtained from Sigma, and used without further purification. Protein solutions used for the electrophoresis were prepared at the appropriate concentration from a stock solution consisting of ~500 nM and stored at 4^{o}C in the dark. Nanopure water with a resistivity above 18 MΩ cm (Nanopure II System, Branstead, Dubuque, IA) was used to prepare all solutions and to rinse the microfluidic devices. Prior to use on the microchip, all solutions were filtered with a 0.2 μm Nylon-66 membrane syringe filter (Cole-Parmer Instrument Co., Vernon, IL) except the protein solutions, which were centrifuged (5 min, 6,000 rpm) to remove particulates.

3.2.6. Protein Labeling and Purification

All proteins, except for BSA, were labeled using an Alexa Fluor 633 protein labeling kit (Molecular Probes). The kit consisted of an amine-reactive dye, sodium hydrogencarbonate, a purification resin, and elution buffer. The labeling was performed according to the manufacture's protocol. Briefly, the protein solution was prepared using 0.1 M sodium hydrogencarbonate buffer and was allowed to react with the amine-reactive dye for 1 h at room temperature. The reaction mixture was subsequently loaded into a size-exclusion column to separate unincorporated dye from the labeled proteins. The columns (Econo-Pac 10 DG, Bio-Rad Laboratories) were packed with Bio-Gel P-6DG gel with a molecular weight cut-off of 6,000 Da. The concentration of labeled-protein and the extent of labeling were measured using a UV/Vis spectrophotometer. Following the labeling, the protein/dye conjugates were diluted to the desired concentration in the electrophoresis buffer and stored at 4^{o}C until required for use.

3.2.7. LIF Detection Apparatus and Power Supply

Fluorescence detection was accomplished using an in-house constructed LIF system. A photograph of the LIF system is shown in Figure 3.2. A Helium-Neon laser with a lasing wavelength of 632.8 nm (NT 54-151, Edmund Industrial Optics, Barrington, NJ) was operated with an external high voltage power supply (LDI LF LAB-1, Laser Drive Inc., Gibsonia, PA) and filtered using an exciter filter (XF-1026, Omega, Brattleboro, VT). The excitation light was reflected off a dichroic mirror into a 40x (NA = 0.65) objective (Melles Griot, Zevenaar, The Netherlands) and focused to a 10 μm diameter spot in the microchannel. The microfluidic device was situated on an x-y-z micro-translational stage to allow positioning of the microchannel with respect to the focused laser beam. The sample fluorescence was collected by the same objective lens, passed through the dichroic mirror (XF-2022, Omega), an emission band pass filter (XF-3030, Omega) and detected using a photomultiplier tube (PMT, RT-1508, Hamamatsu, San Jose, CA). Amplified photoelectrons were converted to a digital signal (IBH Pulse Converter, Glasgow, UK), and processed by a PC computer using a multifunction I/O card (CB-68 LP) and PCI board (PCI-6601) obtained from National Instruments (Austin, TX).

The same LIF system was also used to measure the autofluorescence of polymers excited at 488 nm and 780 nm by switching out the excitation sources and the appropriate filters. The 488 nm detection system consisted of an air-cooled argon-ion laser (532 Omnichrome, Chino, CA), which was directed onto the objective using the appropriate dichroic mirror. The fluorescence emission was filtered through a stack of optical filters and focused onto the PMT. The filter stack consisted of a 520 nm bandpass filter (Oreil, Stanford, CT) and a 520 nm long-pass filter (Edmund Scientific, Barrington, NJ).

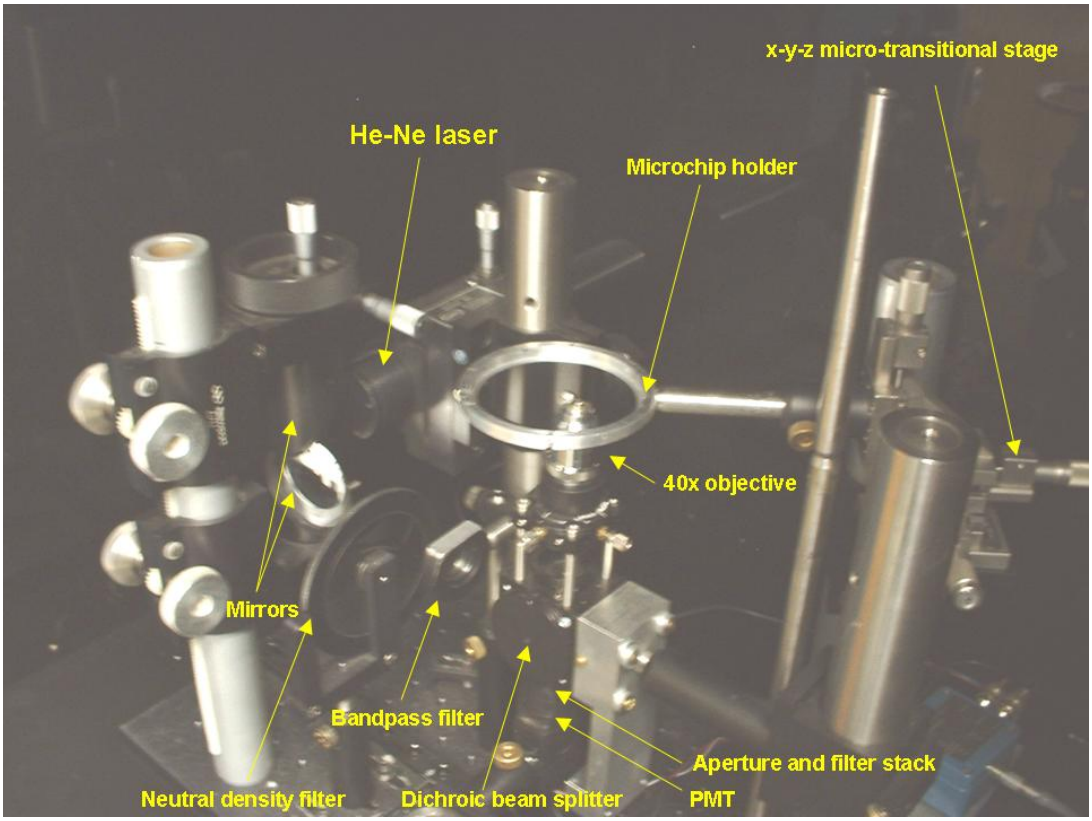

Figure 3.2. LIF 632.8 nm system for detection of proteins labeled with Alexa Fluor 633.

The 780 nm LIF detection system consisted of a diode laser (800 PicoQuant GmbH, Berlin, Germany). The laser excitation beam was passed through a 780 nm line filter (780DF10, Omega Optical, Brattleboro, VT), reflected by a dichroic mirror (795DRLP, Omega Optical) and focused into the microchannel using the 40x microscope objective. The fluorescence excitation was collected by the same objective, transmitted through the dichroic and finally through a filter stack consisting of a long-pass filter (cut-on wavelength 830 nm, Newport Corp., Irvine, CA) and a band-pass filter centered at 825 nm (825RDF30, Omega Optical).

High voltage was applied to the reservoirs of the microchip with four independently controlled high voltage power supplies (EMCO, Sutter Creek, CA). Electrical contact between the solution in the fluid reservoirs and the high voltage leads was achieved using platinum wires (Scientific Instrument Services, Ringoes, NJ). The high voltage power supplies and relays were

controlled by a computer using an analog output (D/A) card (PCI-DDA04/12, National Instruments, Austin, TX). The software for data acquisition and control of the power supply was created using National Instruments LabVIEW.

3.2.8. Electrophoretic Separations

All electrophoretic separations were carried out at ambient temperature in reverse mode (injection end cathodic; detection end anodic). Injection was initiated by applying a positive voltage to the sample waste reservoir and grounding the sample reservoir for the amount of time needed to completely fill the cross channel. The remaining reservoirs were allowed to float during injection. The cross channel was designed for a load volume of 212 pL. Following injection, a positive high voltage was applied to the electrophoresis waste reservoir and the supply buffer reservoir was grounded. The sample and sample waste reservoirs were set to 15% and 10% of the voltage applied to the electrophoresis waste reservoir, respectively, and acted as pullback voltages to prevent sample leakage from these channels during the separation. (Caution! The electrophoresis uses high voltages and special care should be taken when handling the electrodes.) The microfluidic devices were rinsed prior to each electrophoretic run with a 0.01% NaN_3 solution. The device was then rinsed with doubly-distilled H_2O and filled with the appropriate carrier electrolyte and pre-electrophoresed for 10 min. Non-specific adsorption of proteins was reduced by introducing 5 mg/mL BSA dissolved in phosphate buffered saline (PBS), pH 7.2.

MEKC of the proteins labeled with Alexa Fluor 633 dye was performed with a TRIS/HCl electrolyte (100 μM, pH 9.2, Bio-Rad Laboratories) and 1% SDS used above its cmc. The appropriate concentration of protein was diluted in the carrier electrolyte and electrokinetically injected into the cross channel as described above. Electrophoresis of the proteins was performed using an electric field strength of 300 V/cm.

3.3. Results and Discussion

3.3.1. Optimization of Embossing and Assembly Process Steps

Microchip channel dimensions and how reproducible they are formed during the replication steps can affect electrophoresis separation performance and detection. In terms of column performance, the ability of the separation channel and injector to produce narrow peaks, which is quantitatively described by plate numbers, N (N is directly related to the migration time and inversely related to peak width), is critically important. The contributions to peak broadening can arise from Joule heating, which tends to broadened peaks more extensively with larger channel dimensions, reducing separation performance.[37] Joule heating can distort plug geometry due to the establishment of radial temperature profiles across the lumen of the microchip channel. The plate height contribution from Joule heating (H_{Joule}) can be calculated from;

$$H_{Joule} = [1713/T^2]^2 \cdot [\mu_a E^5 k_b^2 (0.5\, d_{chan})^6 / 236.7\, D \cdot k_b^2] \quad (3.1)$$

where T is the absolute temperature, μ_a is the apparent mobility of the solute, E is the applied electric field strength, k_b is the thermal conductivity of the buffer, d_{chan} is the channel depth, and D is the diffusion coefficient.[38] As shown in equation 3.1, $H_{Joule} \alpha d_{chan}^6$, indicating a strong dependence of the plate height on microchannel depth. If the temperature profile gives rise to a parabolic flow over both the width and depth of the channel lumen, the plate height contribution from Joule heating will increase ~8 fold faster than that predicted by equation 3.1 with respect to channel dimensions.[38]

In terms of the limit of detection (LOD), changing the dimensions of the microchannels will produce different injection volumes when using cross-T geometries that can affect the concentration LOD. Deeper channels provide better LODs.[39] However, care must be taken not to produce an injection volume that is >~1% of the separation channel volume, since this can

reduce the plate numbers. In addition, care must be taken when employing "turns" in the separation channel to provide sufficient column lengths for adequate resolving power (plate generation) over a small footprint. This geometrical dispersion artifact scales with channel width, with wider channels providing reduced plate numbers.[40]

Table 3.1 provides a summary of the micromanufacturing data collected for the different polymers investigated in this study in which hot embossing was used to replicate the polymer substrates from metal masters. PMMA and PC are the most common substrates used in microchip electrophoresis. PMMA, is an amorphous, transparent and colorless thermoplastic that is hard and stiff but brittle and notch-sensitive. General purpose grade PMMAs can be extruded and injection molded. Monomer casting is also used to achieve much higher molecular weights. Thin sheets are normally made from impact modified grades, which incorporate a small portion of elastomers in order to improve their flexibility. It should be noted that polymers containing the same monomer units (see Figure. 3.1) are classified differently based on polymer molecular weight, the amount of additives included in the formulation and the method of polymer sheet manufacturing. For example, four different types of PMMA were investigated in this study. PMMA (first entry in Table 3.1), based on manufacturer's information, has good abrasion properties, and excellent optical clarity but poor low temperature fatigue and solvent resistance. The second PMMA listed in Table 3.1 is referred to as clear acrylic (C-PMMA) and according to manufacturer's data is UV stabilized. Gray acrylic (G-PMMA) is made by adding some gray-color additive to C-PMMA during the manufacturing process. Medical grade PMMA (MG-PMMA) is additive-free and the purest (and probably the highest molecular weight) grade of PMMA available and is usually used to make optical lenses.

PC is a crystal clear, colorless, and amorphous thermoplastic. It has good temperature resistance and dimensional stability, low creep, but somewhat limited chemical resistance. Two

types of PC were included in this study and they are listed in Table 3.1 as well. Lexan (LX-PC) contains a special coating, which adds abrasion resistance to the optical grade PC films during manufacturing, but is not present in the native PC material. This offers excellent impact and solvent resistance according to the manufacturer's information.

Polyethylene, PE, is a family of related commodity thermoplastics that traditionally are differentiated by their density or degree of chain branching. PE is made by a low pressure process using Ziegler-Natta or related catalysts. High-density polyethylene, HDPE, (~70 – 80% semi-crystalline) is more rigid, harder and with better chemical resistance than its counterpart, low-density polyethylene, LDPE (~50% semi-crystalline). In addition, its tensile strength is four times higher than LDPE and its compressive strength is three times higher. HDPE is also abrasion resistant, maintains excellent machinability and self-lubricating characteristics. It also has one of the highest impact strengths of any thermoplastic available and maintains its properties at extremely low temperatures.

PET is a hard, stiff, strong dimensionally stable material that absorbs very little water. It has good chemical resistance except to alkalis, which hydrolyse it. Its crystallinity varies from amorphous to fairly high crystalline. Polyethylene terephthalate glycolate (PETG) is the glycol-modified form of PET and consists of the same monomer unit (see Figure 3.1).

PS is an amorphous and colorless commodity thermoplastic that is rigid, relatively hard and brittle. It has good electrical properties, excellent gamma radiation resistance and can be radiation sterilized.

Polypropylene, PP, is a semi-crystalline, white, semi-opaque commodity thermoplastic made in a very wide variety of grades and modifications. It is a linear polyolefin with favorable chemical resistance, which can be compared in many ways to HDPE in that it is manufactured in a similar manner. The catalysts used control the polymer's stereoregularity quite well so that

commercial PPs are usually predominantly isotactic. PP is harder and has higher temperature resistance than HDPE.

Polyurethane, PU, is a unique material that offers the elasticity of rubber combined with the toughness and durability of metal. It is available in a very broad hardness range with an excellent resistance to solvents. Compared to plastics, urethanes offer superior impact resistance, while offering excellent wear properties and elastic memory.

Nylon (NY) is a semi-crystalline, white thermoplastic that can be monomer cast. This allows the production of NY sheets without voiding and gives a product with slightly reduced extensibility and impact strength.

Polysulfone (PSU) is a tough, rigid, high strength transparent thermoplastic, which maintains its properties over a wide temperature range. PSU has very high dimensional stability, it shows very high resistance to acids, alkali, and salt solutions and is not resistant to polar organic solvents, such as ketones, chlorinated hydrocarbons and aromatic hydrocarbons.

Poly(acrylonitrile-butadiene-styrene), ABS, is an amorphous, off-white/grayish thermoplastic that is relatively hard and reasonably tough. Generally ABS is easily processed and bonded but has poor solvent and fatigue resistance.

Table 3.1 shows T_g values obtained for different polymers measured by using DSC. The phase transitions of polymers are considered to occur at a physical state where all materials exhibit the same free fractional volume, independent of the chemical structure of the polymer. The T_g value depends on the thermal expansion coefficient and the heat capacity of the polymer.[41] For example, as can be seen from Table 3.1, different types of PMMA have different T_g's most likely due to differences in the additives present in the polymer formulation as well as differences in their molecular weights. These changes in polymer formulation and/or molecular weight affect the thermal expansion coefficient and heat capacity.

One of the most widely used replication processes to fabricate channel structures for μ-CE applications is hot embossing.[10] After fabrication, a master is mounted in an embossing system together with the polymer substrate. In this work, a Ni master was used to produce the fluidic pattern on the polymer surface using hot embossing, but other materials can be used for the master as well, such as glass or silicon.[10] Both the substrate and master are heated separately in a vacuum chamber and after reaching thermal equilibrium, the master is brought into conformal contact with the polymer substrate between platens with a fixed pressure for a specified amount of time.[10] The parameters reported for embossing including temperature, pressure and time (see Table 3.1), which were optimized using a trial-and-error method to achieve minimal replication errors. Optimization results obtained by this method were verified and controlled in certain cases (e.g., LDPE, PP, PET and PU with large %RE) using a Taguchi optimization methodology with individual optimization matrices for embossing of each polymer chip. Details of this methodology are reported elsewhere.[42] Briefly, a suitable matrix-assisted array (L_{25}) for optimization of the embossing for each desired polymer was used to minimize %RE as the optimization response. This is performed by logically changing the levels of the investigated factors (i.e., embossing temperature, pressure and time), which was determined by optimization matrix-assisted arrays. A surface profiler was used to measure the topographic features of the micro-channels embossed from the master from which REs could be assessed. The %RE values reported in Table 3.1 were obtained from the variation in the channel depth (d_{chan}) of the embossed structure compared to the master height (h_{master}) from the following equation:

$$\%RE = 100\% \, (h_{master} - d_{chan}) / (h_{master}) \qquad (3.2)$$

The optimal embossing temperature for all polymers was found to be slightly above their respective T_g. Both forms of PC showed small %RE values with %RE of 0.4 and 0.9, for PC and LX-PC, respectively. HDPE also showed a relatively small %RE value (0.5), while its

low-density counterpart produced much higher replication errors (13.6, see Table 3.1). For PMMAs, MG-PMMA (%RE = 1.8) showed slightly lower %RE values compared to the other types of PMMA (%RE = 4.2 – 5.5). We suspect that large replication errors are associated with large differences in the thermal expansion coefficients between the embossing master and the particular polymer substrate. For example, the linear thermal expansion coefficient for Ni is ~17 ppm $^{o}C^{-1}$, while for PMMA it is ~70 ppm $^{o}C^{-1}$ and PC the linear thermal expansion coefficient is ~68 ppm $^{o}C^{-1}$.[43] For PMMA and PC, the %RE were relatively small, with values of 1.8 (MG-PMMA) and 0.4 (PC). On the other hand, LDPE and PET were found to produce %REs of 13.6 and 9.6, respectively, and possessed linear thermal expansion coefficients of 250 ppm $^{o}C^{-1}$ for both materials. When using polymer substrates with significantly different thermal expansion coefficients compared to the embossing master, replication errors can be minimized by using other replication techniques, such as injection molding.[10] For example, it has been demonstrated that PP can be replicated with high integrity using injection molding.[44]

All embossed polymers in this study showed similar surface roughnesses with an average value of $(R_a/\lambda_a) = 0.021 \pm 0.004$ μm. The independent nature of surface roughness on microchip substrate is due to the use of embossing, which is able to produce embossed polymer surfaces with similar rugosity to that of the molding die. Therefore, the roughness observed was due to the molding die and not to the embossing process.

The common approach for enclosing fluidic networks formed by replication molding is thermal assembly, in which the substrate and cover plate are clamped together and placed in an oven and heated to a temperature slightly above the T_g of the substrate. When using thermal annealing for chip assembly, it is preferable to match the substrate material to that of the cover plate. This eliminates the creation of a "hybrid" device, in which the EOF generated by the substrate is different from that of the cover plate due to differences in surface chemistry. EOF

mismatch can detrimentally affect electrophoresis performance by producing distorted plug profiles typically associated with electrokinetically driven flows.[45]

As shown in Table 3.1 for the polymers investigated, thermal annealing produced the best results when assembly was performed near the T_g for most of the polymers. The quality of annealing was tested by physically examining how the cover plate was bonded to the embossed substrate (presence of air pockets, microstructure deformation, or solvent leakage when pumping fluid through the fluidic network at constant pressure). For a well annealed chip, no leaks were observed after hydrostatically pumping water through the channel using a syringe pump. For PET, PU, and NY, thermal annealing at temperatures near their T_g was not successful as determined by the observation of significant fluid leakage. Annealing of these particular polymers to prevent leakage required temperatures $>T_g$, which resulted in significant collapsing of the embossed microstructures. Successful annealing of PET was accomplished using a PET/PE copolymer cover sheet.[46]

3.3.2. Optical Clarity

3.3.2.1. Absorbance Background

Many researchers use absorption as a detection mode for microdevices.[2, 7] Therefore, an evaluation of the wavelength-dependent absorption properties of various polymers was carried out to assess usable wavelength regions for UV/Vis detection. The absorbance values for a polymer was measured using a UV/Vis spectrophotometer at six different wavelengths (200, 214, 254, 260, 280, and 320 nm).[2, 7, 23, 26, 47] For comparison, the absorbance value measured at each wavelength was divided by the absorption obtained for glass at that same wavelength. Figure 3.3 shows the results of this investigation.

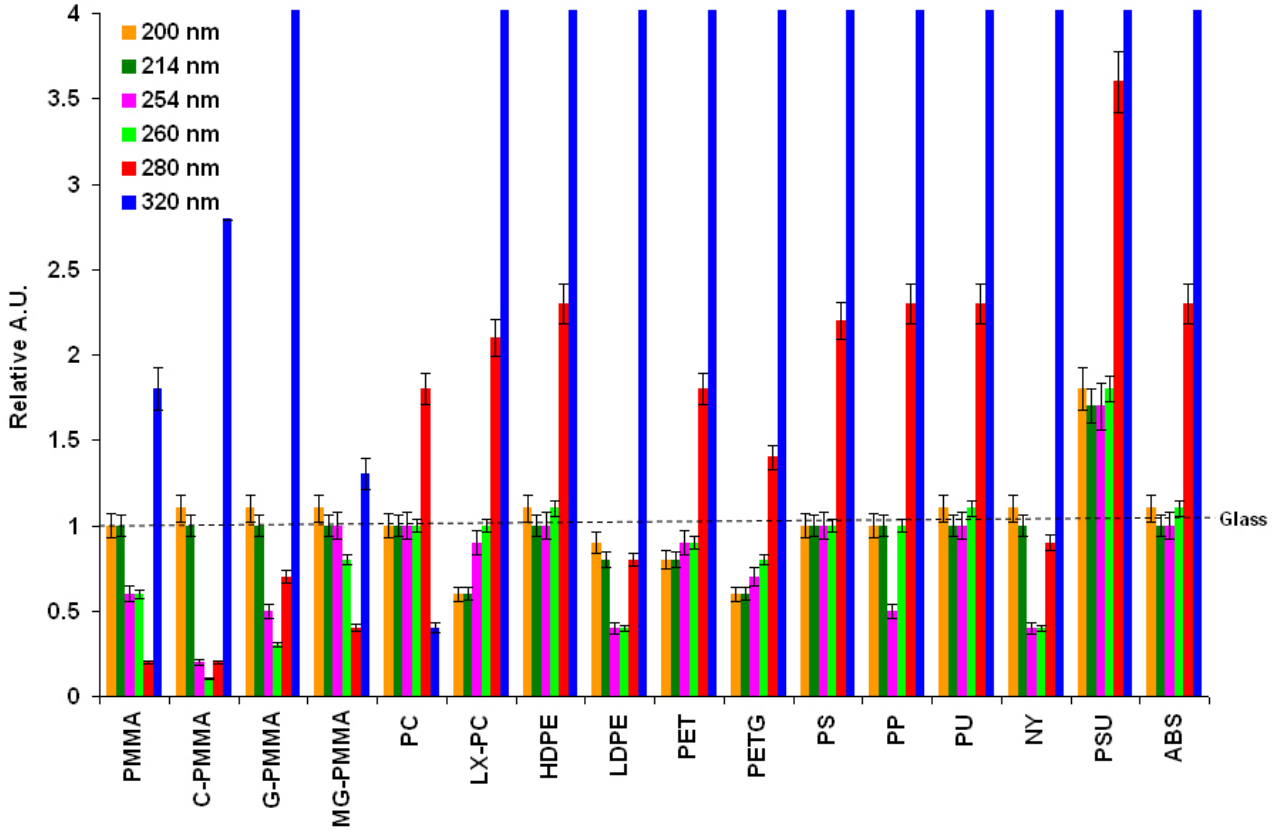

Figure 3.3. Normalized absorbance values of the native polymers evaluated in this study. The normalized absorbance values for each polymer were calculated by dividing the absorbance obtained for glass at each particular wavelength for all six wavelengths investigated.

The absorption of ultraviolet or visible radiation generally correlated to electronic transitions in the polymer under study. There are four types of possible electronic transitions: $\sigma \rightarrow \sigma^*$ (λ_{max} <200 nm), $n \rightarrow \sigma^*$ (λ_{max} ~150 – 250 nm), and $n \rightarrow \pi^*$ or $\pi \rightarrow \pi^*$ (λ_{max} ~200 – 700 nm). The absorbance values reported in Figure 3.2 originate from one or several of these electronic transitions of the polymer and/or transitions from additives or impurities found in the polymer sheet. As shown in Figure 3.2, all polymers showed strong absorbance at 320 nm compared to glass due to possible $n \rightarrow \pi^*$ or $\pi \rightarrow \pi^*$ electronic transitions. Inspection of the monomer units comprising these polymers (see Figure 3.1) shows that in several cases, no chromophores exist in their backbones, such as PP, PE. In addition, the four types of PMMA evaluated in this study indicated that MG-PMMA showed little changes in its UV/Vis clarity

compared to glass at all the wavelengths tested. This data indicates that a major cause of UV/Vis absorbance in most of these materials could be due to additives/impurities found in the sheet polymer since MG-PMMA is free from these types of additives.

3.3.2.2. LIF Background

The LOD for readout is determined partly by the amount of background observed in the measurement. Favorable LODs using LIF can be achieved by reducing the autofluorescence or scattering produced from the microchip substrate.[48] Studies were carried out to determine the amount of autofluorescene produced from commonly used polymer microfluidic substrates. The autofluorescence of polymers was evaluated using three different laser excitation wavelengths that are widely used for the detection of labeled biological samples analyzed electrophoretically.[2, 3] To avoid bleaching, the glass and polymer sheets were slowly translated through the stationary laser spot. In order to compare the results obtained from different lasers, the average fluorescence intensity (n = 5) of the polymers was normalized with respect to the value obtained for glass at the same excitation wavelength. Results of these measurements are presented in Figure 3.4.

Fluorescence from polymers occurs primarily from low energy $\pi \rightarrow \pi^*$ transitions. As a result, polymers with highly conjugated double bond structures with aromatic systems (e.g., ABS, PETG) showed higher fluorescence levels compared to MG-PMMA, which has no aromatic structure or conjugated double bonds in its molecular structure nor additives. All polymers investigated showed lower background levels at 780 nm compared to 632.8 nm or 488 nm. This is consistent with our previous data, which indicated small background levels when using LIF detection at near-IR wavelengths for polymer substrates.[48] Inspection of the autofluorescence levels generated from PMMAs or PCs also demonstrated diverse background levels, even within the same class (i.e., same monomer unit). C-PMMA showed the lowest

background levels at 488, 632.8 and 780 nm with relative autofluorescence values of 1.14 ± 0.05, 0.40 ± 0.01, 0.31 ± 0.02, respectively (see Figure 3.4). On the other hand, G-PMMA showed relative autofluorescence levels of 53.09 ± 2.44, 41.12 ± 0.53, 5.17 ± 0.21 at 488, 632.8 and 780 nm, respectively.

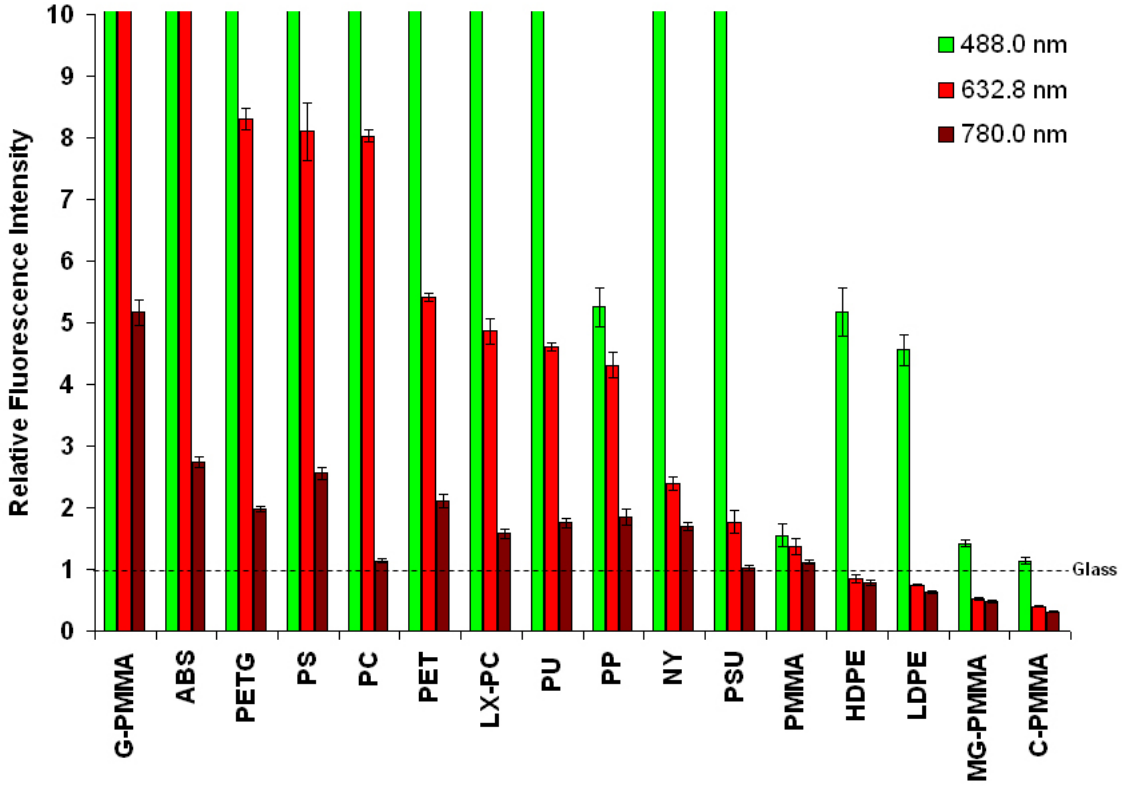

Figure 3.4. LIF background levels measured at three different excitation wavelengths, 488 nm, 632.8 nm, or 780 nm. The LIF system was configured in an epi-illumination format. In all cases, ~2 mW of average laser power was used at the polymer surface. The collected photons were filtered using an interference filter that possessed a center wavelength red-shifted by ~30 nm from the excitation wavelength with a half-band width of ~10 nm. The average fluorescence intensity (cps) of the polymers was normalized with respect to the value obtained for glass at the same excitation wavelength.

3.3.3. Contact Angle Measurements

Water contact angles and EOF measurements have been widely used to characterize channel surfaces, especially those involved in μ-CE applications. Wall surface chemistry is particularly important in microchip devices due to the high surface-to-volume ratio. In order to

prevent adsorption of analytes onto the channel wall and to provide favorable wettability by the aqueous carrier electrolyte, the microchip surface should be sufficiently hydrophilic.[9, 18] Contact angles can be used as a measure of hydrophilicity/hydrophobicity of the polymer surface; polymers with small contact angles show more hydrophilic characteristics than those with higher contact angles.[14, 49] The contact angle of several different embossed polymer microchips was therefore investigated.

A summary of water contact angles for embossed polymer chips are shown in Table 3.2. As can be seen, PP was found to have the most hydrophobic properties of the polymers investigated with a contact angle of 104 ± 3. G-PMMA with a contact angle of 27 ± 2 was found to be the most hydrophilic polymer with a contact angle smaller than that of glass (contact angle = 35 ± 3). The large change in contact angle for G-PMMA compared to C-PMMA is most likely due to the gray color additive added to G-PMMA during the manufacturing process.

Wettability of a polymer surface is dependent on surface energy and surface roughness.[50] Since the surface roughness of embossed polymers was determined primarily by the rugosity of the molding die and not the substrate (see Section 3.3.1), the differences in contact angles for these polymers can be explained primarily through surface energy effects. For example, PP (contact angle = 104 ± 4) has a lower surface energy compared to G-PMMA (contact angel = 27 ± 2). This reverse correlation between the contact angle and surface energy agrees with previous reports.[51]

3.3.4. EOF Values

The value and sign of the EOF can provide information on the nature of the surface of fluidic chips and also, can affect the performance of the electrophoretic separation. For example, EOFs that move from anode to cathode are indicative of a surface with excess negative charge

with the magnitude of the EOF determined by the amount of surface charge. Typically, polymer surfaces show lower surface charge density compared to glass. The surface charge can also be described by the zeta potential, which varies between different polymers as well.[12, 52] Since the EOF can have a negative influence on CE performance, especially for macromolecule separations such as oligonucleotides and proteins, it is necessary many times to suppress or even eliminate the EOF by supplying wall coatings that block charged groups on the surface.[9] EOF suppression coatings can provide more reproducible migration times and also, minimize solute-wall interactions. EOF values of the polymers investigated in this study are shown in Table 3.2. The direction of the EOF in all native or BSA-treated polymers was found to move from anode to cathode.

3.3.4.1. EOF of Native Polymers

As can be seen in Table 3.2, all polymers that were surveyed showed lower EOFs compared to glass. LDPE (EOF = $0.83 \pm 0.03 \times 10^{-4}$ $cm^2/V\ s$) and PC (EOF = $2.22 \pm 0.09 \times 10^{-4}$ $cm^2/V\ s$) showed the lowest and highest EOF values, respectively, at the pH tested. EOF changes were also noticed within the various PMMA and PC types. Inspection of Figure 3.1 indicates that most of the polymers included in this study possessed no charged or ionizable groups in their monomer units. Because the EOF depends on surface charge density, the source of this surface charge could arise from either the additives included in the polymer formulation or photochemical alterations in the polymer backbone.[53]

3.3.4.2. EOF of BSA-Treated Polymers

A BSA solution with a concentration of 5 mg/mL was used to dynamically coat various polymer walls to potentially provide more stable EOF profiles or reduce the magnitude of the EOF. The BSA-treatment was carried out by flooding the microchip channels with BSA solution for 60 min followed by filling them with the buffer used to measure the EOF as described in the

Table 3.2. EOF, separation efficiency (N), migration time (t_{mig}), and intra/inter-chip reproducibilities of myosin in native and BSA-treated polymer microchips. The contact angles are shown for the native polymers only.

Microchip Substrate	Contact Angle	Native Microchip					BSA-Treated Microchip				
		EOF × 10^{-4} [1,2] (cm^2/Vs)	N × 10^4 [3] (plates)	t_{mig} (s)	t_{mig} (RSD%) Intra-Chip	t_{mig} (RSD%) Inter-Chip	EOF × 10^{-4} (cm^2/Vs)	N × 10^4 (plates)	t_{mig} (s)	t_{mig} (RSD%) Intra-Chip	t_{mig} (RSD%) Inter-Chip
PMMA	73 ± 3	2.07 ± 0.07	2.32 ± 0.06	371	2.1	5.1	1.27 ± 0.03	6.67 ± 0.09	115	1.3	2.2
C-PMMA	56 ± 2	1.56 ± 0.05	2.61 ± 0.06	147	1.5	4.1	1.04 ± 0.03	6.06 ± 0.05	89	0.9	1.5
G-PMMA	27 ± 2	0.95 ± 0.02	-	-	-	-	0.73 ± 0.01	-	-	-	-
MG-PMMA	43 ± 1	1.12 ± 0.04	3.01 ± 0.05	98	1.4	3.1	0.76 ± 0.02	6.70 ± 0.05	71	0.7	1.4
PC	80 ± 3	2.22 ± 0.09	2.02 ± 0.08	709	3.4	6.3	1.26 ± 0.04	6.58 ± 0.10	111	1.7	2.5
LX-PC	95 ± 3	2.12 ± 0.07	1.27 ± 0.07	449	6.2	9.2	1.07 ± 0.02	5.24 ± 0.11	93	2.3	3.3
HDPE	90 ± 2	1.58 ± 0.04	1.61 ± 0.07	147	4.0	7.4	0.88 ± 0.01	5.85 ± 0.10	82	1.8	2.8
LDPE	93 ± 3	0.83 ± 0.03	1.43 ± 0.07	78	4.9	7.8	0.45 ± 0.01	5.77 ± 0.10	62	2.0	2.9
PET	77 ± 3	-	-	-	-	-	-	-	-	-	-
PETG	71 ± 2	0.90 ± 0.02	2.46 ± 0.06	82	2.0	4.7	0.57 ± 0.01	6.71 ± 0.07	64	1.1	1.8
PS	94 ± 2	1.54 ± 0.03	1.36 ± 0.08	141	5.1	8.0	0.83 ± 0.01	5.30 ± 0.11	75	2.1	3.2
PP	104 ± 3	1.07 ± 0.03	0.94 ± 0.07	89	6.6	9.8	0.44 ± 0.01	4.40 ± 0.10	59	2.6	3.6
PU	101 ± 4	-	-	-	-	-	-	-	-	-	-
NY	68 ± 2	-	-	-	-	-	-	-	-	-	-
PSU	84 ± 2	-	-	-	-	-	-	-	-	-	-
ABS	79 ± 2	0.92 ± 0.01	-	-	-	-	0.53 ± 0.01	-	-	-	-
Glass	35 ± 3	4.21 ± 0.18	-	-	-	-	2.99 ± 0.10	-	-	-	-

1. No EOF was reported for PET, PU and NY due to the inability to thermally anneal a cover plate to the embossed substrate. 2. No stable EOF using the current monitoring technique could be generated for PSU. 3. No electrophoretic data could be secured for G-PMMA or ABS due to poor optical clarity.

experimental section. The results of this study are shown in Table 3.2. BSA treatment was observed to have a significant damping effect on the EOF for all substrates investigated. The average value of EOF reduction was ~40% across all substrate materials. Polymers such as PP with large contact angles (contact angle = 104 ± 3) showed maximum EOF suppression (59%) following BSA treatment compared to polymers with smaller contact angles, such as G-PMMA.

3.3.5. The μ-CE Performance

In order to determine the effects of different polymer substrates and wall coatings (BSA-treatment) on μ-CE performance, various materials were tested by monitoring the electrophoretic migration and plate number generation of Alexa Fluor 633-labeled myosin as a model with LIF excitation at 632.8 nm. All electrophoretic tests were performed with a running buffer consisting of 100 μM TRIS/HCl, 1% SDS, pH 9.2, a field strength of 300 V/cm and an effective separation length (L_{eff}) of 30 mm. The plate numbers were calculated using,

$$N = [41.7(t_{mig}/w_{0.1})^2]/(A/B + 1.25] \quad (3.3)$$

where t_{mig} is the migration time, $w_{0.1}$ is the band width measured at one-tenth of the maximum height, and A and B are asymmetry peak parameters.[54] Variation in the migration times for myosin was also evaluated in terms of run-to-run (intra-chip, n = 3) and chip-to-chip (inter-chip, n = 3) reproducibility. Due to the high background levels at 632.8 nm (see Figure 3.4), G-PMMA and ABS could not be used in these studies. Also, PET, PU and NY were eliminated from this investigation because of the inability to anneal a cover plate to the substrate. PSU was also eliminated due to its unstable EOF.

The results of this investigation are shown in Table 3.2 both for native and BSA-treated polymers. As shown in Table 3.2, low EOF polymers (e.g., LDPE, EOF = 0.83 ± 0.03 × 10^{-4} cm^2/V s) as compared to high EOF polymers (e.g., PC, EOF = 2.22 ± 0.09 × 10^{-4} cm^2/V s) showed smaller migration times of myosin, with the migration time of myosin increasing from

78 ± 5 s in LDPE to 709 ± 34 s in PC. As noted by Strege and co-workers,[55] one of the disadvantages of using MEKC in the presence of EOF is the relatively long migration times associated with the analytes. Because the charged micelles (negative in this case) possess an electrophoretic mobility that moves in the direction of cathode to anode and is counter to the EOF of the polymers investigated herein, analytes which associate strongly with the micelles tend to migrate very slowly through the channel. Therefore, polymers with larger EOFs should result in longer migration times for the analyte using MEKC with anionic micelles as observed in our data.

Both intra-chip and inter-chip reproducibilities in terms of migration times of myosin were improved using polymers with small contact angles (see Table 3.2). For example, PP showed an RSD of 6.6% and 9.8% for intra-chip and inter-chip reproducibility, respectively, while the RSDs for the intra-chip and inter-chip reproducibilities were 1.4% and 3.1% in MG-PMMA, respectively. Decreased reproducibility in the migration time with polymers possessing large contact angles could be due to non-specific adsorption of myosin to this hydrophobic surface compared to the hydrophilic (i.e., lower contact angles) substrates, which would minimize non-specific adsorption.[9,14,49] In all polymers investigated, lower RSD values were obtained intra-chip (average RSD = 3.7%) compared to inter-chip (average RSD = 6.6%).

Plate numbers for myosin were also found to change for different chip materials as well. The maximum plate number was obtained for MG-PMMA ($N = 3.01 \times 10^4$ plates) while PP showed the lowest number of generated plates ($N = 0.94 \times 10^4$ plates). We suspect that the substrate-dependent plate numbers resulted from potential solute-wall interactions. The interactions of proteins with surfaces can be of two general types: bio-specific or non-specific. Bio-specific interactions, such as the interaction of an antibody with an antigen-bearing surface or binding of avidin to a bio-tinylated surface, rely on close complementarity between the protein

and the surface. On the other hand, non-specific interactions are induced by forces such as electrostatic, hydrophobic interactions, or Van der Waals forces.[56] Non-specific interactions between the channel surfaces and proteins usually involve hydrophobic interactions,[57] although electrostatic interactions may be present as well with charged or polar surfaces.[58]

The effect of BSA pretreatment on myosin microchip separations for selected polymer microchips was next investigated. As shown in Table 3.2, migration times of myosin in all BSA-treated polymers decreased compared to their native polymer counterparts. This was primarily due to EOF suppression of BSA-treated polymers. The maximum change in migration time was observed for PC (709 ± 34 s in native PC compare to 111 ± 2 s in BSA-treated PC, 84.3% change) and the minimum change was observed for LDPE (78 ± 5 s in native LDPE compare to 62 ± 2 s in BSA-treated LDPE, 20.5% change). This result indicates that suppressing EOF effectively accelerates the migration of myosin in MEKC-based separations, especially for high EOF polymer substrates such as PC.

Peak efficiency of myosin was also found to increase in BSA-treated polymers compared to their native counterparts. For example, the plate numbers for myosin in PP improved by 368% when moving to a BSA-coated chip ($N_{native} = 0.94 \times 10^4$ plates, $N_{BSA\text{-}treated} = 4.40 \times 10^4$ plates) while MG-PMMA showed a 122% improvement ($N_{native} = 3.01 \times 10^4$ plates, $N_{BSA\text{-}treated} = 6.70 \times 10^4$ plates). The significant improvement in the plate numbers for PP can be correlated to its large contact angle compared to MG-PMMA, which has a smaller water contact angle. Therefore, in the case of myosin, solute-wall interactions are predominantly mediated by hydrophilic/hydrophobic interactions considering that the pI for myosin is ~5.5 and at the running electrolyte used for these separations (pH = 9.2), the EOF runs from anode to cathode indicating a negatively charged surface. Saturating the microchannel surface with BSA

minimizes solute-wall interactions by BSA occupying the available adsorption sites on the polymer surface.

In Table 3.2 is also shown intra- and inter-chip reproducibilities of our electrophoresis results obtained for myosin in terms of migration time for both native and BSA-treated polymers. The average intra- and inter-chip reproducibility in BSA-treated chips was 1.6% and 2.5%, respectively, while for the native polymers, the average intra-chip and inter-chip RSDs were 3.7% and 6.6%, respectively. These numbers show an improvement in both the intra-chip and inter-chip reproducibilities for BSA-treated materials compared to the native materials due to suppression of both the EOF and non-specific adsorption of myosin to the channel wall. RSDs for myosin migration times appear to be polymer-substrate independent after BSA-treatment compared to the native substrates considering the small gap between the highest and smallest RSDs for the BSA-treated materials (see Table 3.2).

3.3.6. On-Chip Electrophoretic Separations

A number of separations were next performed using four fluorescently-labeled proteins in microchips constructed from different polymers to show how the properties of the polymer alter separation performance. Native PP and BSA-treated PP were selected as the polymer candidates, which showed maximum improvement in terms of separation efficiency, EOF reduction and migration time reproducibility after BSA pretreatment according to the results depicted in Table 3.2. C-PMMA and PETG (pretreated with BSA) were also selected as the polymers for this study due to the large differences in optical clarity at 632.8 nm when using LIF detection (see Figure 3.4). The protein mixture contained carbonic anhydrase, phosphorylase B, β-galactosidase and myosin as used in our previous work.[14] All electrophoreses were performed in reverse mode with the running electrolyte consisting of 100 μM TRIS/HCl, 1% SDS, pH 9.2. The resulting electropherograms are shown in Figure 3.5.

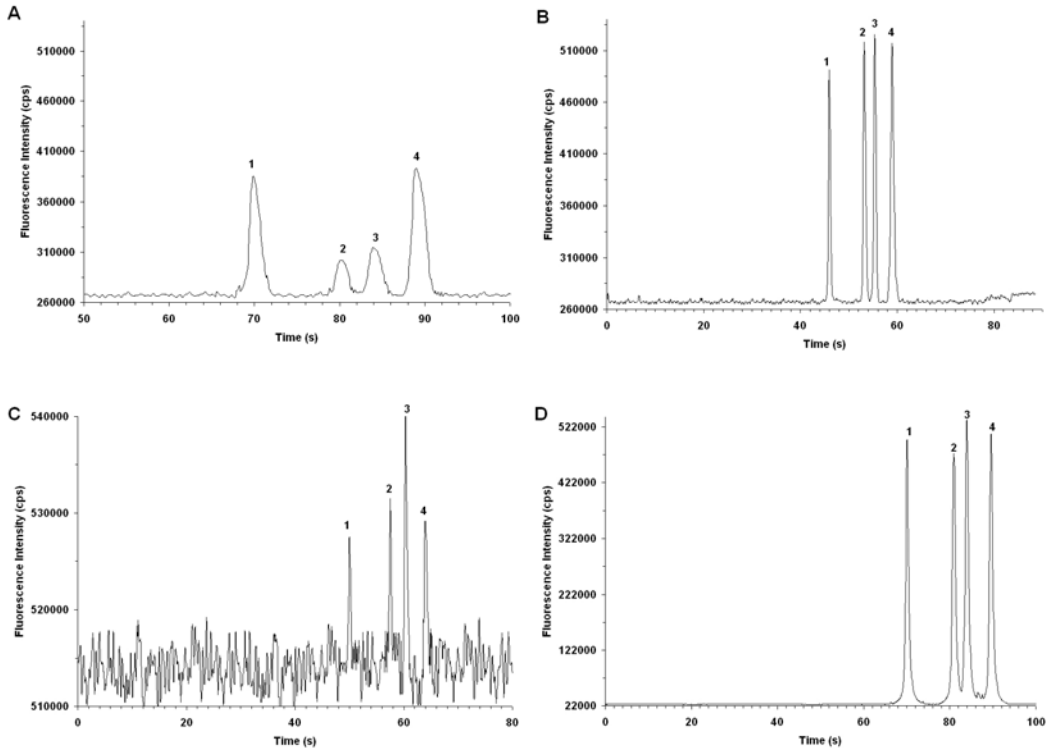

Figure 3.5. Electrophoretic separation of several proteins in polymer microchips: (A) Native PP, (B) BSA-treated PP, (C) BSA-treated PETG, (D) BSA-treated C-PMMA. All separations were performed with a running buffer consisting of 100 μM TRIS/HCl, 1% SDS, pH 9.2; E = 300 V/cm; L_{eff} = 30 mm; LIF detection (excitation = 632.8 nm; ~2 mW average power). The electrophoretic peaks are identified as; 1: Carbonic anhydrase, 2: Phosphorylase B, 3: β-Galactosidase, and 4: Myosin. In all cases, the concentration of the proteins used for the electrophoresis was 300 nM.

The average migration time of the four labeled proteins in native-PP (80.8 s) was longer than the value found in BSA-treated PP (53.2 s), because of the lower EOF associated with the BSA-treated PP. C-PMMA and PETG showed average migration times of 81.0 s and 58.0 s, respectively. The MEKC separation window was calculated to be 19, 19, 14 and 13 s for native-PP, C-PMMA, PETG and BSA-treated PP, respectively. Average separation efficiencies were calculated to be 0.97×10^4 plates and 4.42×10^4 plates, respectively, for native- and BSA-treated PP in agreement with the myosin results. Comparison of Figures 3.5B, C and D shows that by moving from BSA-treated PP to BSA-treated PETG and BSA-treated C-PMMA, migration times increased due to differences in the EOF of these polymers (see Table 3.2). The

average separation efficiency also decreased in the order of BSA-treated PP (4.42×10^4 plates) < BSA-treated C-PMMA (6.01×10^4 plates) < BSA-treated PETG (6.68×10^4 plates).

Resolution (R_s) for selected peak pairs was calculated using $R_s = (t_{mig2}-t_{mig1})/0.5(t_{w1}+t_{w2})$, in which t_{mig1}, t_{mig2} are migration times for species 1 and 2, respectively, and t_{w1}, t_{w2} are their band widths measured at the base of the peak. β-galactosidase and myosin were successfully separated in all BSA-treated polymer chips with a resolution of 1.48, 3.48, 3.69, and 3.96, in native-PP, BSA-treated PP, BSA-treated C-PMMA and BSA-treated PETG, respectively. Phosphorylase and β-glactosidase were also resolved in native-PP, BSA-treated PP, BSA-treated C-PMMA and BSA-treated PETG microchips with a resolution of 1.24, 1.84, 2.12 and 2.61, respectively. Finally, resolution between carbonic anhydrase and phosphorylase were determined to be 3.40, 7.02, 8.48 and 8.56 in native-PP, BSA-treated PP, BSA-treated C-PMMA and BSA-treated PETG chips, respectively. The average resolution of these four model proteins increased in this manner: BSA-treated PETG ($R_{s,ave.} = 5.04$) > BSA treated C-PMMA ($R_{s,ave.} = 4.76$) > BSA treated PP ($R_{s,ave.} = 4.11$) > native-PP ($R_{s,ave.} = 2.04$). This order is in agreement with the increasing efficiency in these polymer chips.

To evaluate the LOD for the labeled proteins using polymer microchips, separations were performed on different concentrations of the protein conjugates. The LOD was evaluated in PP, PETG and C-PMMA microchips by using myosin in the concentration range of ~500 pM to 500 nM. C-PMMA showed the best LOD (800 pM, SNR = 3). PP and PETG provided detection limits that were 4 nM (SNR = 3) and 270 nM (SNR = 3), respectively. The order of polymer chip LODs is in agreement with the background levels observed for these polymers when using 632.8 nm excitation.

The stability of the polymer-based devices was studied by performing multiple electrophoresis runs on a single chip. Figure 3.6 represents the results of this study. The change in separation efficiency of protein mixtures in C-PMMA, PP and PETG microchips after BSA treatment was investigated versus the number of electrophoretic runs for myosin. The chip was initially treated with BSA prior to the first run according to the protocol discussed earlier, electropherograms were collected using LIF excitation at 632.8 nm, and the values of N for myosin calculated. All polymers showed consistent plate numbers even after 7 sequential runs. PP showed the best performance stability (8.1% loss in plate numbers after 7 runs). The stability of the BSA-treated PP is most likely due to stronger BSA adsorption to PP because of the higher hydrophobicity (i.e., larger contact angle) exhibited by PP compared to the other polymer substrates.

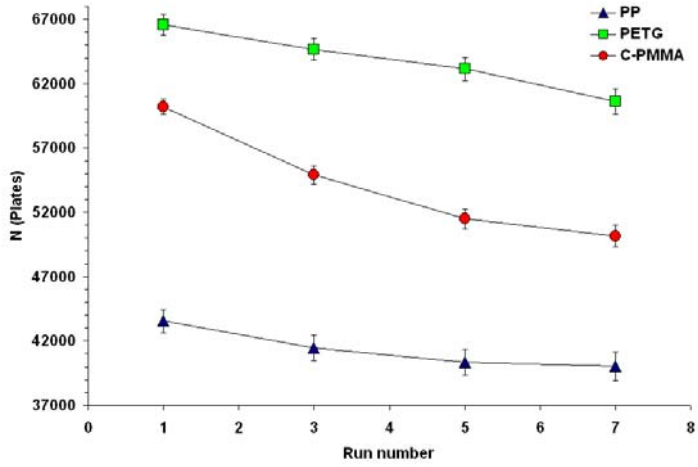

Figure 3.6. Variation of several electrophoretic separation runs in terms of efficiency (plate numbers) for PP, PETG and C-PMMA microchips following BSA treatment using myosin as the model protein. See Figure 3.5 for the electrophoresis conditions.

The effects of pH on μ-CE performance were also studied. A desirable pH should be selected to provide high efficiency MEKC separations, which can be accomplished by suppressing the EOF and minimizing non-specific adsorption of proteins to the microchip channel surface. In terms of MEKC separations, previous works has shown improvements in

separation efficiencies at alkaline pH values when using anionic surfactants, such as SDS.[59] Also, the use of high pH buffers produces similar net charges of all proteins contained in a complex mixture. The buffer pH can also affect the adhesion of a protein to a surface primarily due to changes in hydrogen bonding and electrostatic interactions.[60] In that study, the authors showed that adhesion between a solution protein and a BSA-treated surface decreased when the pH was increased over a range of 4.5 – 10.[6] Therefore, working at high pH values should minimize interactions between the proteins being separated and the BSA layer.

Figure 3.7 represents the results of our pH study. The change in plate numbers of the model protein mixture in C-PMMA, PP and PETG microchips after BSA pretreatment was investigated versus buffer pH. As can be seen, all polymers showed a dramatic increase in plate numbers at higher pH values in concurrence with the aforementioned observations.

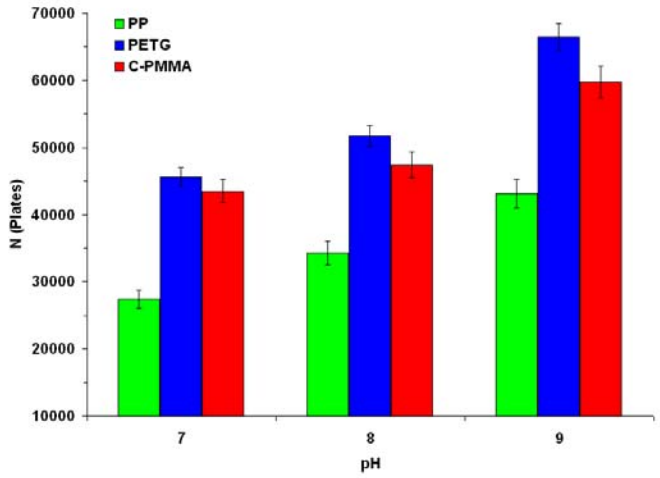

Figure 3.7. Variation of pH buffer in terms of efficiency (plate numbers) for PP, PETG and C-PMMA microchips following BSA treatment. Electrophoresis conditions were similar to those in Figure 3.6 except the pH was altered to the values noted in the figure.

3.4. Conclusions

The substrate material used for a particular microchip application requires careful consideration to its physiochemical properties prior to fabrication in order to provide optimal

performance, both from a manufacturing and operational point of view. The attractive nature of polymer-based substrates is that a wide range of materials can be selected to suite the application. In this chapter, we have demonstrated that several key physiochemical properties must be considered to provide a viable platform for performing microchip electrophoretic separations. For example, replication of microstructures from metal masters require strict attention to such properties as the thermal expansion coefficient, which can impact channel dimensions that can affect separation performance via excessive Joule heating lowering plate numbers or effects on the LOD. Another important parameter to consider is the glass transition temperature of the polymer, which can guide optimization of the replication process and also assembly of the microchip. Thermal assembly is typically used as a procedure to enclose the fluidic network with a cover plate made from the same material as that of the substrate to eliminate formation of a "hybrid" device. In our study, several polymers showed poor thermal annealing properties, such as PET, PU and NY, due to microstructure collapse during thermal processing.

For detection, both the substrate material and the channel dimensions can impact the observed LOD. To obtain favorable LODs, microchip substrates should provide low background levels (i.e., minimal absorption losses or autofluorescence levels at the monitoring wavelengths). The results in our study indicated that a wide variation in background levels existed between different polymers. In addition, microstructure channel dimensions were also viewed as critical to provide favorable LODs, with deeper channels that are narrow producing better LODs while maintaining separation performance by allowing efficient heat transfer and minimal geometrical zone dispersion.[40] While the optical properties of the polymer material vary tremendously, the use of red excitation wavelengths typically provide lower background levels across the entire set of polymers investigated herein.

In terms of the operational characteristics of the material for microchip electrophoresis, a number of physiochemical properties should be carefully evaluated as well, such as the hydrophobicity/hydrophilicity of the material (assessed using sessile water contact angles), EOF and surface modification (covalent or dynamic). For protein separations using polymer-based microchips, efficient and reproducible separations could be achieved using substrates in their native form that provided low EOFs and displayed a hydrophilic character. However, pretreatment of the polymer surfaces evaluated in this study using a dynamic coating of BSA provided significantly improved efficiency and better intra/inter-chip reproducibilities due to suppression of the EOF and the reduction of solute/wall interactions.

3.5. References

(1) Kennedy, R. T.; German, I.; Thompson, J. E.; Witowski, S. R. *Chemical Reviews (Washington, D. C.)* **1999**, *99*, 3081-3131.

(2) Vilkner, T.; Janasek, D.; Manz, A. *Analytical Chemistry* **2004**, *76*, 3373-3386.

(3) Chen, L.; Ren, J. *Combinatorial Chemistry and High Throughput Screening* **2004**, *7*, 29-43.

(4) Lion, N.; Rohner, T. C.; Dayon, L.; Arnaud, I. L.; Damoc, E.; Youhnovski, N.; Wu, Z.-y.; Roussel, C.; Josserand, J.; Jensen, H.; Rossier, J. S.; Przybylski, M.; Girault, H. H. *Electrophoresis* **2003**, *24*, 3533-3562.

(5) Belder, D.; Ludwig, M. *Electrophoresis* **2003**, *24*, 3595-3606.

(6) Yin, X.-B.; Wang, E. *Analytica Chimica Acta* **2005**, *533*, 113-120.

(7) Quigley, W. W. C.; Dovichi, N. J. *Analytical Chemistry* **2004**, *76*, 4645-4658.

(8) Wang, Z.; Swinney, K.; Bornhop, D. J. *Electrophoresis* **2003**, *24*, 865-873.

(9) Dolnik, V. *Electrophoresis* **2004**, *25*, 3589-3601.

(10) Becker, H.; Gartner, C. *Electrophoresis* **2000**, *21*, 12-26.

(11) Rathore, A. S. *Electrophoresis* **2002**, *23*, 3827-3846.

(12) Kirby, B. J.; Hasselbrink, E. F., Jr. *Electrophoresis* **2004**, *25*, 203-213.

(13) Soper, S. A.; Ford, S. M.; Qi, S.; McCarley, R. L.; Kelly, K.; Murphy, M. C. *Analytical Chemistry* **2000**, *72*, 642A-651A.

(14) Galloway, M.; Stryjewski, W.; Henry, A.; Ford, S. M.; Llopis, S.; McCarley, R. L.; Soper, S. A. *Analytical Chemistry* **2002**, *74*, 2407-2415.

(15) Tan, W.; Fan, Z. H.; Qiu, C. X.; Ricco, A. J.; Gibbons, I. *Electrophoresis* **2002**, *23*, 3638-3645.

(16) Xu, J.; Locascio, L.; Gaitan, M.; Lee, C. S. *Analytical Chemistry* **2000**, *72*, 1930-1933.

(17) Abad-Villar, E. M.; Tanyanyiwa, J.; Fernandez-Abedul, M. T.; Costa-Garcia, A.; Hauser, P. C. *Analytical Chemistry* **2004**, *76*, 1282-1288.

(18) Liu, J.; Pan, T.; Woolley, A. T.; Lee, M. L. *Analytical Chemistry* **2004**, *76*, 6948-6955.

(19) Zuborova, M.; Demianova, Z.; Kaniansky, D.; Masar, M.; Stanislawski, B. *Journal of Chromatography, A* **2003**, *990*, 179-188.

(20) Herr, A. E.; Molho, J. I.; Drouvalakis, K. A.; Mikkelsen, J. C.; Utz, P. J.; Santiago, J. G.; Kenny, T. W. *Analytical Chemistry* **2003**, *75*, 1180-1187.

(21) Tabuchi, M.; Kuramitsu, Y.; Nakamura, K.; Baba, Y. *Analytical Chemistry* **2003**, *75*, 3799-3805.

(22) Wen, J.; Lin, Y.; Xiang, F.; Matson, D. W.; Udseth, H. R.; Smith, R. D. *Electrophoresis* **2000**, *21*, 191-197.

(23) Rossier, J. S.; Schwarz, A.; Reymond, F.; Ferrigno, R.; Bianchi, F.; Girault, H. H. *Electrophoresis* **1999**, *20*, 727-731.

(24) Li, Y.; DeVoe, D. L.; Lee, C. S. *Electrophoresis* **2003**, *24*, 193-199.

(25) Li, Y.; Buch, J. S.; Rosenberger, F.; DeVoe, D. L.; Lee, C. S. *Analytical Chemistry* **2004**, *76*, 742-748.

(26) Huang, T.; Pawliszyn, J. *Electrophoresis* **2002**, *23*, 3504-3510.

(27) Chabinyc, M. L.; Chiu, D. T.; McDonald, J. C.; Stroock, A. D.; Christian, J. F.; Karger, A. M.; Whitesides, G. M. *Analytical Chemistry* **2001**, *73*, 4491-4498.

(28) Duffy, D. C.; McDonald, J. C.; Schueller, O. J. A.; Whitesides, G. M. *Analytical Chemistry* **1998**, *70*, 4974-4984.

(29) Xiao, D.; Van Le, T.; Wirth, M. J. *Analytical Chemistry* **2004**, *76*, 2055-2061.

(30) Cui, H.; Horiuchi, K.; Dutta, P.; Ivory, C. F. *Analytical Chemistry* **2005**, *77*, 1303-1309.

(31) Wang, Y.-C.; Choi, M. H.; Han, J. *Analytical Chemistry* **2004**, *76*, 4426-4431.

(32) Bruin, G. J. M. *Electrophoresis* **2000**, *21*, 3931-3951.

(33) Roberts, M. A.; Rossier, J. S.; Bercier, P.; Girault, H. *Analytical Chemistry* **1997**, *69*, 2035-2042.

(34) Huang, X.; Gordon, M. J.; Zare, R. N. *Analytical Chemistry* **1988**, *60*, 1837-1838.

(35) Hitchcock, S. J.; Carroll, N. T.; Nicholas, M. G. *Journal of Materials Science* **1981**, *16*, 714-732.

(36) Schmidtke, S.; Russo, P.; Nakamatsu, J.; Buyuktanir, E.; Turfan, B.; Temyanko, E.; Negulescu, I. *Macromolecules* **2000**, *33*, 4427-4432.

(37) Nelson, R. J.; Paulus, A.; Cohen, A. S.; Guttman, A.; Karger, B. L. *Journal of Chromatography* **1989**, *480*, 111-127.

(38) Petersen, N. J.; Nikolajsen, R. P. H.; Mogensen, K. B.; Kutter, J. P. *Electrophoresis* **2004**, *25*, 253-269.

(39) Liu, S.; Shi, Y.; Ja, W. W.; Mathies, R. A. *Analytical Chemistry* **1999**, *71*, 566-573.

(40) Paegel, B. M.; Hutt, L. D.; Simpson, P. C.; Mathies, R. A. *Analytical Chemistry* **2000**, *72*, 3030-3037.

(41) Elias, H. *An Introduction to Plastics* 2003.

(42) Shadpour, H.; Edrissi, M.; Zanjanchi, M. A. *Journal of Materials Science: Materials in Electronics* **2002**, *13*, 139-148.

(43) Brandrup, J. *Polymer Handbook*, 1999.

(44) Weber, L. *Kunststoffe--Plast Europe* 1998.

(45) Johnson, T. J.; Waddell, E. A.; Kramer, G. W.; Locascio, L. E. *Applied Surface Science* **2001**, *181*, 149-159.

(46) Wu, Z.; Xanthopoulos, N.; Reymond, F.; Rossier, J. S.; Girault, H. H. *Electrophoresis* **2002**, *23*, 782-790.

(47) Heiger, D. *High Performance Capillary Electrophoresis*, 2000.

(48) Wabuyele, M. B.; Ford, S. M.; Stryjewski, W.; Barrow, J.; Soper, S. A. *Electrophoresis* **2001**, *22*, 3939-3948.

(49) Henry, A. C.; Tutt, T. J.; Galloway, M.; Davidson, Y. Y.; McWhorter, C. S.; Soper, S. A.; McCarley, R. L. *Analytical Chemistry* **2000**, *72*, 5331-5337.

(50) Teshima, K.; Sugimura, H.; Inoue, Y.; Takai, O.; Takano, A. *Langmuir* **2003**, *19*, 10624-10627.

(51) Shimizu, R. N.; Demarquette, N. R. *Journal of Applied Polymer Science* **2000**, *76*, 1831-1845.

(52) Kirby, B. J.; Hasselbrink, E. F., Jr. *Electrophoresis* **2004**, *25*, 187-202.

(53) Wei, S.; Vaidya, B.; Patel, A. B.; Soper, S. A.; McCarley, R. L. *Journal of Physical Chemistry B* **2005**, *109*, 16988-16996.

(54) Bidlingmeyer, B. A.; Warren, F. V., Jr. *Analytical Chemistry* **1984**, *56*, 1583A.

(55) Strege, M. A.; Lagu, A. L. *Journal of Chromatography, A* **1997**, *780*, 285-296.

(56) Doherty, E. A. S.; Meagher, R. J.; Albarghouthi, M. N.; Barron, A. E. *Electrophoresis* **2003**, *24*, 34-54.

(57) Ostuni, E.; Chapman, R. G.; Liang, M. N.; Meluleni, G.; Pier, G.; Ingber, D. E.; Whitesides, G. M. *Langmuir* **2001**, *17*, 6336-6343.

(58) Egodage, K. L.; de Silva, B. S.; Wilson, G. S. *Journal of the American Chemical Society* **1997**, *119*, 5295-5301.

(59) Strege, M. A.; Lagu, A. L. *Analytical Biochemistry* **1993**, *210*, 402-410.

(60) Xu, L.-C.; Vadillo-Rodriguez, V.; Logan, B. E. *Langmuir* **2005**, *21*, 7491-7500.

CHAPTER 4

TWO-DIMENSIONAL ELECTROPHORETIC SEPARATION OF PROTEINS USING POLYMERIC MICROCHIPS*

4.1. Introduction

In the last few years, significant research has been invested into developing CE and LC methods to enable the separation and identification of all proteins in a given proteome. This task is not a trivial separation exercise because, for example, a serum proteome may contain up to 20,000 different components with a concentration dynamic range of 10^{10}.[1, 2] The peak capacity (P) describes the maximum number of components that can be resolved in any given separation.[3] Unfortunately, the peak capacity is typically not adequate using a single LC or CE procedure by itself to resolve such a complex mixture.[4] Therefore, attempts have been made using different LC or CE modes and a combination of these techniques (multi-dimensional separations) to generate the required peak capacity for proteome analysis.[5-8]

A requirement of any successful multi-dimensional procedure is orthogonality, which means that the selected dimensions possess different, but compatible, separation mechanisms. Furthermore, the subsequent dimension in any multi-dimensional separation should not destroy the resolution achieved by the previous one.[5, 6] According to Giddings,[6] the peak capacity of a multi-dimensional separation is the product of the peak capacities of its constituent 1-D methods ($P_1 \ldots P_n$). This definition is valid only when the modes of separation are completely orthogonal.[6] Unfortunately, this condition is rarely fulfilled, limiting the overall peak capacity of most multi-dimensional separations.

The interfacing of 2-D column-based separations, which are typically used for proteome analyses, can be performed off-line or on-line.[9] The on-line coupled 2-D systems offer many

advantages, such as minimizing the loss of analyte due to non-specific adsorption to the walls of small volume transfer containers, which are used with many off-line 2-D methods.[4] Moreover, poor reproducibility can result in off-line methods due to the manual sample transfer from the first to the second dimension,[10] and plates generated in the first dimension can be lost due to the transfer step if the transfer volume is not kept smaller than the peak volume.[10]

Recently, several on-line 2-D CE separations have been reported by investigators, which offer high column efficiencies, favorable resolution and convenient coupling MS. Researchers have demonstrated column-based coupling of ITP and CZE,[11] IEF and ITP,[12] CZE and CGE,[13] capillary sieving electrophoresis (CSE) and MEKC,[14-18] MEKC and IEF,[19] IEF and CGE,[20] IEF and CSE,[21] or CE and CZE using different run buffers.[22] These 2-D capillary-based separations routinely produce peak capacities in the range of 500 – 1,000.[23]

While CE systems have become readily available with automated sample handling capabilities and integration to mass spectrometry for protein identification, μ-CE is evolving as a viable separation platform for proteome analysis due to the unique opportunities μ-CE may offer such as, reduced consumption of sample and reagents; shorter analysis times; minimal dead volumes when coupling multiple separation dimensions and the ability to integrate complex geometries into a small area. In addition, microchips fabricated in polymers can provide the potential for producing devices from a large variety of substrates suitable for the particular separation application using a single replication master.[24]

However, only a few 2-D μ-CE separation developmental efforts have been reported.[23, 25-33] On-chip multi-dimensional CE separations were described by Ramsey and co-workers[23, 25, 26] for peptides by using fluorescence detection in a glass microchip. In those reports, the proteins were digested into peptides off-chip prior to the separation. 2-D μ-CE

separation of proteins without digestion have been reported by coupling IEF with CZE,[27, 29] and IEF with CGE.[28-33] The 2-D separations in these examples were completed within a few minutes to hours.

Most reports for 2-D separations of proteins on microchips utilized IEF as one of the separation dimensions. However, IEF is not compatible with fluorescence labeling because the incorporation of a fluorescent tag changes the pI of the molecule.[34] Furthermore, for the analysis of complex samples, inter-diffusion between focused bands following IEF decreases the efficiency and resolution following transfer into the second dimension.[29] In addition, some investigators have reported low reproducibility in the IEF dimension.[35] In some cases proteins need a few minutes for focusing in IEF channel which also raises the overall 2-D developing time.[32] On the other hand, some studies have been performed to improve the resolving power of the microchip-based IEF with an expense of longer developing time (up to several minutes).[36]

In this chapter, we describe a 2-D separation of a set of proteins using a PMMA microchip. The separation in the first dimension was based on size using SDS μ-CGE. The second dimension consisted of a fast MEKC separation, which sorted proteins based on differences in their interactions with SDS surfactants poised well above their cmc. Effluents from the SDS μ-CGE dimension were transferred into the MEKC dimension by using a pulsed sample transfer protocol. LIF was used at the end of the MEKC separation for detection of the dye-labeled proteins.

4.2. Experimental Details

4.2.1. Microchip Fabrication

PMMA was obtained from MSC (Melville, NY) and was selected for these studies because of its favorable physiochemical properties such as, good optical clarity at 632.8 nm,

minimal replication errors following hot embossing, high separation efficiency, good migration time reproducibility and suitable wettability.[24] The PMMA microchips were replicated from a brass master that was fabricated using high precision micromilling and hot embossing following the procedure that is described herein. A 0.25" thick brass sheet (alloy 353 engravers brass, McMaster-Carr, Atlanta, GA) was machined into a 12 cm diameter circular plate. Plate flatness was typically within ±2 μm and was verified by a surface profiler (Tencor P11, KLA-Tencor, San Jose, CA). Microstructures were milled onto the brass plate with a micro-milling machine (KERN MMP 2522, KERN Micro-und Feinwerktechnik GmbH & Co. KG, Germany). 500, 200, 100, 50, and 25 μm solid carbide milling bits were used (McMaster-Carr or Quality Tools, Hammond, LA) for micro-milling, which was carried out at 40,000 rpm feed rates that were optimized for maximum machining speed and quality of the microstructures. Feed rates were dependent on the size of the milling tool and were typically in the range of 200 mm/min for the 500 μm milling bit, 100 – 150 mm/min for the 200 μm bit, 50 – 75 mm/min for the 100 μm bit, 10 – 20 mm/min for the 50 μm bit, and 2 – 4 mm/min for the 25 μm bit. A typical milling cycle consisted of a pre-cut of the entire surface with the 500 μm milling bit to ensure parallelism between both faces of the brass plate, a rough milling of the microstructures using the 500 or 200 μm milling bit, and a finishing cut with the required smaller diameter milling bit. In the final step, burrs produced at the top of the microstructures were removed by mechanical polishing. Polishing was performed on a 3 μm grain size polishing paper (Fibrmet Discs - PSA, Buehler, Lake Bluff, IL) followed by polishing on a polypropylene cloth (Engis, Wheeling, IL) with a 1 μm diamond suspension (Metadi Diamond Suspension, Buehler).

Before hot embossing, the PMMA wafers were kept in an oven (80^{o}C) overnight to

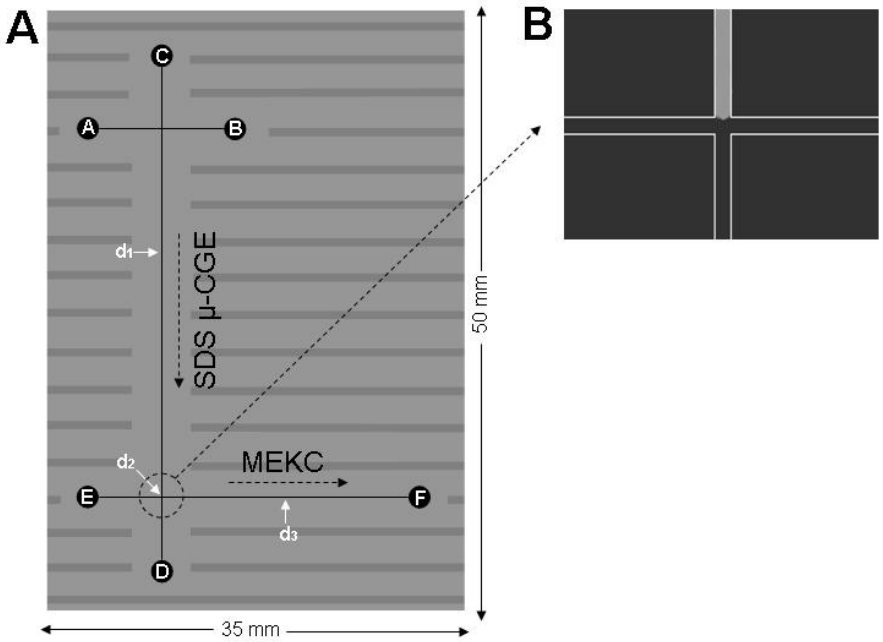

Figure 4.1. (A) Geometrical layout of the micro-electrophoresis chip used for 1-D and 2-D separations. The chip was fabricated using hot embossing from a brass master into PMMA: with a channel width = 20 µm; channel depth = 50 µm. The solution reservoirs are; (a) sample reservoir, (b) sample waste reservoir, (c) SDS µ-CGE buffer reservoir, (d) SDS µ-CGE buffer waste reservoir, (e) MEKC buffer reservoir, (f) MEKC buffer waste reservoir. (B) Fluorescence image of the sieving matrix/MEKC interface at the intersection of the SDS µ-CGE and MEKC dimensions. The fluorescence was generated by seeding the sieving matrix with fluorescein.

remove any absorbed water. During embossing, the mold master was heated (160^{o}C) and pressed into the polymer wafer with a pressure of 1,100 psi for 410 s. The embossing plates were then retracted and the polymer substrate removed and cooled to room temperature. The entire fluidic network was sealed with a thin polymer cover plate by clamping the plastic pieces between two glass plates and thermally annealing in a GC oven (120^{o}C, 20 min).[24] Figure 4.1A shows the geometrical layout of the micro-electrophoresis chip used for our 1-D and 2-D separations. The microchip channel lengths were 5 mm for each injection leg, 40 mm for the SDS µ–CGE dimension and 25 mm for the MEKC separation dimension. All channels were 20 µm wide and 50 µm deep.

4.2.2. Samples and Reagents

Alexa Fluor 633 (excitation/emission ~ 633/652 nm) conjugated proteins, including wheat germ agglutinin (WG, 38 kDa), actin (AC, 43 kDa), ovalbumin (OV, 45 kDa), protein A (PA, 45 kDa), streptavidin (ST, 53 kDa), BSA (66 kDa), *Helix pomatia* lectin (HPA, 70 kDa), transferrin (TR, 80 kDa), concanavalin A (CO, 104 kDa), and lectin peanut agglutinin (PNA, 110 kDa) were purchased from Molecular Probes Inc. (Eugene, OR). The conjugation reactions were carried out with a dye-to-protein molar ratio of 1.5-to-1. Dye-labeled protein solutions were made by suspending in 150 mM PBS, pH 7.2 (Sigma, St. Louis, MO), with the addition of 2 mM sodium azide (Sigma, St. Louis, MO), and stored at 4 ^{o}C until required for use. For long term storage, the protein conjugates were divided into 100 μL aliquots and stored at –20^{o}C. A protein mixture was prepared in the desired concentrations by adding 12 mM TRIS/HCl, 1% w/v (35 mM) SDS, pH 8.5 (Beckman, Fullerton, CA) with 0.05% w/v methyl hydroxyl ethyl cellulose, MHEC, (Sigma), which was used as a dynamic coating of the PMMA to suppress the EOF.[37] The solutions were heated to 95^{o}C for 4 min to denature the proteins. SDS μ-CGE was performed by using a SDS 14 – 200 matrix (Beckman, Fullerton, CA) and 12 mM TRIS/HCl, 0.1% w/v (3.5 mM) SDS, pH 8.5, run buffer. Both the sieving matrix and run buffer in the SDS μ-CGE separations contained 0.05% w/v MHEC to suppress the EOF. MEKC was carried out with 12 mM TRIS/HCl, 0.4% w/v (14 mM) SDS, pH 8.5, containing 0.05% w/v MHEC. Additional SDS (Sigma) was added to the TRIS/HCL buffer to adjust the SDS concentration above its cmc (~0.24% w/v or ~8.3 mM in water and somewhat less in buffer solutions)[30] for the MEKC separations. Prior to use in the microchip, all solutions were filtered using a 0.2 μm

Nylon-66 membrane filter (Cole-Parmer Instrument Co., Vernon, IL) and degassed (10 min). Proteins solutions were centrifuged for 5 min at 6,000 rpm to remove any particulates. Mixtures of proteins with a total concentration of 30 nM were used for all 1-D and 2-D electrophoretic separations.

4.2.3. LIF Detection and Electrophoresis Power Supply

Fluorescence was detected at positions d_1, d_2 and d_3 (see Figure 4.1A) from the microchip using an instrument constructed in-house. Figure 4.2 shows block diagram of the LIF system. A Helium-Neon laser beam, with a lasing wavelength of 632.8 nm (NT 54-151, Edmund Industrial Optics, Barrington, NJ) and operated with an external power supply (LDI LF LAB-1, Laser Drive Inc., Gibsonia, PA), was passed through an excitation filter (XF-1026, Omega, Brattleboro, VT) and reflected off a dichroic mirror (XF-2022, Omega) into a 40x (NA = 0.65) objective (Melles Griot, Zevenaar, The Netherlands). The beam was focused to a ~10 μm diameter spot into the microchannel, which was situated on an x-y-z micro-translational stage to allow the position of the microchip to be adjusted with respect to the focused laser beam. The fluorescence from the labeled proteins was collected by the same objective lens, passed through the dichroic mirror, then through a 1 mm aperture and onto an emission band pass filter (XF-3030, Omega). The photons were detected using a photomultiplier tube (RT-1508, Hamamatsu, San Jose, CA). Photoelectron events were amplified and shaped with a pulse converter (TB-01, HORIBA Jobin Yvon Inc., Edison, NJ), and processed by a PC computer using a multifunction I/O card (CB-68 LP) and PCI board (PCI-6601) obtained from National Instruments (Austin, TX).

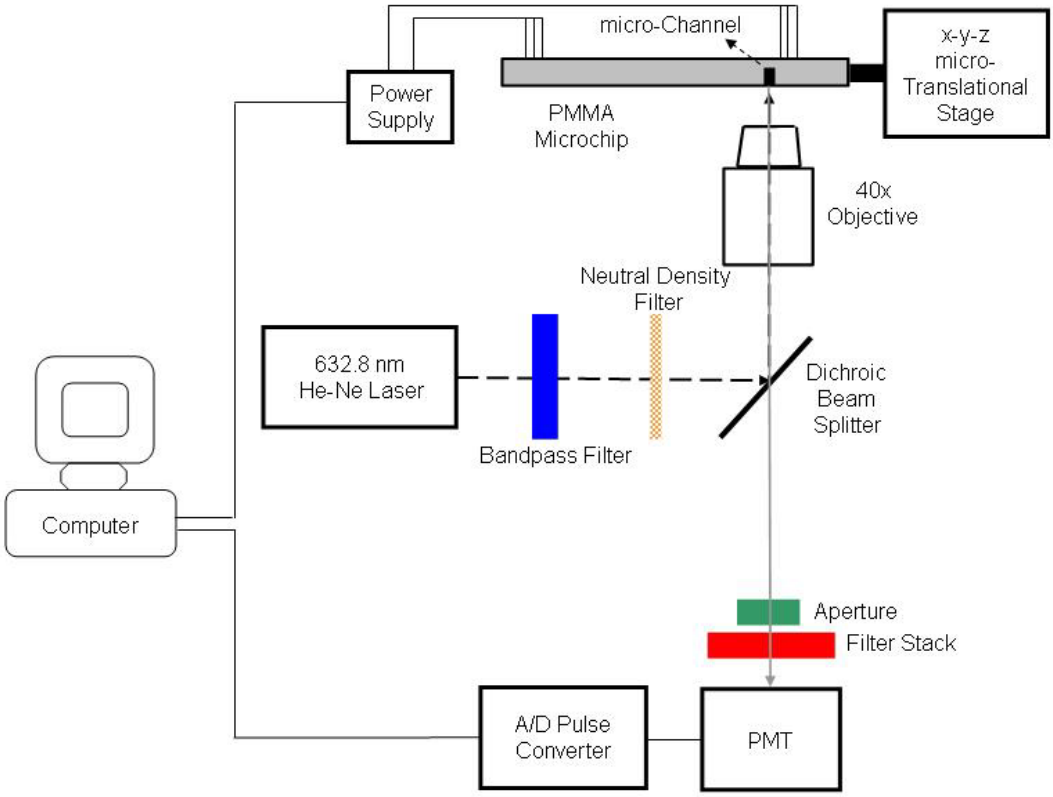

Figure 4.2. Block diagram of the in-house built LIF detection system used for 1-D and 2-D microchip separations of the proteins labeled with Alexa Fluor 633. The LIF system was configured in an epi-illumination format with a 40x microscope objective (NA = 0.65) used to focus the laser light into the PMMA microchip channel, which was positioned on a x-y-z micro-transitional stage, and also collected the resulting fluorescence photons. In all cases, ~2 mW of average laser power was used. The collected photons were filtered using an interference filter that possessed a center wavelength red-shifted by 20 nm from the excitation wavelength (632.8 nm) with a half-band width of ~10 nm. The photons were analyzed using a Hamamatsu RT-1508 photomultiplier tube.

High voltage for the electrophoresis was applied to the reservoirs of the microchip with six independently controlled power supplies (EMCO, Sutter Creek, CA). Electrical contact between the solution in the fluid reservoirs and the high voltage was achieved using 0.30 mm diameter platinum wires (Scientific Instrument Services, Ringoes, NJ) situated in buffer reservoirs. The high voltage power supplies and relays were controlled by a computer using an analog output (D/A) card (PCI-DDA04/12, National Instruments).

The program for data acquisition and control of the power supply was created using National Instruments LabVIEW software. The LabVIEW controller program was capable of importing user-defined parameters for the separation and detector, such as electrophoresis voltages and their duration, sampling and switching times between reservoirs and channels, and also collecting/monitoring the fluorescence intensity during the course of the separations.

4.2.4. Microchip Operation

The microfluidic chips were cleaned with a 0.01% w/v sodium azide solution dissolved in nano-pure water. Prior to each use, the microchip was rinsed by filling all reservoirs with 2 mg/mL MHEC dissolved in PBS, pH 7.2, and applying vacuum to reservoir F (see Figure 4.1A) for at least 10 min to provide sufficient EOF suppression. A 5-min electrophoretic pre-run was performed using the separation buffers prior to each electrophoresis run to obtain a stable current during the separations. Peak identities were confirmed through migration time matching by injecting the analytes individually.

All electrophoretic separations were carried out at ambient temperature in reverse mode (detection end anodic). Individual 1-D SDS μ-CGE and MEKC separations were evaluated using A-B and C-D paths serving as injection and separation channels, respectively. The LIF detection positions for the 1-D separations were set at points d_2 for SDS μ-CGE and d_1 for MEKC (see Figure 4.1A) to provide effective separation lengths of 30 and 10 mm, respectively. These 1-D separations were used to evaluate separation performance for each dimension and also, orthogonality between the individual dimensions.

To perform an effective 2-D separation, one must be able to introduce and isolate two different separation media within the individual dimensions of the fluidic network. In our case, the sieving matrix must be filled between reservoir C and point d_2 only. To accomplish this, the

SDS μ-CGE channel (C-D channel, see Figure 4.1A) was filled with the sieving matrix using a plastic syringe from reservoir C and applying vacuum to reservoir D while reservoirs E and F were sealed. Matrix movement was monitored using an optical microscope. The filling process was continued until the sieving matrix reached point d_2 (see Figure 4.1A). Then, the MEKC buffer was introduced into the MEKC channel (Figure 4.1A) from reservoir F with a syringe and sealing all reservoirs except E and D, which were left open to the atmosphere. This not only filled the MEKC channel with its appropriate run buffer, but also removed any extra sieving matrix in the MEKC channel. Excess sieving matrix in reservoirs A-C was carefully removed and replaced with sample or SDS μ-CGE run buffer. Finally, to obtain a smooth sieving matrix / solution interface and also to ensure proper buffer composition in each channel, a two step electrokinetic run was performed. This was performed just prior to the 2-D separation and consisted of applying +0.8 kV and +0.5 kV to reservoirs C and F, respectively, and grounding the remaining reservoirs. This was followed by switching the polarity of reservoirs C and F and electrophoresing again. Each step continued for ~3 min. The microchip filled with sieving matrix was checked by adding fluorescein (Sigma, $\lambda_{excitation}$ = 465 - 495 nm, $\lambda_{emission}$ = 520 nm,) into this matrix and using a fluorescence microscope (Nikon EFD-3, Optical Apparatus, Ardmore, PA) to image matrix/solution interface (see Figure 4.1B for the resulting image).

For both the 1-D SDS μ-CGE and MEKC separations after pressure filling channels with the sieving matrix or run buffer, the sample reservoir (reservoir A, see Figure 4.1A) was filled with the protein mixture and the rest of the reservoirs were filled with run buffer. Injection into the A-B channel was initiated by applying a positive voltage (0.20 kV) to the sample waste reservoir (reservoir B, see Figure 4.1A) and grounding the sample reservoir (reservoir A) for the amount of time needed to completely fill the cross channel (reservoirs C to F were floated during

injection). Following injection, a positive voltage was switched to reservoir D and reservoir C was grounded (see Figure 4.1A). Pull back voltages (10 – 15% of applied voltage at reservoir D) were applied to the sample and waste reservoirs (reservoirs A and B, see Figure 4.1A). The electric field strength used for SDS μ-CGE and MEKC separations were 350 V/cm and 400 V/cm, respectively. The current measured within each dimension was found to be 11 μA and 9 μA for the SDS μ-CGE and MEKC dimensions, respectively. By plotting the applied electric field versus current for each dimension, Ohm plots indicated insignificant Joule heating at these applied voltages.[38] Injection was performed using an electric field of 200 V/cm.

After introducing the appropriate separation media within the individual dimensions of the fluidic network, the laser beam for LIF detection was positioned at point d_3 (see Figure 4.1A) for the full 2-D separation. This provided an effective separation length of 30 mm for the first dimension and 10 mm for the second dimension. Table 4.1 represents the high voltage protocol adopted for the 2-D separation. As shown in this Table, the injection and run steps were the same as discussed previously. SDS μ-CGE was started by switching the high voltage applied to reservoir D to +1.40 kV and grounding C. Reservoirs A and B (see Figure 4.1A) were kept at +0.14 kV until the end of the run. Reservoirs E and F (see Figure 4.1A) were floated during the SDS μ-CGE separation.

Table 4.1. High voltage protocol for 2-D separations using the PMMA microchip. Letters A to F refer to reservoirs on the 2-D platform as shown in Figure 4.1A

	Applied Voltages (kV)[1]					
Step	**A**	**B**	**C**	**D**	**E**	**F**
Injection	G	+ 0.20	F	F	F	F
SDS μ-CGE	+ 0.14	+ 0.14	G	+ 1.40	F	F
Second MEKC cycle	+ 0.14	+ 0.14	F	F	G	+ 1.00
First to second sample transfer	+ 0.14	+ 0.14	G	+ 1.40	F	F

1. G: grounded, F: floating.

Sample transfer into the second dimension was performed every 0.5 s run time in the first dimension by switching the applied high voltage to reservoir F (+1.00 kV) and grounding E. This provided an electric field of 400 V/cm for MEKC in the second dimension. After a 0.5-s sample transfer time from the first to second dimension, each MEKC cycle was performed for 10 s. During each MEKC cycle, the components in the SDS μ-CGE dimension were parked by grounding point D (see Table 4.1). After the 10-s run time, MEKC electrophoresis was paused for 0.5 s by floating points E and F. This resulted in the movement of components in the SDS μ-CGE dimension into the junction between the separation dimensions (point d_2) and provided a new sample plug to be introduced into the second dimension (i.e., MEKC). As this was a serially implemented 2-D separation, the transfer/separation cycles were repeated until all bands from the first dimension were transferred into the MEKC dimension.

LIF data was collected continuously from the start of the SDS μ-CGE at point d_3 and the separation landscape (see Results and Discussion) was generated by dividing the temporal LIF signal into successive runs representing each MEKC cycle. This was performed using ImageJ 1.34s (National Institute of Health, Bethesda, MD) and TableCurve 3D 4.0 (Systat Software Inc., Point Richmond, CA) software.

4.3. Results and Discussion

To evaluate the orthogonality of the SDS μ-CGE and MEKC separation dimensions and to compare the efficiency of the final 2-D separation with its respective SDS μ-CGE and MEKC dimensions, individual 1-D separations were performed using the fluorescently labeled protein mixture described in the Experimental Section. These results are presented in the following sections.

4.3.1. SDS μ-CGE Separation of Proteins

The presence of a highly viscous gel can change the separation mechanism to a size-based separation and also minimizes solute diffusion, prevents analyte adsorption to the microchip channels, and suppresses EOF.[13] Separation of native (un-denatured) proteins typically results poor migration time reproducibility, band smears, and less distinct protein spots.[39] The electrophoretic mobilities of native proteins depend on their charge-to-mass ratios rather than their molecular sizes.[29] As a conclusion, formation of SDS-protein complexes after denaturing not only establishes the foundation for performing electrokinetic protein transfer due to their negative charge but also prepares protein analytes for a size-based separation.[30]

A typical SDS μ-CGE electropherogram using our PMMA microchip is shown in Figure 4.3. Six peaks were visible in the electropherogram. Three bands were found to be composed of several co-migrated proteins due to their similar molecular weights. The co-migrated groups of proteins were AC-OV-PA, BSA-HPA, and CO-PNA. Although N and thus R_s could be improved by increasing separation distance,[23, 40] this will not allow for the separation of proteins with similar molecular weights, such as OV and PA using SDS μ-CGE. Longer separation channels also increase separation time and sample dispersion due to diffusional or geometrical spreading, or both, if turns are used to keep a compact footprint of the microchip to accommodate microfabrication capabilities.[23] Furthermore, filling long microchannels with highly viscous sieving matrixes is difficult due to the high pressure drop across the channel. Therefore, simple increases in column length do not necessarily translate into improved electrophoretic performance.

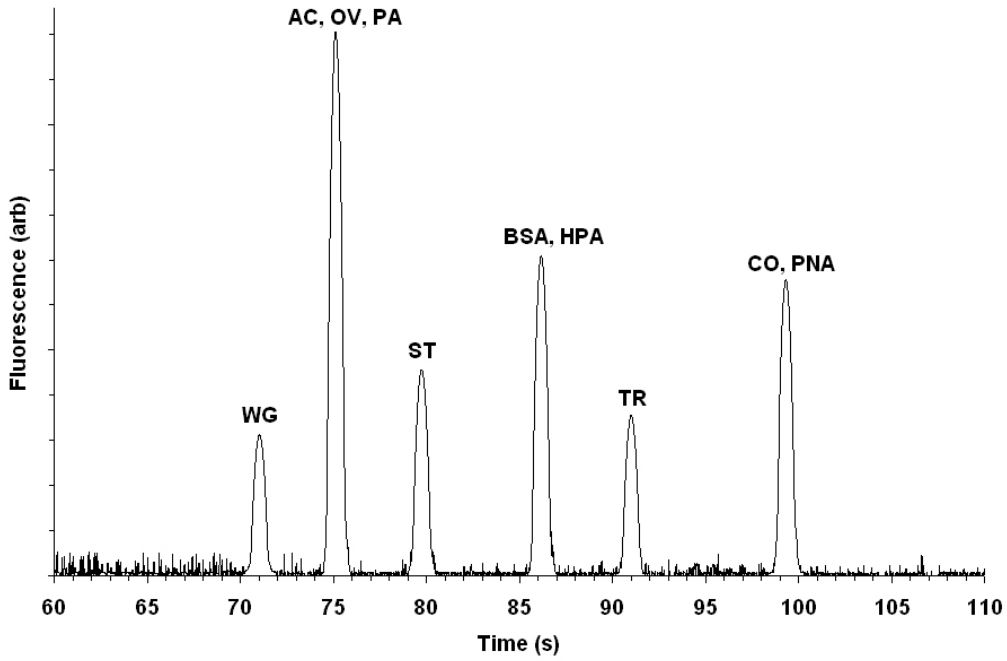

Figure 4.3. SDS μ-CGE analysis (1-D separation) of a 30 nM protein mixture using the PMMA microchip. The electrophoresis was performed using SDS 14 – 200 sieving matrix with 12 mM TRIS/HCl, 0.1% w/v (3.5 mM) SDS, pH 8.5 containing 0.05% w/v MHEC.

The average separation efficiency for the SDS μ-CGE electropherogram was calculated to be 4.83×10^4 plates (plate height, H = 0.62 μm). An apparent average R_s of 2.81 was calculated based solely on the spatial separation and peak width of the observed electrophoretic bands in the 1-D separation and did not take into account components that exhibited co-migration. The peak capacity for this 1-D separation was calculated to be 19.[41] Figure 4.4 represents a linear plot of log(MW) versus the corresponding migration times (MT) obtained by SDS μ-CGE (see Figure 4.3).

The equation for the linear fit of the average data in this figure was;

$$Log_{10}(MW) = 1.5 \times 10^{-2} MT + 3.45 \quad (4.1)$$

The plot shows good linearity ($r^2 = 0.996$) across the molecular weight range studied (38,000 – 110,000). The SDS served to not only to denature the proteins, but also to eliminate

any charge density differences among the proteins, which reduced the effect of variability in the partial specific volume and hydration,[42] producing high linearity in the plot as shown in Figure 4.4.

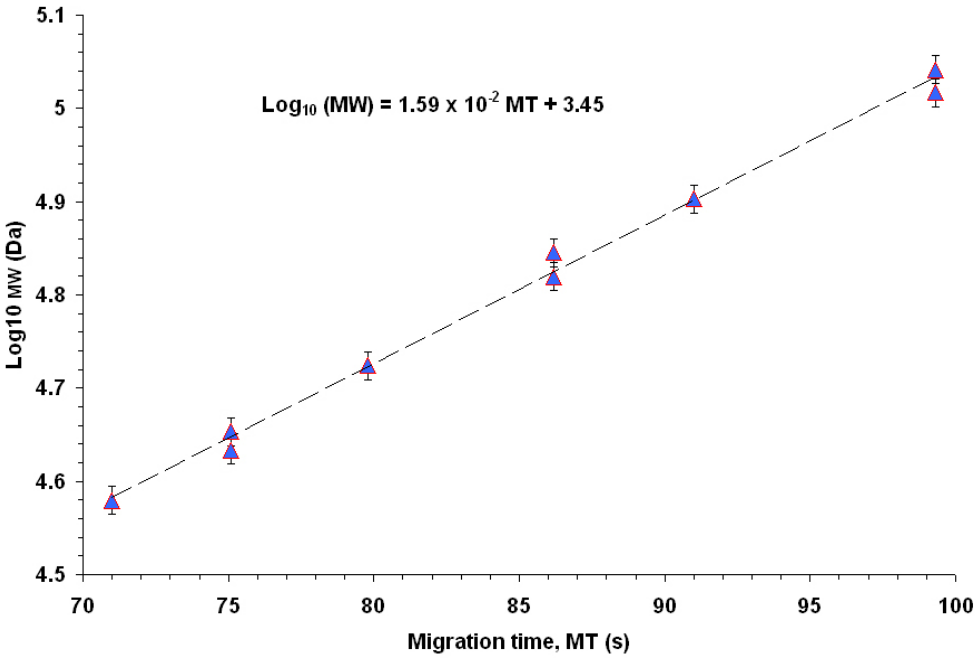

Figure 4.4. Plot of the logarithm of molecular mass versus corresponding migration times for the SDS μ-CGE separation of the labeled-proteins ranging in size from 38 to 110 kDa. The data used to construct this plot was secured from Figure 4.3.

4.3.2. MEKC Separation of Proteins

The use of buffers containing micellar concentrations of surfactants facilitate the ability to separate proteins using CE via a hydrophobic or other protein/micelle interaction mechanism.[43, 44] While the exact mechanism of separation is not well understood for large molecules, such as proteins due to their inability to easily partition within the hydrophobic core of the micelle, the degree of denaturing/unfolding that different proteins experience in the presence of surfactant-monomer-based micelles may provide greater surface area and therefore

alter their frictional drag affecting the electrophoretic mobility. Whatever the separation mechanism, we were interested in evaluating the use of MEKC as the second dimension when coupled to SDS μ-CGE.

In comparison to other CE techniques, MEKC provides superior separation selectivity and peak capacity for a wide range of analytes. For protein separations, another advantage due to the presence of surfactants in the separation buffer is minimizing non-specific protein-surface interactions in the separation channels, which can be highly deleterious to the separation.[44] In terms of biological applications, for example, since the proteins expressed in *E. coli* in the form of inclusion bodies exist in a denatured inactive state,[45] it is beneficial to perform analyses under denaturing conditions using ionic micellar mobile phases, where analyte solubility is maximized. As a result, when current microchip 2-D separation technique is used for analysis of proteins extracted form a cell (e.g., *E. Coli*), the MEKC is a favorable separation technique in combination with SDS μ-CGE since both separation techniques provide SDS environments to maximize the analyte solubility.

Although buffers containing cationic surfactants (e.g., CTAB, see Chapter 1) may be employed to separate most proteins at neutral or acidic pH, electrostatic interactions of these surfactants with negatively charged moieties predominant for acidic proteins at high pH, which can result in electrostatic neutrality and subsequent precipitation. As an alternative, improvements in separation efficiency are realized in an alkaline environment and the use of anionic surfactants, such as SDS.[43]

Eliminating or suppressing the EOF is a way to significantly decrease the separation time in MEKC while still preserving the selectivity of the separation, especially when using anionic micelles. To reduce the EOF, we used a dynamic coating of MHEC on the PMMA channels (see

Experimental Section).[37] It should be noted that no sieving properties are afforded by buffers containing methylcellulose derivatives (e.g., MHEC) when set to a concentration below 0.1%.[46] The EOF measured for pristine PMMA was $1.56 \pm 0.05 \times 10^{-4}$ cm^2/V s and was reduced to $1.20 \pm 0.07 \times 10^{-5}$ cm^2/V s using MHEC in the MEKC run buffer.

MEKC runs of the protein mixture were performed using a shorter effective separation length than that used for SDS μ-CGE to assist in shortening the development time (d_2, see Figure 4.1A). A typical MEKC electropherogram obtained on the PMMA microchip is shown in Figure 4.5. As shown in Figure 4.5, HPA, with a relatively high molecular weight (70,000), eluted first. On the other hand, WG eluted last despite its small molecular weight (38,000). Similar to SDS μ-CGE, some proteins, such as OV-BSA, PNA-ST-PA, and CO-TR-WG, co-migrated.

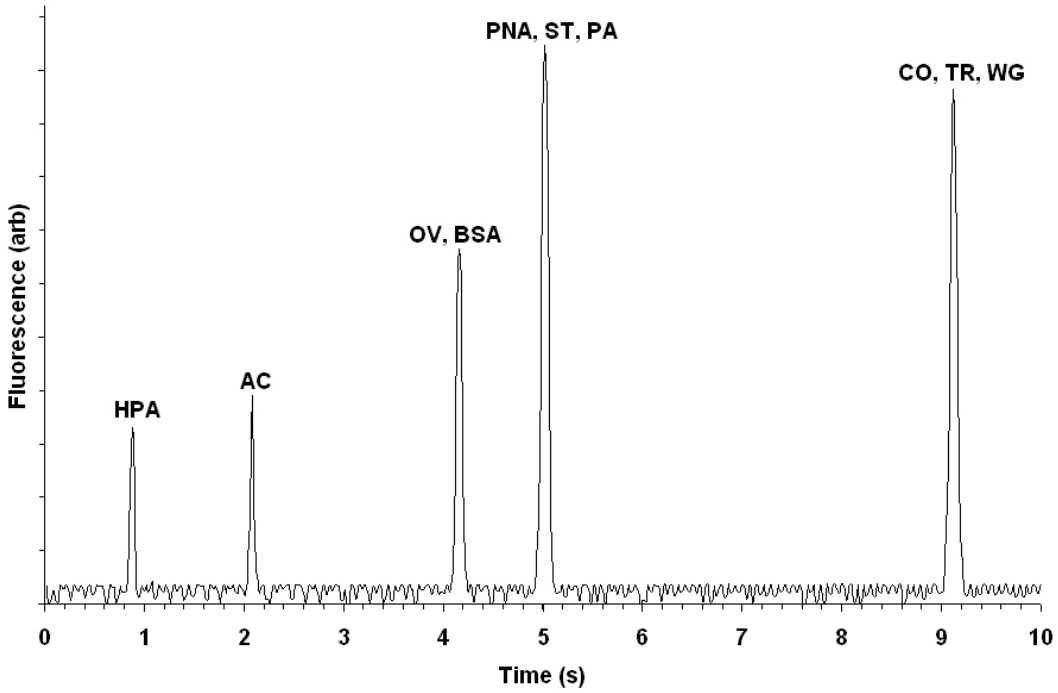

Figure 4.5. MEKC separation (1-D separation) of a 30 nM protein mixture using the PMMA microchip. The electrophoresis was conducted using 12 mM TRIS/HCl, 0.4% w/v (14 mM) SDS, pH 8.5 containing 0.05% w/v MHEC as the dynamic EOF suppressor.

As reported previously,[44] higher concentrations of SDS in the run buffer can result in better separation of proteins due to differential tendencies of the protein-SDS complexes to associate with SDS micelles, the number of which grows as the surfactant concentration increases. But, increasing the SDS concentration also increases the MEKC separation window. In this study, increasing the SDS concentration did not eliminate the co-migration observed for several of the proteins studied herein. We also noticed that increasing the SDS concentration increased the buffer conductivity, producing higher current flow in the microchannel degrading separation performance due to excessive Joule heating effects. Finally, the high SDS concentration minimized protein transfer efficiency from the first to the second dimension when performing a 2-D run was performed. Therefore, the optimal SDS concentration was set at 0.4% w/v (14 mM) well above its cmc, which provided high transfer efficiency from the first to second dimension and maintained separation efficiency.

The average separation efficiency, peak width and peak capacity in MEKC were calculated to be 1.15×10^4 plates (H = 0.87 μm), 0.14 s, and 59, respectively. An apparent average resolution of 4.91 was calculated for the separation, which did not take into account co-migration. Sample migration time reproducibility, in particular, is dependent upon the chemical environment inside the separation channels.[43] Poor migration time reproducibility and peak tailing in MEKC separations can be produced by high EOF or non-specific adsorption of proteins, or both to the microchip wall.[24] In this study, the EOF and protein non-specific adsorption were minimized by using MHEC, which accounted for the relatively high plate numbers obtained for the MEKC dimension. The peaks in the MEKC electropherogram showed an average asymmetry factor (A_s) of 1.07 ± 0.04 indicating a lack of significant peak tailing that would be indicative of potential solute / wall interactions.

4.3.3. Orthogonality of SDS μ-CGE and MEKC Separation Techniques

Since the potential peak capacity of a 2-D electropherogram is the arithmetic product of the peak capacities of the constituent dimensions (i.e., SDS μ-CGE and MEKC in this case), extremely large peak capacities can be obtained even if the constituent dimensions produce only modest peak capacities.[8] A 2-D separation actually generates this theoretically available peak capacity only if the constituent 1-D dimensions are completely orthogonal. A high degree of retention correlation between the dimensions can reduce a 2-D separation to what is, in fact, a 1-D separation with peaks distributed along the diagonal of a plot of retention times between the constituent dimensions.[47] The information content of any multi-dimensional system is the sum of the mean information content of each individual dimension minus the cross-information.[48] Minimizing cross-information is therefore important in any multi-dimensional separation.[47]

Changes in migration order and migration time can serve as indicators of different separation mechanisms responsible for the migration behavior in each dimension.[26] In the present case to evaluate the orthogonality of SDS μ-CGE and MEKC,[49-51] protein migration maps were constructed. To perform this, the migration times (MT_i) for all ten proteins were acquired for each separation mode according to the 1-D results. Then, the normalized migration times ($MT_{i,norm}$) for both SDS μ-CGE and MEKC were calculated using the following equation;

$$MT_{i,norm} = [MT_i - MT_{min}]/[MT_{max} - MT_{min}] \quad (4.2)$$

where MT_{max} and MT_{min} represent the migration times of the most and least retained proteins, respectively, for both the SDS μ-CGE and MEKC electropherograms. The migration times for this investigation were obtained by testing each protein individually, and also confirmed by spiking proteins into both the SDS μ-CGE and MEKC microchip separations. The values of $MT_{i,norm}$ range from 0 to 1. The normalization serves two purposes: First, it allows for

comparison of SDS μ-CGE and MEKC as two different sets of μ-CE data in a uniform 2-D migration space regardless of the absolute migration time values, which can change due to electrophoretic conditions such as electric field and the effective length of the separation channel. Second, it removes the void spaces in the 2-D separation plot where no peaks migrated.[49]

Normalized 2-D relative migration time plots were constructed and are shown in Figure 4.6 for the ten investigated proteins. The orthogonality of the two individual dimensions can be qualitatively estimated by looking at the position of each protein on this 2-D map with respect to the main diagonal (shown by a dashed line in Figure 4.6). Figure 4.6 illustrates that the combination of SDS μ-CGE and MEKC can provide good orthogonality as only two proteins fell along the diagonal (AC and CO).

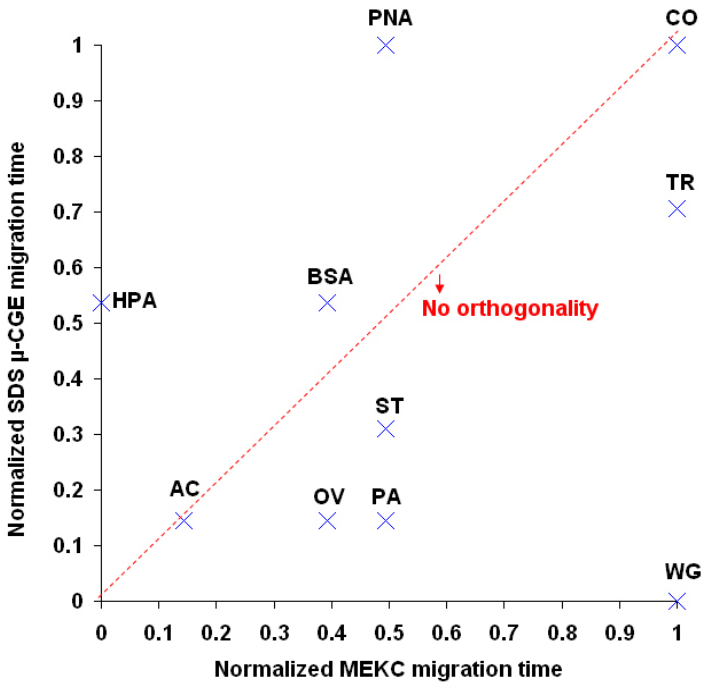

Figure 4.6. Scatter plot of the normalized migration times for SDS μ-CGE versus MEKC separation dimensions for the investigated proteins. The normalized migration times were calculated using equation 4.2 and secured from the data shown in Figures 4.3 and 4.5.

4.3.4. 2-D SDS μ-CGE × MEKC Separation of the Labeled Proteins

The ability to adequately sample the components from the first dimension into the second dimension is very important for any successful 2-D separation strategy employing a serial transfer as used herein. In particular, electrophoretic band aliasing due to low sampling into the second dimension must be avoided. Band aliasing can be reduced by employing a rapid analysis time in the second dimension and/or long development times in the first dimension, or both.[23] In this study, SDS μ-CGE was selected as the first separation dimension because the development time of MEKC is much shorter than that of SDS μ-CGE. Another reason for selecting MEKC as the second separation dimension is mainly a consideration of diffusional contributions from each dimension. During each MEKC cycle while protein bands in the first dimension are parked until being transferred into the MEKC dimension (see Table 4.1), minimal amounts of diffusional spreading are expected primarily due to the sieving network, which significantly reduces the diffusion coefficient of the proteins compared to the free solution used in MEKC (see Section 4.3.6).

Coupling SDS μ-CGE with MEKC for a full 2-D separation was next investigated using the PMMA microchip shown in Figure 4.1A with LIF detection placed at point d_3. Details of the injection and separation protocols are shown in Table 4.1. The time to start the second dimension (i.e., MEKC) in our on-chip 2-D run depends on the migration time of the smallest protein or co-migrated proteins in the SDS μ-CGE dimension. This migration time can be estimated by using equation 4.1 for the smallest component (lowest MW) in any given mixture. In this study, equation 4.1 estimated a MT ~71 s for WG as the smallest protein (MW = 38,000) in the mixture. Therefore, the first MEKC cycle was set to start at 70 s. However, for a mixture

consisting of components with unknown molecular weights, the second dimension can be started by extrapolating the plot given in Figure 4.4 to 0 MT (~2,200), which basically describes the column holdup time. The MEKC cycles were then performed by proper switching of the high voltage applied to points E and F as discussed previously (see Experimental Section). The word "cycle" refers to a complete MEKC electrophoretic run that was used for the second dimension. Since all proteins used here were found to elute from the MEKC channel within a 10 s separation window, the MEKC cycles were fixed at 10 s. For different protein mixtures, longer separation windows could be selected at the expense of longer 2-D development times.

The linear output of the detector from the 2-D analysis of the proteins is shown in Figure 4.7. The 2-D analysis shown in Figure 4.7 was able to resolve all 10 proteins in this mixture including species that could not be separated using individual 1-D separations under similar experimental conditions (see Figures 4.3 and 4.5). The final 2-D electropherogram was obtained from 61 MEKC cycles following an initial SDS μ-CGE electrophoresis of 70 s.

An important aspect when separation dimensions are serially coupled is making injections from the first dimension into the second dimension that maintain separation efficiency and result in efficient sample transfer (i.e., minimal sample loss).[28] In a comprehensive 2-D system, the effluent from the first dimension should be sampled into the second dimension at regular intervals and with fixed volumes without being diluted or experience dispersion. To maintain continuity between the two dimensions, run buffer pH, MHEC, and the presence of other buffer constituents should be similar with similar concentrations in both dimensions. In our case, the run buffers were essentially identical except that the SDS concentration was set in the MEKC dimension to provide the formation of micelles.

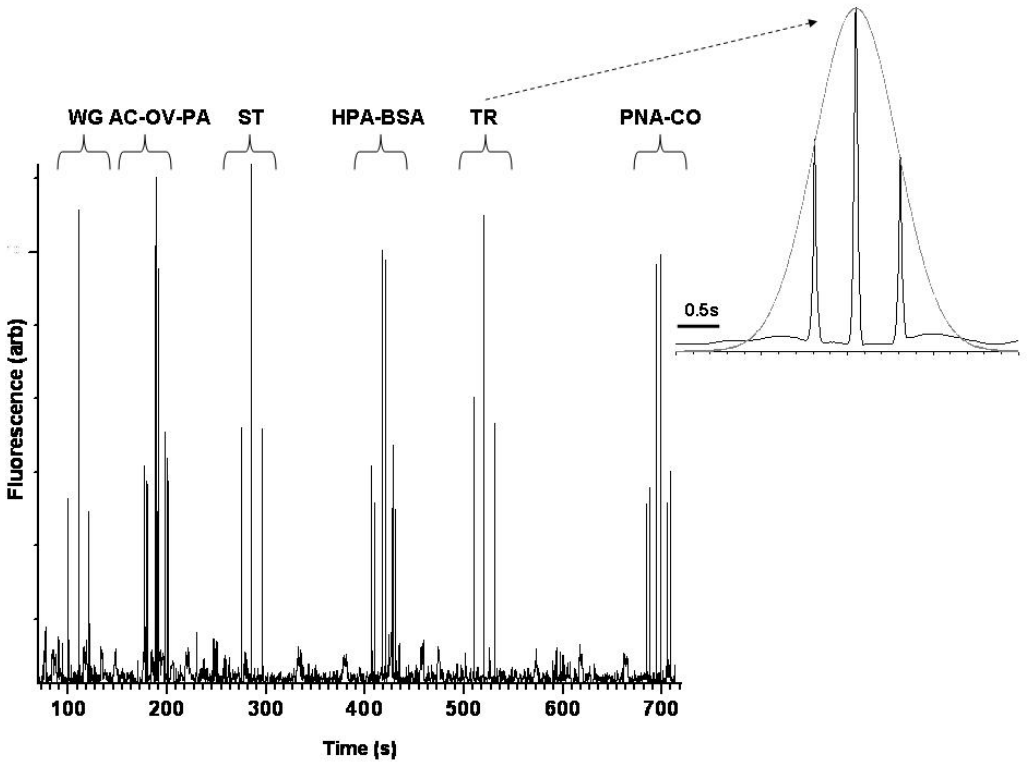

Figure 4.7. 2-D μ-CE separation of a 30 nM protein mixture in the PMMA chip. A 0.5 s pulse injection of the SDS μ-CGE peaks starting at 70 s was performed in channel E–F (see Table 4.1 and related text for details). All separation conditions were the same as those stated in Figures 4.3 and 4.5. Shown in figure is a linear output of the LIF 632.8 nm detector system from the 2-D analysis of the protein sample.

To maintain separation performance and minimize band aliasing, each peak from the first dimension should be sampled approximately three times in the second dimension.[25, 52] This "oversampling" from the first dimension into the second enhances the overall separation performance of the 2-D system.[27] In our study, the average peak width (4σ) just prior to the second dimension (point d_2, see Figure 4.1A) produced by the SDS μ–CGE dimension was 1.52 s. Therefore, for a transfer time of 0.5 s, the average protein band eluting from the first dimension would be sampled approximately three times. Inspection of Figure 4.7 shows an expanded view of a band (TR) that has been oversampled, producing approximately 3 peaks in

the linear electropherogram. Fitting these oversampled peaks to a Gaussian (and removing the 2 intervening MEKC cycles), produced a bandwidth (formal width at half maximum) of 2.4 s, yielding plate numbers for the 2-D separation of 7.2×10^5 plates (H_{TOT} = 0.056 μm; see Section 4.3.6).

The duration of our serially coupled SDS μ-CGE and MEKC is determined by the product of the number of MEKC cycles, 61, sample transfer time (0.5 s), and the development time for each MEKC cycle (10 s) as well as the initial first dimension run time (70 s). As a result, the 2-D separation of the proteins studied in this work was complete in <12 min (see Figure 4.7). Shorter 2-D separation times can be achieved by reducing the initial SDS μ-CGE development time, reducing the number of MEKC cycles, reducing the sample transfer time or reducing the MEKC development time. Shortening the MEKC development time could simply be affected by reducing the column length, which would sacrifice resolution. But, as noted in the MEKC 1-D results, the apparent average resolution (4.91) using the 10 mm length column indicated that much shorter columns could be envisioned. If we assume that $R_s \alpha L^{1/2}$,[40] and requiring R_s ~1.5, a column length for the MEKC dimension of 5 mm would be sufficient, yielding a development time of only ~5 s. This would reduce the separation time to ~6.7 min. It should be noted that reducing the MEKC development time would also reduce the diffusional spreading contribution (H_D) to the total plate height (H_{TOT}). In the present case, H_D represents ~39% to H_{TOT} (see Section 4.3.6). The data depicted in Figure 4.7 were converted into a landscape (see Figure 4.8).

The width of the first dimension channel approximately defines the injection plug width into the second dimension for coupled 2-D systems. The application of separation channels with narrow widths and large depths is advantageous because it improves peak capacity by

minimizing zone variances induced by the finite injection plug introduced into the second MEKC dimension and also improves the detection limit by lengthening the effective detection path length.[53] The average peak width for each MEKC cycle was 0.15 ± 0.03 s, comparable to the corresponding value in the 1-D MEKC (0.14 ± 0.02 s) runs. For the sample tested in our microchip, the sieving matrix and run buffers with their respective compositions provided the best reproducibility in terms of migration times and highest separation efficiencies in a minimal amount of analysis time.

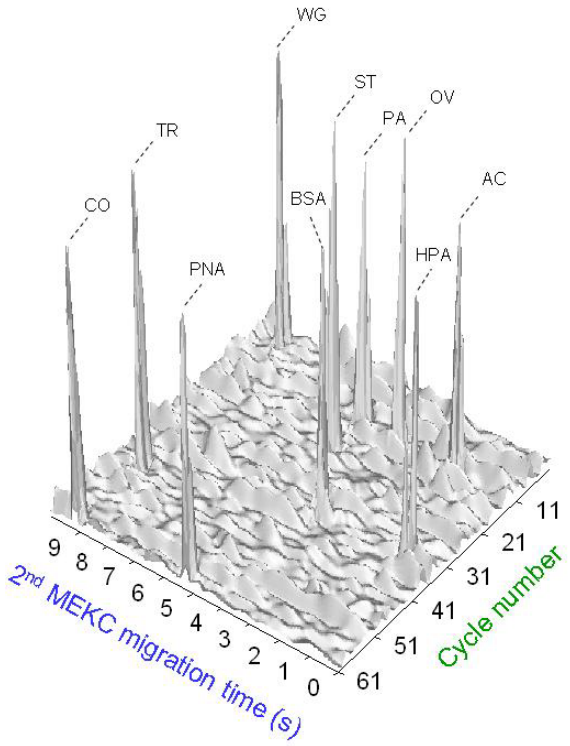

Figure 4.8. 2-D μ-CE separation of a 30 nM protein mixture in the PMMA chip. A 3-D image of the data shown in Figure 4.7 with the cycle number plotted versus the MEKC migration time.

The benefit of a coupled 2-D separation is demonstrated by its peak capacity as compared to its constituent 1-D peak capacities. For SDS μ-CGE, the proteins studied produced a peak capacity of 19. The MEKC dimension had a peak capacity of 59. Therefore, the theoretical peak capacity of the 2-D separation ($P_{2\text{-}D}$) would be 1,121 (19 × 59).[23] The actual peak capacity could

be considered smaller due to an increase in peak width in the SDS μ-CGE dimension produced by protein diffusion during the MEKC separation period, cross-information, or both from the individual separation dimensions (see Section 4.3.6).[14]

The data shown in Figure 4.7 were imported into ImageJ software to draw the representative 2-D image (see Figure 4.9). Once the 2-D separation was converted into a 2-D image, the separation resolving power could be determined from the number of pixels in each axis (x and y). As can be seen from Figure 4.9, the total area for this 2-D analysis includes 258,000 (400 × 645) pixels. It is obvious that more MEKC cycles, longer MEKC development times or both can provide 2-D separation images consisting of a higher number of pixels. Analyzing the spots in Figure 4.9 using ImageJ, a total of 10 components were found from this 2-D analysis corresponding to all of the proteins comprising the sample. An average area of 257.7 pixels was obtained for each protein in this 2-D separation image. Assuming no free space between the protein spots, a maximum number of ~1,000 (258,000/257.7) elements is estimated for this 2-D separation, which is in close agreement to the peak capacity calculated above.

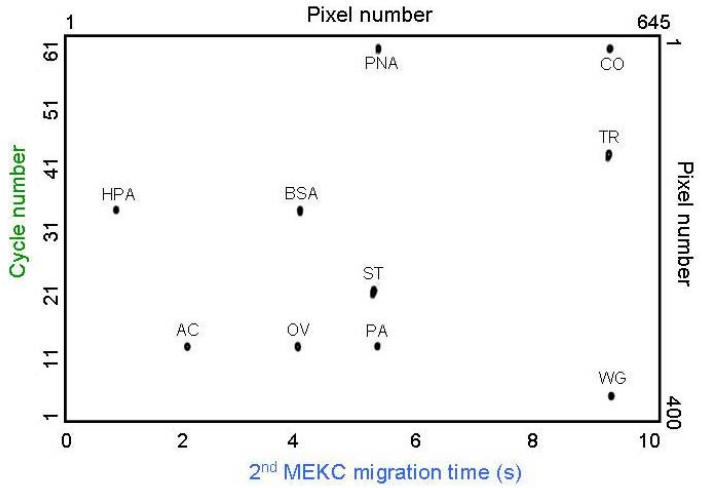

Figure 4.9. 2-D μ-CE separation of a 30 nM protein mixture in the PMMA chip. A converted image of Figure 4.8 formatted to resemble a stained gel.

4.3.5. Geometric Orthogonality of the 2-D Separation

The degree of orthogonality between the SDS μ–CGE and MEKC techniques in our 2-D separation using the PMMA microchip can be calculated based on the data presented in Figure 4.9.[49, 51, 54] The orthogonality (O) can be calculated using the following equation;

$$O = [\sum bins - \sqrt{P_{max}}]/[0.63\ P_{max}] \quad (4.3)$$

where ∑bins is the number of bins in the 2-D plot containing data points, and P_{max} is the total peak capacity obtained as a sum of all bins.[49] Figure 4.10 represents the 2-D separation image (see Figure 4.9), which was divided into 10 (2 × 5) rectangular bins. See Figure 4.7 for separation details.

Figure 4.10. Geometric orthogonality description of the 2-D separation of model proteins obtained in a PMMA microchip.

Considering 8 bins that contained data points and a total capacity of 10, the orthogonality of this 2-D system was calculated to be 77% using equation 4.3. This value compared well to values reported previously (0 – 69%) using a similar calculation method for different combinations of separation techniques to perform a 2-D analysis.[49] Practical peak capacity (N_p) is usually lower than the theoretical peak capacity because only a fraction of the surface is

utilized for separation.[49] The practical peak capacity can be evaluated using the following equation;[49]

$$N_p = P_{2\text{-}D}\,[\sum bins]/P_{max} \qquad (4.4)$$

Considering the values obtained above and using equation 4.4, $N_p = 897$ is expected for our 2-D analysis using SDS μ-CGE and MEKC.

4.3.6. Zonal Spreading due to the Coupled 2-D Process

Loss of peak capacity due to zonal dispersion induced by the on-line coupled 2-D separation can result from either the interface of the two-dimensions of the 2-D separation, incompatibility of the individual separation dimensions or "parking" of zones for a serial multidimensional separation as that used herein. We evaluated the effects of zonal spreading due to longitudinal diffusion in the first dimension during the development phases of the separations in the second dimension. This was accomplished by calculating the height equivalent of a theoretical plate for longitudinal diffusion only (H_D) of the 1-D SDS μ-CGE dimension and comparing that value to H_{TOT} secured from the complete 2-D separation. A representative diffusion coefficient for proteins in a sieving matrix as used herein was taken as ~10^{-8} cm^2 s^{-1}, which is the measured diffusion coefficient of cytochrome C in polyacrylamides[55] resulting in $H_D = 2.6 \times 10^{-6}$ cm (H_D = 2Dt / L; t = time; L = column length, cm). The number of plates for a typical band migrating from the 2-D separation (TR, see Figure 4.7) was 7.2×10^5, resulting in $H_{TOT} = 5.6 \times 10^{-6}$ cm. Therefore, the diffusional component to H_{TOT} was calculated to be approximately 46%. For 61 10 s MEKC cycles, which represents the parking time (610 s), and a total separation time of 720 s, the percent contribution of diffusional spreading during the parking phases only to H_D is roughly 85% or 2.2×10^{-6} cm. Clearly, reductions in the development time for the MEKC cycles can reduce H_D resulting from the parking phases of the separation, producing higher peak

capacities. Interestingly, the diffusion coefficient for cytochrome C in free solution has been reported to be ~10^{-6} cm^2 s^{-1},[55] two-orders of magnitude higher than that in the viscous polyacrylamide sieving matrix. Therefore, using MEKC in the first dimension, where parking is required to allow development in the second dimension, would be inadvisable due to significant degradations in peak capacity arising from large values of H_D.

Another process that could add to the total plate height of this coupled 2-D separation is protein de-stacking at the interface of the sieving matrix with the pseudo-stationary phase of the MEKC dimension due to mobility mismatches. Inspection of an injection band produced by a single MEKC cycle (see inset of Figure 4.7) resulted in an electrophoretic band width (FWHM) of 0.15 s. The band width obtained solely from the 1-D MEKC run was 0.14 s. Therefore, the coupling process resulted in a 6.7% increase in the observed 2-D band width. The relatively small increase in the band width resulted from the narrow channel used in the first dimension and the lack of sieving matrix (see Figure 4.1A) in the path defining the second dimension, which produced acceleration of material entering into the second dimension due to the analytes lower mobility in the first dimension. Both of these observations define the width of the injection plug introduced into the second dimension, which would be $\leq$ 20 μm, which is 0.07% of the total column length for the MEKC dimension.

4.4. Conclusions

Integrating two different separation modes, SDS μ-CGE and high speed MEKC, has been demonstrated using a PMMA microchip. The 2-D separation operates by rapidly sampling effluent from the first dimension into the second dimension. Results from the 2-D analysis suggested higher peak capacity over that of the corresponding uncoupled 1-D separations as peaks that were not resolvable using the 1-D separation under identical conditions were

effectively resolved in the 2-D format. The system consisted of an on-chip serial transfer, in which electrokinetic control of sample from the first to the second dimension channels resulted in efficient transfer maintaining overall separation performance.

The complete 2-D system was estimated to have a peak capacity of ~1,000. The peak capacity and resolution could be further improved by reducing the size of each fluid volume sampled into the second dimension, increasing the channel length in the first dimension and/or further reducing dispersion during sample transfer between the first and second dimensions. In addition, using higher transfer frequencies of effluent from the first dimension into the second dimension can improve peak capacity of the 2-D system as well,[25] but at the expense of increasing the 2-D electrophoresis development time.

All data reported herein were obtained using PMMA as the fluidic substrate due to its favorable optical properties permitting sensitive fluorescence readout as well as its ease in micromachining using replication technologies. Fabrication of both separation channels in PMMA minimized dead volumes between separation dimensions, improving peak capacity of the 2-D system by removing any interconnect paths. Further work in our laboratory is underway to couple the 2-D separation system with on-line mass spectrometry and solid-phase proteolytic digestion to provide a fully automated microfluidic processing system of proteins.

4.5. References

(1) Regnier, F.; Amini, A.; Chakraborty, A.; Geng, M.; Ji, J.; Riggs, L.; Sioma, C.; Wang, S.; Zhang, X. *LCGC North America* **2001**, *19*, 200-213.

(2) Anderson, N. L.; Anderson, N. G. *Mol. Cell. Proteomics* **2002**, *1*, 845-867.

(3) Giddings, J. C. *Analytical Chemistry* **1967**, *39*, 1027-1028.

(4) Stroink, T.; Ortiz, M. C.; Bult, A.; Lingeman, H.; de Jong, G. J.; Underberg, W. J. M. *Journal of Chromatography, B: Analytical Technologies in the Biomedical and Life Sciences* **2005**, *817*, 49-66.

(5) Giddings, J. C. *Analytical Chemistry* **1984**, *56*, 1258A-1270A.

(6) Giddings, J. C. *HRC & CC, Journal of High Resolution Chromatography and Chromatography Communications* **1987**, *10*, 319-323.

(7) Cortes, H. J. *Journal of Chromatography* **1992**, *626*, 3-23.

(8) Cortes, H. J.; Editor *Chromatographic Science Series, Vol. 50: Multidimensional Chromatography: Techniques and Applications*, 1990.

(9) Stroink, T.; Schravendijk, P.; Wiese, G.; Teeuwsen, J.; Lingeman, H.; Waterval, J. C. M.; Bult, A.; de Jong, G. J.; Underberg, W. J. M. *Electrophoresis* **2003**, *24*, 1126-1134.

(10) Powell, M. *Multidimensional Chromatography Edited by L. Mondello, A. C. Lewis, K. D. Bartle*, 2002.

(11) Bowerbank, C. R.; Lee, M. L. *Journal of Microcolumn Separations* **2001**, *13*, 361-370.

(12) Mohan, D.; Lee, C. S. *Electrophoresis* **2002**, *23*, 3160-3167.

(13) Liu, Y.-M.; Sweedler, J. V. *Analytical Chemistry* **1996**, *68*, 3928-3933.

(14) Michels, D. A.; Hu, S.; Dambrowitz, K. A.; Eggertson, M. J.; Lauterbach, K.; Dovichi, N. J. *Electrophoresis* **2004**, *25*, 3098-3105.

(15) Hu, S.; Michels, D. A.; Fazal, M. A.; Ratisoontorn, C.; Cunningham, M. L.; Dovichi, N. J. *Analytical Chemistry* **2004**, *76*, 4044-4049.

(16) Kraly, J. R.; Jones, M. R.; Gomez, D. G.; Dickerson, J. A.; Harwood, M. M.; Eggertson, M.; Paulson, T. G.; Sanchez, C. A.; Odze, R.; Feng, Z.; Reid, B. J.; Dovichi, N. J. *Analytical Chemistry*, **2006,** *78*, 5977-5986.

(17) Abul Fazal, M.; Palmer, V. R.; Dovichi, N. J. *Journal of Chromatography, A* **2006**, *1130*, 182-189.

(18) Harwood, M. M.; Christians, E. S.; Abul Fazal, M.; Dovichi, N. J. *Journal of Chromatography, A* **2006**, *1130*, 190-194.

(19) Sheng, L.; Pawliszyn, J. *Analyst (Cambridge, United Kingdom)* **2002**, *127*, 1159-1163.

(20) Yang, C.; Liu, H.; Yang, Q.; Zhang, L.; Zhang, W.; Zhang, Y. *Analytical Chemistry* **2003**, *75*, 215-218.

(21) Liu, H.; Yang, C.; Yang, Q.; Zhang, W.; Zhang, Y. *Journal of Chromatography, B: Analytical Technologies in the Biomedical and Life Sciences* **2005**, *817*, 119-126.

(22) Michels, D. A.; Hu, S.; Schoenherr, R. M.; Eggertson, M. J.; Dovichi, N. J. *Molecular and Cellular Proteomics* **2002**, *1*, 69-74.

(23) Ramsey, J. D.; Jacobson, S. C.; Culbertson, C. T.; Ramsey, J. M. *Analytical Chemistry* **2003**, *75*, 3758-3764.

(24) Shadpour, H.; Musyimi, H.; Chen, J.; Soper, S. *Journal of Chromatography A* **2006**, *1111*, 238-251.

(25) Gottschlich, N.; Jacobson, S. C.; Culbertson, C. T.; Ramsey, J. M. *Analytical Chemistry* **2001**, *73*, 2669-2674.

(26) Rocklin, R. D.; Ramsey, R. S.; Ramsey, J. M. *Analytical Chemistry* **2000**, *72*, 5244-5249.

(27) Herr, A. E.; Molho, J. I.; Drouvalakis, K. A.; Mikkelsen, J. C.; Utz, P. J.; Santiago, J. G.; Kenny, T. W. *Analytical Chemistry* **2003**, *75*, 1180-1187.

(28) Griebel, A.; Rund, S.; Schoenfeld, F.; Doerner, W.; Konrad, R.; Hardt, S. *Lab on a Chip* **2004**, *4*, 18-23.

(29) Wang, Y.-C.; Choi, M. H.; Han, J. *Analytical Chemistry* **2004**, *76*, 4426-4431.

(30) Li, Y.; Buch, J. S.; Rosenberger, F.; DeVoe, D. L.; Lee, C. S. *Analytical Chemistry* **2004**, *76*, 742-748.

(31) Sluszny, C.; Yeung, E. S. *Analytical Chemistry* **2004**, *76*, 1359-1365.

(32) Chen, X.; Wu, H.; Mao, C.; Whitesides, G. M. *Analytical Chemistry* **2002**, *74*, 1772-1778.

(33) Xu, A.; Sluszny, C.; Yeung, E. S. *Journal of Chromatography, A* **2005**, *1087*, 177-182.

(34) Richards, D. P.; Stathakis, C.; Polakowski, R.; Ahmadzadeh, H.; Dovichi, N. J. *Journal of Chromatography, A* **1999**, *853*, 21-25.

(35) Tsai, S.-W.; Loughran, M.; Karube, I. *Journal of Micromechanics and Microengineering* **2004**, *14*, 1693-1699.

(36) Cui, H.; Horiuchi, K.; Dutta, P.; Ivory, C. F. *Analytical Chemistry* **2005**, *77,* 7878-7886.

(37) Zuborova, M.; Demianova, Z.; Kaniansky, D.; Masar, M.; Stanislawski, B. *Journal of Chromatography, A* **2003**, *990*, 179-188.

(38) Fonslow, B. R.; Bowser, M. T. *Analytical Chemistry* **2005**, *77*, 5706-5710.

(39) Jungblut, P.; Thiede, B.; Zimny-Arndt, U.; Mueller, E.-C.; Scheler, C.; Wittmann-Liebold, B.; Otto, A. *Electrophoresis* **1996**, *17*, 839-847.

(40) Foley, J. P. *Analyst (Cambridge, United Kingdom)* **1991**, *116*, 1275-1279.

(41) Giddings, J. C. *Unified Separation Science*, 1991.

(42) Tsai, S.-W.; Loughran, M.; Suzuki, H.; Karube, I. *Electrophoresis* **2004**, *25*, 494-501.

(43) Strege, M. A.; Lagu, A. L. *Analytical Biochemistry* **1993**, *210*, 402-410.

(44) Strege, M. A.; Lagu, A. L. *Journal of Chromatography, A* **1997**, *780*, 285-296.

(45) Williams, D. C.; Van Frank, R. M.; Muth, W. L.; Burnett, J. P. *Science (Washington, DC, United States)* **1982**, *215*, 687-689.

(46) Strege, M. A.; Lagu, A. L. *Journal of Chromatography* **1992**, *630*, 337-344.

(47) Venkatramani, C. J.; Xu, J.; Phillips, J. B. *Analytical Chemistry* **1996**, *68*, 1486-1492.

(48) Erni, F.; Frei, R. W. *Journal of Chromatography* **1978**, *149*, 561-569.

(49) Gilar, M.; Olivova, P.; Daly, A. E.; Gebler, J. C. *Analytical Chemistry* **2005**, *77*, 6426-6434.

(50) Slonecker, P. J.; Li, X. D.; Ridgway, T. H.; Dorsey, J. G. *Analytical Chemistry* **1996**, *68*, 682-689.

(51) Gray, M.; Dennis, G. R.; Wormell, P.; Shalliker, R. A.; Slonecker, P. *Journal of Chromatography A* **2002**, *975*, 285-297.

(52) Murphy, R. E.; Schure, M. R.; Foley, J. P. *Analytical Chemistry* **1998**, *70*, 1585-1594.

(53) Liu, S. R.; Shi, Y. N.; Ja, W. W.; Mathies, R. A. *Analytical Chemistry* **1999**, *71*, 566-573.

(54) Slonecker, P. J.; Li, X.; Ridgway, T. H.; Dorsey, J. G. *Analytical Chemistry* **1996**, *68*, 682-689.

(55) Lewus, R. K.; Carta, G. *Industrial & Engineering Chemistry Research* **2001**, *40*, 1548-1558.

CHAPTER 5

HIGH-THROUGHPUT ELECTROPHORETIC SEPARATION OF PROTEINS AND OTHER BIOMOLECULES USING POLYMERIC MICROCHIPS*

5.1. Introduction

Microchip capillary electrophoresis is becoming a powerful new tool in separation science because of the high performance separation capacity it offers for a variety of bio-molecules arising from the high speed separations it affords as well as the reduced sample/reagent consumption and low cost of producing this separation platform. Another attractive feature associated with μ-CE is its ability to perform high-throughput analyses by fabricating wafers that incorporate multiple separation columns onto a single wafer.[1]

High-throughput analyses are extremely desirable for many types of bio-analytical analyses. For example, in order to understand molecular interactions and the role they play in cellular functioning, a large number of protein mixtures in many different samples must be analyzed in concert.[2-4] Another example of the need for high-throughput processing capabilities is in drug discovery, which has produced significant analytical separation challenges due in part to the advent of combinatorial chemistry with automated parallel synthesis techniques. Advances in combinatorial chemistry has dramatically increased the number of compounds that must be analyzed in a reasonable timeframe and at modest costs.[5-7] High-throughput analytical separation techniques have become critical for determining the identity and purity of these synthesized substances and also understanding their potential inhibitory effects on targets by invoking mobility shift assays that use electrophoresis techniques in multi-channel formats to achieve the necessary high-throughput processing capacity demanded for drug discovery.[8, 9]

The throughput of a capillary array electrophoresis (CAE) system is directly proportional to the number of separation capillaries contained within the instrument. Many commercial instruments are now available that can run 96 individual separations in parallel using the CAE

format and this number has recently increased to 384-capillary-based machines.[10] However, as the number of capillaries increases, it becomes more challenging to control sample injection and to detect signals from all of the capillaries simultaneously. In addition, the cost of maintaining the machine increases as well. For example, a 96-capillary CAE system may cost nearly $3,600 to replace all of the capillaries. On the other hand, microchip capillary array electrophoresis (μ-CAE) can increase system throughput by simply machining a higher number of independently operating separation units onto a single wafer using high-precision microfabrication techniques producing the required number of independently operating separation columns at a fraction of the cost associated with capillary arrays. In addition, the analysis times afforded by μ-CAE can be shorter than CAE because of the use of shorter separation columns, further increasing the throughput capacity of the system.[11]

The μ-CAE on glass microchips coupled with fluorescence detection have been developed by several groups for high-throughput genetic analyses,[11-19] and separation of biomolecules[18, 20] and drugs.[21] μ-CAE for genomic analyses has been reviewed recently.[22, 23] Simultaneous immunoassays have also been reported on glass[24] and polymer[25] microchips. A multi-channel PMMA microchip equipped with a CCD-based fluorescence detection system was also reported for high-throughput genetic analysis.[26] The use of polymer-based wafers for μ-CAE applications are particularly compelling because polymer-based devices are conducive to mass production when using microreplication-type technologies, significantly lowering the cost of the device.[27-29]

The readout strategy used for most μ-CAE separations has relied primarily on fluorescence detection due to the fact that it provides exquisite sensitivity with limits of detection that can approach the single molecule level.[30-33] The major challenge associated with fluorescence is the fact that the analytes, for the most part, must be labeled either covalently or

non-covalently with a fluorophore due to the fact that most do not display intrinsic fluorescence properties at the excitation wavelengths used. In addition, miniaturization and integration of the detector into a μ-TAS, especially those designed for multi-channel readout, is difficult to accomplish when using fluorescence detection.[34, 35]

Another readout strategy for microfluidic applications is electrochemical detection.[36-39] Electrochemical detection requires very simple hardware in order to affect detection and at the same time, offers reasonable sensitivities and LODs.[38] Additionally, electrochemical detection techniques are not mass-sensitive but concentration sensitive, implying that scaling down the detector cell size does not necessarily result in a loss in the LOD. Miniaturization of the detection electrodes, which defines the detector volume, could even result in improving the LOD as a result of the reduced noise afforded by smaller electrode geometries. Furthermore, since the detector response is derived directly from an electrical property of the solution, conversions between different physical parameters, such as light intensity to electricity, are eliminated thereby removing an additional source of noise.[40]

For amperometric detection, the analytes must be electroactive or electroactive species must be appended to the target molecules. On the other hand, conductivity detection is considered as a technique with the ability to detect any analyte irrespective of whether it contains an electroactive species or not.[41] Conductivity detection often displays inferior LODs compared to other electrochemical detection methods such as amperometry, but has the advantage of being a universal detection technique, thereby obviating the need for pre-labeling the analytes prior to detection.[42] The only requirement is that the migrating analyte zones hold a solution conductance that is different from the carrier electrolyte.[41]

Recently, μ-CE with conductivity detection in single channel microfluidic devices has been reviewed.[38, 41-45] The majority of μ-CE integrated with contact conductivity detection

technique was focused on separation of small / organic ions or pharmaceuticals.[38, 41-45] For biological samples, contact conductivity detection was used in single channel microchips for CZE[46, 47] or ITP[48] of amino acids, CZE of peptides,[42, 47, 49] CZE,[49-51] CZE-ITP[52] or MEKC[47] of proteins, and CEC of oligonucleotides.[47]

To the best of our knowledge, there has been no report on μ-CAE utilizing an integrated conductivity sensor array for detection. In this chapter, we will describe the fabrication and testing of a novel 16-channel PC microfluidic device to perform parallel micro-capillary zone electrophoresis (μ-CZE) of amino acids, peptides and proteins, and also micro-capillary electrochromatography (μ-CEC) of oligonucleotides detected by a gold (Au) conductivity sensor array. The sensor array was patterned onto a PC cover plate before thermal bonding this cover plate to the fluidic network. The fabrication approach with parallel arrangement of the conductivity electrodes has the potential for integrating large numbers of fluidic channels onto a single wafer for parallel operation with integration of several processing steps including injection, separation and detection for the rapid and high-throughput analyses of unlabeled species using a universal detection technique and inexpensive polymeric microchip.

5.2. Experimental Details

5.2.1. Fabrication of Microfluidic Chip

Fabrication of the microfluidic chips used herein involved the following steps: (i) design and fabrication of a metal mold master; (ii) hot-embossing of polymer devices; (iii) patterning of the electrode array onto a polymer film and (iv) device assembly. Both the microfluidic network and electrode array were designed using AutoCAD (Autodesk, Inc., San Rafael, CA; see Figure 5.1A). The mold master was fabricated in brass using high-precision micromilling (KERN MMP, KERN Micro-und Feinwerktechnik GmbH & Co.KG; Germany) according to procedures described elsewhere.[54] Fluidic parts were hot embossed (180^{o}C, 2 min, 20 kN) using

a HEX-02 hot-embossing machine (Jenoptik Mikrotechnik GmbH, Jena, Germany) into the PC wafers (Lexan PC, MSC, Melville, NY). Following embossing, devices were cut into 66 mm × 81 mm rectangles and 40 holes (1.5 mm in diameter) were drilled using a computer numerical control (CNC) machine at designated locations on the fluidic microchip to serve as reservoirs.

The gold electrodes used for conductivity detection were fabricated onto a thin PC plate using standard lithographic techniques (see Figure 5.2). Briefly, an AutoCAD design of the electrode array (see Figure 5.1A, red pattern) was transferred to a 5" UV photomask blank (Nanofilm, Westlake Village, CA) using a GCA Mann 3600 pattern generator (D.W. Mann/GCA Corp., USA) and the optical mask was developed according to the manufacturer's procedure. A 1,000 Å thick layer of Ti and 500 Å of Au were deposited (BJD-1800 E-beam evaporator, TES, CA) on the surface of the PC cover plate (500 μm thickness, Lexan PC, MSC, Melville, NY). The Au layer served as the conductivity electrodes and the thick layer of Ti was used to improve both the adhesion of Au to the PC substrate and the mechanical strength of the final pattern. A 2 μm layer of positive photoresist (S1813, Shipley, NJ) was then spin-coated onto the metal-coated PC substrate (2,000 rpm for 20 s, PWM101 spinner, Headway Research Inc., TX). After a pre-bake for 1 min at 90°C, the resist-coated PC substrate was exposed under UV light for 10 s (Oriel UV Exposure System, Stratford, CT) through an optical mask. The substrate was then developed (354 Developer, Shipley, NJ) for 40 s to remove the UV-exposed photoresist followed by etching of the exposed metal layers. The Au was etched in a commercial Au-etching solution (Transene Comp., Inc., Danvers, MA) for 1 min and the Ti layer was etched in a 1% HF solution diluted from 49% concentrated HF (General Chemical Corp., Hollister, CA) to distilled water with a ratio of 1:50 for 1 min. After etching, the PC substrate was flood-exposed under UV light for 10 s and the remaining photoresist was developed to reveal the electrode pattern.

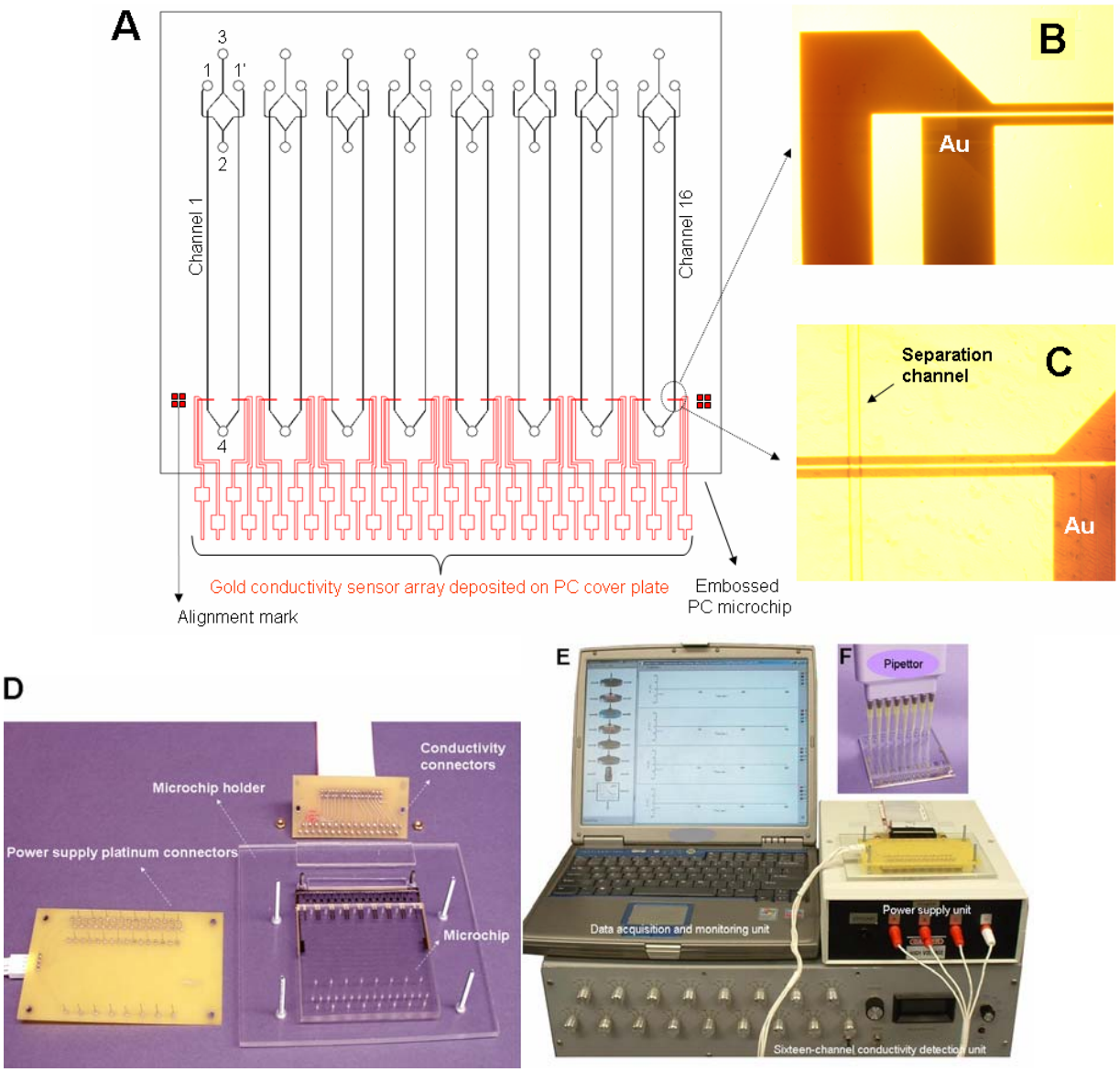

Figure 5.1. (A) Topographical layout of the multi-channel microfluidic network. Injection channel length = 9 mm; total separation channel length = 54 mm; effective separation channel length (L_{eff}) = 40 mm; channel width = 60 µm; channel depth = 40 µm. The reservoirs for each microfluidic channel pair are; (1) and (1') sample reservoirs; (2) sample waste reservoir; (3) buffer reservoir; (4) buffer waste reservoir. All reservoirs were 1.5 mm in diameter. The center-to-center spacing of each fluidic reservoir was fixed at 9 mm. The line trace shown in red provides a topographical layout of the lithographically printed-Au conductivity sensor array. The outlet end consisted of 16 Au-electrodes (7.62 mm long × 500 µm wide) serving as the conductivity sensors. Shown is the detection region of one Au-electrode pair before (B), and after (C) thermal annealing of the cover plate to the microfluidic chip. Each contact conductivity electrode was 60 µm in diameter with an end-to-end spacing of 5 µm. (D) Photograph showing the microchip and the holder setup with connectors for the high voltage power supply and conductivity detection units. (E) Overview of entire system including 16-channel conductivity detection, power supply and data acquisition/monitoring units. (F) Filling all 40 reservoirs in 5 steps using multi-channel pipettor.

In the final step of the multi-channel microfluidic device fabrication, the microfluidic channels were tightly sealed to the Au-patterned cover plate. To accomplish this, both PC parts were cleaned with 50% isopropanol and distilled water, dried using compressed air with the embossed PC substrate placed in an oven at 85°C overnight to remove all residual water from this piece. Then, the patterned cover plate was aligned with the hot embossed PC chips using alignment marks (see Figure 5.1A) incorporated into both parts during fabrication. Both pieces were then clamped between glass plates and thermally bonded using a GC oven (150°C, 20 – 30 min).[29] Prior to any electrophoresis experiment, the Au microfabricated electrodes were inspected using an optical microscope for any possible damage/deformation during the thermal assembly step.

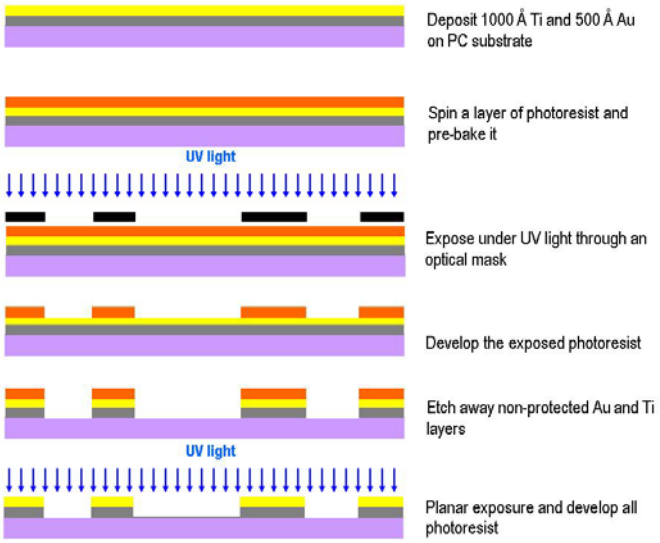

Figure 5.2. Flow chart showing the processing steps used for patterning the Au conductivity sensor array onto a PC cover plate (layers are not drawn to scale).

5.2.2. Conductivity Detection and High Voltage Power Supply Units

The conductivity detection unit was designed to perform simultaneous conductivity measurements on 16 microchannels (see Figure 5.1E). The conductivity was measured using a previously reported bipolar technique.[47] The bipolar pulse waveform for the conductivity array was generated by an in-house fabricated circuit, which was controlled by a National Instruments

controller board (PCI-6071E, Austin, TX) programmed using Visual Basic. The instrument outputs a bipolar pulse waveform that could be adjusted in both amplitude and frequency. A 12 bit digital–to-analog converter (D/A) covered a range of 0 to ±5 V with 1.2 mV resolution. The potential of one conductivity electrode was maintained at virtual ground while the potential at the other electrode was the bipolar waveform. The detector gathered instantaneous current readings between the electrode pair ~100 ns prior to the rising edge of every bipolar pulse (up to ±2.5 V) at the input port. The readings were averaged over the electrophoresis sampling time to improve the SNR in the measurement. The resulting signal from each detector in the array was processed by an adjustable gain amplifier (four resistors ranging from 1 kΩ to 1 MΩ) and passed to a sample-and-hold amplifier whereby the output was filtered by a low-pass filter with a cut-off frequency of 16 Hz. To further preserve signal integrity, the filtered output was transmitted to the data acquisition board via a differential amplifier driving a shielded twisted pair wire. The signals were amplified and converted to a 12-bit word.

The high voltage power supply used for the electrophoresis was assembled in-house using four independent high voltage modules (EMCO, Sutter Creek, CA) configured into separate electrokinetic modes. The high voltage power supplies and relays were controlled by a computer using an analog output card (PCI-DDA04/12, National Instruments, Austin, TX) and software written in Visual Basic.

Interfacing the electrical signals from both the conductivity array detector and the high voltage power supplies for the electrophoresis to the multi-channel microfluidic chip was provided by two printed circuit boards (PCB). The PCBs, with spring-loaded Au-coated pins, were used to connect the conductivity detection unit to the conductivity array connector pads patterned on the cover plate of the microfluidic chip. The PCB with platinum wire electrodes (Scientific Instrument Services, Ringoes, NJ) was used to distribute high voltage to all of the

fluidic reservoirs used for capillary electrophoresis. Caution! The electrophoresis uses high voltages and special care should be taken when handling the electrodes.

5.2.3. Electrophoretic Separations

All electrophoretic separations were carried out at ambient temperature and run in reverse mode (injection end cathodic). Injection was initiated by applying +50 V to the sample waste reservoir (reservoirs 2, see Figure 5.1A) and grounding the sample reservoir (reservoirs 1 and 1', see Figure 5.1A) for the appropriate amount of time to completely fill the cross channel injector. Reservoirs 3 and 4 were allowed to float during injection. Following injection, –480 V (E = 90 V/cm) was applied to reservoirs 3 while reservoirs 4 were grounded. The field strength used herein was selected to minimize solvent electrolysis occurring between the two conductivity electrodes. Potentials of +20 V and +10 V were applied to the sample and sample waste reservoirs, respectively, to serve as pullback voltages that minimized sample leakage into the separation channels during the separation step.

Prior to loading into receiving reservoirs, the samples were centrifuged (6,000 rpm for 10 min) to remove any particulates. The electrolyte solutions were filtered using a 0.2 μm Nylon-66 membrane filter (Cole-Parmer Instrument Co., Vernon, IL), and degassed for 10 min prior to filling the microchip. All electrophoresis were performed simultaneously in the multi-channel PC chip using a bipolar amplitude of ±0.6 V and a frequency of 6.0 kHz.

The current-monitoring method was used to measure the EOF in a straight channel of the microfluidic device by using 1X and 0.5X TBE buffers, pH 8.3 (BioRad Laboratories, Hercules, CA) that were mixed with 0.05% w/v MHEC (Sigma, St. Louis, MO) which served as a dynamic EOF suppressor.[29] Standard KCl solutions (Sigma) were used to evaluate the analytical figures of merit of the conductivity sensor array.

5.2.4. Multi-Channel μ-CZE and μ-CEC

The μ-CZE was carried out on the amino acid mixture (Sigma), which included alanine, valine, glutamine and tryptophan, using a running buffer that contained triethylammonium acetate (TEAA, 8 mM, pH 7.0, Fluka, Milwaukee, WI). 0.05% w/v MHEC was also added to the carrier electrolyte to assist in suppressing the EOF.[51] The μ-CZE was also carried out on a peptide mixture, which consisted of leucine enkephalin, methionine enkephalin and oxytocin (Sigma), using a running buffer that was comprised of 2 mM Na_3PO_4 and 0.05% w/v MHEC, pH 7.3 (Sigma). The μ-CZE of the protein sample, consisting of chymotrysinogen (MW = 25 kDa, pI = 9.3), cytochrome C (MW = 12.5 kDa, pI = 10.6) and bovine serum albumin (MW = 68 kDa, pI = 4.9), was conducted using 2.5 mM NaH_2PO_4, 0.5 mM SDS, and 0.05% w/v MHEC, pH 2.5 (Sigma).

The μ-CEC of the double-stranded oligonucleotides (1 kbp DNA ladder, Invitrogen, Carlsbad, CA) used ion-pair reverse-phase chromatography which has been reported by our group.[47] The carrier electrolyte was 25% acetonitrile (Sigma) and 75% water containing 50 mM TEAA (Fluka, serving as the ion pairing agent), pH 7.0. The oligonucleotides consisted of 517, 1018, 1636, 2036, 3054, 4072, 5090, 6108, 7126, 8144, 10000, 15000, 20000 and 40000 bp fragments.

For both high-throughput μ-CZE and μ-CEC experiments, the required concentrations of samples were made from stock solutions diluted in the appropriate carrier electrolyte (except for proteins, which were dissolved in protein running buffer with a total concentration of SDS = 2 mM) and electrokinetically injected into the system using the voltage pattern described above.

5.3. Results and Discussion

5.3.1. Multi-Channel Microelectrophoresis Chip with Contact Conductivity Detection

Figure 5.1A represents the design of both the microfluidic network and the conductivity electrode array. The microfluidic network consisted of 8 pairs of independently operated separation channels. Each pair of channels shared common buffer and waste reservoirs. All channels in this microchip were 60 μm wide and 40 μm deep with L_{eff} = 40 mm. In order to facilitate loading of the sample and buffer solutions into the microchip prior to analysis, all reservoirs were spaced with the same pitch as an 8-channel automatic pipettor (9 mm). This way, all 40 reservoirs could be loaded in only 5 pipetting steps; 3 steps for buffer, buffer waste and sample waste reservoirs, and 2 steps for loading sample into the appropriate reservoirs. The Au electrode array consisted of 32 independent Au traces (see Figure 5.1A). Each trace consisted of square metal pads for external contact with a 500 μm wide conduction path and a 60 μm wide microelectrode pair used for conductivity detection. The pair of conductivity microelectrodes was spaced by 5 μm, which was kept small to reduce the potential drop across the electrode pair arising from the electrophoresis field. To facilitate the assembly process and to ensure that the microelectrodes were accurately and uniformly aligned to all microchannels, alignment marks were incorporated onto both the microfluidic chip and the cover plate. Figures 5.1B and 4.1C show optical micrographs of a typical printed Au conductivity sensor array on a PC cover plate before and after thermal assembly to the microfluidic network. A photograph of the multi-channel PC microchip and the microchip holder with its high voltage and conductivity PCBs is shown in Figure 5.1D.

5.3.2. Analytical Figures of Merit for the Conductivity Sensor Array

The contact conductivity sensor array geometry used here had an electrode area that was in contact with the solution of 7.2×10^{-5} cm^2 providing a calculated cell constant (K_c) of 7 cm^{-1}

for each pair of electrodes.[55] Two 60-μm wide microelectrodes with a 5 μm spacing between them provided a 125 μm length detection region for each parallel micro-channel. Since the conductivity sensors were placed 40 mm (i.e., L_{eff}) from the injector, the length of the detection region was calculated to be ~0.3% of L_{eff}. The injection cross channel (simple cross) was designed to have an approximate load volume of 144 pL (injection length, L_{inj}, ~60 μm). Calculation of the detection and injection variances (σ_{det}^2, σ_{inj}^2, respectively) from L_{det}^2 / 12 or L_{inj}^2 / 12 yielded values of 1.3×10^{-5} cm^2 and ~3.0×10^{-6} cm^2 for σ_{det}^2 and σ_{inj}^2.[47] For typical electrophoretic separations using this microchip design, a representative total variance, σ_{tot}^2, was determined to be, σ_{tot}^2 ~3.2×10^{-3} cm^2, which was calculated for alanine based on its migration time and peak width (see Figure 5.3B). Therefore, σ_{inj}^2 and σ_{det}^2 were less than ~0.4% of σ_{tot}^2.

Using a 90 V/cm separation field and the ±0.6 V bipolar voltage for this high-throughput conductivity analysis system, the measured potential difference between the electrode pair was determined to be 350 mV. This voltage drop did not cause any noticeable electrolysis or bubble formation in our experiments with the carrier electrolytes and pH values used for our separations. It should be noted that reducing the spacing between each pair of the conductivity electrodes and/or reducing the electrode width would further minimize this potential drop and would allow for higher electric fields used for the electrophoresis to shorten development times.

The effects of the MHEC EOF suppression coating and the electrophoretic analyses on the response of the contact conductivity sensor array was studied by using injections of a 100 μM KCl solution used as a reference following electrophoretic runs of model analytes. The results indicated that the conductance response decreased by about 4% in the presence of 0.05% w/v MHEC added into a 1X TBE running buffer (data not shown). Following 20 repetitive electrophoretic analyses, the conductivity detector response decreased by ~17% for the 20th run when compared to the initial run (data not shown).

5.3.3. Multi-Channel Electrophoresis with Conductivity Detection

As a proof-of-concept for the μ-CAE platform with the integrated conductivity array detector, the performance of the system was tested for the simultaneous μ-CZE of amino acids, peptides and proteins and also μ-CEC of oligonucleotides. To perform this, channels 1-4, 5-8, 9-12 (see Figure 5.1A, left-to-right) and the corresponding reservoirs were selected for μ-CZE of the amino acids, peptides and proteins, respectively, and were filled with the appropriate running buffers (see Experimental Section). For each analyte type, the sample reservoirs were filled with different concentrations of the analyte ranging from 10 μM to 100 μM. μ-CEC of the oligonucleotides was carried out in channels 13-16 with each channel containing a different concentration of the oligonucleotide ladder ranging from 0.1 μg/μL to 1.0 μg/μL. A typical output for these samples is shown in Figure 5.3A. The x-axis shows the electrophoresis migration time and the y-axis represents the normalized conductivity response for each microchannel. Normalization of the conductivity responses was performed by dividing the detector response received from each microfluidic channel by the average conductivity value obtained for each running buffer in that particular channel. The normalization process was carried out in order to correct for differences in the conductivity response for each buffer system used in these separations. A summary of the separation results for these analytes is shown in Table 5.1.

The PC used herein showed an EOF that ran from anode to cathode with a magnitude of 2.1×10^{-4} cm^2/Vs.[29] At the pH used for these separations, the amino acids, peptides and oligonucleotides existed in their anionic form; therefore, these analytes migrated toward the anodic reservoir because their electrophoretic mobility was slightly greater than the EOF of the PC. Although the proteins carried a positive charge in the acidic pH buffer that was used herein (pH 2.5, pI of proteins listed in the Experimental Section), association of the proteins with

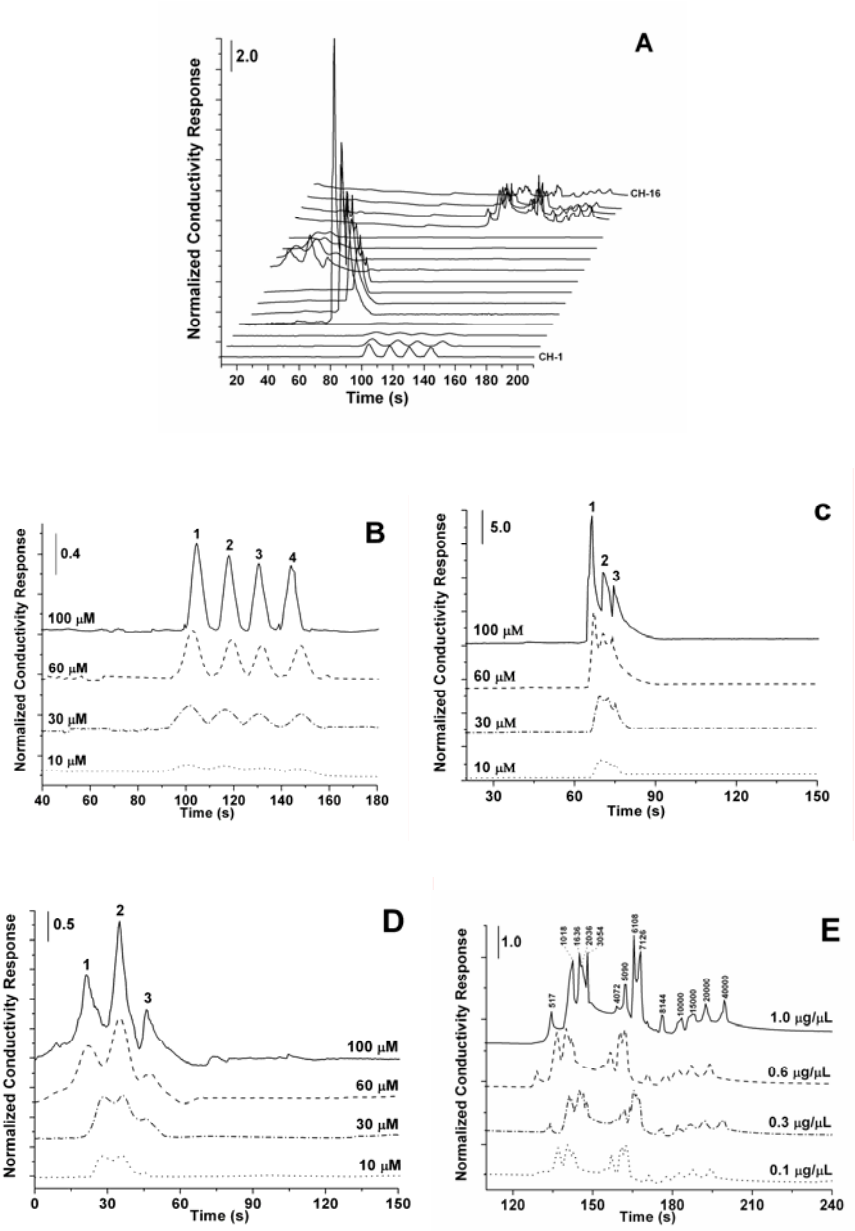

Figure 5.3. (A) Sixteen-channel microchip electrophoresis of different samples using the PC microchip and setup shown schematically in Figure 5.1. Channels 1-4 - μ-CZE of amino acids; channels 5-8 - μ-CZE of peptides; channels 9–12 - μ-CZE of proteins; channels 13-16 - μ-CEC of oligonucleotides. The electrophoresis was performed at 90 V/cm with a bipolar pulse amplitude of ±0.6 V and a bipolar frequency of 6.0 kHz. Details on the separation buffers used for each sample can be found in the Experimental Section. (B) An expanded view of the electrophoretic trace for the μ-CZE analysis of amino acids, which consisted of; 1 – alanine; 2 – valine; 3 – glutamine; and 4 - tryptophan. (C) An expanded view of the μ-CZE analysis of peptides, which contained; 1 - leucine enkephalin; 2 - methionine enkephalin; and 3 - oxytocin. (D) Expanded view of the electrophoretic trace for the μ-CZE analysis of proteins consisting of; 1 - chymotrypsinogen A; 2 - cytochrome C; and 3 - bovine serum albumin. (E) Expanded view for the μ-CEC analysis of a 1 kbp oligonucleotide ladder comprised of 517, 1018, 1636, 2036, 3054, 4072, 5090, 6108, 7126, 8144, 10000, 15000, 20000 and 40000 bp fragments. All concentrations used for the analyses are shown in the Figure. Figures 3B to 3E were re-constructed from the data shown in Figure 5.3A.

negatively charged SDS made their apparent mobilities direct them toward the anode as well. However, since the EOF moved in the cathodic direction, the apparent mobility was small for these analytes extending the analysis time. In order to reduce the electrophoretic development time, the EOF was suppressed by adding 0.05% w/v MHEC into all μ-CZE running buffers.[56] The EOF value of the PC microchip in the presence of MHEC was measured to be 3.6×10^{-5} cm^2/Vs, providing an approximate 80% reduction in the EOF compared to native PC. As a result, the separations were completed in less than 4 min for all species analyzed in this set of experiments.

Table 5.1. Mean N, R_s and channel-to-channel migration time reproducibility (RSD%) resulting from the analysis of various analytes using a multi-channel PC microdevice with an integrated conductivity sensor array for detection. Regression equations and the statistical parameters calculated from the calibration plots are also shown.[1]

Sample	CE Type	N (plates)	R_s	RSD%	Regression Equation	r^2	Concentration Range
Amino acids	μ-CZE	2.0×10^3	1.0	1.4	y = 0.037x + 0.060	0.990	10 – 100 μM
Peptides	μ-CZE	4.8×10^3	0.9	1.6	y = 0.39x + 1.652	0.993	10 – 100 μM
Proteins	μ-CZE	3.4×10^2	1.0	6.3	y = 0.16x + 0.127	0.990	10 – 100 μM
Oligonucleotides	μ-CEC	6.4×10^4	4.6	1.8	y = 3.9x + 0.156	0.986	0.1 – 1.0 μg/μL

1.y: Normalized conductivity peak area; x: analyte concentration; r^2: square of correlation coefficient.

In Figures 5.3B to D are shown μ-CZE analyses of the amino acids (channels 1-4, extracted from Figure 5.3A), peptides (channels 5-8) and proteins (channels 9-12). Separation of the amino acids, peptides and proteins with resolution near baseline (R_s = 0.9-1.0, see Table 5.1) was completed in the 12 microfluidic channels in approximately 160 s, 90 s and 70 s, for the amino acids, peptide and proteins, respectively, using a 90 V/cm electric field strength. The proteins showed the lowest separation efficiency (plate numbers) and poorest channel-to-channel migration time reproducibility due most likely to their potential non-specific interactions to the walls of the microfluidic separation channels. The average value for the migration time reproducibility was calculated to be 3.1% for all 12 parallel μ-CZE separations.

We have developed a C18 modified PMMA microchip that was used for the high-resolution separation of DNA oligonucleotides via CEC, in which the C18 phase, serving as the stationary phase, was covalently strapped to the PMMA surface.[47] In this work, we were interested in adapting these types of μ-CEC separations for oligonucleotides using pristine PC as the stationary phase. The last four channels (channels 13-16, see Figure 5.1A) were used for the μ-CEC separation of an oligonucleotide ladder. Figure 5.3E shows the corresponding results re-constructed from Figure 5.3A. The mobile phase used here contained acetonitrile as the organic modifier and an ion-pairing agent, TEAA. As shown in Figure 5.3E, successful separation (see Table 5.1) was completed in less than 210 s with a migration time reproducibility between the parallel microfluidic channels being 1.8%. The high separation efficiency and resolution obtained using pristine PC was due to the relatively strong hydrophobic nature of the Lexan PC surface (contact angle = $95^{o}\pm3$),[29] allowing extensive partitioning of the hydrophobic ion-pair complexes to this support. As reported in our previous work, pristine PMMA was unable to separate ion-paired oligonucleotides due to this material's smaller water contact angle.[47] As a comparison, μ-CZE analysis of this oligonucleotide ladder using only 1X TBE buffer only did not show any separation of these oligonucleotides (data not shown).[47]

The capability of the conductivity array detector for securing quantitative data was evaluated by analyzing the average peak area of the normalized conductivity signals (extracted from Figure 5.3) of the amino acids, peptides and proteins as a function of different concentrations (i.e., 10 – 100 μM) and also for the μ-CEC of the oligonucleotides in a 0.1 – 1.0 μg/μL concentration range. The resulting calibration plots are shown in Figure 5.4. A summary of a linear regression analyses carried out on these data sets is also shown in

Table 5.1. For each sample mixture, a different regression equation and correlation coefficient was obtained with an overall $r^2 = 0.990$ calculated as an average for these analytes. The value obtained for the correlation coefficient was comparable to literature values using contact conductivity detection run in a single channel format.[47, 51] Inspection of the data indicated an average concentration LOD of 7.1 μM at a SNR = 3 for alanine. On the basis of the known injection volume (~144 pL), the mass detection limit for this concentration was calculated to be ~1.0 fmol. It should be noted that the SNR depends intimately on the carrier electrolyte concentration as well with lower concentrations of the carrier electrolyte improving LODs.[47] The limitation of using lower concentrations of the carrier electrolyte is a loss of separation efficiency;[57] therefore, a trade-off between separation efficiency and detector performance must always be considered. As a matter of reference, the mass LOD for contact conductivity detection reported in our previous publication using a single channel microchip electrophoresis platform was 3.4 amol, but used electrodes that were larger in area and were poised orthogonal to the electric field.[47, 55]

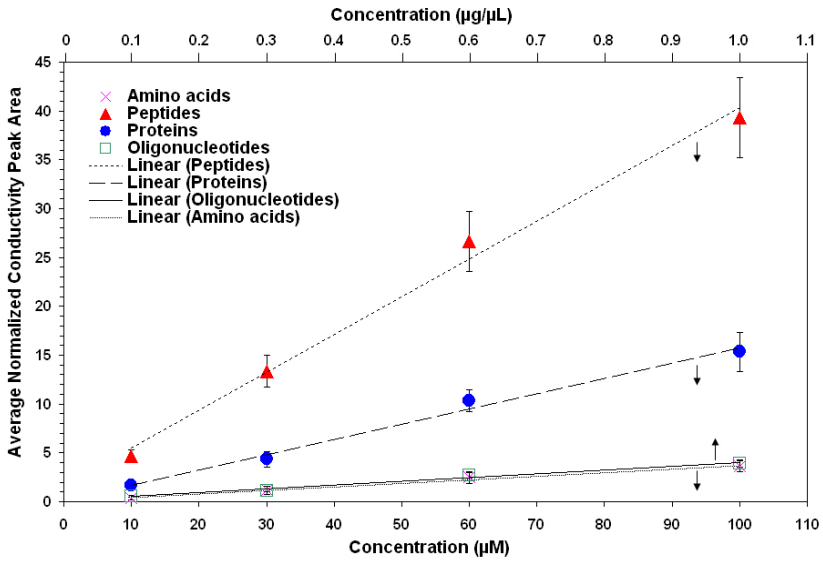

Figure 5.4. Linear calibration plots obtained from the results shown in Figure 5.3 for the electrophoretic analyses of amino acids, peptides, proteins and oligonucleotides using the integrated conductivity sensor array.

5.4. Conclusions

A 16-channel PC microfluidic chip integrated with a contact conductivity sensor array was developed and successfully tested for the high-speed, parallel μ-CZE and μ-CEC separations of 16 different samples, which consisted of amino acids, peptides, proteins or oligonucleotides. The separation and detection of all 16 mixtures required less than 210 s with baseline resolution accomplished using a 40 mm effective length separation channel. In addition, the device was flexible enough to simultaneously carry out different separation mechanisms selected for the individual sample under investigation. The detection was accomplished using a label-less technique consisting of contact conductivity detection configured in a sensor array for reading the bulk solution conductance. The electrode sensor array was lithographically patterned onto the fluidic cover plate and assembled to an embossed substrate using a thermal bonding process. While the LOD for this sensor array was poorer than our previous publication using contact conductivity detection configured in a single channel format due to the electrode geometry,[40] the electrode configuration adopted herein provided simple integration with the fluidic network, especially when configured in a multi-channel format.

While we have demonstrated the ability to perform 16-simultaneous separations with contact conductivity detection, it would be desirable to consider the integration of more separation units along with the conductivity sensor array onto one microfluidic wafer to increase sample throughput. Using an 8" plastic wafer fabricated via micro-replication technologies (~20 cm), we could pattern 40 separation units in this footprint leaving the fluidic geometry similar to that depicted in Figure 5.1A (20 separation units on each side of the wafer with L_{tot} = 54 mm). This would maintain the 9 mm spacing between the individual fluidic reservoirs to allow loading the chip using a multi-channel pipettor. As the number of channels (n) is increased with our

current chip design, 2.5n reservoirs, 2.5n Pt wire electrodes and n pairs of Au-patterned conductivity electrodes are required.

5.5. References

(1) Vilkner, T.; Janasek, D.; Manz, A. *Analytical Chemistry* **2004**, *76*, 3373-3386.

(2) Mann, M.; Hendrickson, R. C.; Pandey, A. *Annual Review of Biochemistry* **2001**, *70*, 437-473.

(3) Gygi, S. P.; Rist, B.; Gerber, S. A.; Turecek, F.; Gelb, M. H.; Aebersold, R. *Nature Biotechnology* **1999**, *17*, 994-999.

(4) Pandey, A.; Mann, M. *Nature (London)* **2000**, *405*, 837-846.

(5) Gordon, E. M.; Barrett, R. W.; Dower, W. J.; Fodor, S. P. A.; Gallop, M. A. *Journal of Medicinal Chemistry* **1994**, *37*, 1385-1401.

(6) Gallop, M. A.; Barrett, R. W.; Dower, W. J.; Fodor, S. P. A.; Gordon, E. M. *Journal of Medicinal Chemistry* **1994**, *37*, 1233-1251.

(7) Ecker, D. J.; Crooke, S. T. *Bio/Technology* **1995**, *13*, 351-360.

(8) Krchnak, V.; Dalton, C. *Modern Drug Discovery* **2002**, *5*, 22-28.

(9) Labute, P.; Nilar, S.; Williams, C. *Combinatorial Chemistry and High Throughput Screening* **2002**, *5*, 135-145.

(10) http://www.genteon.net/products/capella-400.asp.

(11) Liu, S.; Ren, H.; Gao, Q.; Roach, D. J.; Loder, R. T., Jr.; Armstrong, T. M.; Mao, Q.; Blaga, I.; Barker, D. L.; Jovanovich, S. B. *Proceedings of the National Academy of Sciences of the United States of America* **2000**, *97*, 5369-5374.

(12) Woolley, A. T.; Sensabaugh, G. F.; Mathies, R. A. *Analytical Chemistry* **1997**, *69*, 2181-2186.

(13) Simpson, P. C.; Roach, D.; Woolley, A. T.; Thorsen, T.; Johnston, R.; Sensabaugh, G. F.; Mathies, R. A. *Proceedings of the National Academy of Sciences of the United States of America* **1998**, *95*, 2256-2261.

(14) Medintz, I.; Wong, W. W.; Berti, L.; Shiow, L.; Tom, J.; Scherer, J.; Sensabaugh, G.; Mathies, R. A. *Genome Research* **2001**, *11*, 413-421.

(15) Simpson, J. W.; Ruiz-Martinez, M. C.; Mulhern, G. T.; Berka, J.; Latimer, D. R.; Ball, J. A.; Rothberg, J. M.; Went, G. T. *Electrophoresis* **2000**, *21*, 135-149.

(16) Xu, H.; Roddy, E. S.; Roddy, T. P.; Lapos, J. A.; Ewing, A. G. *Journal of Separation Science* **2003,** *27*, 7-12.

(17) Tian, H.; Emrich, C. A.; Scherer, J. R.; Mathies, R. A.; Andersen, P. S.; Larsen, L. A.; Christiansen, M. *Electrophoresis* **2005**, *26*, 1834-1842.

(18) Shen, Z.; Liu, X.; Long, Z.; Liu, D.; Ye, N.; Qin, J.; Dai, Z.; Lin, B. *Electrophoresis* **2006**, *27*, 1084-1092.

(19) Liu, C. N.; Toriello, N. M.; Mathies, R. A. *Analytical Chemistry* **2006**, *78*, 5474-5479.

(20) Xu, H.; Roddy, T. P.; Lapos, J. A.; Ewing, A. G. *Analytical Chemistry* **2002**, *74*, 5517-5522.

(21) Gao, Y.; Shen, Z.; Wang, H.; Dai, Z.; Lin, B. *Electrophoresis* **2005**, *26*, 4774-4779.

(22) Kelly, R. T.; Woolley, A. T. *Analytical Chemistry* **2005**, *77*, 96A-102A.

(23) Khandurina, J.; Zhu, T.; Guttman, A. *Chemical Genomics* **2004**, 101-136.

(24) Cheng, S. B.; Skinner, C. D.; Taylor, J.; Attiya, S.; Lee, W. E.; Picelli, G.; Harrison, D. J. *Analytical Chemistry* **2001**, *73*, 1472-1479.

(25) Wakida, S.-I.; Wu, X.; Yoshino, K.; Matsuoka, K.; Niki, E. *Chemical Sensors* **2002**, *18*, 88-90.

(26) Dang, F.; Shinohara, S.; Tabata, O.; Yamaoka, Y.; Kurokawa, M.; Shinohara, Y.; Ishikawa, M.; Baba, Y. *Lab on a Chip* **2005**, *5*, 472-478.

(27) McDonald, J. C.; Duffy, D. C.; Anderson, J. R.; Chiu, D. T.; Wu, H.; Schueller, O. J. A.; Whitesides, G. M. *Electrophoresis* **2000**, *21*, 27-40.

(28) Reyes, D. R.; Iossifidis, D.; Auroux, P.-A.; Manz, A. *Analytical Chemistry* **2002**, *74*, 2623-2636.

(29) Shadpour, H.; Musyimi, H.; Chen, J. F.; Soper, S. A. *Journal of Chromatography A* **2006**, *1111*, 238-251.

(30) Effenhauser, C. S.; Bruin, G. J. M.; Paulus, A.; Ehrat, M. *Analytical Chemistry* **1997**, *69*, 3451-3457.

(31) Fister, J. C., III; Jacobson, S. C.; Davis, L. M.; Ramsey, J. M. *Analytical Chemistry* **1998**, *70*, 431-437.

(32) Haab, B. B.; Mathies, R. A. *Analytical Chemistry* **1999**, *71*, 5137-5145.

(33) Wabuyele, M. B.; Ford, S. M.; Stryjewski, W.; Barrow, J.; Soper, S. A. *Electrophoresis* **2001**, *22*, 3939-3948.

(34) Burns, M. A.; Johnson, B. N.; Brahmasandra, S. N.; Handique, K.; Webster, J. R.; Krishnan, M.; Sammarco, T.; Man, P. M.; Jones, D.; Heldsinger, D.; Mastrangelo, C. H.; Burke, D. T. *Science (Washington, D. C.)* **1998**, *282*, 484-487.

(35) Webster, J. R.; Burns, M. A.; Burke, D. T.; Mastrangelo, C. H. *Analytical Chemistry* **2001**, *73*, 1622-1626.

(36) Lacher, N. A.; Garrison, K. E.; Martin, R. S.; Lunte, S. M. *Electrophoresis* **2001**, *22*, 2526-2536.

(37) Uchiyama, K.; Nakajima, H.; Hobo, T. *Analytical and bioanalytical chemistry* **2004**, *379*, 375-382.

(38) Vandaveer, W. R. I. V.; Pasas-Farmer, S. A.; Fischer, D. J.; Frankenfeld, C. N.; Lunte, S. M. *Electrophoresis* **2004**, *25*, 3528-3549.

(39) Wang, J. *Electroanalysis* **2005**, *17*, 1133-1140.

(40) Zemann, A. J. *TrAC, Trends in Analytical Chemistry* **2001**, *20*, 346-354.

(41) Solinova, V.; Kasicka, V. *Journal of Separation Science* **2006**, *29*, 1743-1762.

(42) Guijt, R. M.; Evenhuis, C. J.; Macka, M.; Haddad, P. R. *Electrophoresis* **2004**, *25*, 4032-4057.

(43) Chen, G.; Lin, Y.; Wang, J. *Current Analytical Chemistry* **2006**, *2*, 43-50.

(44) Hergenroeder, R.; Grass, B. *Methods in Molecular Biology (Totowa, NJ, United States)* **2006**, *339*, 113-126.

(45) Tanyanyiwa, J.; Leuthardt, S.; Hauser, P. C. *Electrophoresis* **2002**, *23*, 3659-3666.

(46) Grass, B.; Hergenroder, R.; Neyer, A.; Siepe, D. *Journal of Separation Science* **2002**, *25*, 135-140.

(47) Galloway, M.; Stryjewski, W.; Henry, A.; Ford, S. M.; Llopis, S.; McCarley, R. L.; Soper, S. A. *Analytical Chemistry* **2002**, *74*, 2407-2415.

(48) Olvecka, E.; Masar, M.; Kaniansky, D.; Johnck, M.; Stanislawski, B. *Electrophoresis* **2001**, *22*, 3347-3353.

(49) Silvertand, L. H. H.; Machtejevas, E.; Hendriks, R.; Unger, K. K.; van Bennekom, W. P.; de Jong, G. J. *Journal of Chromatography B-Analytical Technologies in the Biomedical and Life Sciences* **2006**, *839*, 68-73.

(50) Deyl, Z.; Miksik, I.; Eckhardt, A. *Journal of Chromatography, A* **2003**, *990*, 153-158.

(51) Zuborova, M.; Demianova, Z.; Kaniansky, D.; Masar, M.; Stanislawski, B. *Journal of Chromatography, A* **2003**, *990*, 179-188.

(52) Olvecka, E.; Kaniansky, D.; Pollak, B.; Stanislawski, B. *Electrophoresis* **2004**, *25*, 3865-3874.

(53) Horng, R.-H.; Han, P.; Chen, H.-Y.; Lin, K.-W.; Tsai, T.-M.; Zen, J.-M. *Journal of Micromechanics and Microengineering* **2005**, *15*, 6-10.

(54) Hupert, M. L.; Guy, J. W.; Llopis, S. D.; Shadpour, H.; Rani, S.; Nikitopoulos, D. E.; Soper, S. A. *Microfluidics and Nanofluidics* **2006**, in press.

(55) Grass, B.; Siepe, D.; Neyer, A.; Hergenroeder, R. *Fresenius' Journal of Analytical Chemistry* **2001**, *371*, 228-233.

(56) Shadpour, H.; Soper, S. A. *Analytical Chemistry* **2006**, *78*, 3519-3527.

(57) Rasmussen, H. T.; McNair, H. M. *Journal of Chromatography* **1990**, *516*, 223-231.

CHAPTER 6

COLLABORATIVE WORK AND FUTURE DIRECTIONS

6.1. Collaborative Work

Microchip technology can be used for a voracity of chemical, biological and engineering applications. In the previous chapters, work was reported on the development of devices that could be integrated into a system for processing proteins. I was also involved in a number of different projects during the course of my graduate studies in conjunction with colleagues in the microfluidics area. The following sections briefly describe these collaborative works (only published work). More detail on each work of these projects can be found elsewhere.[1-3]

6.1.1. Evaluation of Micromilled Metal Mold Masters for the Replication of Microchip Electrophoresis Devices*,[2]

As discussed in Chapter 2, the most complicated and often expensive step in manufacturing microstructures through replication processes, is fabrication of the mold master, the quality of which determines the quality of the final product. There are few materials and processes that are being used for mold master fabrication, the selection of which depends on the type of replication process, physical dimensions of the microstructures, and life expectancy of the mold master. An attractive material for replication processes are metals, as they offer both high thermal and mechanical strength and high thermal conductivity required for fast heating and cooling cycles during replication.[2]

Various techniques for microfabricating metal mold masters have been established over recent years as briefly discussed in Chapter 2.[4-6] Simpler methods of metal master fabrication include conventional machining techniques, such as μ-EDM and high-precision micromilling.[7, 8] High-precision micromilling offers some distinct advantages over other commonly used techniques for preparing mold masters such as only three fabrication steps are required; design,

*_Microfluidics and Nanofluidics_, 2006, in press (the original publication is available at www.springerlink.com).

CNC milling, and finishing as compared to ~15 steps required for x-ray LiGA or ~10 steps for UV lithography-based techniques.[5, 6] A typical micro-milling system is shown in Figure 6.1.

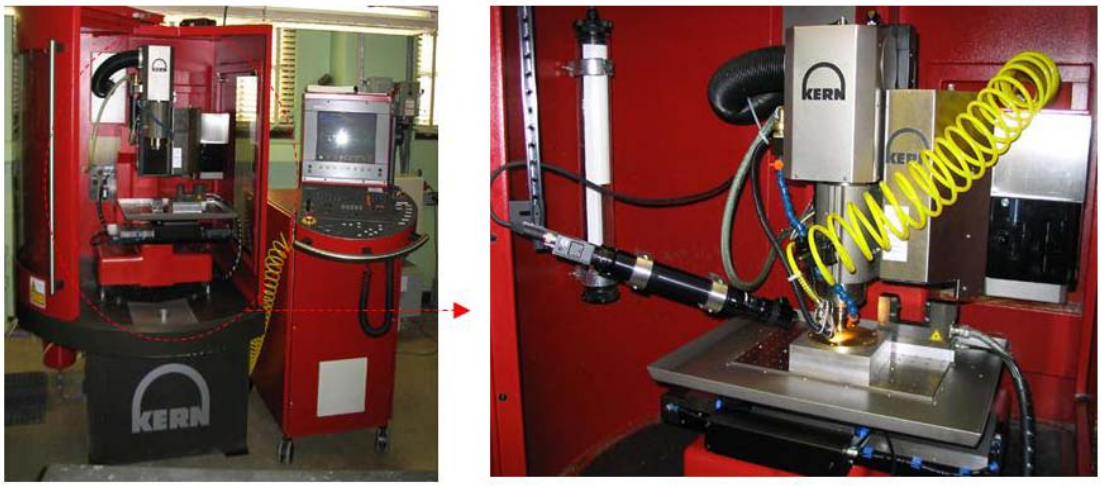

Figure 6.1. Kern micromilling system that was used for the microfabrication of metal mold masters used in this study.

In this work, we successfully used high-precision micromilling to fabricate molding masters that could be used for hot embossing microfluidic chips in polymers. The entire fabrication process from the design to the finished device was less than 6 h (~3 h for brass master fabrication, ~3 h for hot embossing, post-machining, cleaning, and final assembly) making this technique a very attractive method for rapid prototyping of polymer-based microfluidic devices.[2]

As an example of using micromilled masters for fabricating polymer microdevices, a microchip electrophoresis device was fabricated and tested via experimentation and numerical simulations. The results of the numerical simulations (see Figure 6.2) indicated that additional injection volume present in a cross injector due to the curvature in the micromilled corners led to increased sample plug size, which could produce extra-column variances lowering the effective plate number for electrophoretic separations. This artifact could be minimized by using a milling bit with a radius of curvature to channel width ratio (R/W) less than 0.5. In order to generate

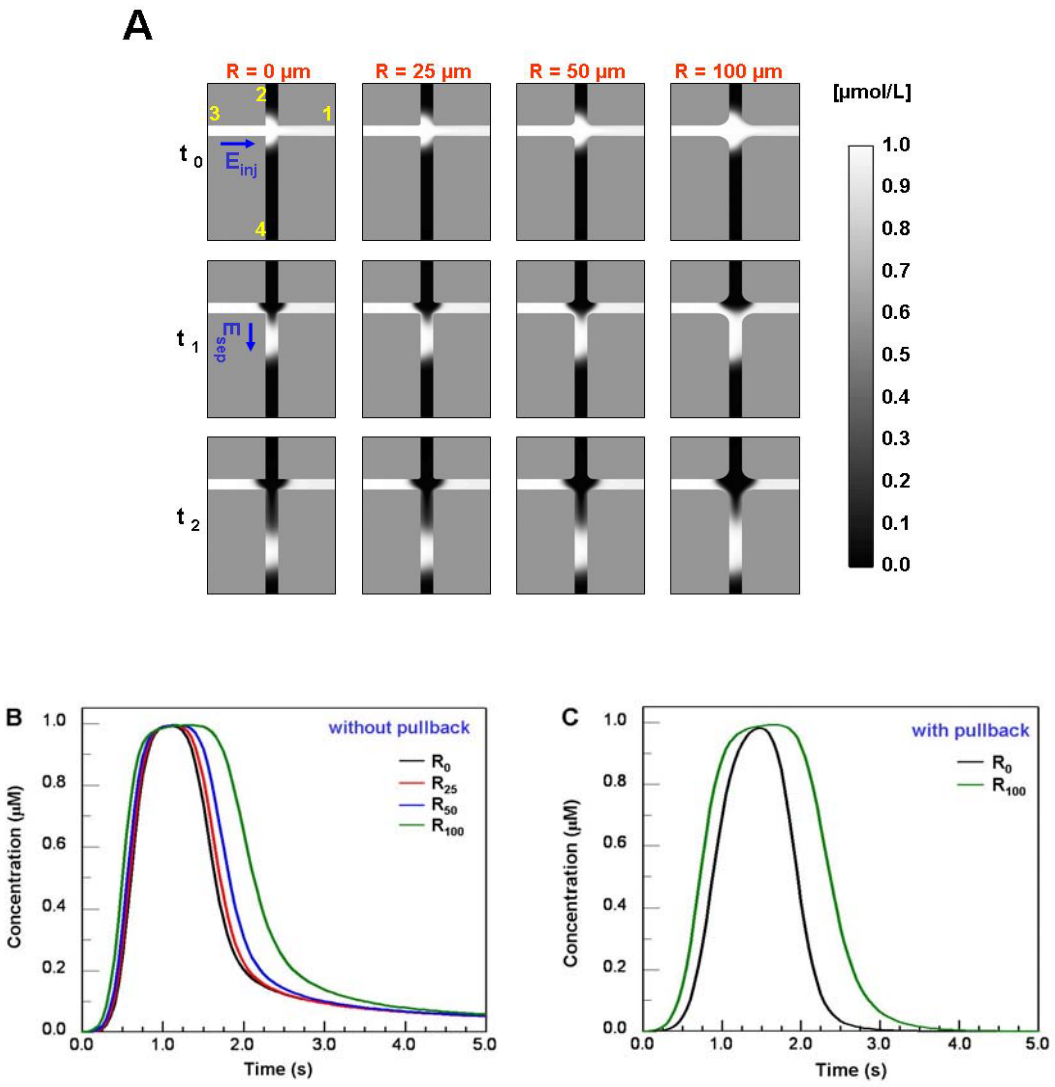

Figure 6.2. Numerical simulations of loading and dispensing of sample using cross injectors with different geometries. (A) The pictures present only the central part of the simulated microchannels: 1. Waste, 2. buffer, 3. sample, and 4. separation microchannel. Loading: 1 at 33.4 V, 3 at ground, 2 and 4 float. Dispensing: 1 and 3 float, 2 at ground, 4 at 66.8 V. $E_{inj} = E_{sep}$ = 167 V/cm; t_{inj} = 7.5 s, t_{sep} = 11 s. t_0 corresponds to the start of dispensing; t_1 and t_2 were taken at 1 s increments. (B) and (C) Each data point is the average concentration across the separation channel obtained 350 µm downstream from the center of the injector. B Loading and dispensing parameters were the same as in A. C loading parameters were the same as in A, dispensing: 1 and 3 at 28 V, 2 at ground, 4 at 66.8 V.[2]

short sample plugs pinched injections with strong pinching potentials can be used as well. Increased wall roughness for the microdevice replicated from a master fabricated via micromilling did not seem to affect the performance of the device in any significant way

compared to LiGA-prepared microchips as determined from a direct comparison of plate numbers for similar separations. Direct comparison of a microchip electrophoresis device produced from a micromilled master to one made using LiGA indicated that the number of theoretical plates for the separation of double-stranded DNA for both chips exceeded one million plates/m.[2]

6.1.2. Electrokinetically Synchronized PCR Microchip Fabricated in PC*,[1]

PCR is a powerful tool used for creating large numbers of copies of specific DNA fragments for both sequencing and genotyping applications.[9-11] PCR has the potential to rapidly amplify even a single DNA molecule into billions of identical molecules, making it attractive for the analysis of low-abundant targets in heterogeneous samples. The common devices used for PCR consist of metal blocks that are repetitively cycled between various temperatures required for the amplification process. The advantage of these "block" thermal cyclers is that they can simultaneously amplify 96 to 384 samples placed in titer wells that are sandwiched between the thermal block and a cover plate. The disadvantage associated with this format is the poor thermal management produced by the need for heating/cooling large thermal masses and the slow thermal equilibrium between the block and the fluid contained within the titer well. The result is limitations on the amplification speed due to slow thermal equilibration. In addition, block thermal cyclers set limits on reducing the volume of a PCR reaction to ~0.5 μL due to the need for manually pipetting reagents into the wells.[1]

In this work, a novel electrokinetically driven synchronized PCR chip was developed (see Figure 6.3). This microchip allowed DNA amplifications to be carried out in a continuous flow mode using synchronized electrokinetic pumping. Compared to well-type PCR formats, continuous-flow PCR (CF-PCR) offers the advantage of rapid analysis due to a faster rate of

problems associated with hydrodynamic flow in a continuous flow PCR format include, leakage from the high back pressure required for pumping in long and small cross-sectional area microchannels, sample dilution due to the hydrodynamic flow profile, the chip can only be used for a fixed number of thermal cyclers, which is determined by the architecture of the chip, and the necessity for off-chip pumps. Using an electrokinetic, synchronized format for the continuous flow PCR also allowed for adjusting the number of PCR cycles required for the reaction without the need for redesigning the microchip.[1]

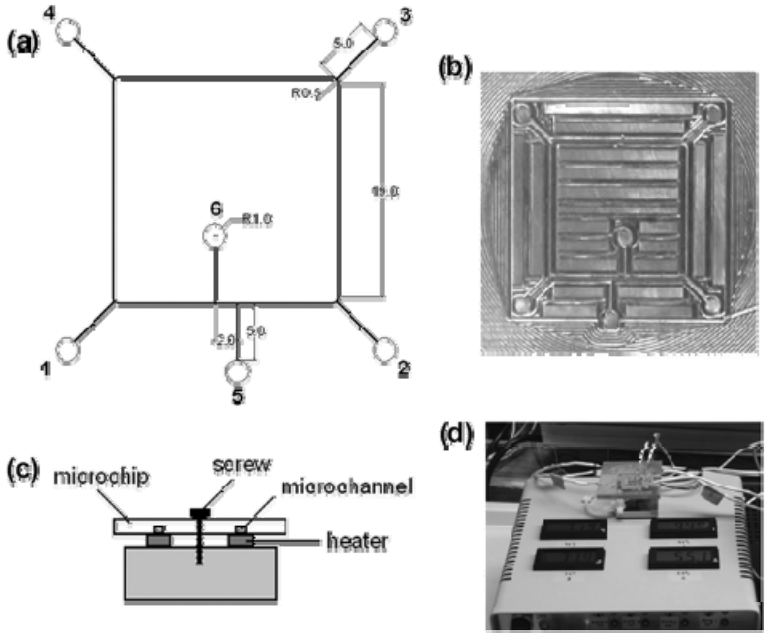

Figure 6.3. (A) Topographical layout of the PC-based microchip (units are in mm). Each side of the main square channel serving as the PCR reactor was 19.0 mm. The width of the microchannel was 100 μm, and the depth was 70 μm. The access channels (connecting reactor to solution reservoirs) had the same size as the reactor channel. The reservoirs marked as 1 to 4 were used to set up the synchronized pattern. Reservoirs 5 and 6 were used for sample injection (V_{inj} = 14 nL). (B) Micrograph of the brass molding die used for hot embossing replicates in PC. (C) A simple holding apparatus for microchip. The microchip was screwed down over the heaters to eliminate the air gap between microchannel and heaters. (D) PCR electronics system.[1]

Another attractive feature of this PCR format is the potential to easily integrate this chip to microchip electrophoresis without requiring active mechanical valving, simplifying operation

of the integrated device. In addition, the short effective channel length used herein (1.9 cm) permitted the use of small power supplies for generating the electric field, which will allow reducing the footprint of the device for potential field-deployable applications. The speed of the PCR amplification reaction can simply be adjusted by increasing the field strength used for moving the sample through the device and carefully controlling the direction and magnitude of the EOF. In the present case (300 V/cm), we completed 27 PCR cycles in ~18.1 min (40 s/cycle) and this could potentially be reduced to 5.2 s/cycle for a 500-bp amplicon (see Figure 6.4).[12]

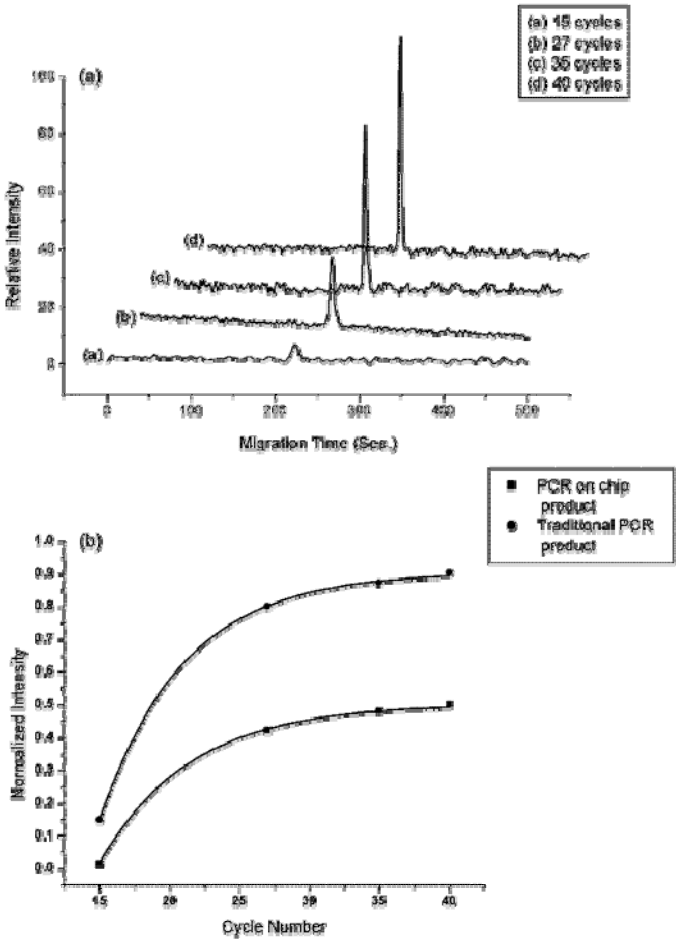

Figure 6.4. Effect of PCR cycle number on the amount of product generated. (A) 15, 27, 35, and 40 cycles of PCR products were collected from the PCR chip. (B) Relative fluorescence yield of PCR product obtained from the CF-PCR product vs. cycle number. The curves were normalized to the electrophoretic peak area for the conventional thermal cycler.[1]

6.1.3. A Continuous Flow Thermal Cycler Microchip for DNA Cycle Sequencing*[3]

Recently, attention has focused on developing microfabricated devices for a variety of biomedical and biological discovery applications with a number of devices directed toward DNA amplifications that require temperature cycling, such as PCR[12-18] and dideoxy cycle sequencing.[19] These efforts have been driven by the importance of thermal cycling reactions in DNA analyses and the fact that micro-thermal reactors can offer several advantages compared to their bench top counterparts including lower thermal capacitance, smaller amounts of reagents required for the reaction, and the ability to provide a high degree of automation in the assay by integrating the micro-PCR to subsequent processing steps configured on chips as well.[3]

While new strategies for high-throughput DNA sequencing are evolving that do not require Sanger dideoxynucleotide formats,[20-27] Sanger methods based on cycle sequencing continue to be a work horse in most large-scale genome sequencing projects.[28-30] Therefore, micro-based thermal cyclers (TC), especially those using a continuous flow format, could potentially provide another tool for developing fully automated instrument platforms for large-scale, high-throughput DNA sequencing.[31-37]

The results reported herein represent the first example of performing Sanger thermal cycle sequencing reactions in a continuous flow microchip thermal cycler (see Figure 6.5). For cases where rapid thermal cycling is required, for example to improve throughput by reducing processing time, the continuous flow thermal cycler (CF-TC) microchip provides superior performance compared to block thermal cyclers in terms of DNA read length when using rapid cycling times due to its better thermal management capabilities. As shown in Figure 6.5, the CF-TC chip had three well-defined temperature zones poised at 95, 55, and 60°C for denaturation, renaturation, and DNA extension, respectively. The sequencing mixture was hydrodynamically pumped through the microreactor channel at different linear velocities ranging

from 1 to 12 mm/s. At a linear velocity of 4 mm/s resulting in a 36 s extension time, a read length of >600 bp could be obtained in a total reaction time of 14.6 min. The CFTC chip could be reused for subsequent sequencing runs (>30) with negligible amounts of carryover contamination or degradation in the sequencing read length.

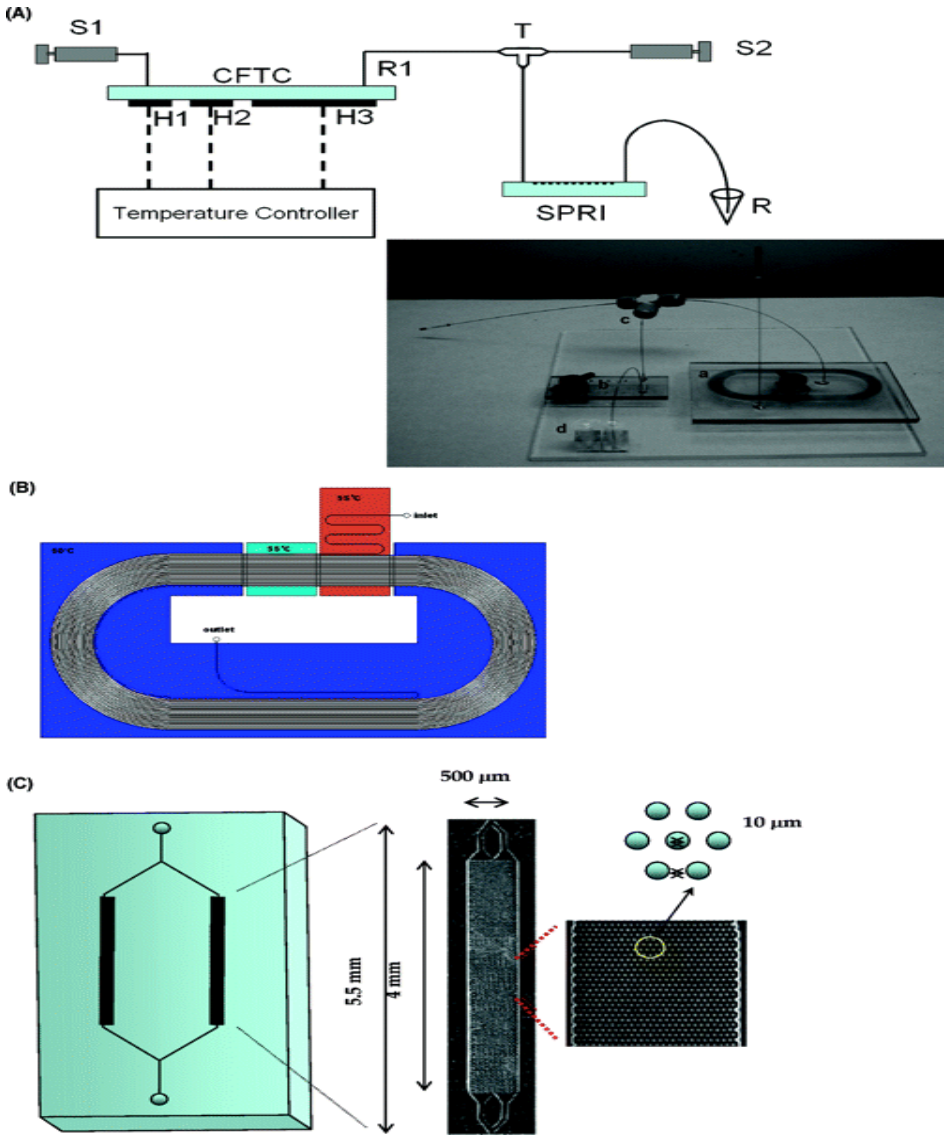

Figure 6.5. (A) Schematic diagram of the integrated CFTC-SPRI microchips for producing cycle sequencing DNA ladders that can be directly processed via CGE. CF-TC chip; SPRI chip; S_1 and S_2, syringe pumps; H_1, H_2, and H_3, heaters; T, micro-tee connector; R, sample receiving microfuge tube. Also shown is a picture of the integrated CFTC-SPRI system consisting of the (a) CF-TC, (b) the SPRI microchip, (c) micro-tee, and (d) the receiving microfuge tube for the purified cycle sequencing reactions. (B) Layout of the thermal cycler chip and the isothermal zones placed on the chip. (C) Topographical layout and optical micrograph of the SPRI bed, which contain microposts for increasing the DNA load.[3]

By coupling the CF-TC chip to a solid phase reversible immobilization (SPRI) purification chip, we could prepare a sample for electrophoretic sorting in less than 30 min. When the chips are configured into a multichannel format, they can be used to prepare cycle sequencing reactions in an automated, rapid and high-throughput fashion to deliver electrophoresis-ready products into a capillary array instrument (see Figure 6.6). In addition, if the coupled CF-TC-SPRI chips are interfaced to a microchip electrophoresis unit, which would eliminate the need for off-chip sample handling, sample volumes much smaller than 1 µL could be envisioned significantly reducing reagent consumption required for performing DNA cycle sequencing.[3]

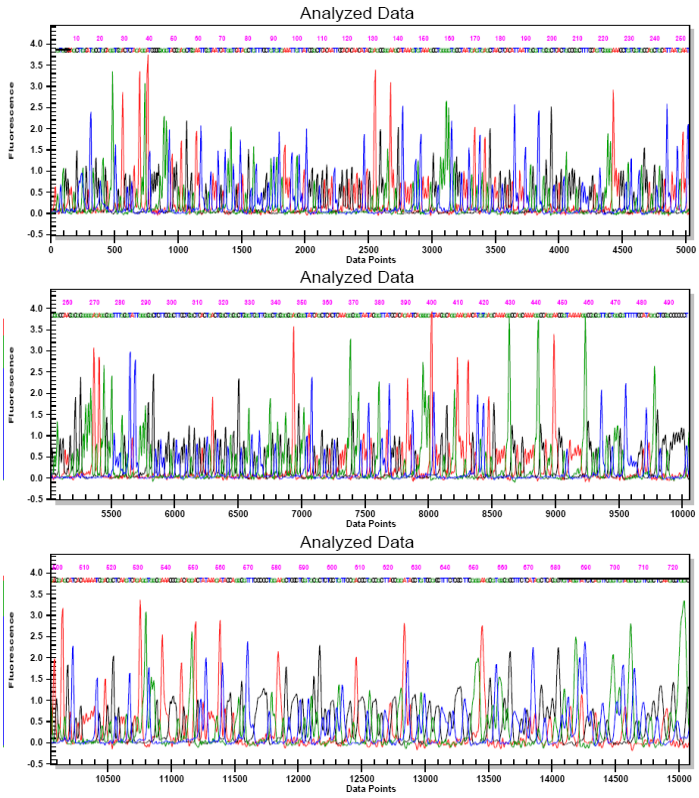

Figure 6.6. Four color fluorescence sequencing trace obtained from the thermal cycler microchip coupled to the SPRI microchip. The sequencing trace was analyzed (i.e., DNA electrophoretic sorting) with the default parameters set by the Sequence Analysis Module in the CEQ 8000 system. The sequencing reaction was run through the CF-TC chip at a linear flow rate of 1 mm/s, with the same flow rate used to introduce this sample into the SPRI chip. The binding buffer was infused into the SPRI chip at a linear velocity of 3.6 mm/s. Following air drying of the SPRI chip, the purified sequencing fragments were eluted form the SPRI bed using 20 µL of electrophoresis loading buffer (deionized formamide).[3]

6.2. Future Directions

6.2.1. 2-D Electrophoresis of Proteins with Combination of SDS PAGE and Microemulsion Electrokinetic Chromatography (MEEKC) Using Polymeric Microchips

In Chapter 4, we reported a microchip 2-D separation of proteins with combination of 30 mm SDS μ-CGE and 10 mm MEKC. To further reduce the footprint size of the 2-D separation platform reported on in this work, one can envision using a photo defined cross-linked polyacrylamide gels and coupling this dimension to MEEKC in a polymeric (PC preferred) microchip. Using a microchip of this configuration, fluorescently labeled proteins can be separated using SDS PAGE × MEEKC technique to evaluate the efficiency of using a 2-D separation platform possessing a column length of 20 mm (10 mm each dimension). Figure 6.7 represents the new 2-D microchip design. The channel depth was selected to be 30 μm to obtain homogeneous photopolymerization efficiency from top to bottom of the SDS PAGE channel. In addition, this helps to use high E to improve separation performance and speed without Joule heating.

For many years, SDS PAGE has been used as a separation technique for proteomic analyses due to is excellent resolving power.[38-40] As discussed previously (see Chapter 1), electrophoresis of SDS-denatured proteins through a gel or sieving matrix allows size-based separation of eluting species.

To aid patterning of very small localized gels within microfluidic devices, cross-linked polymer matrices in conjunction with photolithographic fabrication processes can be used. Historically, photodefined cross-linked polymers have been shown to possess superior performance for on-chip DNA sizing,[41] DNA and protein localization,[42-46] chromatography[47-49] and protein sizing.[50] The use of an *in situ* polymerized gel fabrication technique is essential for the direct adaptation of cross-linked gel SDS PAGE to a chip-based format. The nature of the

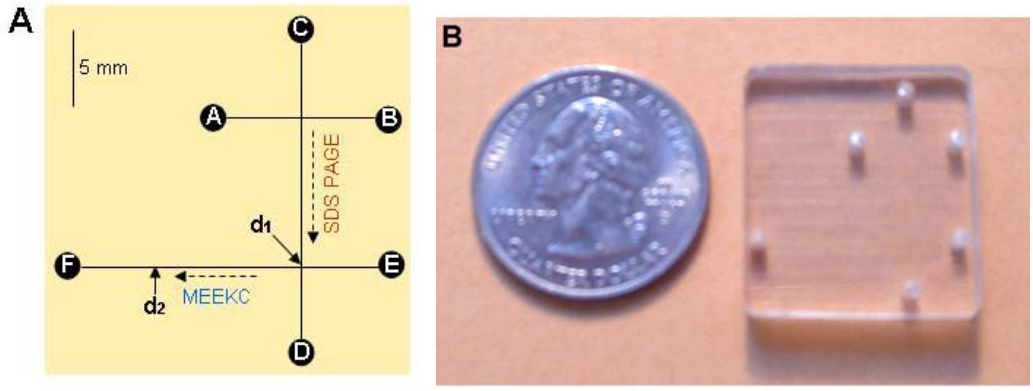

Figure 6.7. (A) Topographic layout of the micro-electrophoresis chip used for 1-D and 2-D separations. The microchip was hot embossed on PC from a brass master fabricated using high-precision micromilling: channel width ~20 µm; channel depth ~30 µm. The solution reservoirs are; A: sample reservoir, B: sample waste reservoir, C: SDS PAGE buffer reservoir, D: SDS PAGE buffer waste reservoir, E: MEEKC buffer reservoir, F: MEEKC buffer waste reservoir. All were 1.5 mm in diameter. Pt wires were used to apply high voltages to all reservoirs. SDS PAGE channel: Injection length was 10 mm, L_{tot} = 20 mm, L_{eff} = 10 mm; MEEKC channel: L_{tot} = 20 mm, L_{eff} = 10 mm. Letters d_1 and d_2 represent LIF detection positions for 1-D and 2-D separations providing effective separation lengths of 10 mm, and 20 mm, respectively. (B) A photograph of the PC microchip for 2-D separation.

cross-linked gels renders introduction of a pre-made gel into a microfluidic device difficult. In addition, photolithographically patterned soft polymers[51, 52] offer numerous advantages as compared to chemically polymerized gels such as easier fluid handling than high-viscosity bulk polymer solutions, facile tailoring of the sieving matrix porosity for specific applications, and improved separation resolution.[53] Therefore, *in situ* polymerized polymer gels could assist in the development of complex and integrated chip-based systems such as 2-D separation schemes that possess a small footprint. To the best of our knowledge, there is no report showing application of a photopolymerized gel for on-chip 2-D separations. Figure 6.8 shows the photopatterning steps for a PC microchip containing a photopolymerized cross-linked gel. The microchip preparation to perform 2-D analyses with photopolymerized gel in the first dimension consists of four easy steps: (i) flushing monomer into all channels, (ii) masking the injection and second dimension areas by a UV mask (e.g., tape or aluminum foil), (iii) UV exposure to produce the

cross-linked acrylamide polymer in unprotected regions, and finally (iv) UV mask removal and filling the non-polymerized channels (i.e., injection and second dimension channels) by suitable buffers after cleaning and removing the non-polymerized acrylamide solution.

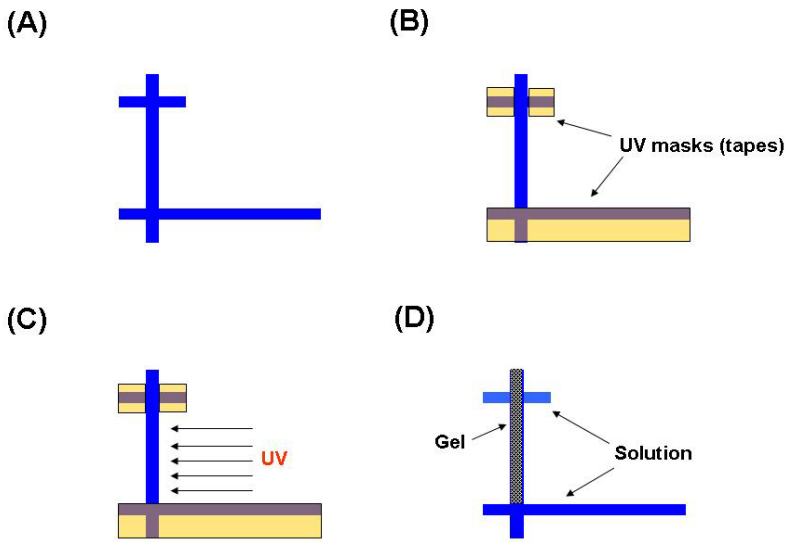

Figure 6.8. Photopatterning steps for a PC microchip. (A) Monomer is flushed into all channels. (B) All channel were masked by UV mask except the SDS PAGE channel. (C) Chip was exposed to a UV source and cross-linked acrylamide polymer fabricated in non-masked regions. (D) The mask was removed and the rest of channels filled by MEEKC buffer after cleaning and removing the non-polymerized acrylamide solution.

PC is an ideal microchip substrate in this application due to its favorable transparency at 365 nm and also its large EOF value,[54] which can be used as the driving force in the MEEKC dimension. Therefore, PC can be used for the photopolymerization, which requires 365 nm light. Using a very thin PC cover plate is suggested to minimize photopolymerization development time.

MEEKC was selected as a complementary separation technique in the second dimension. In MEEKC, the separation medium is a microemulsion, i.e., a transparent solution consisting of a surfactant, a co-surfactant, oil and water. [19, 55-60] Microemulsions are heterogeneous liquids, which are optically transparent and thermodynamically stable. Usually MEEKC solutions are mixtures of SDS to enhance separation between sample compounds, an alkane (e.g, heptane) to

form microemulsion droplets in the aqueous solution, some alkyl alcohol (e.g., 1-butanol) to reduce the surface tension between the alkane and water phases.[61-63] Figure 6.9 shows a potential diagram of microemulsion formation and the separation mechanism during MEEKC. As shown in figure, the surfactant and co-surfactant are located on the surface of the droplet in order to stabilize it.[64] This leads to higher separation efficiencies for MEEKC in comparison to MEKC, providing more efficient separations.

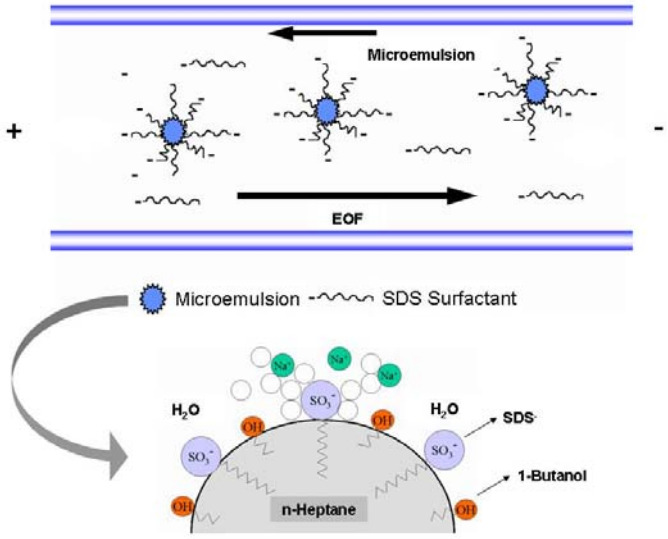

Figure 6.9. A potential demonstration of microemulsions and MEEKC mechanism based on partitioning analytes between microemulsions and the aqueous phase. See text for detail.

MEEKC has great potential for the separation of very complex samples.[65] Although MEEKC has been reported for successfully analyzing a wide variety of analytes, only a few reports have been made for MEEKC separation of proteins.[65] Among the recent reports, it has been described that MEEKC can resolve protein mixtures with high efficiency and could be used to separate both basic and acidic proteins simultaneously.[64]

Separation of compounds in MEEKC is based on both compound partitioning between the microemulsion droplets and the water phase, as well as on their electrophoretic mobilities.[61, 63] Manipulation of the microemulsion phase influences the separation of the

compounds.[26, 56, 57, 61, 63, 66, 67] Polar compounds favor the aqueous electrolyte solution rather than partitioning into the microemulsion droplets. For neutral compounds, they move with both the EOF and the microemulsion droplets in water and organic phases, respectively. Cationic analytes with pK_a values higher than the pH of the microemulsion solvent can form ion-pairs (IP) with the anionic SDS surfactant layer on the emulsion droplet. Possibly, they may even totally adsorb into the microemulsion droplets. If ion-pair formation is to be excluded, cationic sample compounds in the presence of anionic surfactants are better separated in uncharged or co-charged microemulsion phases to exclude the IP effect.[68] Macromolecules such as proteins have been shown to have very low affinity towards the anionic surface molecules, but, to the best of our knowledge, the role of nonionic MEEKC has not been thoroughly studied.[68] A microemulsion medium can be used for the separation of proteins. However, in this case, the large molecules are not able to partition into the core of the microemulsion droplet, but only on its surface. In spite of that, the analysis is more possible than in MEKC medium, where the large macromolecules cannot penetrate the micelles.[68] As a result, a combination of MEEKC and SDS PAGE may provide enhanced 2-D separation performance and peak capacity compared to our previous on-chip combination.[1]

6.2.2. Heart-Cut On-Chip 2-D Separation of Proteins with Integrated Conductivity Sensors

2-D separations can be classified into two categories, comprehensive or heart-cut separations. Comprehensive 2-D separations are based on the frequent transfer of samples from the first dimension to the second. This implies that the second dimension operates on a much faster time scale than the first one as we have reported previously.[69] In this separation platform, all analytes reach the end of the first dimension and are injected at regular time intervals into the second dimension for further analysis. As shown in Chapter 4, comprehensive 2-D separations on microchips can be performed using only one detector (e.g., LIF) at the end of the second

dimension. In contrast, the heart-cut 2-D separation technique transfers only a section of the first separation dimension to the second dimension.[70, 71] An advantage of this technique is that only the components of interest are analyzed, which dramatically speeds the overall separation process. Heart-cut is also essential in method development for comprehensive 2-D systems because the elution of the components in the second dimension can be assessed in a simplified system without the complication of peak overlap or wrap-around effects.[72] Furthermore, in some instances, such as those where peak wrap around effects cannot be avoided, a heart-cut approach is the only process that can be applied to a 2-D separation. Also, when an isolation process is required to obtain sample 'in-hand' a heart-cut approach may prove to be the most appropriate, especially in separation systems that display a high degree of chaotic band displacement. Under such circumstances, solute crowding, disordered solute displacement and oversampling may make it difficult to identify the component of interest (e.g., on-chip digestion and MS identification of the resolved proteins coming from a 2-D separation unit in an integrated microchip for complete protein analysis as will be discussed later, see Section 6.2.4) and separate the species with a high degree of purity and recovery. Application of a comprehensive process under such circumstances may prove to be too complicated.[73] In some cases, the separation can be optimized and accelerated to resolve only the components of interest that are heart-cut to the second dimension, leaving behind the components that are of little interest.[74] In addition, in comprehensive 2-D separations any two components separated in the first dimension must remain separated when subjected to a second dimension and elution profiles from both dimensions must be preserved.[75] For 2-D separations, heart-cut techniques are more routine in liquid phase separations because in these separations, the mobile phase plays an active role in the separation process, in contrast to the passive role of the carrier gas in GC.[74]

In an attempt to overcome some of the disadvantages of comprehensive 2-D techniques and also to facilitate the entire 2-D separation of proteins in cases that speed is more desirable, we have investigated the possibility of performing heart-cut 2-D separations in a plastic microchip. In our previous work, the orthogonality and separation performance of a size-based separation (i.e., SDS μ-CGE) and MEKC electrophoresis of model labeled-protein samples in a polymeric microchip was evaluated using LIF detection.[76] To perform a similar 2-D combination in a heart-cut format, a fraction coming from the first dimension of the 2-D separation is selected. This fraction then is electrokinetically transferred to the second separation dimension for further separation. Figure 6.10 shows an illustration of an on-chip heart-cut 2-D system with conductivity detection.

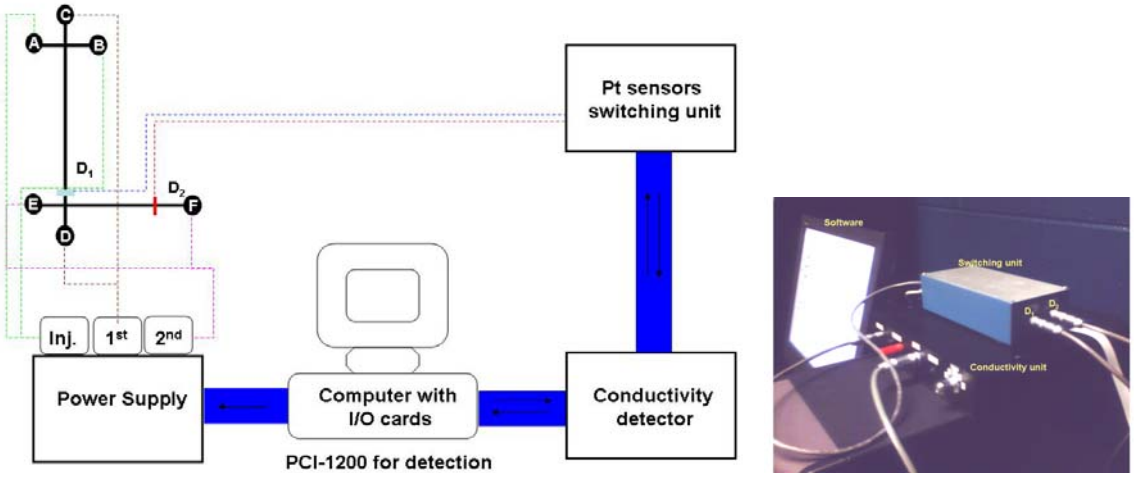

Figure 6.10. The diagram of the on-chip heart-cut 2-D system with conductivity detection (left), and a photograph of system with conductivity, sensors switching box and software/monitoring units (right). The detection system consists of one conductivity unit and a swathing relay box to measure the conductivity signals received from each Pt sensor integrated inside microchip channels. Letters D_1 and D_2 refer to conductivity detection for the first and second dimensions of the microchip, respectively.

As shown in the figure, the process of cutting fractions in the first dimension and then transferring them to the second dimension was monitored and processed by integration of two conductivity sensors at the end of the first and second dimensions. Platinum ribbons (500 μm

wide, 50 μm deep) were assembled inside the microchip channels according to our previous work.[77] The attractive feature of this format is that the electrodes can be configured directly on-column maintaining 2-D separation performance without the need for labeling the proteins.

We have built a prototype of this device, which is shown in Figure 6.11. The conductivity and electrophoresis power supplies were controlled using a custom designed LabVIEW program. After injecting samples and during the separation step, the conductivity signals received from D_1 are monitored (up to 20 readouts/s) until the signal exceeds a threshold value (defined as the ratio of receiving signal to average background value in each data collection step) the value of which is determined by the user. At this moment, sensor readings will be switched in a relay box (see Figure 6.10) from D_1 to D_2 causing a segment of fluid to enter the second dimension of the separation from the first (e.g., MEKC).

The feasibility of this novel approach can be demonstrated using a simple mixture of un-labeled proteins. The first dimension of the separation consists of SDS μ-CGE (see Chapter 4) or photopolymerized SDS PAGE (see Section 6.2.1) to obtain a separation of the proteins according to their size. The second dimension consists of MEKC (see Chapter 4) or MEEKC (see Section 6.2.1) separation of the isolated fraction containing co-migrated proteins, which are similar or close in size and thus, can be sorted via SDS PAGE. The results obtained in a heart-cut technique in this microchip can be compared with similar comprehensive separations by using only one conductivity sensor (the one located at end of the second dimension, D_2, see Figure 6.10) and using a pulse injection transfer protocol as described previously.[76]

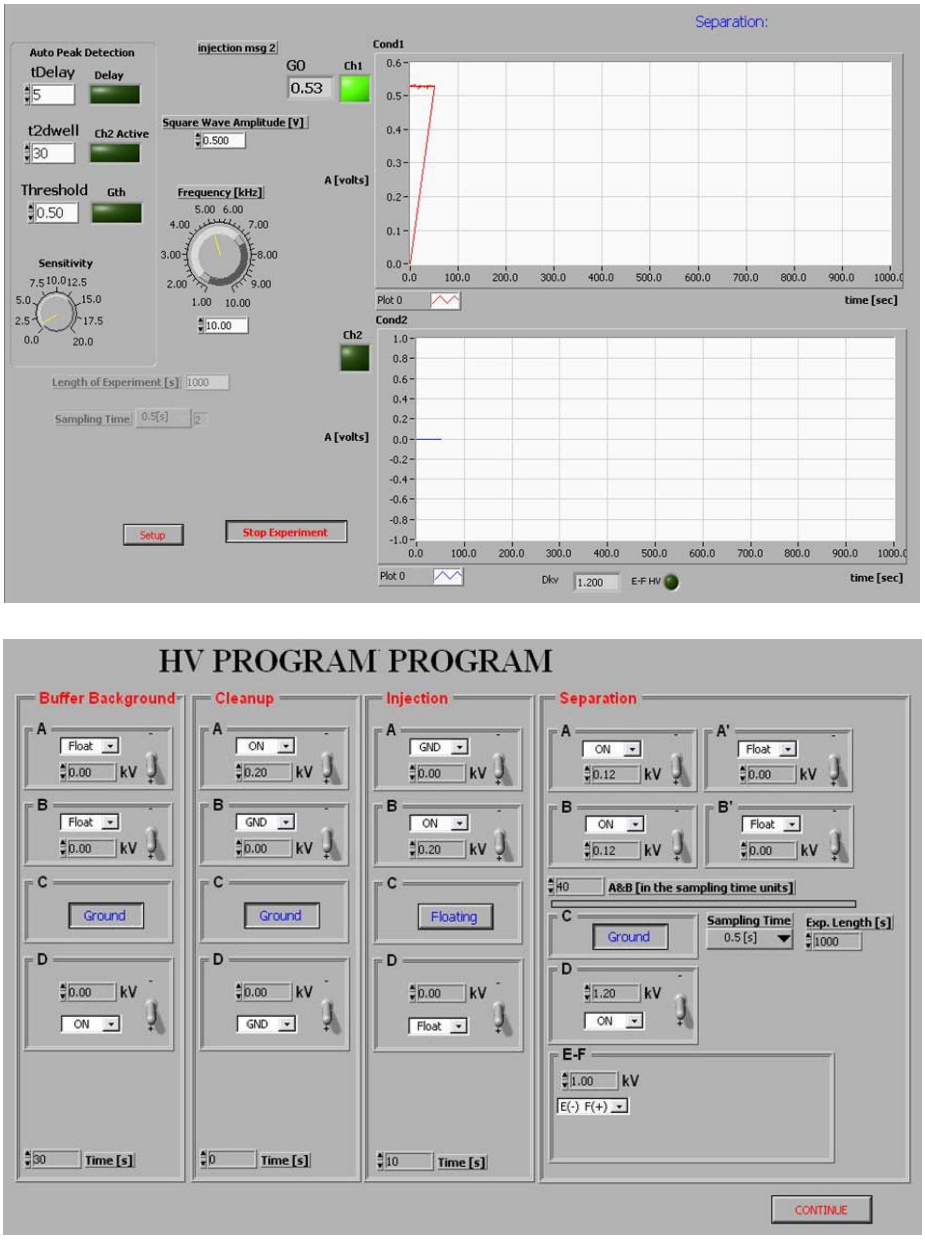

Figure 6.11. Top: LabVIEW program (written-in-house) for microchip heart-cut 2-D conductivity detection system. The user screen consists of two detection windows, each monitoring conductivity signals receiving from first and second dimension Pt sensors. The variable parameters are bipolar amplitude, bipolar frequency, threshold, delay time and separation window for second dimension. The signal received from D_1 is monitored frequently until it passes threshold value which is defined by user. At this moment, after passing delay time due to distance between D_1 and two dimension channels cross section, the signals will be collected from D_2 corresponding to second dimension. The power supplies are also changed in manner suitable with sensor changes. See text for detail. Bottom: software unit to control power supplies including buffer background measurement, clean up, injection and separation steps. The buffer background is measured by D_1 and averaged to be used for threshold comparison of the receiving conductivity from samples in a separation run. To perform 1-D separations, system can be switched to "manual" mode from software menu.

6.2.3. 2-D and High-Throughput Separation of Membrane Proteins Extracted from Adult Stem Cells Using Polymeric Microchip

Although membrane proteins correspond to one-third of the proteins encoded by the human genome, they represent more than two-thirds of the known protein targets for drugs. As a result, high-throughput approaches to characterize membrane proteins are of significant interest for drug discovery. Membrane proteins are also poised at the interface between the cell and the surrounding environment, and perform key biological functions such as cell-to-cell recognition and transport of ions and solutes, as well as acting as receptors for relaying diverse signals that bombard the cell. Therefore, separation, identification and quantification of membrane proteins is key to understanding the role of membrane proteins in fundamental biology.[78]

Despite recent progress in proteomics, technology to analyze a large number of membrane proteins is lacking. This is mainly due to their insolubility. This is especially true of integral membrane proteins, those with intracellular, extra-cellular, and membrane-spanning domains. This class of membrane proteins is particularly difficult to analyze because these proteins contain both hydrophilic and hydrophobic domains. A large part of the system optimization process can be devoted to proper solubilization conditions, whereas large-scale studies that aim for massively parallel analysis of membrane proteins must rely upon more robust and versatile techniques that can deal with proteins of varying solubility and hydrophobicity. In addition, membrane proteins are present generally in low abundance making their analysis more challenging. Finally, membrane proteins don't show significant difference from soluble proteins in that they can be extensively modified via PTMs, which can greatly alter their function.[78]

Adult stem cells are undifferentiated cells that reproduce daily to provide certain specialized cells and are created from hemopoietic stem cells. Pluripotent stem cells offer the possibility of a renewable source of replacement cells and tissues to treat a myriad of diseases. To develop more treatments, however, two basic questions concerning stem cells must be answered. First,

how do stem cells remain unspecialized and regenerate for many years, and second, what factors inside and outside of the cells trigger stem cell differentiation.[79, 80] As a result, identifying the surface membrane proteins in stem cells at various stages of differentiation and in different developing tissue types is essential for controlling stem cell differentiation for various biomedical applications.[81]

Classic approaches for studying membrane proteins at the proteomic level often begin with the separation of whole membrane proteins using 2-D IEF/SDS PAGE. As an alternative, we are pursuing an approach using our 2-D microchip to separate membrane proteins isolated from adult stem cells. To perform this, cells are suspended in 0.15 M PBS, pH 7.0 – 8.5 with Biotin/DMF solution and allowed to incubate for 40 min. The unreacted biotin is removed by centrifugation of the product for 3 minutes. This is repeated twice. Cells are stored at 4°C in 0.05% sodium azide.[81] The extracted membrane proteins are then labeled with Alexa Fluor 633 dye, purified using resin columns, and finally thermally denatured with SDS solution prior to performing the on-chip 2-D separation. 2-D maps of the resolved membrane proteins obtained for stem cells can then be correlated to the differentiation capacity of the stem cell. With thousands of membrane proteins in the mixture, we are close to reaching the chip's predicted peak capacity of ~1000.

6.2.4. Integrated Microchip for Complete Protein Analysis

As we described previously (see Chapter 2, Section 2.1.2), our goal to overcome the labor-intensive issues and extensive sample handling problems associated with proteomic studies by developing an integrated microchip for protein analysis, which covers all the major protein processing steps in one wafer adopting a top-down proteomic strategy. Figure 6.12 shows a photograph of an embossed PMMA microchip, which was designed based on the platform that was discussed in Chapter 2 (see Figure 2.10 for more detail).

The integrated microchip includes a total number of 21 reservoirs. Each reservoir requires one power supply connector (e.g., Pt wire) since the entire microchip uses electrokinetics to shuttle fluids inside channels and between reservoirs. In cases where conductivity detection is required and as shown in this Figure and considering four connectors for two conductivity sensors (D_1 and D_2, see Figure 6.12), 25 connectors will be required between the microchip, power supply and detector units.

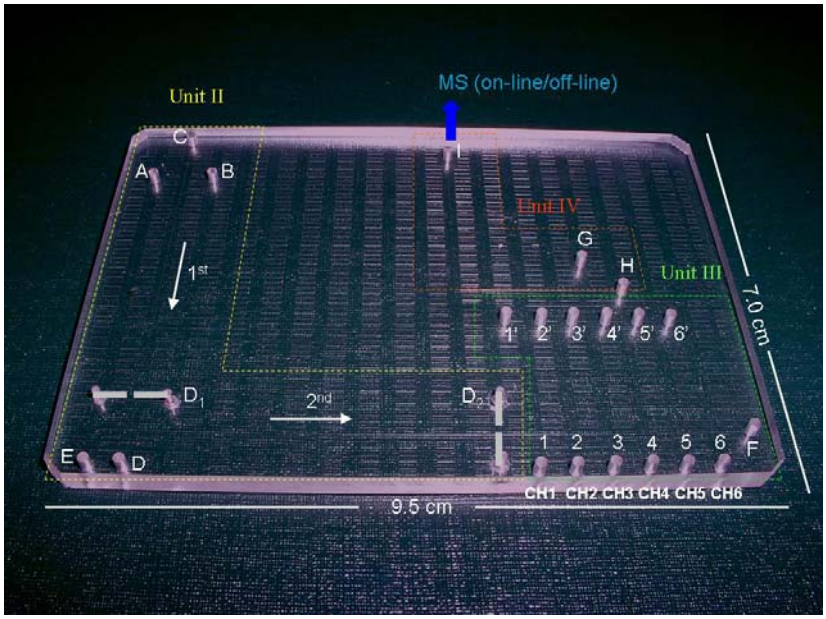

Figure 6.12. Integrated PMMA microchip for complete protein analysis. The microchip consisted of three unites: 2-D electrophoresis (unit II), protein digestion (unit III) and electrophoretic separation of resulting peptide fragments (unit IV). Letters A-E refer to sample, sample waste, first dimension buffer, buffer waste, second dimension buffer and buffer waste reservoirs, respectively. D_1 and D_2 are the conductivity sensors for first and second separation dimensions, respectively. Numbers 1 to 6 and 1' to 6' represent buffer and buffer waste reservoirs for each individual parallel protein digestion channel. G, H and I represent common ground for all parallel digestion channels, buffer reservoir for unit IV, and buffer waste reservoir for unit IV, respectively. All reservoirs shown in picture are 1.5 mm in diameter. The resolved peptide fragments can be collected and analyzed using MS technique in an off-line (shown in figure) or on-line manner. All channels are 50 μm deep and ~20 μm wide. See text for detail.

Depending on the method of detection, the protein samples can be fluorescently labeled (e.g., Chapters 3 and 4) for LIF detection, or simply can be native proteins when using contact

conductivity detection (see Chapter 5) with the two sensors that are shown in Figure 6.12. Although both comprehensive (See Chapter 4) and heart-cut (see Section 6.2.2) 2-D separation techniques can be used in this unit, heart-cut is preferred mainly due to eliminating over sampling of effluents from the first to second dimension and better screening of both dimensions, which also minimizes the system complexity.

The separated proteins are electronically forwarded to unit III for rapid digestion using surface-immobilized proteolytic enzymes. Details of this unit were briefly described elsewhere.[82] The number of theses digestion reactors will not be limited and primarily depends on the sample complexity and the requested total protein analysis speed; more parallel reactors increases the throughput of digestion and consequently minimizes the time required for digestion of all resolved proteins eluted from unit II.

In unit IV, the peptide fragments in each parallel digestion channel (i.e., CH1 to CH6, see Figure 6.12) will be further separated using a simple electrophoretic separation technique such as μ-CZE or μ-CEC. As shown in Figure 6.12, the resolved peptide fragments will be directly transferred to any MS for further analysis either using off-line or an on-line technique.[83]

According to the initial evaluations obtained for each unit operated separately, a total analysis time of less than 1 h is estimated for complete protein analysis using this microchip format. This will result in a tremendous improvement in processing speed as well as efficiency compare to conventional methods of protein analysis, which usually take several days to one week as discussed in Chapter 1. Using this microchip will also minimize the amount of reagents and protein samples required for the anlaysis, which are usually limited especially those obtained from a limited source such as human cells, tissues or organs. Another advantage of this system as a miniaturized analytical system, a high-throughput layout of this microchip can also be developed in a fashion similar to the approach discussed in Chapter 5.

6.3. References

(1) Chen, J.; Wabuyele, M.; Chen, H.; Patterson, D.; Hupert, M.; Shadpour, H.; Nikitopoulos, D.; Soper, S. A. *Analytical Chemistry* **2005**, *77*, 658-666.

(2) Hupert, M.; Guy, J. W.; Llopis, S. D.; Shadpour, H.; Rani, S.; Nikitopoulos, D.; Soper, S. A. *Microfluidics and Nanofluidics* **2006**, in press.

(3) Wang, H.; Chen, J.; Zhu, L.; Shadpour, H.; Hupert, M.; Soper, S. A. *Analytical Chemistry* **2006**, *78*, 6223-6231.

(4) Holger Becker, C. G. *Electrophoresis* **2000**, *21*, 12-26.

(5) Soper, S. A.; Ford, S. M.; Qi, S.; McCarley, R. L.; Kelly, K.; Murphy, M. C. *Analytical Chemistry* **2000**, *72*, 642A-651A.

(6) Boone, T.; Fan, Z. H.; Hooper, H.; Ricco, A.; Tan, H. D.; Williams, S. *Analytical Chemistry* **2002**, *74*, 78A-86A.

(7) Ehrfeld, W.; Lehr, H.; Michel, F.; Wolf, A.; Gruber, H. P.; Bertholds, A. 1996; Proceedings of SPIE—the international society for optical engineering; 332-337.

(8) Guber, A. E.; Heckele, M.; Herrmann, D.; Muslija, A.; Saile, V.; Eichhorn, L.; Gietzelt, T.; Hoffmann, W.; Hauser, P. C.; Tanyanyiwa, J.; Gerlach, A.; Gottschlich, N.; Knebel, G. *Chemical Engineering Journal* **2004**, *101*, 447-453.

(9) White, T. J.; Arnheim, N.; Erlich, H. A. *Trends in Genetics* **1989**, *5*, 185-189.

(10) Mullis, K. B.; Faloona, F. A. *Methods in Enzymology* **1987**, *155*, 335-350.

(11) Vosberg, H. P. *Human Genetics* **1989**, *83*, 1-15.

(12) Hashimoto, M.; Chen, P. C.; Mitchell, M. W.; Nikitopoulos, D. E.; Soper, S. A.; Murphy, M. C. *Lab on a Chip* **2004**, *4*, 638-645.

(13) Burns, M. A.; Mastrangelo, C. H.; Sammarco, T. S.; Man, F. P.; Webster, J. R.; Johnson, B. N.; Foerster, B.; Jones, D.; Fields, Y.; Kaiser, A. R.; Burke, D. T. *Proceedings of the National Academy of Sciences of the United States of America* **1996**, *93*, 5556-5561.

(14) Khandurina, J.; McKnight, T. E.; Jacobson, S. C.; Waters, L. C.; Foote, R. S.; Ramsey, J. M. *Analytical Chemistry* **2000**, *72*, 2995-3000.

(15) Koh, C. G.; Tan, W.; Zhao, M. Q.; Ricco, A. J.; Fan, Z. H. *Analytical Chemistry* **2003**, *75*, 6379-6379.

(16) Kopp, M. U.; de Mello, A. J.; Manz, A. *Science* **1998**, *280*, 1046-1048.

(17) Lagally, E. T.; Emrich, C. A.; Mathies, R. A. *Lab on a Chip* **2001**, *1*, 102-107.

(18) Obeid, P. J.; Christopoulos, T. K.; Crabtree, H. J.; Backhouse, C. J. *Analytical Chemistry* **2003**, *75*, 288-295.

(19) Oda, R. P.; Strausbauch, M. A.; Huhmer, A. F. R.; Borson, N.; Jurrens, S. R.; Craighead, J.; Wettstein, P. J.; Eckloff, B.; Kline, B.; Landers, J. P. *Analytical Chemistry* **1998**, *70*, 4361-4368.

(20) Shendure, J.; Mitra, R. D.; Varma, C.; Church, G. M. *Nature Reviews Genetics* **2004**, *5*, 335-344.

(21) Gharizadeh, B.; Nordstrom, T.; Ahmadian, A.; Ronaghi, M.; Nyren, P. *Analytical Biochemistry* **2002**, *301*, 82-90.

(22) Ronaghi, M. *Genome Research* **2001**, *11*, 3-11.

(23) Deamer, D. W.; Akeson, M. *Trends in Biotechnology* **2000**, *18*, 147-151.

(24) Drmanac, S.; Kita, D.; Labat, I.; Hauser, B.; Schmidt, C.; Burczak, J. D.; Drmanac, R. *Nature Biotechnology* **1998**, *16*, 54-58.

(25) Nowak, R. *Science* **1995**, *267*, 172-174.

(26) Drmanac, R.; Drmanac, S.; Strezoska, Z.; Paunesku, T.; Labat, I.; Zeremski, M.; Snoddy, J.; Funkhouser, W. K.; Koop, B.; Hood, L.; Crkvenjakov, R. *Science* **1993**, *260*, 1649-1653.

(27) Metzker, M. L. *Genome Research* **2005**, *15*, 1767-1776.

(28) Collins, F. S.; Green, E. D.; Guttmacher, A. E.; Guyer, M. S. *Nature* **2003**, *422*, 835-847.

(29) Collins, F. S.; Guyer, M. S.; Chakravarti, A. *Science* **1997**, *278*, 1580-1581.

(30) Sanger, F.; Nicklen, S.; Coulson, A. R. *Proceedings of the National Academy of Sciences of the United States of America* **1977**, *74*, 5463-5467.

(31) Kan, C. W.; Fredlake, C. P.; Doherty, E. A. S.; Barron, A. E. *Electrophoresis* **2004**, *25*, 3564-3588.

(32) Paegel, B. M.; Blazej, R. G.; Mathies, R. A. *Current Opinion in Biotechnology* **2003**, *14*, 42-50.

(33) Paegel, B. M.; Yeung, S. H. I.; Mathies, R. A. *Analytical Chemistry* **2002**, *74*, 5092-5098.

(34) Salas-Solano, O.; Schmalzing, D.; Koutny, L.; Buonocore, S.; Adourian, A.; Matsudaira, P.; Ehrlich, D. *Analytical Chemistry* **2000**, *72*, 3129-3137.

(35) Schmaizing, D.; Koutny, L.; Salas-Solano, O.; Adourian, A.; Matsudaira, P.; Ehrlich, D. *Electrophoresis* **1999**, *20*, 3066-3077.

(36) Zhang, Y. H.; Tan, H. D.; Yeung, E. S. *Analytical Chemistry* **1999**, *71*, 5018-5025.

(37) Tan, H. D.; Yeung, E. S. *Analytical Chemistry* **1998**, *70*, 4044-4053.

(38) Raymond, S. *Annals of the New York Academy of Sciences* **1964**, *121*, 350-365.

(39) Shapiro, A. L.; Vinuela, E.; Maizel, J. V., Jr. *Biochemical and Biophysical Research Communications* **1967**, *28*, 815-820.

(40) Laemmli, U. K. *Nature (London, United Kingdom)* **1970**, *227*, 680-685.

(41) Burns, M. A.; Johnson, B. N.; Brahmasandra, S. N.; Handique, K.; Webster, J. R.; Krishnan, M.; Sammarco, T.; Man, P. M.; Jones, D.; Heldsinger, D.; Mastrangelo, C. H.; Burke, D. T. *Science (Washington, D. C.)* **1998**, *282*, 484-487.

(42) Timofeev, E. N.; Kochetkova, S. V.; Mirzabekov, A. D.; Florentiev, V. L. *Nucleic Acids Research* **1996**, *24*, 3142-3148.

(43) Guschin, D.; Yershov, G.; Zaslavsky, A.; Gemmell, A.; Shick, V.; Proudnikov, D.; Arenkov, P.; Mirzabekov, A. *Analytical biochemistry* **1997**, *250*, 203-211.

(44) Proudnikov, D.; Timofeev, E.; Mirzabekov, A. *Analytical Biochemistry* **1998**, *259*, 34-41.

(45) Vasiliskov, A. V.; Timofeev, E. N.; Surzhikov, S. A.; Drobyshev, A. L.; Shick, V. V.; Mirzabekov, A. D. *BioTechniques* **1999**, *27*, 592-606.

(46) Olsen, K. G.; Ross, D. J.; Tarlov, M. J. *Analytical Chemistry* **2002**, *74*, 1436-1441.

(47) Yu, S. M.; McQuade, D. T.; Quinn, M. A.; Hackenberger, C. P. R.; Krebs, M. P.; Polans, A. S.; Gellman, S. H. *Protein Science* **2000**, *9*, 2518-2527.

(48) Shediac, R.; Ngola, S. M.; Throckmorton, D. J.; Anex, D. S.; Shepodd, T. J.; Singh, A. K. *Journal of Chromatography, A* **2001**, *925*, 251-263.

(49) Throckmorton, D. J.; Shepodd, T. J.; Singh, A. K. *Analytical Chemistry* **2002**, *74*, 784-789.

(50) Herr, A. E.; Singh, A. K. *Analytical Chemistry* **2004**, *76*, 4727-4733.

(51) Han, J.; Singh, A. K. *Micro Total Analysis Systems 2002, Proceedings of the μ-TAS 2002 Symposium, 6th, Nara, Japan, Nov. 3-7,* **2002**, *1*, 596-598.

(52) Shediac, R.; Pizzaro, S. A.; Herr, A. E.; Singh, A. K. *Micro Total Analysis Systems 2002, Proceedings of the μ-TAS 2003 Symposium, OH, USA, Oct. 5-9,* **2003**, 971-974.

(53) Schwartz, H.; Palmieri, R.; Brown, R. *capillary electrophoresis Theory and Practice*; CRC Press: Boca Raton, FL, 1993.

(54) Shadpour, H.; Musyimi, H.; Chen, J.; Soper, S. A. *Journal of Chromatography, A* **2006**, *1111*, 238-251.

(55) Vomastova, L.; Miksik, I.; Deyl, Z. *Journal of Chromatography, B: Biomedical Applications* **1996**, *681*, 107-113.

(56) Boso, R. L.; Bellini, M. S.; Miksik, I.; Deyl, Z. *Journal of Chromatography, A* **1995**, *709*, 11-20.

(57) Pedersen-Bjergaard, S.; Gabel-Jensen, C.; Honore Hansen, S. *Journal of Chromatography, A* **2000**, *897*, 375-381.

(58) Mrestani, Y.; El-Mokdad, N.; Ruettinger, H. H.; Neubert, R. *Electrophoresis* **1998**, *19*, 2895-2899.

(59) Debusschere, L.; Demesmay, C.; Rocca, J. L.; Lachatre, G.; Lofti, H. *Journal of Chromatography, A* **1997**, *779*, 227-233.

(60) Hilder, E. F.; Klampfl, C. W.; Buchberger, W.; Haddad, P. R. *Journal of Chromatography, A* **2001**, *922*, 293-302.

(61) Altria, K. D. *Journal of Chromatography, A* **1999**, *844*, 371-386.

(62) Riekkola, M.-L.; Wiedmer, S. K.; Valko, I. E.; Siren, H. *Journal of Chromatography, A* **1997**, *792*, 13-35.

(63) Altria, K. D.; Clark, B. J.; Mahuzier, P. E. *Chromatographia* **2000**, *52*, 758-768.

(64) Zhou, G.-H.; Luo, G.-A.; Zhang, X.-D. *Journal of Chromatography, A* **1999**, *853*, 277-284.

(65) Hansen, S. H. *Electrophoresis* **2003**, *24*, 3900-3907.

(66) Terabe, S.; Matsubara, N.; Ishihama, Y.; Okada, Y. *Journal of Chromatography* **1992**, *608*, 23-29.

(67) Miola, M. F.; Snowden, M. J.; Altria, K. D. *Journal of Pharmaceutical and Biomedical Analysis* **1998**, *18*, 785-797.

(68) Siren, H.; Karttunen, A. *Journal of Chromatography, B: Analytical Technologies in the Biomedical and Life Sciences* **2003**, *783*, 113-124.

(69) Cottet, H.; Biron, J. P.; Taillades, J. *Journal of Chromatography, A* **2004**, *1051*, 25-32.

(70) Matsui, T.; Tamaya, K.; Kawasaki, T.; Osajima, Y. *Journal of Chromatography, B: Biomedical Sciences and Applications* **1999**, *729*, 89-95.

(71) Anon *Lab on a Chip* **2002**, *2*, 31N-36N.

(72) Gray, M. J.; Sweeney, A. P.; Dennis, G. R.; Slonecker, P. J.; Shalliker, R. A. *Analyst (Cambridge, United Kingdom)* **2003**, *128*, 598-604.

(73) Gray, M. J.; Dennis, G. R.; Slonecker, P. J.; Shalliker, R. A. *Journal of Chromatography, A* **2004**, *1028*, 247-257.

(74) Sweeney Alan, P.; Shalliker, R. A. *Journal of chromatography. A* **2002**, *968*, 41-52.

(75) Liu, S.; Ren, H.; Gao, Q.; Roach, D. J.; Loder, R. T., Jr.; Armstrong, T. M.; Mao, Q.; Blaga, I.; Barker, D. L.; Jovanovich, S. B. *Proceedings of the National Academy of Sciences of the United States of America* **2000**, *97*, 5369-5374.

(76) Shadpour, H.; Soper, S. A. *Analytical Chemistry* **2006**, *78*, 3519-3527.

(77) Galloway, M.; Stryjewski, W.; Henry, A.; Ford, S. M.; Llopis, S.; McCarley, R. L.; Soper, S. A. *Analytical Chemistry* **2002**, *74*, 2407-2415.

(78) Rabilloud, T. *Nature Biotechnology* **2003**, *21*, 508-510.

(79) Gregory, C. A.; Gunn, W. G.; Reyes, E.; Smolarz, A. J.; Munoz, J.; Spees, J. L.; Prockop, D. J. In *Stem Cell Biology: Development and Plasticity*, 2005; Vol. 1049, pp 97-106.

(80) Munoz, J. R.; Stoutenger, B. R.; Robinson, A. P.; Spees, J. L.; Prockop, D. J. *Proceedings of the National Academy of Sciences of the United States of America* **2005**, *102*, 18171-18176.

(81) Witek, M. A.; Chen, G.; Shadpour, H.; Khaterpal, I.; Prockop, D.; Gregory, C. A.; McCarley, R. L.; Soper, S. A. *Micro Total Analysis Systems 2006, Proceedings of the μ-TAS 2006 Symposium,* **2006**, in press.

(82) Musyimi, H.; Shadpour, H.; Murray, K. K.; Soper, S. A., **2006**, in submission.

(83) Musyimi, H. K.; Guy, J.; Narcisse, D. A.; Soper, S. A.; Murray, K. K. *Electrophoresis* **2005**, *26*, 4703-4710.

APPENDIX

LETTERS OF COPYRIGHT PERMISSION

Hamed

From: Smith, Stephanie (ELS-OXF) [ST.Smith@elsevier.com]
Sent: Thursday, September 07, 2006 6:44 AM
To: hshadp1@lsu.edu
Subject: RE: Obtain Permission

We hereby grant you permission to reproduce the material detailed below in your thesis at no charge subject to the following conditions:

1. If any part of the material to be used (for example, figures) has appeared in our publication with credit or acknowledgement to another source, permission must also be sought from that source. If such permission is not obtained then that material may not be included in your publication/copies.

2. Suitable acknowledgment to the source must be made, either as a footnote or in a reference list at the end of your publication, as follows:

"Reprinted from Publication title, Vol number, Author(s), Title of article, Pages No., Copyright (Year), with permission from Elsevier".

3. Reproduction of this material is confined to the purpose for which permission is hereby given.

4. This permission is granted for non-exclusive world English rights only. For other languages please reapply separately for each one required. Permission excludes use in an electronic form. Should you have a specific electronic project in mind please reapply for permission.

5. This includes permission for UMI to supply single copies, on demand, of the complete thesis. Should your thesis be published commercially, please reapply for permission.

Yours sincerely

Steph Smith
Rights Assistant

Elsevier Ltd
The Boulevard
Langford Lane
Kidlington
Oxford OX5 1GB

-----Original Message-----
From: hshadp1@lsu.edu [mailto:hshadp1@lsu.edu]
Sent: 06 September 2006 18:09
To: permissions@elsevier.com
Subject: Obtain Permission

This Email was sent from the Elsevier Corporate Web Site and is related to Obtain Permission form:

Product: Customer Support
Component: Obtain Permission
Web server: http://www.elsevier.com
IP address: 10.10.24.149
Client: Mozilla/4.0 (compatible; MSIE 6.0; Windows NT 5.1; SV1)
Invoked from:
http://www.elsevier.com/wps/find/obtainpermissionform.cws_home?isSubmitted=y

es&navigateXmlFileName=/store/prod_webcache_act/framework_support/obtainpermission.xml

Request From:
Ph.D. Candidate Hamed Shadpour
Louisiana State University
232 Choppin Hall
70803
Baton Rouge
United States

Contact Details:
Telephone: 225-578-7709
Fax: 225-578-3458
Email Address: hshadpl@lsu.edu

To use the following material:
ISSN/ISBN:
Title: Journal of Chromatography A
Author(s): Hamed Shadpour, Steven A. Soper, et al.
Volume: 1111
Issue: 2
Year: 2006
Pages: 238 - 251
Article title: Physiochemical properties of various ...

How much of the requested material is to be used:
The entire article.

Are you the author: Yes
Author at institute: Yes

How/where will the requested material be used: [how_used]

Details:

My Ph.D. Dissertation, Department of Chemistry, Louisiana State University.

Additional Info:

- end -

For further info regarding this automatic email, please contact:
WEB APPLICATIONS TEAM (esweb.admin@elsevier.co.uk)

American Chemical Society

Publications Division
Copyright Office

1155 Sixteenth Street, NW
Washington, DC 20036
Phone: (1) 202-872-4368 or -4367
Fax: (1) 202-776-8112 E-mail: copyright@acs.org

VIA FAX: 225-578-3458 DATE: September 19, 2006

TO: Hamed Shadpour, Department of Chemistry and Center for BioModular Multi-Scale Systems
Louisiana State University, 232 Choppin Hall, Baton Rouge, LA 70803

FROM: C. Arleen Courtney, Copyright Associate C. Arleen Courtney

Thank you for your request for permission to include **your** paper(s) or portions of text from **your** paper(s) in your thesis. Permission is now automatically granted; please pay special attention to the implications paragraph below. The Copyright Subcommittee of the Joint Board/Council Committees on Publications approved the following:

Copyright permission for published and submitted material from theses and dissertations
ACS extends blanket permission to students to include in their theses and dissertations their own articles, or portions thereof, that have been published in ACS journals or submitted to ACS journals for publication, provided that the ACS copyright credit line is noted on the appropriate page(s).

Publishing implications of electronic publication of theses and dissertation material
Students and their mentors should be aware that posting of theses and dissertation material on the Web prior to submission of material from that thesis or dissertation to an ACS journal may affect publication in that journal. Whether Web posting is considered prior publication may be evaluated on a case-by-case basis by the journal's editor. If an ACS journal editor considers Web posting to be "prior publication", the paper will not be accepted for publication in that journal. If you intend to submit your unpublished paper to ACS for publication, check with the appropriate editor prior to posting your manuscript electronically.

If your paper has **not** yet been published by ACS, we have no objection to your including the text or portions of the text in your thesis/dissertation in **print and microfilm formats**; please note, however, that electronic distribution or Web posting of the unpublished paper as part of your thesis in electronic formats might jeopardize publication of your paper by ACS. Please print the following credit line on the first page of your article: "Reproduced (or 'Reproduced in part') with permission from [JOURNAL NAME], in press (or 'submitted for publication'). Unpublished work copyright [CURRENT YEAR] American Chemical Society." Include appropriate information.

If your paper has already been published by ACS and you want to include the text or portions of the text in your thesis/dissertation in **print or microfilm formats**, please print the ACS copyright credit line on the first page of your article: "Reproduced (or 'Reproduced in part') with permission from [FULL REFERENCE CITATION.] Copyright [YEAR] American Chemical Society." Include appropriate information.

Submission to a Dissertation Distributor: If you plan to submit your thesis to UMI or to another dissertation distributor, you should not include the unpublished ACS paper in your thesis if the thesis will be disseminated electronically, until ACS has published your paper. After publication of the paper by ACS, you may release the entire thesis (**not the individual ACS article by itself**) for electronic dissemination through the distributor; ACS's copyright credit line should be printed on the first page of the ACS paper.

Use on an Intranet: The inclusion of your ACS unpublished or published manuscript is permitted in your thesis in print and microfilm formats. If ACS has published your paper you may include the manuscript in your thesis on an intranet that is not publicly available. Your ACS article cannot be posted electronically on a publicly available medium (i.e. one that is not password protected), such as but not limited to, electronic archives, Internet, library server, etc. The only material from your paper that can be posted on a public electronic medium is the article abstract, figures, and tables, and you may link to the article's DOI or post the article's author-directed URL link provided by ACS. This paragraph does not pertain to the dissertation distributor paragraph above.

06/07/06

Karen Buehler

From: Hamed Shadpour [hshadp1@lsu.edu]
Sent: Tuesday, September 19, 2006 2:38 PM
To: copyright@acs.org
Subject: Request for copyright permission

Copyright Office,

I am currently writing my Ph.D. dissertation and would like to request your permission to include my paper (full article) listed below:

Two-Dimensional Electrophoretic Separation of Proteins Using Poly(methyl methacrylate) Microchips, Analytical Chemistry, 2006, 78 (11), 3519-3527.

Sincerely,

Hamed Shadpour

Department of Chemistry and Center for BioModular Multi-Scale Systems
Louisiana State University
232 Choppin Hall
Baton Rouge, LA 70803
U.S.A
E-mail: hshadp1@lsu.edu
Phone: 225-578-7709
Fax: 225-578-3458

9/19/2006

American Chemical Society

Publications Division
Copyright Office

1155 Sixteenth Street, NW
Washington, DC 20036
Phone: (1) 202-872-4368 or -4367
Fax: (1) 202-776-8112 E-mail: copyright@acs.org

VIA FAX: 225-578-3458 DATE: November 8, 2006

TO: Hamed Shadpour, Department of Chemistry and Center for BioModular Multi-Scale Systems
Louisiana State University, 232 Choppin Hall, Baton Rouge, LA 70803

FROM: C. Arleen Courtney, Copyright Associate C. Arleen Courtney

Thank you for your request for permission to include your paper(s) or portions of text from your paper(s) in your thesis. Permission is now automatically granted; please pay special attention to the implications paragraph below. The Copyright Subcommittee of the Joint Board/Council Committees on Publications approved the following:

Copyright permission for published and submitted material from theses and dissertations
ACS extends blanket permission to students to include in their theses and dissertations their own articles, or portions thereof, that have been published in ACS journals or submitted to ACS journals for publication, provided that the ACS copyright credit line is noted on the appropriate page(s).

Publishing implications of electronic publication of theses and dissertation material
Students and their mentors should be aware that posting of theses and dissertation material on the Web prior to submission of material from that thesis or dissertation to an ACS journal may affect publication in that journal. Whether Web posting is considered prior publication may be evaluated on a case-by-case basis by the journal's editor. If an ACS journal editor considers Web posting to be "prior publication", the paper will not be accepted for publication in that journal. If you intend to submit your unpublished paper to ACS for publication, check with the appropriate editor prior to posting your manuscript electronically.

If your paper has not yet been published by ACS, we have no objection to your including the text or portions of the text in your thesis/dissertation in **print and microfilm formats**; please note, however, that electronic distribution or Web posting of the unpublished paper as part of your thesis in electronic formats might jeopardize publication of your paper by ACS. Please print the following credit line on the first page of your article: "Reproduced (or 'Reproduced in part') with permission from [JOURNAL NAME], in press (or 'submitted for publication'). Unpublished work copyright [CURRENT YEAR] American Chemical Society." Include appropriate information.

If your paper has already been published by ACS and you want to include the text or portions of the text in your thesis/dissertation in **print or microfilm formats**, please print the ACS copyright credit line on the first page of your article: "Reproduced (or 'Reproduced in part') with permission from [FULL REFERENCE CITATION.] Copyright [YEAR] American Chemical Society." Include appropriate information.

Submission to a Dissertation Distributor: If you plan to submit your thesis to UMI or to another dissertation distributor, you should not include the unpublished ACS paper in your thesis if the thesis will be disseminated electronically, until ACS has published your paper. After publication of the paper by ACS, you may release the entire thesis (**not the individual ACS article by** itself) for electronic dissemination through the distributor; ACS's copyright credit line should be printed on the first page of the ACS paper.

Use on an Intranet: The inclusion of your ACS unpublished or published manuscript is permitted in your thesis in print and microfilm formats. If ACS has published your paper you may include the manuscript in your thesis on an intranet that is not publicly available. Your ACS article cannot be posted electronically on a publicly available medium (i.e. one that is not password protected), such as but not limited to, electronic archives, Internet, library server, etc. The only material from your paper that can be posted on a public electronic medium is the article abstract, figures, and tables, and you may link to the article's DOI or post the article's author-directed URL link provided by ACS. This paragraph does not pertain to the dissertation distributor paragraph above. 06/07/06

Arleen Courtney

From: Hamed Shadpour [hshadp1@lsu.edu]
Sent: Monday, November 06, 2006 11:18 AM
To: Copyright
Subject: Request for copyright permission

Copyright Office,

I am currently writing my Ph.D. dissertation and would like to request your permission to include portion of my contributed paper (Figure 1, Figure 4, and related information in text as marked in attachment) listed below:

Continuous Flow Thermal Cycler Microchip for DNA Cycle Sequencing, Analytical Chemistry, 2006, 78 (17), 6223-6231.

Sincerely,

Hamed Shadpour

Department of Chemistry and Center for BioModular Multi-Scale Systems
Louisiana State University
232 Choppin Hall
Baton Rouge, LA 70803
U.S.A
E-mail: hshadp1@lsu.edu
Phone: 225-578-3458
Fax: 225-578-3458

11/6/2006

Arleen Courtney

From: Hamed Shadpour [hshadp1@lsu.edu]
Sent: Monday, November 06, 2006 11:20 AM
To: Copyright
Subject: Request for copyright permission

Copyright Office,

I am currently writing my Ph.D. dissertation and would like to request your permission to include my submitted manuscript (full article) listed below:

Multi-channel microchip electrophoresis device fabricated in polycarbonate with an integrated contact conductivity sensor array, Analytical Chemistry, 2006, in review.

Obviously, there will not be any web posting of this article prior publication by the ACS.

Sincerely,

Hamed Shadpour

Department of Chemistry and Center for BioModular Multi-Scale Systems
Louisiana State University
232 Choppin Hall
Baton Rouge, LA 70803
U.S.A
E-mail: hshadp1@lsu.edu
Phone: 225-578-3458
Fax: 225-578-3458

11/6/2006

American Chemical Society

Publications Division
Copyright Office

1155 Sixteenth Street, NW
Washington, DC 20036
Phone: (1) 202-872-4368 or -4367
Fax: (1) 202-776-8112 E-mail: copyright@acs.org

VIA FAX: 225-578-3458 DATE: November 9, 2006

TO: Hamed Shadpour, Department of Chemistry and Center for BioModular Multi-Scale Systems
Louisiana State University, 232 Choppin Hall, Baton Rouge, LA 70803

FROM: C. Arleen Courtney, Copyright Associate C. Arleen Courtney

Thank you for your request for permission to include **your** paper(s) or portions of text from **your** paper(s) in your thesis. Permission is now automatically granted; please pay special attention to the implications paragraph below. The Copyright Subcommittee of the Joint Board/Council Committees on Publications approved the following:

Copyright permission for published and submitted material from theses and dissertations
ACS extends blanket permission to students to include in their theses and dissertations their own articles, or portions thereof, that have been published in ACS journals or submitted to ACS journals for publication, provided that the ACS copyright credit line is noted on the appropriate page(s).

Publishing implications of electronic publication of theses and dissertation material
Students and their mentors should be aware that posting of theses and dissertation material on the Web prior to submission of material from that thesis or dissertation to an ACS journal may affect publication in that journal. Whether Web posting is considered prior publication may be evaluated on a case-by-case basis by the journal's editor. If an ACS journal editor considers Web posting to be "prior publication", the paper will not be accepted for publication in that journal. If you intend to submit your unpublished paper to ACS for publication, check with the appropriate editor prior to posting your manuscript electronically.

If your paper has **not** yet been published by ACS, we have no objection to your including the text or portions of the text in your thesis/dissertation in **print and microfilm formats**; please note, however, that electronic distribution or Web posting of the unpublished paper as part of your thesis in electronic formats might jeopardize publication of your paper by ACS. Please print the following credit line on the first page of your article: "Reproduced (or 'Reproduced in part') with permission from [JOURNAL NAME], in press (or 'submitted for publication'). Unpublished work copyright [CURRENT YEAR] American Chemical Society." Include appropriate information.

If your paper has already been published by ACS and you want to include the text or portions of the text in your thesis/dissertation in **print or microfilm formats**, please print the ACS copyright credit line on the first page of your article: "Reproduced (or 'Reproduced in part') with permission from [FULL REFERENCE CITATION.] Copyright [YEAR] American Chemical Society." Include appropriate information.

Submission to a Dissertation Distributor: If you plan to submit your thesis to UMI or to another dissertation distributor, you should not include the unpublished ACS paper in your thesis if the thesis will be disseminated electronically, until ACS has published your paper. After publication of the paper by ACS, you may release the entire thesis (**not the individual ACS article by itself**) for electronic dissemination through the distributor; ACS's copyright credit line should be printed on the first page of the ACS paper.

Use on an Intranet: The inclusion of your ACS unpublished or published manuscript is permitted in your thesis in print and microfilm formats. If ACS has published your paper you may include the manuscript in your thesis on an intranet that is not publicly available. Your ACS article cannot be posted electronically on a publicly available medium (i.e. one that is not password protected), such as but not limited to, electronic archives, Internet, library server, etc. The only material from your paper that can be posted on a public electronic medium is the article abstract, figures, and tables, and you may link to the article's DOI or post the article's author-directed URL link provided by ACS. This paragraph does not pertain to the dissertation distributor paragraph above. 06/07/06

Karen Buehler

From: Hamed Shadpour [hshadp1@lsu.edu]
Sent: Monday, November 06, 2006 11:15 AM
To: Copyright
Subject: Request for copyright permission

Copyright Office,

I am currently writing my Ph.D. dissertation and would like to request your permission to include portion of my contributed paper (Figure 1, Figure 6, and related information in text as marked in attachment) listed below:

Electrokinetically Synchronized Polymerase Chain Reaction Microchip Fabricated in Polycarbonate, Analytical Chemistry, 2005, 77 (2), 658-666.

Sincerely,

Hamed Shadpour

Department of Chemistry and Center for BioModular Multi-Scale Systems
Louisiana State University
232 Choppin Hall
Baton Rouge, LA 70803
U.S.A
E-mail: hshadp1@lsu.edu
Phone: 225-578-3458
Fax: 225-578-3458

11/9/2006

VITA

Hamed Shadpour was born in Rasht, Iran, and has one brother. Hamed attended Beheshti (Azadegan) High School in Rasht. Upon graduation, he enrolled at University of Guilan, Iran, in 1993. He graduated as a first rank alumnus with a bachelor degree with honors from the Chemistry Department in 1997. Then, the same year, he moved to the capital city of Iran, Tehran, to begin his master's education at Amirkabir University of Technology (Tehran Polytechnic). Then, he graduated as a first rank alumnus with a master's degree with honors from the Department of Chemical Engineering in 2000.

After two years of work in both academia and industry and establishing a company in Tehran, he moved to the United States to pursue his doctorate in 2002. He joined Professor Soper's research group in the Chemistry Department of Louisiana State University (LSU) in Baton Rouge, Louisiana, and started his doctoral work on developing Bio-MEMS for proteomics and genomics. He successfully passed the doctoral general examination in 2004. He was selected as the honorable doctoral candidate in North America for the year 2006 by the American Chemical Society division of analytical chemistry. He also received several national and international awards during his doctoral research and presentations. He also is a member of many national or international scientific societies including the American Chemical Society (ACS), American Association for the Advancement of Science, (AAAS), American Electrophoresis Society (AES), National Postdoctoral Association (NPA), American Institute of Chemical Engineers (AIChE), American Association of Clinical Chemistry (AACC) and California Separation Science Society (CASSS). He is receiving the degree of Doctor of Philosophy in chemistry at the December 2006 commencement.